



HAL
open science

Characterization and targeting of cancer stem cells in gastric adenocarcinoma

Phu Hung Nguyen

► **To cite this version:**

Phu Hung Nguyen. Characterization and targeting of cancer stem cells in gastric adenocarcinoma. Human health and pathology. Université de Bordeaux, 2015. English. NNT : 2015BORD0052 . tel-01519379

HAL Id: tel-01519379

<https://theses.hal.science/tel-01519379>

Submitted on 7 May 2017

HAL is a multi-disciplinary open access archive for the deposit and dissemination of scientific research documents, whether they are published or not. The documents may come from teaching and research institutions in France or abroad, or from public or private research centers.

L'archive ouverte pluridisciplinaire **HAL**, est destinée au dépôt et à la diffusion de documents scientifiques de niveau recherche, publiés ou non, émanant des établissements d'enseignement et de recherche français ou étrangers, des laboratoires publics ou privés.

THÈSE PRÉSENTÉE
POUR OBTENIR LE GRADE DE
DOCTEUR DE
L'UNIVERSITÉ DE BORDEAUX

ÉCOLE DOCTORALE
Sciences de la Vie et de la Santé

Par Phu Hung NGUYEN

**Caractérisation et ciblage des cellules souches
cancéreuses dans l'adénocarcinome gastrique**

***Characterization and targeting of cancer stem cells
in gastric adenocarcinoma***

Sous la direction de : Christine VARON

Soutenue le 30 avril 2015

Membres du jury :

| | |
|--|---------------------|
| Mme Tamara MATYSIAK-BUDNIK, Professeur, CHU Nantes | Présidente |
| M. MEGRAUD Francis, Professeur, INSERM U853, Université de Bordeaux | Examineur |
| M. Gerardo NARDONE, Professeur, Université de Naples, Federico II, Italie | Rapporteur |
| Mme Julie PANNEQUIN, DR CNRS, Institut de Génomique Fonctionnelle, Montpellier | Rapporteur |
| Mme Christine VARON, Maître de conférences, Université de Bordeaux | Directrice de thèse |

Titre : Caractérisation et ciblage des cellules souches cancéreuses dans l'adénocarcinome gastrique

Résumé :

Les cellules souches cancéreuses (CSC) représentent une sous-population de cellules tumorales à l'origine de l'hétérogénéité et de la croissance tumorale. Les CSC sont plus résistantes aux traitements, et à l'origine de la rechute et des métastases. L'identification des CSC constitue actuellement un enjeu majeur dans le développement de nouvelles thérapies ciblées pour inhiber la croissance tumorale et éradiquer le cancer. Dans ce travail, nous avons cherché à identifier, caractériser, et cibler les CSC dans l'adénocarcinome gastrique. Des modèles murins de xéno greffe de tumeurs primaires de patients atteints d'adénocarcinome gastrique hors cardia de types intestinal et diffus ont été développés, ainsi qu'un modèle de tumorsphere *in vitro* afin d'évaluer les capacités tumorigéniques de sous-populations tumorales. Nous avons identifié CD44 et l'aldéhyde déshydrogénase (ALDH) comme marqueurs d'enrichissement des CSC dans les 2 types d'adénocarcinomes gastriques, l'ALDH représentant un marqueur plus spécifique que CD44. Nous avons ensuite étudié l'effet de l'acide rétinoïque tout trans (ATRA), et nous avons montré que l'ATRA inhibe la formation et la croissance des tumorspheres *in vitro* ainsi que la croissance tumorale *in vivo*. Cet effet de l'ATRA passe par l'inhibition de l'expression des marqueurs souches et des capacités d'auto-renouvellement des CSC. En conclusion, CD44 et ALDH sont des marqueurs de CSC dans les adénocarcinomes gastriques hors cardia de types intestinal et diffus, et le traitement par l'ATRA constituerait une stratégie commune de traitement pour cibler spécifiquement les CSC et inhiber la croissance tumorale dans ces deux types de cancer gastrique.

Mots clés :

Cancer gastrique, cellule initiatrice de tumeur, acide rétinoïque, aldéhyde déshydrogénase, CD44, xéno greffe, tumorsphère

Title: Characterization and targeting of cancer stem cells in gastric adenocarcinoma

Abstract:

Cancer stem cells (CSCs) are a subpopulation of tumor cells at the origin of the heterogeneity and growth of tumors. CSCs are more resistant to treatment, and are responsible for relapse and metastasis. The identification of CSCs is a major challenge for the development of new targeted therapies to inhibit tumor growth and eradicate cancer. In this work, we aimed to identify, characterise, and target CSCs in gastric adenocarcinoma. Mouse models of primary tumor xenografts from intestinal and diffuse type non-cardia gastric adenocarcinomas from patients were developed, as well as an *in vitro* tumorsphere assay, to assess the tumorigenic capacity of subpopulations of tumor cells. We identified CD44 and aldehyde dehydrogenase (ALDH) as CSC enrichment markers in the two types of gastric adenocarcinoma, ALDH representing a more specific marker than CD44. We then studied the effect of All-trans retinoic acid (ATRA), and showed that it inhibited the formation and growth of tumorspheres *in vitro* and tumor growth *in vivo*. This effect of ATRA is due to the inhibition of stem marker expression and the self-renewal capacity of CSCs. In conclusion, CD44 and ALDH are effective CSC markers in intestinal and diffuse type non-cardia gastric adenocarcinomas, and treatment with ATRA provides a common treatment strategy to specifically target CSCs and inhibit tumor growth in both subtypes of this gastric cancer.

Keywords:

Gastric cancer, tumor initiating cell, retinoic acid, aldehyde dehydrogenase, CD44, xenograft, tumorsphere

Unité de recherche

Infection à Helicobacter, inflammation et Cancer,

INSERM U853, Université de Bordeaux,

146 rue Léo Saignat, 33076 Bordeaux

Substantial abstract (4-5 pages):

Context of the research

Gastric cancer is the fourth most common cancer in frequency and the third leading cause of cancer mortality in the world. Ninety-five percent of all gastric cancers are gastric adenocarcinomas and the main driving factor is the chronic infection by *Helicobacter pylori*.

Tumors are heterogeneous, composed of cells which are more or less differentiated and not all proliferative. The cancer stem cell (CSC) hypothesis that is now widely accepted shows that CSCs are a subpopulation of tumor cells with self-renewal and asymmetrical division properties giving rise to the more or less differentiated cells composing the tumor mass. These cells are at the origin of the heterogeneity of the tumors, and have tumor initiating properties which are responsible for tumor growth. CSCs are more resistant to treatment, and at the origin of relapse and metastasis. Several CSC markers, such as CD133, CD44 and CD24, have been characterized in tumors of different organs. More recently, detection of aldehyde dehydrogenase (ALDH) activity was also used to identify CSCs in acute myeloid leukemia (AML) and in solid tumors in the breast, lung, colon, and other organs.

In the stomach, their existence has been subject to debate. The first study performed by Takaishi *et al.* on gastric cancer cell lines proposed CD44 as a marker of gastric CSCs, but this marker was expressed in 3 out of 6 gastric cell lines, and confirmation in primary tumors was lacking. Then, the study performed by Rocco *et al.* on 12 human primary cases of gastric adenocarcinoma failed to demonstrate tumor-initiating properties of CD133+ and CD44+ sorted cells in xenograft assays in both NOD/SCID and nude immunodeficient mice.

On the other hand, the discovery of the CSCs in tumors has opened the window for the development of new anti-cancer therapies based on CSC targeting. One strategy concerns the targeting of the self-renewal and differentiation properties of CSCs. All-trans retinoic acid (ATRA) has been used in the treatment of leukemia in clinics for the past three decades for its properties to induce cell differentiation. More recently, studies suggested that ATRA induced cell differentiation via CSC targeting.

In this study, we aimed: first, to confirm the existence of CSCs and to characterize markers allowing their identification and isolation in human primary intestinal and diffuse type non-cardia gastric adenocarcinomas; and second, we assessed the effect of ATRA treatment on gastric CSC self-renewal and tumorigenic properties.

Experimental procedures

In the first part of the study, mouse xenograft models using primary non-cardia gastric adenocarcinoma from patients were successfully developed for 20% of the cases included. Among these cases, 1 diffuse and 5 intestinal histological variants showed similar histopathological features to the primary tumors after serial transplantation in mice, and were studied. The expression of 11 putative cell surface markers of CSCs described in other cancers was evaluated on these cases and on gastric cancer cell lines. Tumorigenic properties of FACS-sorted cells were evaluated by *in vitro* tumorsphere assays and *in vivo* xenografts using extreme limiting dilution assays in mice.

In the second part of the study, in order to assess the inhibitory effect of ATRA on gastric CSCs, 3 different models of ATRA treatment of gastric cancer cells were developed including 2D and 3D *in vitro* cultures and *in vivo* xenografts in NSG immunodeficient mice. ATRA-induced growth inhibition of gastric cancer cell lines in 2D *in vitro* culture was evaluated by MTT assay. A tumorsphere assay was used to assess the effect of ATRA on self-renewal in 3D *in vitro* cultures. The effect of ATRA on tumor growth was assessed on mouse xenograft models. Flow cytometry analyses were carried out to assess the effects of ATRA on cell cycle progression and apoptosis. The expression markers of cell cycle progression, apoptosis, stemness and CSCs were analyzed by RTqPCR, tumorspheres by immunofluorescence, and tumor xenografts by immunohistochemistry.

Results

Establishment of a mouse model of primary xenografts from human gastric adenocarcinomas

Fresh gastric tissue samples were collected by pathologists upon surgical resection from consenting patients who underwent gastrectomy for non-cardia gastric adenocarcinoma at the University Hospital and the Bergonié Regional Cancer Center in Bordeaux. Among the 37 tumor cases xenografted in mice, only 8 cases led to the growth of a secondary tumor; 7 were intestinal type and 1 was diffuse type according to the Lauren classification. Tumors reached a the size of 500 mm³ 16.6±3.4 weeks after the first passage (P) (P1) in mice. Among them, 6 tumor cases including 1 diffuse and 5 intestinal cases were serially transplanted successfully in mice and preserved similar histopathological features to the primary tumors of the patients until at least P5. Tumors between P2, P3 and P5, reaching a 500 mm³ tumor size after 10±5.9, 10.6±6.9 and 7.2±0.8 weeks, were removed from the mice and freshly dissociated for each experiment in the study.

CD133 and CD44 cells with tumorigenic CSC properties identified

CD133 and CD44 expression was observed in tumor cells of both diffuse and intestinal type primary gastric adenocarcinoma. Among them, CD44 expression was restricted to a subpopulation of cells representing approximately one quarter of the tumor cells. Cell sorting based on CD133 and CD44 expression was then performed on live (7-AAD-), ESA+ (to detect human carcinoma cells) cells freshly dissociated from tumors collected from mice. Concerning the three cases studied (GC10, GC06 and GC04), both CD133+ and CD44+ FACS-sorted cells formed significantly more tumorspheres after 10 days of *in vitro* culture than their CD133- and CD44- respective counterparts. The number of tumorspheres obtained was higher in all cases with the CD44+ cells compared to the CD133+ cells. This suggested that the CD44+ cell subpopulation contained the higher number of CSCs. These FACS-sorted cells were then subcutaneously xenografted in mice in a limiting dilution assay, and tumor growth was recorded periodically. Results revealed that CD133+ cells and CD44+ cells led to the development of tumors in mice, whereas CD133- or CD44- did not or, when present, at a very lower frequency. The observed CSC frequency was between 1/105 to 1/1,911 ESA+CD133+ cells versus 1/781 to 1/66,876 ESA+CD133- cells, and between 1/29 to 1/1,020 ESA+CD44+ cells versus 1/568 to 1/28,963 ESA+CD44- cells. These results confirmed that CSCs exist in both primary diffuse and intestinal type non-cardia gastric adenocarcinomas, and they express CD133 and CD44. In addition, CD44 was more specific than CD133 for the isolation of CSCs.

ALDH is a more specific marker of gastric CSCs than CD44

The expression of 7 additional putative markers of CSCs, CD10, CD49f, CD73, CD166, CD90, CD105, which were described in carcinomas of other organs, and ALDH activity were analyzed by flow cytometry on 5 cases of primary gastric tumor xenografts and 5 gastric cancer cell lines. Results showed that ESA and CD49f were the most highly expressed markers in both cancer cell lines and primary tumors, followed by CD90 expressed in nearly half of the cells, then CD73 in more than a third of the cells. In primary tumors, CD166 was expressed in 21±13% of the tumor cells while CD105 expression and ALDH activity were detected in only 9±6% and 8±5% of the cells, respectively. CD10 was negative except in 2 of the 10 cases studied. Flow cytometry experiments of CD44 co-staining with these markers demonstrated that CD166 and CD44 were co-expressed. CD73 was expressed in a high percentage of CD44+ cells as well as in CD44- cells. CD90+ and CD105+ cells were found in equal amounts in CD44+ and CD44- cells. Interestingly, most of the ALDH+ cells expressed CD44, and the ALDH+CD44+ cells represented less than half of the CD44+ cells.

Tumorsphere assays from FACS-sorted cells showed that cells forming tumorspheres were essentially ALDH+ and CD166+, and to a lesser extent CD73+, CD90- and CD105-. Xenograft experiments in mice, in the 4 cases studied, revealed that ALDH+ cells developed tumors at a significantly higher frequency than the respective ALDH- cells (ranging between 1/38 to 1/273 for ALDH+ cells versus 1/368 to 1/21,208 ALDH- cells) and the CD133+ cells (1/105 and 1/1658, respectively) and CD44+ cells (1/49 and 1/352, respectively).

Immunohistochemistry analyses revealed that ALDH1, the main isoform of ALDH enzymes, was expressed in a smaller number of tumor cells than CD44 in most of the cases studied, except one for which its high expression did not match the low ALDH activity detected by the flow cytometry assay. *In vitro*, ALDH and CD44 were expressed in all cells composing small young tumorspheres, and in bigger and older tumorspheres, some CD44+ALDH- cells were detected, representing more differentiated cells. Interestingly, CD44+ALDH+ cells, corresponding to CSCs, but not CD44+ALDH- cells corresponding to more differentiated cells, excluded the Hoechst 33342 stain, suggesting drug efflux properties. Verapamil treatment restored Hoechst 33342 incorporation and staining in ALDH+ cells, confirming that CD44+ALDH+ cells have drug efflux properties and may correspond to cells in the so-called side population previously proposed by others as CSCs in gastric cell lines. Finally, these results confirmed that ALDH is a more selective marker than CD133 and CD44 for the identification and isolation of CSCs in intestinal and diffuse variants of non-cardia gastric adenocarcinomas.

In the second part of this work, we assessed the effects of ATRA treatment on gastric CSCs and tumor growth of gastric primary tumors and cell lines in three complementary models including an *in vitro* mono-layer culture (2D), an *in vitro* tumorsphere assay under non-adherent culture conditions (3D), and an *in vivo* xenograft in mice.

Optimization of cell culture conditions for studying the effects of ATRA

Under 2D culture conditions of gastric cancer cell lines treated with 5 µM ATRA, MKN7, MKN74 and MKN28 responded to ATRA only under conditions of total serum deprivation, whereas others like AGS or NCI-N87 tolerated a concentration as low as 0.2% to become ATRA sensitive. Quantitative RT-PCR analyses demonstrated that RAR-γ but not RXR-α and

RXR- β were expressed at a substantial level in these cell lines, and were upregulated under serum free-conditions. With a growth inhibition of 70%, the MKN45 and MKN74 cell lines appear to be the most sensitive to ATRA under serum-free culture conditions.

Flow cytometry experiments revealed that ATRA treatment at 5 μ M under serum-free conditions induced a cell cycle arrest in the G0/G1 phase.

ATRA inhibits gastric tumorsphere formation and growth

In vitro tumorsphere assays under serum-free conditions revealed that ATRA inhibited significantly the number and the size of tumorspheres. The number of tumorspheres was inversely correlated with the ATRA doses, suggesting that the drug reduced the number of CSCs with a dose-effect. Flow cytometry analyses showed that ATRA blocked cell cycle progression, in the G0/G1 phase for MKN45 and in the G2/M phase for MKN74. The downregulation of expression of A, B, E1 and D1 cyclins, CDK2, CDC25C and E2F1, which control cell cycle progression was detected by quantitative RT-PCR. In addition, an increased expression of cyclin inhibitors, P21 and P27, was observed in both cell lines as well as P16 in MKN74 cells and P53 in MKN45 cells. PCNA, an important gene which controls DNA replication in the S phase, was also downregulated in both cell lines.

This inhibitory effect of ATRA on tumorsphere formation and growth was associated with a downregulation of the expression of the CSCs marker, CD44 and ALDH1, as well as the stemness markers, Klf4 and Sox2. These results suggest that ATRA treatment targets CSC self-renewal properties. In addition, the expression of MUC5AC, a marker of gastric differentiation, was increased; this suggests that ATRA may also favor differentiation, as reported in the treatment of promyelocytic leukemia.

ATRA inhibited the growth of gastric tumors *in vivo*

Cells from two gastric cancer cell lines (MKN45 and MKN74) and two gastric primary tumors (C06 and GC10) were subcutaneously xenografted in NSG mice, and tumor size was recorded periodically. When tumors reached the size of 100 mm³, treatment was started and ATRA (33 or 3.3 μ mol/kg) or DMSO as a control vehicle was injected once a day for 15 days. ATRA at 33 μ mol/kg noticeably inhibited tumor growth, while DMSO-treated tumors continued to actively grow. The ATRA anti-tumor effect was particularly visible in the GCO6 and GC10 primary tumors, in which ATRA seemed to be effective as early as 3 days of treatment. ATRA treatment for 15 days was not sufficient to inhibit totally the growth of tumors from gastric cancer cell lines, but in some cases of primary tumors xenografts, there was no palpable residual tumor. Tumor relapse was indeed observed in all cases after stopping ATRA treatment, however it is important to note that ATRA treatment was able to maintain the tumor size up to 28 days for GC06, MKN45, and MKN74 and up to 14 days for GC06.

Immunohistochemical analysis of the residual tumors after ATRA (33 μ mol/kg) or DMSO treatment showed that ATRA noticeably decreased the expression of specific gastric CSC markers including CD44 and ALDH. On other hand, the downregulation of expression of proteins involved in tumor growth including PCNA and Ki67 was also observed. ATRA-induced caspase expression was increased in three of the four cases studied.

Conclusion:

(1). CD44 and ALDH are two enrichment markers of gastric CSCs in primary tumors, and ALDH can be considered as a more specific CSC marker than CD44 in diffuse and intestinal types of non-cardia gastric adenocarcinoma.

(2). In this study, we demonstrated that ATRA regulated the expression of genes involved in the cell cycle to inhibit cellular proliferation, and downregulated the expression of stemness genes as well as the CSC markers, CD44 and ALDH. Consequently, ATRA inhibited gastric cancer cell growth both *in vitro* and *in vivo* by targeting gastric CSCs, suggesting that it may be a potent strategy to consider to complement/in addition to the treatment of both intestinal and diffuse type gastric adenocarcinomas.

Remerciements

Achever une thèse est comme une aventure pleine de défi, et personne ne peut le faire tout seul. J'ai eu vraiment de la chance de recevoir l'aide précieuse de ma famille, des directeurs de thèse, de nombreux amis et collègues.

Tout d'abord, je tiens à remercier profondément Madame le Docteur Christine Varon, une chercheuse très compétente et enthousiaste, de m'avoir encadré avec beaucoup de dévouement tout au long de ces quatre années de thèse. Grâce à elle, j'ai pu acquérir des théories avancées et une expérience précieuse en vue de concevoir et mener un projet de recherche.

En particulier, je tiens à adresser mes sincères remerciements au Professeur Francis Mégraud de m'avoir accueilli au sein de son équipe et m'avoir fait rencontrer des scientifiques internationaux. Il m'a toujours encouragé et m'a offert de meilleures conditions pour travailler au laboratoire durant ces quatre années.

Je voudrais remercier profondément Madame le Docteur Cathy Staedel pour son aide et ses conseils. Elle m'a montré comment avoir les compétences nécessaires d'un chercheur scientifique.

Je souhaite également exprimer toute ma reconnaissance à Lucie, une amie, une collègue qui m'a beaucoup aidé au travail. Je remercie également à tous les collègues de l'unité INSERM U853 pour leur implication pendant ma thèse.

Mes remerciements vont également à Madame Lindsay Mégraud pour avoir accepté de corriger cette rédaction de recherche et aussi tous mes articles en anglais. En absence de votre aide, je ne pourrais pas les finir.

Merci à Benoit Rousseau, Vincent Pitard, Santiago Gonzalez, Edith Chevret et les collaborateurs de l'unité INSERM U853 pour votre aide pendant ma thèse.

Je suis très reconnaissant aux membres du jury d'avoir accepté de juger ces travaux.

Pour finir, je voudrais remercier mon plus grand soutien qui est ma femme Le Thi Thanh Huong, mon garçon Nguyen Phu Binh –Tin, mes parents et ma famille, merci pour votre soutien, votre patience et votre compréhension pendant cette belle aventure.

CONTENTS

LIST OF ABBREVIATIONS

LIST OF TABLES

LIST OF FIGURES

| | |
|---|----|
| PART I. Introduction..... | 6 |
| I. GASTRIC EPITHELIUM..... | 6 |
| I.1 Cardiac region | 7 |
| I.2 Fundus and body region..... | 7 |
| I.3 Pyloric region..... | 7 |
| I.4 Gastric gland structure..... | 8 |
| I.4.1. Surface mucous cells and mucous neck cells..... | 8 |
| I.4.2. Parietal cells | 8 |
| I.4.3. Chief cells | 10 |
| I.4.4. Enteroendocrine cells | 11 |
| I.4.5. Stem cells | 11 |
| II. GASTRIC CARCINOMA..... | 11 |
| II.1 Epidemiology..... | 11 |
| II.2 Classification of gastric cancer | 13 |
| II.2.1 Classification of gastric cancer | 14 |
| II.2.2 The Japanese classification of gastric cancer | 14 |
| II.2.3 The WHO classification | 14 |
| II.2.4 The Laurén classification..... | 15 |
| II.3 Risk factors for development of gastric cancer..... | 17 |
| II.3.1 Environmental factors..... | 17 |
| II.3.2 Genetic factors..... | 18 |
| II.3.3 <i>Helicobacter pylori</i> and gastric cancer | 19 |

| | | |
|---------|---|----|
| II.4 | Gastric carcinogenesis..... | 22 |
| II.5 | Signaling pathways in gastric cancer..... | 25 |
| II.5.1 | Wnt/beta-catenin signaling pathway..... | 25 |
| II.5.2 | Signaling pathway of growth factors | 27 |
| II.5.3 | Notch signaling pathway..... | 30 |
| II.5.4 | Epithelial-mesenchymal transition | 33 |
| III. | STEM CELLS AND CANCER STEM CELLS..... | 36 |
| III.1 | Normal stem cells..... | 36 |
| III.1.1 | General Introduction | 36 |
| III.1.2 | Mechanism of self-renewal of stem cells | 38 |
| III.1.3 | Gastric stem cells | 39 |
| III.2 | Cancer stem cells | 40 |
| III.2.1 | Concept of cancer stem cells | 41 |
| III.2.2 | Evidence of cancer stem cells | 42 |
| III.2.2 | Origin of cancer stem cells..... | 43 |
| III.2.3 | Cells-of-origin in gastric cancer..... | 45 |
| IV. | IDENTIFICATION OF CANCER STEM CELLS | 45 |
| IV.1 | Methods of identification and isolation of cancer stem cells..... | 46 |
| IV.1.1 | Colony formation assays..... | 46 |
| IV.1.2 | 'Side population' assay..... | 46 |
| IV.1.3 | Tumorsphere assay..... | 48 |
| IV.1.4 | Cancer stem cell isolation based on surface marker expression..... | 48 |
| IV.1.5 | ALDH activity assay | 49 |
| IV.1.6 | <i>In vivo</i> xenotransplantation models for cancer stem cell identification | 49 |
| IV.2 | Marker of cancer stem cells..... | 50 |
| IV.3 | Aldehyde dehydrogenase | 54 |
| IV.3.1 | Human ALDH gene superfamily..... | 55 |

| | |
|---|------------|
| IV.3.2 Role of ALDH in protection of normal and cancer stem cells | 58 |
| IV.3.3 ALDH is a common marker of cancer stem cells..... | 60 |
| IV.4 CD44 and cancer stem cells | 64 |
| IV.4.1 Structure of CD44 | 64 |
| IV.4.2 Role of CD44 in cancer..... | 66 |
| IV.4.3 CD44 is a universal marker of cancer stem cells..... | 69 |
| IV.5 Role of CD133 in cancer stem cells..... | 71 |
| V. RETINOIC ACID IN CANCER THERAPY | 73 |
| V.1. Retinoid metabolism..... | 74 |
| V.1.1. Retinoids | 74 |
| V.1.2. Synthesis and degradation of retinoic acids..... | 75 |
| V.2. Retinoic acid receptors and their roles..... | 78 |
| V.2.1. Retinoic acid receptor (RAR)..... | 78 |
| V.2.2. Retinoic X receptor (RXR)..... | 79 |
| V.2.3. Role of retinoic acid receptors in gene transcription regulation..... | 80 |
| V.3. Role of retinoic acid in anticancer treatment..... | 89 |
| V.3.1. RA in acute promyelocytic leukemia | 90 |
| V.3.2. RA in solid tumors..... | 92 |
| V.4. Retinoic acid signaling pathway and gastric carcinoma | 93 |
| V.4.1 Modifications of RA signaling in gastric cancer | 93 |
| V.4.2 Role of RA in gastric cancer treatment..... | 94 |
| PART II. Results | 96 |
| Article 1 – CD44 and Aldehyde dehydrogenase are markers of cancer stem cells in intestinal and diffuse types of non-cardia gastric carcinoma..... | 98 |
| Article 2 – All-trans retinoic acid targets cancer stem cells and inhibits tumor growth in gastric carcinoma | 154 |
| PART III. DISCUSSION AND PERSPECTIVES | 200 |
| PART IV. REFERENCES | 214 |

ANNEXES246

Article 3 – *Helicobacter pylori* infection generates cells with cancer stem cells properties via epithelial to mesenchymal-like changes 248

Article 4 – Inhibition of gastric tumor cell growth using seed-targeting LNA as specific, long-lasting microRNA inhibitors..... 250

List of abbreviations

| | |
|------------------|---|
| ABCG2 | ATP-binding cassette sub-family G member 2 |
| ADH | Alcohol dehydrogenase |
| ALDH | Aldehyde dehydrogenase |
| ALDH1A1 | Aldehyde dehydrogenase 1 family, member A1 |
| ATRA | All-Trans Retinoic Acid |
| BMDC | Bone Marrow-Derived Cell |
| CCNA | Cyclin A gene |
| CCNB | Cyclin B gene |
| CCND1 | Cyclin D1 gene |
| CCNE1 | Cyclin E1 gene |
| CDC2 | Cell division cycle 2 |
| CDC25C | Cell division cycle 25 homolog C |
| cDNA | Complementary deoxyribonucleic acid |
| CDKs | Cyclin-dependent kinase |
| CDKN1A | Cyclin-dependent kinase inhibitor 1A |
| CHECK1 | CHK1 checkpoint homolog |
| <i>CIP/KIP</i> | CDK interacting protein/Kinase inhibitory protein |
| CKIs | Cyclin-dependent kinases inhibitors |
| CRABP | Cellular Retinoic Acid Binding Protein |
| CRBP | Cellular Retinol Binding Protein |
| CSC | Cancer Stem Cells |
| <i>CYP26A1</i> | Cytochrome P450, Family 26, Subfamily A, Polypeptide 1 |
| DBD | DNA Binding Domain |
| DEAB | Diethylaminobenzaldehyde |
| DNA | Deoxyribonucleic Acid |
| E2F1 | E2F transcription factor 1 |
| EC cells | Embryonic Carcinoma cells |
| EGF | Epidermal growth factor |
| EGFR | Epidermal growth factor receptor |
| eGFP | Enhanced Green Fluorescent Protein |
| ESA | Epithelial Specific Antigen |
| ESCs | Embryonic Stem cells |
| FACS | Fluorescence activated cell sorter |
| FGF | Fibroblast Growth Factor |
| FISH | Fluorescence <i>in situ</i> hybridization |
| GADD45A | Growth arrest and DNA-damage-inducible protein, alpha |
| HAT | Histone acetyl transferase |
| HDAC | Histone deacetylase |
| HER2 | Human EGF receptor 2 |
| HMT | Histone methyl transferase |
| <i>H. pylori</i> | <i>Helicobacter pylori</i> |
| HSCs | Hematopoietic stem cells |
| ID1 | Inhibitor of differentiation 1 |
| Klf4 | Kruppel-Like Factor 4 |
| LBD | Ligand Binding Domain |
| Lgr5 | Leucine-rich repeat-containing G-protein coupled receptor 5 |
| MAPK | Mitogen Associated Protein Kinase |
| mRNA | messenger Ribonucleic Acid |
| NSG | Non obese diabetous (NOD) severe combined |

| | |
|--------------|---|
| | immunodeficiency (SCID)-interleukin2-Rag- γ null |
| Oct4 | Octamer-binding transcription factor 4 |
| PBS | Phosphate Buffered Saline |
| PCNA | Proliferating cell nuclear antigen |
| PCR | polymerase chain reaction |
| RA | Retinoic Acid |
| RALDH | Retinaldehyde Dehydrogenase |
| RAR α | Retinoic Acid Receptor alpha |
| RAR β | Retinoic Acid Receptor beta |
| RAR γ | Retinoic Acid Receptor gamma |
| RARE | Retinoic Acid Response Element |
| RNA | Ribonucleic Acid |
| RXR | Retinoid X receptor |
| shRNA | Small hairpin RNA |
| siRNA | Small interfering RNA |
| Sox2 | SRY (sex determining region Y)-box 2 |
| TGF β | Transforming Growth Factor beta |
| UTR | Untranslated Regions |

List of tables

- Table 1** Surface markers of cancer stem cells
- Table 2** Isotype of RA receptors
- Table 3** Target genes that are directly regulated by Retinoic acid

List of Figures

- Figure 1** Anatomical regions of the stomach
- Figure 2** The mucosa of three different regions of the stomach
- Figure 3** Structure of a gastric gland
- Figure 4** Age-standardized gastric cancer incidence rates
- Figure 5** Age – standardized incidence rates for stomach cancer
- Figure 6** Two types of gastric adenocarcinoma
- Figure 7** Factors contributing to gastric pathology and disease outcome in H.pylori infection
- Figure 8** Cellular activities of CagA
- Figure 9** Histological progression of a Helicobacter-induced gastric cancer in a mouse model
- Figure 10** Wnt/beta-catenin pathway
- Figure 11** The FGF signalling pathway
- Figure 12** The EGFR-signalling pathway
- Figure 13** Notch signalling pathway
- Figure 14** Contribution of EMT to cancer progression
- Figure 15** The stem-cell hierarchy
- Figure 16** Restricted expression of Lgr5 at the base of adult pyloric glands
- Figure 17** Stochastic and hierarchical model in tumor initiation
- Figure 18** Methods for the identification and enrichment of CSCs
- Figure 19** Multiplex function of aldehyde dehydrogenase
- Figure 20** Dendrogram of 19 human aldehyde dehydrogenase genes of the ALDH superfamily
- Figure 21** CD44 gene and protein structure
- Figure 22** Schematic representation of the transmembrane glycoprotein CD133
- Figure 23** Chemical structures of retinoids used
- Figure 24** Retinoic acid synthesis and signalling
- Figure 25** Mechanisms of transcriptional repression and activation by RAR–RXR
- Figure 26** Crosstalk between the RA-activated p38MAPK pathway and the expression of RAR target genes
- Figure 27** Retinoids and rexinoids can interfere with events leading to tumorigenicity at several levels
- Figure 28** Expression level of putative CSC markers in human primary non-cardia gastric carcinoma
- Figure 29** CSC frequency determined by the capacity of FACS sorted cancer cells to initiate a new tumor in mouse xenograft experiments in limiting dilution assays.

PART I. Introduction

I. GASTRIC EPITHELIUM

The stomach is one of the principal parts of the digestion system in most vertebrates and functions as the main food storage tank of the body. The contraction of the stomach wall and the enzymes secreted by the gastric mucosa contribute to this function. Anatomically, the stomach is comprised of four regions including the cardia, fundus, body and pylorus (Figure 1). Sometimes referred to as a fifth anatomical region, the antrum is located between the body and the pylorus.

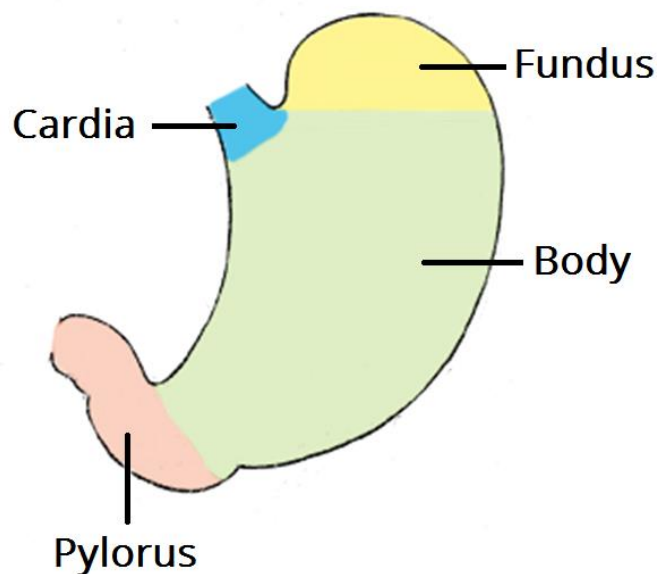


Figure 1. Anatomical regions of the stomach

Source: (teachmeanatomy.info)

I.1 Cardiac region

The cardia is a small region approximately 3 to 5 cm wide and serves as the junction between the esophagus and the upper part of the stomach. Cardiac glands are composed almost entirely of mucous-secreting cells which form a columnar epithelium in which enteroendocrine cells are present. Glands in the cardiac region are lined entirely with surface mucous cells (Figure 2.a).

Their secretion plays an important role in lubrication of the incoming foods as well as esophagus protection against gastric reflux.

I.2. Fundus and body region

The glands of this region are the principal producers of gastric juice and are comprised of three parts: (1) the crypt with surface mucous cells, (2) the collar containing mucous neck cells, stem cells with mitotic activity and parietal cells, and (3) the body gland, corresponding to the major part of the gland length. The upper and lower body portions contain different proportions of cells lining the gastric gland. Approximately 15 million gastric glands open into 3.5 million gastric crypts. Two to seven gastric glands open into a single crypt (Figure 2.b).

I.3. Pyloric region

The pyloric region consists of short, coiled and branched tubular glands with a wide lumen (Figure 2.c). Epithelial cells constituting pyloric glands resemble the mucous neck cells of the gastric glands. Occasionally parietal cells may locate in the pyloric glands. Enteroendocrine cells (G cells) which secrete gastrin are frequently found in

the pyloric antrum region. In addition, lymphoid islands can be observed in the chorion. Superficial mucous cells cover the surface of the mucosa and gastric pits.

I.4. Gastric gland structure

The six major cell types in gastric glands are surface mucous cells, mucous neck cells, parietal cells, principal cells, enteroendocrine cells and stem cells (Figure 3).

I.4.1. Surface mucous cells and mucous neck cells

Surface mucous cells cover the pit of the gastric units. Mucous neck cells are situated at the level where glands open into a crypt. These cells are shorter than surface mucous cells and both cell types produce mucin proteins, which are high weight molecular glycoproteins. Mucous neck cells contain 95% water and 5% mucins, and form an insoluble gel which adheres to the gastric mucosal surface. These cells also play a role as a barrier, approximately 100 μm thick, to protect the gastric lining by secreting mucous.

I.4.2. Parietal cells

The parietal cells are mainly distributed in the upper part of the gastric glands. These are large pyramidal cells, with a central and spherical nucleus and intense eosinophilic cytoplasm due to its high density of mitochondria. Parietal cells secrete both hydrochloric acid (HCl) and intrinsic factor, an essential glycoprotein for the absorption of vitamin B12 in the small intestine. Carbonic anhydrase produces H_2CO_3 which dissociates into H^+ and HCO_3^- in the cytoplasm. The active cell also releases K^+ , and Cl^- combines with H^+ to form HCl. Numerous mitochondria provide the energy needed by ion pumps located mainly in the cell membrane microvilli projecting into the canaliculus. The secretory activity of the parietal cells is stimulated by both cholinergic nerve endings (parasympathetic stimulation), and histamin and gastrin, the latter secreted by local enteroendocrine cells.

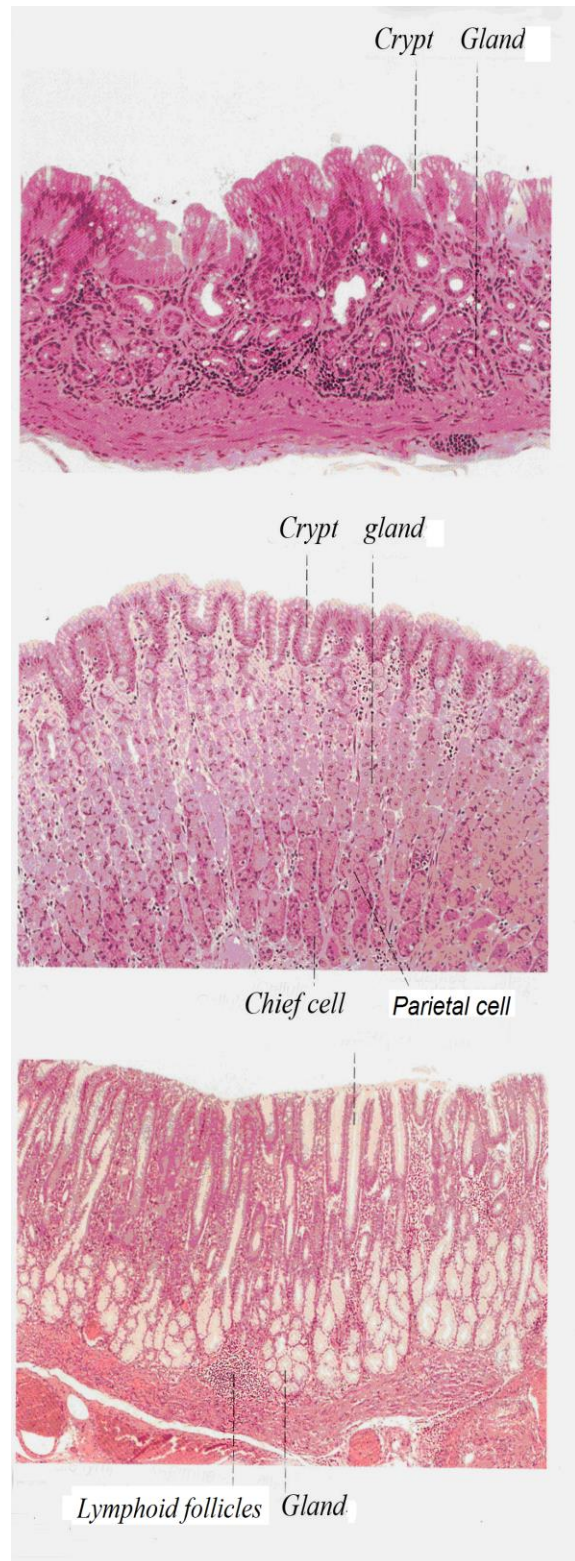
Figure 2. The mucosa of three different regions of the stomach.

a. Mucosa of the stomach cardia, human. The epithelium is relatively thin; gastric crypts are dimple-shaped invaginations of the superficial epithelium which, in the cardia, represent approximately half the thickness of the

b. Mucosa of the gastric fundus, human. Gastric crypts constitute approximately one fifth to one fourth of the mucosa width. The epithelium which lines the crypts, is formed by cylindrical cells. The glands, slightly curved and partially branched, have an upper “neck”, a middle part, and a deep part. One fourth to one third of the lower portion of the glands are composed primarily of chief cells, i.e. basophils with apical grains which elaborate/release a proteolytic enzyme, pepsin.

c. Mucosa of the pyloric portion of the stomach, human. The different layers of the gastric glands correspond to approximately half of the mucosal width; the tubular glands, curved and branched, produce mucus and lysozyme, but also contain numerous endocrine cells, especially those which produce gastrin. Lymphoid follicles can be present, but they can also be found in other parts of the stomach.

Source: Antoine de Hem, 2002 Citation complete



I.4.3. Chief cells

Chief cells (or zymogen cells) predominate in the lower third of the gastric glands and have the characteristics of cells synthesizing and exporting proteins. Chief cells have an analogous structure to zymogen cells of the exocrine pancreas: the basal area of their cytoplasm comprises a well-developed rough endoplasmic reticulum. Secretory granules containing pepsinogen (zymogen granules) are observed at the cell's apical pole. Pepsinogen, a proenzyme stored in zymogen granules, is released into the lumen of the gland and converted in the acidic environment of the stomach into pepsin, a proteolytic enzyme capable of digesting most proteins. The pepsinogen production is fast and stimulated by food.

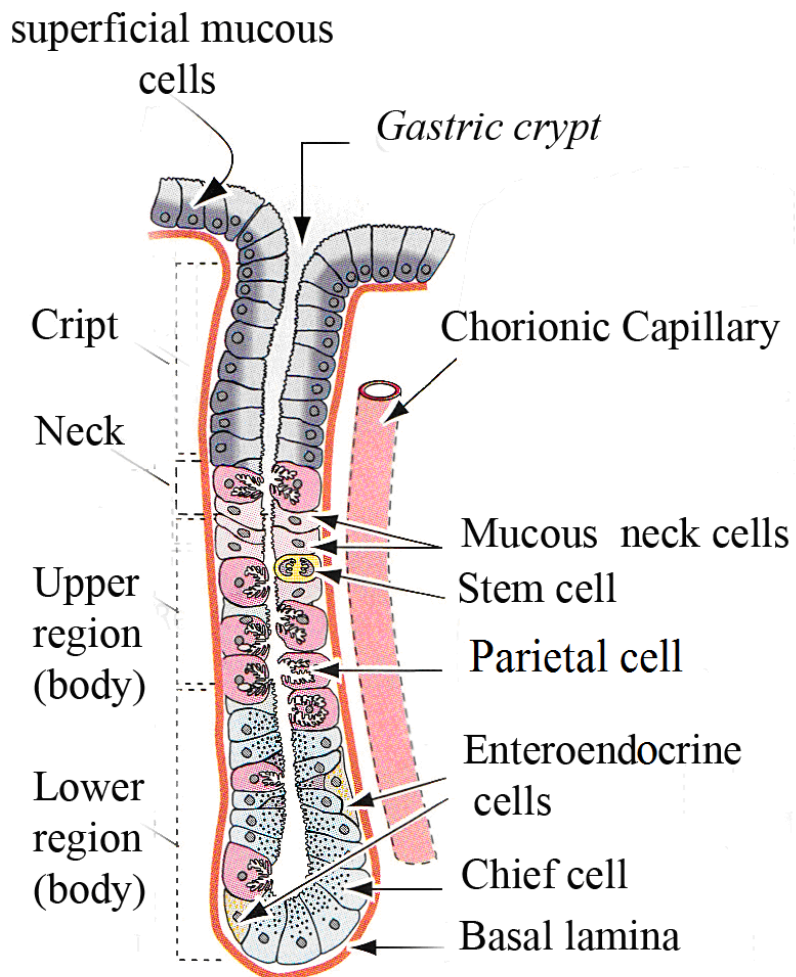


Figure 3. Structure of a gastric gland. Source: (Kierszenbaum, 2006).

I.4.4. Enteroendocrine cells

Enteroendocrine cells are dispersed throughout the digestive tract, but are difficult to detect by routine HE staining. Different types of enteroendocrine cells secrete various hormones, mostly corresponding to short polypeptides. In the fundus, enterochromaffin cells based on the basal lamina of the gastric glands secrete primarily serotonin (5-hydroxytryptamine). In the pylorus and the lower part of the body, other enteroendocrine G cells are arranged in contact with glandular lumen and produce gastrin. Gastrin stimulates acid secretion of the parietal cells, and has a trophic effect on the gastric mucosa.

I.4.5. Stem cells

Stem cells are the precursors of all epithelial cells of the gastric mucosa. They are small undifferentiated cells with an oval nucleus at the base and they show no cytoplasm specialization. However, they can differentiate into mucous, parietal, chief and endocrine cells. Normally present in very small numbers in humans, their number and activity increase when the gastric epithelium undergoes continual attacks and when there is chronic inflammation. An increase in the activity of stem cells allows rapid re-epithelialization of an ulcerated area. Such regeneration is the final stage of the healing of a gastric ulcer.

II. GASTRIC CARCINOMA

II.1 Epidemiology

Gastric cancer is one of the cancer types with the highest incidence and related mortality. Gastric cancer is the fourth most common cancer in the world preceded by lung, breast and colorectal cancer with a worldwide incidence of 989,000 new cases each year. Gastric cancer is the third leading cause of cancer death in the world, with 738,000 deaths recorded in 2008 (Jemal et al., 2011). There is a large geographic difference in the distribution of gastric cancer worldwide. The high gastric cancer

rates concern mainly East Asia (China, Japan, and South Korea), Eastern Europe, and South America (Figures 4 and 5). In general, the incidence rates are approximately twice as high in men than in women. For example, the rates are 49.6 vs. 22.5 in men and women, respectively, per 100,000 cases in China (Chinese Cancer Registry Annual Report, 2011), 84.8 vs 38.2 in Japan, and 80.8 vs. 39.8 in South Korea. In France, there are about 6,500 new cases of gastric cancer registered annually, while the total estimated number of deaths was 4420 in 2010 (INCa – 2011). Similar to the incidence, the mortality rates of gastric cancer patients vary depending on the regions of the world, and they are particularly high in developing countries (Jemal et al., 2011). The five-year survival rate for patients with gastric cancer is less than 25% in most countries (Forman and Burley, 2006). Mortality rates are noticeably high because most of the cases are diagnosed at late stages. In a study performed in the United States, more than 65% of patients with gastric cancer were diagnosed at the T3 or T4 stage, and amongst them approximately 85% had lymph node metastasis (Macdonald et al., 2001). However, much improvement has been made in Japan with more than 60% of gastric cancer patients now surviving more than five years (Nashimoto et al., 2013). This is considered to be the result of the implementation of X-ray based screening programs for gastric cancer over a long time which allows to detect early gastric cancer (Hisamichi and Sugawara, 1984; Hamashima et al., 2008).

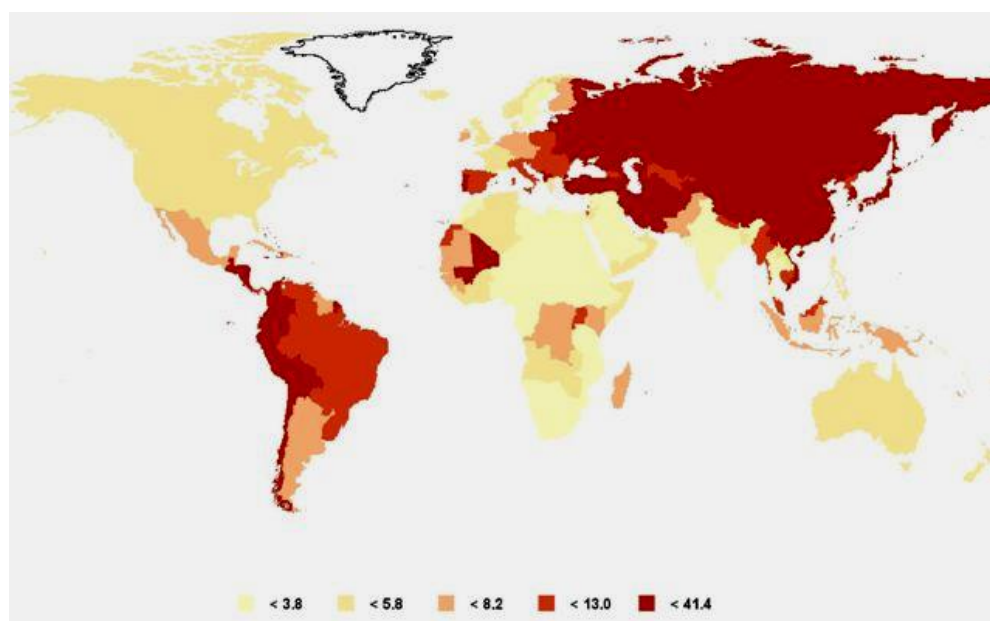


Figure 4. Age-standardized gastric cancer incidence rates. Source: (GLOBOCAN 2008).

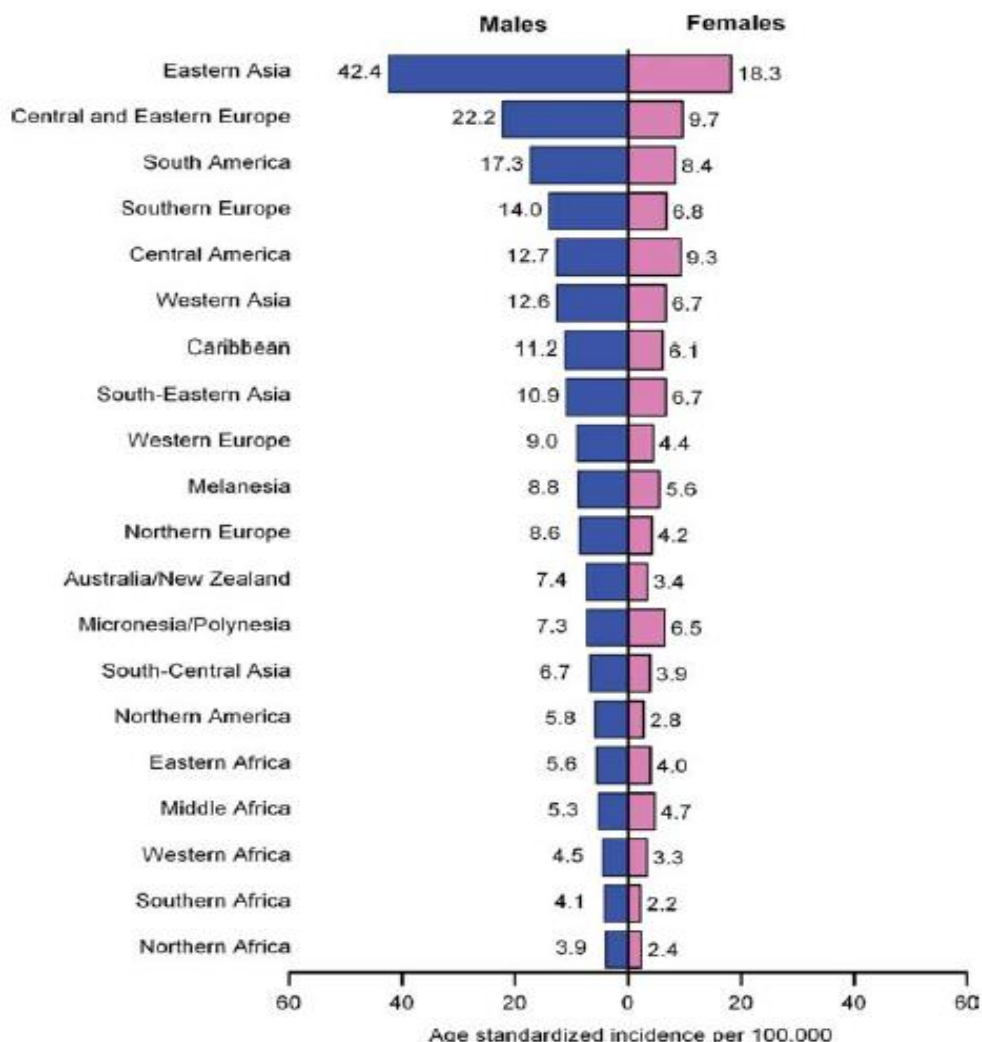


Figure 5. Age – standardized incidence rates for stomach cancer. Source: (Jemal et al., 2011).

II.2 Classification of gastric cancer

There are four main classification systems which have been used to categorize gastric cancers based on histological and anatomical features: the Japanese classification, the Bormann classification, the Lauren classification and the World Health Organization (WHO) classification.

II.2.1 Classification of gastric cancer

The Bormann classification, based on the gross features of gastric cancer, is the most widely used for classification of advanced gastric carcinoma (AGC). Bormann segregated AGCs into four types as follows: Type I (polypoid), type II (fungating), type III (ulcerative) and type IV (infiltrating/diffuse). While type II is frequently found in the lesser curvature of the antrum, type I and type III are usually located in the greater curvature of the corpus of the stomach. Bormann type IV is found in the greater curvature near the pylorus and the 5-year survival rate of patients carrying type IV tumors is lower than that of other types. Furthermore, this type has poor clinicopathological features (Ma et al., 2012).

II.2.2 The Japanese classification of gastric cancer

The gastric cancer classification system of the Japanese Gastric Cancer Association is now used worldwide. The 3rd English edition of this system divides gastric cancer into six different subtypes including type 0 (superficial), type I (mass), type II (ulcerative), type III (infiltrative ulcerative), type IV (diffuse infiltrative) and type V (unclassifiable). In addition, type 0 is subdivided further into different subtypes from type 0-I to type 0-III according to the Macroscopic Classification of Early Gastric Cancer of the Japanese Endoscopy Society Classification of 1962 (Japanese Gastric Cancer Association, 2011).

II.2.3 The WHO classification

The most recent WHO classification system divides gastric carcinoma into four principal histological patterns involving tubular, papillary, mucinous adenocarcinoma and Signet ring cell carcinoma. The tubular type of gastric adenocarcinoma is characterized as irregular-shaped and fused neoplastic glands with intraluminal mucus. It can form fungating or polypoid masses. Papillary adenocarcinoma is commonly connected with liver metastasis and lymph node invasion. Tubular and papillary subtypes are often found in early gastric cancer. Histologically, mucinous adenocarcinoma is characterized by extracellular mucin pools. Tumor cells can form

irregular cell clusters and glandular architecture. Signet ring cell carcinoma is defined as diffuse with signet ring cells that are predominantly at the superficial layer of the lamina propria of gastric tumors (Hu et al., 2012).

II.2.4 The Laurén classification

The Laurén classification system is most frequently used worldwide for gastric carcinoma. This classification was first described in 1960 at the University of Turku in Finland, based on an examination of 1,344 cases of gastric cancer (Laurén, 1965). The Laurén classification divides gastric adenocarcinoma into two main types. One, which presents a similar structure to colon cancer, is defined as the intestinal type. The other, specific to gastric cancer and more frequently found in younger people, is defined as the diffuse type (Figure 6).

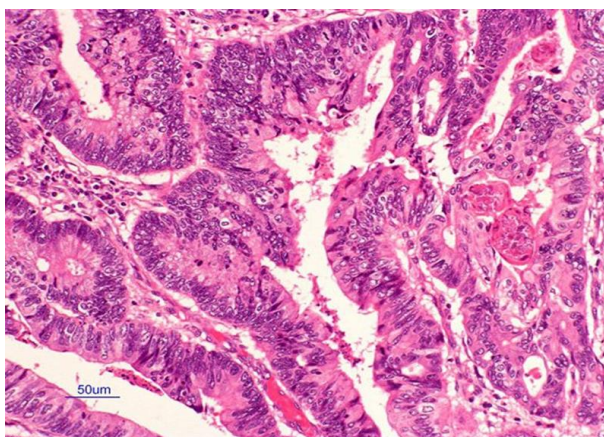
Intestinal type:

Intestinal type adenocarcinoma is more common than the diffuse type. The intestinal type is characterized by the presence of glandular structures with mitotically active columnar cells. These tumors frequently arise in the older population, and are found twice as much in males as in females (Henson et al., 2004). Intestinal type adenocarcinomas are usually located in the antrum of the stomach and tend to spread hematogeneously. The development of these tumors is hypothesized as a stepwise sequence, starting with *Helicobacter pylori* infection and gastritis, evolving towards atrophic gastritis, intestinal metaplasia, dysplasia, and finally cancer (Correa, 1992). However, this multistep process only corresponds to the intestinal type of gastric adenocarcinoma and not to the diffuse type. Beside *H. pylori* infection, other environmental factors such as a high-salt diet, smoking have been identified as risk factors for intestinal type gastric adenocarcinoma (Wang et al., 2009).

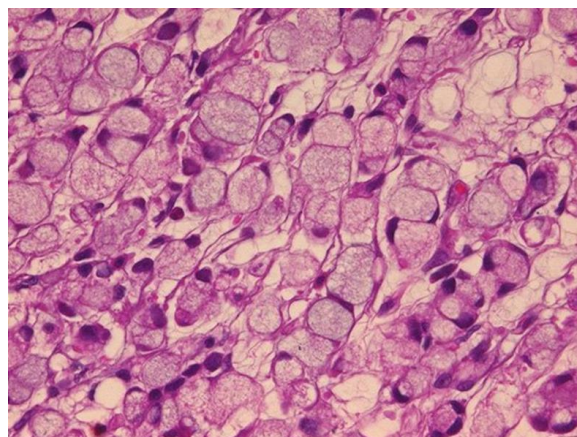
Diffuse type:

Diffuse type adenocarcinomas are characterized by small signet ring cells, which are uniform in shape and in nuclear size, and show inferior mitotic activity. Gastric tumors of this type are more commonly found in the gastric corpus and are recognized by the lack of gland formation and cellular adhesion. The diffuse type tends to occur more

frequently in the younger population, and there is no difference in distribution between men and women (Noda et al., 1980). The peripheral stem cells of the gastric gland neck zone are thought to be the origin of diffuse type adenocarcinoma. Genetic instabilities are closely related to the development of diffuse type gastric tumors. E-cadherin play an essential and fundamental role in cellular adhesion and also maintain the cellular architecture. Germline point mutations in the *cdh1* gene of E-cadherin tumor suppressor frequently occur in hereditary diffuse type gastric tumors (HDGC), accounting for approximately 30% (Pharoah et al., 2001). HDGCs are rarely related to autosomal dominant disorder, which accounts for less than 1% of all cases of gastric carcinoma (Piazuelo et al., 2010). Deletion mutations occur on exons 1, 2, 15 and 16 of the CDH1 gene, 4% of which are large deletions also identified for HDGCs (Oliveira et al., 2009). Currently the CDH1 gene is the only marker used to screen family members when one of them has confirmed diffuse gastric cancer, according to the recommendations of the International Gastric Cancer Consortium (Fitzgerald et al., 2010).



Intestinal type



Diffuse type

Figure 6. Two types of gastric adenocarcinoma. Source: Japanese Society of Pathology

II.3 Risk factors for development of gastric cancer

Different factors such as *H. pylori* infection, other factors from the environment, genetic factors such as the inflammatory response against this bacterial infection (El-Omar et al., 2000) have been proven as major risk factors for gastric cancer.

II.3.1 Environmental factors

Gastric cancer may arise from environmental factors such as smoking, alcohol consumption and salty foods. Among them the dietary factor seems to be the most important risk factor for gastric cancer. Many studies indicate that a diet high in vegetables and fruits protects against this cancer, while high consumption of foods rich in nitrates or nitrosamines play a role in the development of gastric cancer (Kim et al., 2002).

A number of cohort and case–control studies suggested that consumption of red and/or processed meat, and especially red meat, increased the risk of gastric cancer (Zhu et al., 2013). An increased intake of protein and sugar may increase the risk of gastric cancer. (Palli et al., 2001).

Vitamin C also decreases risk of gastric cancer as it inhibits the growth of *H. pylori* strains (Zhang et al., 1997). Furthermore, high intake of vitamin D, vitamin A and pro-vitamin A were also shown to reduce the risk of gastric cancer (Ren et al., 2012; Larsson et al., 2007).

Alcohol drinking and cigarette smoking have been identified as two independent factors which may raise the incidence of gastric cancer (Moy et al., 2010). However, the incidence rate is further increased when both cigarette smoking and heavy alcohol consumption are present (Sung et al., 2007). Moreover, individuals who carry the genotype CYP2E1 c1/c1 and smoke have high risk of gastric cancer.

II.3.2 Genetic factors

Most gastric cancer cases appear sporadically, while approximately 10% of the cases are diagnosed in individuals with an inherited familial component (Oliveira et al., 2006). Hereditary gastric cancer is often found in young people before the age of 50. Studies with Poisson regression analyses have confirmed that individuals with blood group A have a higher risk of gastric cancer than those with other blood groups, while a high risk of peptic ulcer was demonstrated among those with blood group O (Edgren et al., 2010; Yaghoobi et al., 2004).

Germline mutations in the gene encoding the cell adhesion protein E-cadherin are the most important genetic aberrations found in hereditary gastric adenocarcinomas (Carneiro et al., 2008; Oliveira et al., 2006; Everett and Axon, 1998). Genetic alterations in E-cadherin can cause the loss of cell–cell adhesion and an increase in invasiveness (Oda et al., 1994). Recently, genetic polymorphism analysis of the CDH1 gene showed that the ATCTG haplotype was associated with an increased risk of gastric cancer, while the CTTTG haplotype showed a decreased risk in a Japanese gastric cancer population (Yamada et al., 2007). Other single mutations with the +54C allele (C/C or C/T) in this gene significantly increased the risk of gastric cancer adenocarcinoma compared to the +54T/T genotype (Zhang et al., 2008).

Germline mutations in the BRCA1 and BRCA2 genes, associated with a high risk of breast and ovarian cancers, were also confirmed in gastric stomach cancers and other cancers related to the pancreas, prostate, and colon (Friedenson, 2005; Breast Cancer Linkage Consortium, 1999).

Recently, the role of cytokine polymorphisms and the risk of gastric cancer has been a subject of interest. A number of studies have shown that interleukin-1 (IL-1) is pro-inflammatory and also an inhibitor of gastric acid secretion. A study showed a 2.6 fold increase in the risk of gastric cancer in individuals who carried the T/T genotype at this locus (El-Omar et al., 2000). Furthermore, a recent study showed an increased risk of distal gastric cancer related to the combination of the specific bacterial genotype and specific host cytokine polymorphism (Perez-Perez et al., 2005). A genetic polymorphism in the promoter of mannose–binding lectin-2 was also related to a 1.8 fold increased risk of gastric cancer (Baccarelli et al., 2006).

MicroRNAs (miRNAs) are known as small non-coding RNAs that function in transcriptional and post-transcriptional regulation of target genes. MiRNAs may act as tumor suppressors or oncogenes and miRNA sequence polymorphisms may be related to gastric carcinogenesis. In recent studies, other genetic polymorphisms on different miRNA genes have been reported to cause an increased risk of gastric cancer such as the Rs4919510 G allele, miR-196a-2 CC genotype (Peng et al., 2010) and rs895819 G and GG genotypes (Sun et al., 2010). In contrast, individuals carrying the Rs2910164 C allele have been shown to have a low risk of gastric cancer (Xu et al., 2011).

II.3.3 *Helicobacter pylori* and gastric cancer

H. pylori is a Gram-negative, spiral-shaped bacterium with oxidase, catalase and urease activities and polar flagella. It is the first formally recognized bacterial carcinogen. It is adapted to the life in the antrum but can be found in other parts of the stomach.

H. pylori infection affects approximately 50% of the world population and about 20-25% of the French adult population. Approximately 10-20% of the infected individuals develop gastroduodenal diseases such as peptic ulcer disease, gastric adenocarcinoma and mucosa associated lymphoid tissue (MALT) gastric lymphoma (Lacy and Rosemore, 2001) (Kusters et al., 2006) (figure 7)

Higher infection rates are found in developing countries with low socioeconomic levels and poor sanitary conditions, representing 80% compared to 10% in developed countries (Torres et al., 2000; Mégraud et al., 1989). The infection occurs mainly during early childhood, and the current impact of acquisition in adulthood is less 0.5% per year (Mégraud and Broutet, 2000).

H. pylori was the first bacterium to be identified as a type I carcinogen by the International Agency for Research in 1994. More aggressive virulence factors have been associated with the pathogenicity of *H. pylori* including CapA, the vacuolating cytotoxin A (VacA), the HtrA protease, lipopolysaccharide (LPS) and others. In fact, CagA is one of the most studied factors (Matysiak-Budnik and Mégraud, 2006; Backert and Clyne, 2011). A number of studies have demonstrated that infection with

CagA positive strains increases the risk of noncardia gastric cancer by 2.0-fold compared to CagA negative strains (Huang et al., 2003).

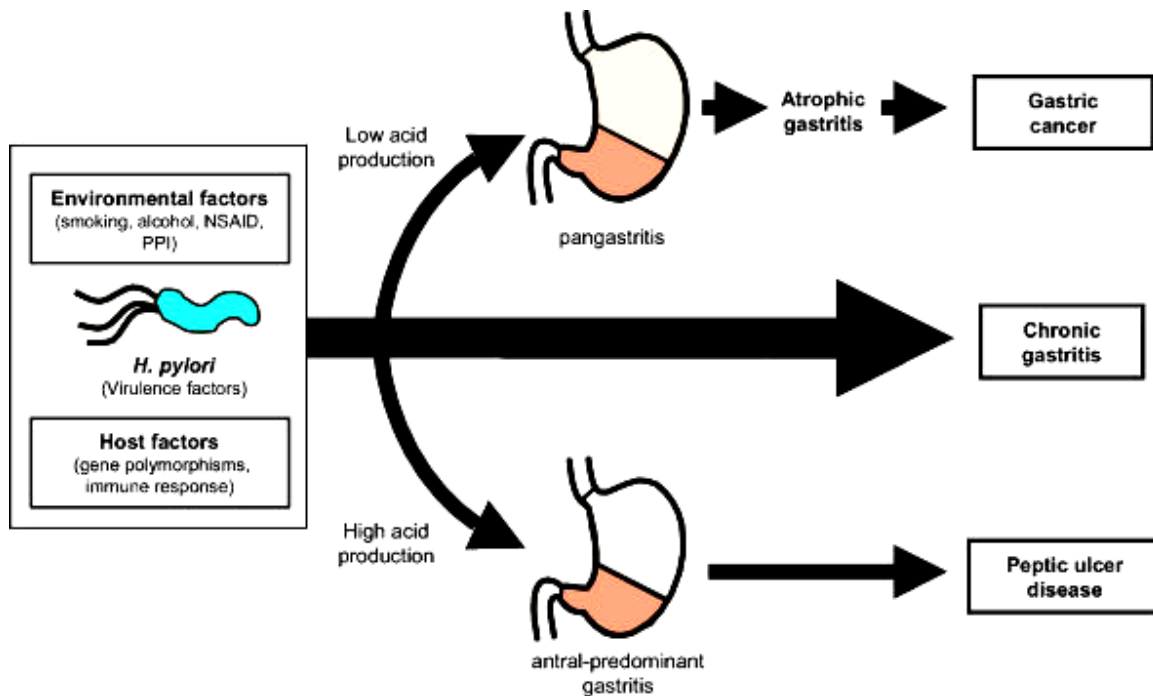


Figure 7. Factors contributing to gastric pathology and disease outcome in *H. pylori* infection. Source: Kusters et al., 2006

cag pathogenicity island:

The *cag* pathogenicity island (*cagPAI*) is a chromosome region of approximately 40 kb which has been studied the most. The *cagPAI* contains approximately 32 genes encoding a type IV secretion system (SST4) which are needed to inject the CagA protein into the epithelial gastric cells (Backert et al., 2000). The CagA protein is present in nearly 90% of the strains from East Asian countries such as Japan, Korea and China (Maeda et al., 1998), however, only 60% of *H. pylori* isolates in Western countries (North America, Africa & Europe) carry the *cagA* gene. This is agreement with epidemiological data showing that the incidence of gastric cancer is higher in East Asian countries than in Western countries. *cagA*-positive strains are strongly associated with inflammatory lesions of the gastric mucosa and they also increase the risk of gastric cancer compared to *cagA*-negative strains (Blaser et al., 1995; Occhialini et al., 2001).

The molecular mechanism for the pathogenic activity of CagA on gastric epithelial cells was also investigated (Figure 8). After *H. pylori* adheres to gastric epithelial cells, the CagA protein is injected into the cell via the Type IV secretion system which is encoded by the *cagPAI*. There, the protein is phosphorylated at a specific site in the C-terminal region of the protein on EPIYA motifs. The variation inside the EPIYA motifs results in more different subtypes: EPIYA-A, EPIYA-B, EPIYA-C, and EPIYA-D, based on the amino acid sequences flanking each of them (Hatakeyama, 2004). The phosphorylation of the CagA protein then stimulates the cell signaling via activation of the eukaryotic kinase, Src homology region 2-containing protein tyrosine phosphatase-2 (SHP-2), which plays an important role in mitosis, chromosome stability and cancer (Liu et al., 2012), as well as extracellular signal-regulated kinase.

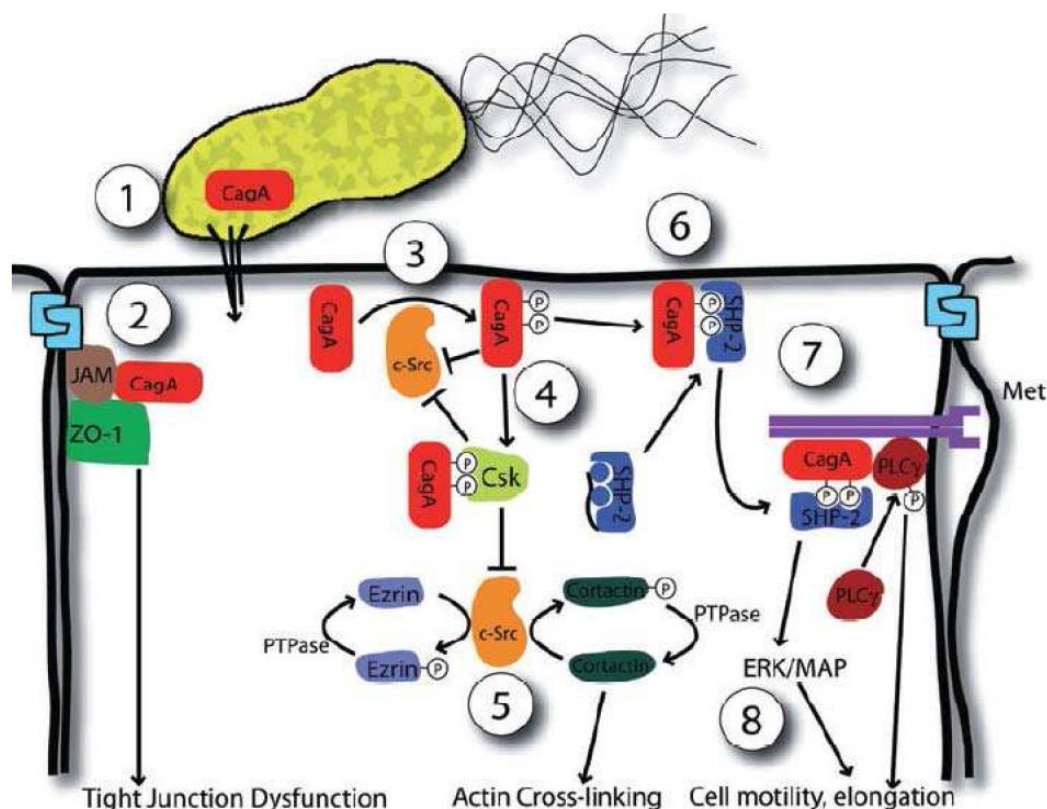


Figure 8. Cellular activities of CagA. A type 4 secretion system allows CagA delivery into host cells cytoplasm (1) where it associates with the proteins JAM and ZO-1. CagA can also be phosphorylated by c-Src kinase at EPIYA sites (3). CagA^{P-Tyr} inhibits c-Src directly and by activation of Csk (4). Inhibition of c-Src may contribute to cell morphology changes and motility (5). CagA^{P-Tyr} also activates SHP-2 (6), the c-Met receptor and with PLCγ (7). SHP-2 stimulates ERK kinase activity (8). All those activations are required for CagA-induced cell elongation and motility. Source: (Bourzac and Guillemin, 2005)

Vacuolating cytotoxin VacA:

VacA is also known to be a virulence factor associated with gastric carcinogenesis, in addition to CagA. The *vacA* gene is present in all *H. pylori* strains but only 50% of them express an active vacuolating cytotoxin (Cover, 1996). This difference is due to the presence of variable regions on the *vacA* gene (Atherton et al., 1995; Gangwer et al., 2010). Interestingly, in the East Asian countries, known for their high incidence of gastric cancer, most *H. pylori* strains are VacA/CagA positive (Yamaoka et al., 2008). Besides their diverse functions on epithelial cells and ability to induce apoptosis, more recent studies on VacA show that *vacA* activates the immunomodulatory system (Rieder et al., 2005) and inhibits the proliferation of CD4(+)T and B cells (Torres et al., 2007).

The *vacA* gene encodes a protein of 140 KDa that is secreted by the autotransporter or type-IV secretion mechanism (Fischer et al., 2001). VacA is comprised of two domains, p33 and p55, congregating into large “snowflake”-shaped oligomers (Chambers et al., 2013). Mutations in the *vacA* gene result in the inhibition of VacA-induced cell vacuolation via the formation of mixed oligomers (Vinion-Dubiel et al., 1999). The *vacA* alleles have a high level of genetic diversity, and sequence diversity in specific regions led to different types of VacA. Genetic diversity at the s-region (5' end) with s1a, s1b and s2 types and the m-region (middle region) with m1 and m2 types of *vacA* has been highlighted (Atherton et al., 1995). A number of studies demonstrated that individuals infected with *H. pylori* strains carrying s1 m1 *vacA* alleles have a higher risk of developing gastric cancer than those with strains carrying type s2 or m2 *vacA* alleles (Van Doorn et al., 1999; Atherton et al., 1997). A third region of *vacA* has been later identified, called i region, which is of particular importance in peptic ulcers (Basso et al., 2008).

II.4 Gastric carcinogenesis

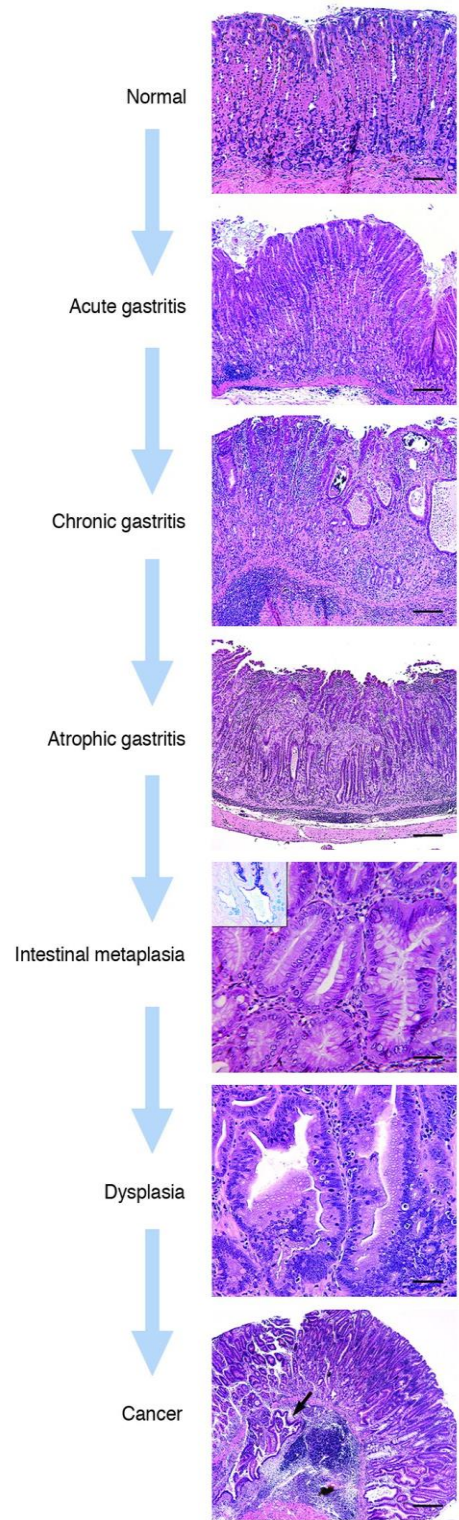
The pathogenesis of gastric cancer is a complex process, involving an interaction of multiple factors including genetic and environment factors. There are actually many differences to fully understand gastric carcinogenesis. Until recently, the hypothesis

firstly described by Correa in 1975 was largely accepted to explain the mechanism of gastric carcinogenesis. Correa proposed a multistep model of gastric carcinogenesis with the following sequence: chronic gastritis, atrophy, intestinal metaplasia, and dysplasia (Figure 9).

Chronic infection and inflammation are suggested as strongly associated factors in the evolutionary process of gastric cancer according to evidence from clinical and epidemiological studies (Matysiak-Budnik and Mégraud, 2006; Fox and Wang, 2007). Atrophic gastritis is defined as the focal loss of glands containing parietal and chief cells in the gastric corpus. The reduction of HCl secretion by the loss of parietal cells led to a more favorable environment for *H. pylori* and other microorganisms growth. *H. pylori* overgrowth and inflammation result in increasing genetic mutations in epithelial cells of the stomach. Gastric adenocarcinomas are frequently found in areas of chronic atrophic inflammation (Edgren et al., 2010). Gastric atrophy is the final stage of chronic gastritis, confirming its role as a precursor of gastric cancer in the Correa model. Epidemiological studies suggest that *H. pylori* infection is strongly associated with chronic atrophic gastritis (Weck et al., 2009). A higher risk of gastric cancer was more frequently observed in individuals with a high prevalence of atrophic gastritis than in individuals without atrophic gastritis (Whiting et al., 2002). Other cohort studies have shown atrophic gastritis as a crucial step in the evolution toward gastric cancer, they have also confirmed the model of gastric carcinogenesis with the following sequence: the gastritis-metaplasia-carcinoma (Ohata et al., 2004).

Figure 9. Histological progression of a *Helicobacter*-induced gastric cancer in a mouse model.

Normal: Histology of the body of the stomach. Acute gastritis: Infiltration of mucosal and submucosal lymphocytes with pockets of polymorphonuclear cells, accompanied by mild mucosal defects and edema. Chronic gastritis: Moderate to severe inflammation with marked epithelial defects including gland dilatation and mineralization. Atrophic gastritis: Chronic inflammation with focal fibrosis and complete loss of oxyntic parietal and chief cells. Intestinal metaplasia: Acquisition of an intestinal phenotype characterized by columnar elongation, mucous droplets occasionally forming goblet cells, and production of mixed acidic (blue, intestinal-type) and neutral (red, gastric-type) mucins as shown by pH 2.5 Alcian blue/PAS stain (inset). Dysplasia: High-grade, with irregular size and shape of glands, infolding, branching and cell piling, and marked cellular and nuclear atypia. Cancer: Gastric intraepithelial neoplasia, here with intramucosal invasion (arrow), develops in *H. pylori*-infected wild-type B6129 mice, as well as in certain genetically engineered models (124–126). Scale bars: 160 μm (first panel); 400 μm (second through fourth panels); 80 μm (fifth panel; inset, original magnification, $\times 400$); 40 μm (sixth panel); 800 μm (seventh panel).
Source: Fox and Wang, 2007



Intestinal metaplasia is a step in the multistep model. *H. pylori* infection with atrophic gastritis and intestinal metaplasia contributes to the pathology of gastric carcinoma (Sipponen and Kimura, 1994). In contrast to atrophic gastritis, intestinal metaplasia is characterized by the replacement of gastric epithelial cells by intestinal type cells. Recent studies on a C57BL/6 mouse model of gastric cancer suggest that bone marrow-derived cells participate in metaplasia and dysplasia in gastric cancer (Houghton et al., 2004; Varon et al., 2012).

Further lesions in this multistep model of gastric cancer lead to dysplasia, which is recognized by variations in size, form and orientation of epithelial cells. *H. pylori* infection, smoking, and low levels of dietary vitamin C are associated with an increased risk of dysplasia, known as the ultimate precancerous lesions in gastric carcinogenesis (You et al., 2000).

II.5 Signaling pathways in gastric cancer

II.5.1 Wnt/beta-catenin signaling pathway

The Wnt family is one of the most important protein families, which includes 19 secreted proteins that are key regulatory factors of cell proliferation, differentiation, migration and apoptosis. Aberrant activation of Wnt pathway is associated with many cancers, including gastric cancer. The Wnt pathway may be divided into two sub-pathways: canonical and non-canonical pathways. The canonical pathway is more common than the other and the β -catenin protein plays a role as a key signaling intermediate, hence it is also known as the Wnt/ β -catenin pathway. In contrast, in the non-canonical pathway, an intracellular calcium ion but not β -catenin, is the signaling intermediate; in vertebrate development, it is known to regulate stem cells and it has also been found in gastric carcinogenesis (Sugimura and Li, 2010) (Gencer et al., 2010) (Kurayoshi et al., 2006). Many studies have described the mechanism of the Wnt/ β -catenin pathway in detail, (Figure 10). Wnt signals are thought to stabilize β -catenin, thereby activating target genes through interaction with transcription factors in the cell nucleus (Polakis, 2000; Reya and Clevers, 2005). Mutations in the APC, β -

catenin or axin genes may lead to deregulation of this signaling pathway and an increase in malignant lesions.

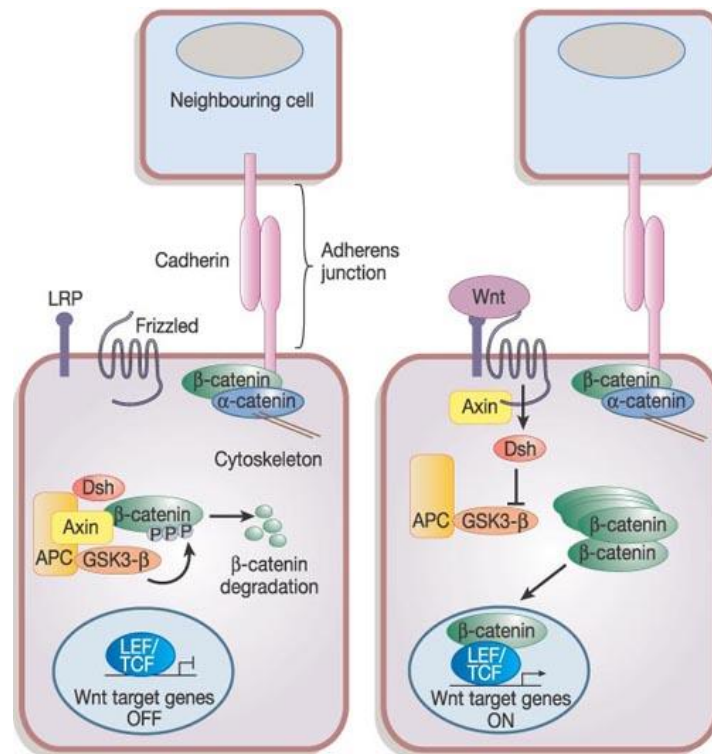


Figure 10. Wnt/beta-catenin pathway. Without Wnt signaling (left), β -catenin is retained by an Axin, APC and GSK3- β complex, where it gets phosphorylated and targeted for degradation. β -catenin may as well regulate intercellular adhesion by bounding cadherins. In the presence of Wnt signaling (right panel), β -catenin is not in the degradation complex and translocates to the nucleus, where it binds to Lef/Tcf transcription factors, thus activating target genes. Source: (Reya and Clevers, 2005).

Immunohistochemistry and molecular genetic analysis have provided strong evidence of the role of β -catenin in gastric carcinogenesis. β -catenin is expressed in most gastric cancers and β -catenin over-expression is frequently found in intestinal type gastric cancer compared to the diffuse type (Ebert et al., 2002). Evidence suggesting that *H. pylori* infection induces the transcription of β -catenin and its accumulation in the nucleus via LRP6 phosphorylation, a co-receptor of the Wnt/ β -catenin signaling pathway, has been widely accepted (Gnad et al., 2010; Franco et al., 2005). Furthermore, the latest studies have shown an important role of the Wnt/ β -catenin pathway in the regulation of gastric CSCs. Overexpression of the Wnt1 protein, was strongly associated with enhanced proliferation of gastric CSCs and tumorsphere

formation capacity, which expressed surface markers of CSCs such as CD44 and Oct4 (J Mao et al., 2014). In gastric tumors, the mutation rate of the APC gene accounts for 20%, and more frequently in the intestinal type than in the diffuse type (Fang et al., 2002). Together with APC, axin has a role as co-factor in promoting β -catenin degradation, and is suggested to be a tumor suppressor. Axin mutations may relate to the development of gastric cancers (Kim et al., 2009). Recent understanding of the Wnt/ β -catenin signaling pathway led to an effective application for the development of targeted therapies for gastric cancer (Luu et al., 2004; Mao et al., 2014).

II.5.2 Signaling pathway of growth factors

FGFR signaling:

Fibroblast growth factor (FGF) family proteins play pivotal roles during embryogenesis, and deregulation of FGF/FGFR signaling is associated with many developmental disorders including carcinogenesis (Kunath et al., 2007; Turner and Grose, 2010). To date, 22 human FGF proteins have been identified and characterized, they are proteins comprised of a conserved core of 140 amino acids, and they express their biological activity by binding to FGF receptors (FGFRs) on the cell surface. FGF proteins are also thought to have high affinity with heparin or heparin sulphate glycosaminoglycans (HSGAGs) within the extracellular matrix. This complex plays an important role in protecting the FGFs from extracellular protease and increases the binding capacity with FGFRs (Knights and Cook, 2010).

The FGFR family has four members, namely FGFR1, FGFR2, FGFR3, and FGFR4. Receptor activation is promoted by a FGFR transphosphorylation based on the formation of HSGAG/FGF/FGFR. Activated FGFRs lead to the activation of a series of intracellular signals, including phosphoinositide-3 (PI(3)K), extracellular signal-regulated kinase (ERK), and finally Akt. Akt then promote the transcription of target genes and modulates processes of cell proliferation, adhesion and differentiation (Dudley and Tabin, 2003) (Figure 11). The FGF signaling pathway can increase mitogenic activity and anti-apoptosis in cells, each of which has been shown to be a critical feature of cancer cells when there is deregulation. FGFs and FGFRs can act

as oncogenes, and their overexpression are found in a variety of cancers such as prostate cancer, thyroid cancer, head cancer, colonic cancer, cervical cancer, T cell lymphoma and gastric cancer (reviewed in Knights and Cook, 2010). FGFR2 amplification was first identified in gastric cancer (Hattori et al., 1990).

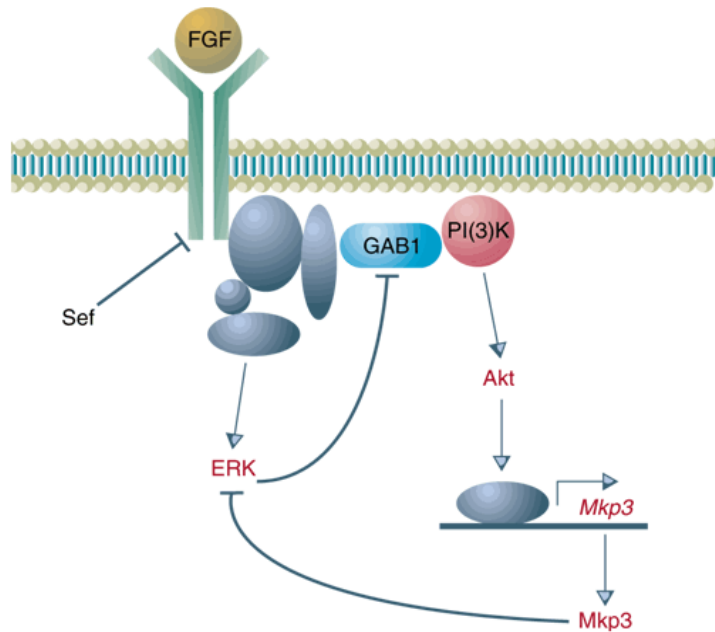


Figure 11. FGF signaling pathway.

Recognition of FGF by its receptor leads to recruitment and activation of PI(3)K- and ERK-activating proteins. PI(3)K phosphorylates Akt, and its target genes like the Mkp3 phosphatase. This phosphatase Mkp3 dephosphorylates ERK, inhibiting the ERK-mediated signaling pathway. Active ERK inhibits PI(3)K-mediated activation of Akt by decreasing association of PI(3)K and adaptor proteins.. Source: (Dudley and Tabin, 2003)

H. pylori, a key risk factor for chronic atrophic gastritis and gastric cancer, is thought to induce FGF signaling activation via FGF2 upregulation and SHP2 activation (Katoh and Katoh, 2006). Recently, it has become apparent that FGFR2 plays an important role in gastric carcinogenesis and amplification of this receptor has been found in both gastric cancer cell lines and primary gastric tumors. Mutations on FGFR2 and FGFR3 genes which may result in deregulation of FGF signaling in gastric carcinoma have been reported (Jang et al., 2001). Interestingly, cases of gastric cancer showing an overexpression of the FGFR2 gene were extremely sensitive to FGFR2 inhibitors such as AZD2171 (Takeda et al., 2007), AZD4547 (Xie et al., 2013) and PD173074 (Matsumoto et al., 2012).

EGFR signaling:

The epidermal growth factor receptor (EGFR), known to be a tyrosine kinase receptor and a member of the ERbB family, regulates proliferation, differentiation and apoptosis in various tumors including gastric cancer. EGFR is a cell-surface receptor and is activated by interaction of the EGFR extracellular domain with its ligands, such as epidermal growth factor (EGF) and transforming growth factor α (TGF α). The ligand binding of EGFR results in the initiation of a series of intracellular signals, including PI3-K/Akt/mTOR and the Ras/Raf/MAPK pathway, and finally, initiation of transcription and cell cycle activation in the cell nucleus (Figure 12).

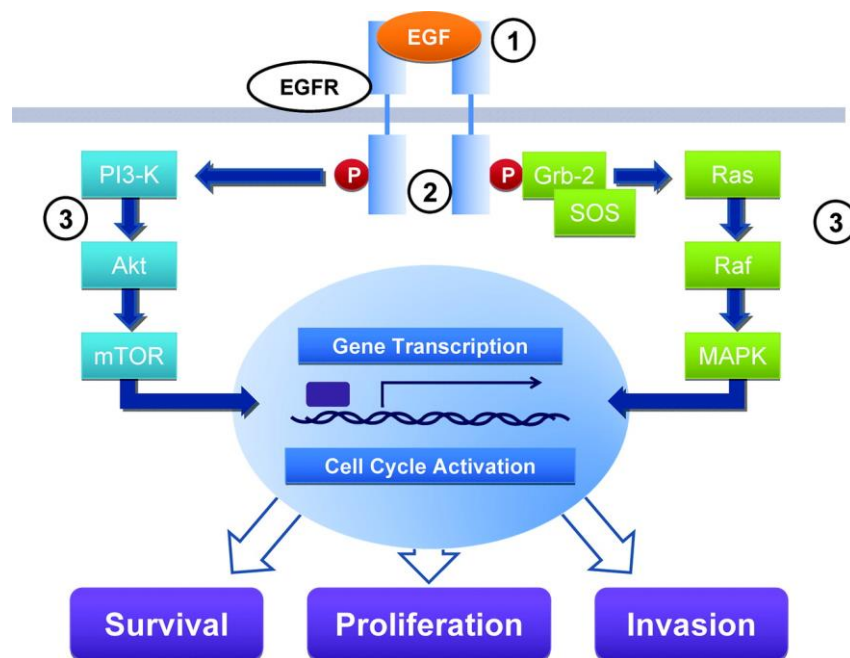


Figure 12. The EGFR signaling pathway. Scheme showing potential inhibition levels for EGFR-signaling pathway and examples of inhibitor are numbered: (1) EGFR interaction with ligand (cetuximab); (2) RTK activity (erlotinib); (3) downstream signaling inhibitors (ISIS 2503 [Ras] or LY294002 [PI3-K]). PI3-K = phosphatidyl inositol-3 kinase; Grb-2 = growth factor receptor-bound protein-2; SOS = son of sevenless; MAPK = mitogen-activated protein kinase; mTOR = mammalian target of rapamycin. Source: (Hodkinson et al., 2008)

EGFR and other members of the ErbB family including c-erbB-2 and c-erbB-3 are highly expressed in specimens from primary gastric cancer patients, accounting for 50% to 80% of all cases (Slesak et al., 1998; Galizia et al., 2007; Takehana et al., 2003). EGFR is expressed at a higher level in gastric cancer patients in advanced stages (III/IV) than those in the early stages (I/II). Furthermore, one or more members of the ErbB family could be expressed at an early stage of gastric cancer (Galizia et

al., 2007). Fluorescence in situ hybridization (FISH) analysis also showed that a number of copies of the EGFR gene could be amplified up to more than 10 fold in gastric cancer cases compared to non-cancerous cases (Takehana et al., 2003).

Structure alterations of EGFR and other members in its signaling pathway are rare but they could lead to gastric carcinogenesis (Mammano et al., 2006; Moutinho et al., 2008). Mutations have been found in EGFR, MLK3, PIK3CA, and KRAS genes, among them, deletions of the A13 repeats of EGFR are known to be common, and are an important biomarker for treatment of gastric cancer patients with EGFR inhibitors (Corso et al., 2011).

Many studies have shown that *H. pylori* induced EGFR and EGF gene transcription leading to activation of EGFR signaling, followed by neoplastic transformation of gastric epithelial cells in gastric cancer (Wallasch et al., 2002; Kim et al., 2013). Interestingly, EGFR activation by *H. pylori* was able to protect gastric epithelial cells from *H. pylori* induced-apoptosis. This is important to more thoroughly understand the mechanism of progression of *H. pylori*-associated gastric cancer (Yan et al., 2009).

II.5.3 Notch signaling pathway

Notch signaling is known to be a highly conserved pathway which plays a crucial role in the regulation of many cellular processes including proliferation, differentiation, apoptosis, and stem cell self-renewal during development (Borggreffe and Oswald, 2009). The Notch gene was first described by Morgan *et al.* in a *Drosophila melanogaster* model in the 1990s. Notch genes encode four transmembrane receptors, namely Notch1, 2, 3 and 4. The precursor form of the Notch protein is composed of three domains: extracellular, transmembrane and intracellular. Notch precursors are then cleaved by a particular enzyme in the Golgi apparatus to generate the complete form including two subunits that can interact with the Notch ligand. Five members of the Notch ligand family have been identified including Jagged1, Jagged2 and Delta (Dll1, Dll3 and Dll4) (Bray, 2006). Ligand binding to the Notch extracellular domain which has been shown to contain 36 EGF-like repeats essential for ligand binding permit a cleavage by metalloproteases, releasing the

Notch intracellular domain (NICD) which then translocates to the cell nucleus and plays a role as a transcriptional coactivator (Fiúza and Arias, 2007). In the cell nucleus, NICD binds to the DNA binding protein RBP-J and other coactivators before activating the transcription of target genes containing RBP-J binding sites (Figure 13). Several genes which are regulated by the Notch signaling pathway have been identified in both normal cells and cancer cells, in particular, Hes and Hey genes, which encode for helix-loop-helix transcription factors and the CD25 gene of T cells (Borggreffe and Oswald, 2009). Many important Notch target genes which control the cell cycle are deregulated in different cancers, such as c-myc in T-cell acute lymphoblastic leukemia (Weng et al., 2006) and breast cancer (Efstratiadis et al., 2007), cyclinD1 in breast cancer (Cohen et al., 2010), and p21(waf1/cip1) and p27kip1p21 in small cell lung cancer (Sriuranpong et al., 2001).

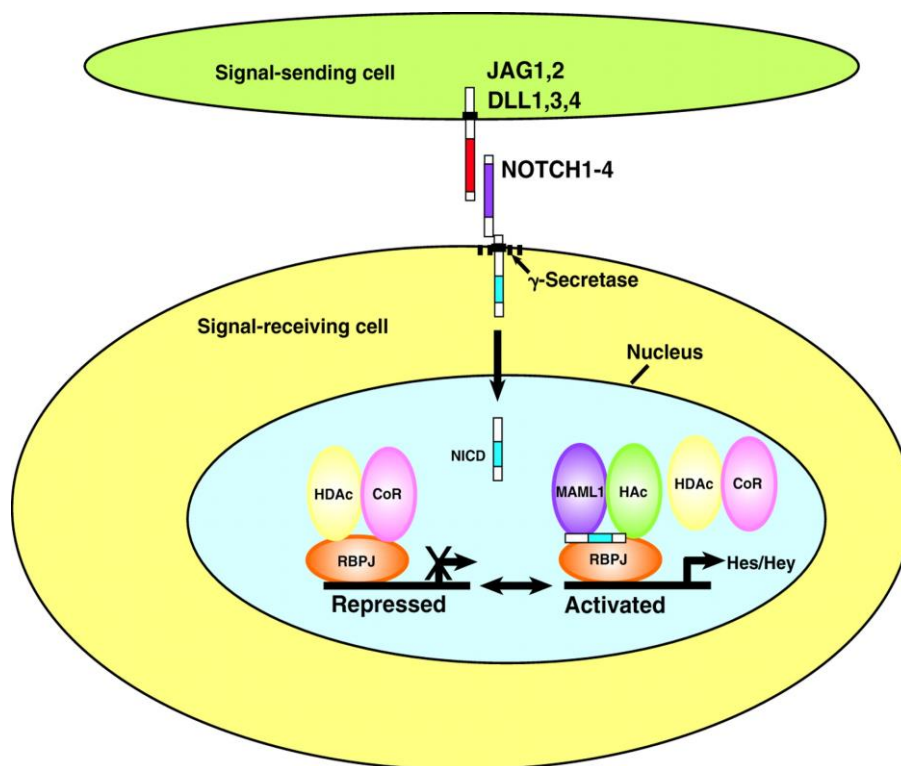


Figure 13. Notch signaling pathway. The Jagged (JAG1 and JAG2) and Delta-like (DLL1, DLL3, DLL4) families proteins are ligands of Notch family receptors (NOTCH1-4). These are heterodimeric cell surface receptors with a large ectodomain and a membrane-tethered intracellular domain. The receptor-ligand interaction induces the proteolytic cleavage and liberation of the Notch intracellular domain (NICD), that then translocates to the nucleus and forms a complex with the RBPJ protein and displacing a histone deacetylase (HDAC)–co-repressor (CoR) complex. Other components like MAML1 and histone acetyltransferases

(HAc) are recruited and are lead to the transcriptional activation of Notch target genes. Source: (Gridley, 2007).

Many recent studies have confirmed the role of the Notch signaling pathway in gastric carcinogenesis. Expression of all four Notch receptors (Notch1-4) (Sun et al., 2011; Hashimoto et al., 2010) and their ligands including jagged1 and Jagged2 (Kang et al., 2012) were found in human gastric cancer. Interestingly, Notch1 was undetected in non-cancerous gastric mucosa and it was found more often in intestinal gastric cancer (more 50%) than in diffuse gastric cancer (23%) (Sun et al., 2011). Other Notch ligands including DLL1 and DLL4 were also upregulated and strongly associated with an increase in the Notch1 intracellular domain and hes1 in gastric cancer cells (Piazzini et al., 2011; Li et al., 2013).

STAT3 and Twist pathways are also recognized for the activation of gastric carcinogenesis. Interaction between Twist and STAT3 promoters were enhanced by an overexpression of Notch1 receptors in gastric cancer cells. Furthermore, Notch1 expression promote phosphorylation of STAT3, induce Twist promoter activity and enhance colony formation, migration and invasion of gastric cancer cells (Hsu et al., 2012).

Notch1 and Notch2 signaling is able to promote gastric cancer progression via the induction of COX-2 expression. Yel *et al.* demonstrated that the activated form of the Notch1 receptor encouraged colony formation in *vitro*, xenografted tumor growth, migration and invasion abilities via COX-2 in gastric cancer cells (Yeh et al., 2009). In another study, Notch2 expression enhanced colony formation, migration, invasion and epithelial-mesenchymal transition (EMT) of gastric cancer cells. Moreover, the interaction between the Notch2 intracellular domain and a COX-2 promoter, leading to stimulation of COX-2 expression in a CBF1-dependent manner in gastric cancer cells, was suggested (Tseng et al., 2012). The inhibition of COX-2 expression with NS-398, known as a COX-2 inhibitor, downregulates the effect of the Notch2 intracellular domain in gastric cancer progression (Tseng et al., 2012). More interestingly, the differentiation of gastric epithelial stem and/or progenitors could be inhibited by activation of the Notch signaling pathway. The Notch activated enhancement within parietal cells confers stem cell properties which finally induces the formation of adenomas (Kim and Shivdasani, 2011).

II.5.4 Epithelial-mesenchymal transition

Epithelial and mesenchymal cells are two of the main cell types in humans. EMT is known as a biological process by which epithelial cells change to a mesenchymal phenotype which confers migratory ability, invasiveness and enhanced resistance to apoptosis (Kalluri and Weinberg, 2009). EMT plays an important role during development as well as cancer progression (Figure 14). EMT was initiated by the activation of transcription factors such as Snail, zinc-finger E-box-binding (ZEB1/ZEB2), Slug, FOXC2, expression of specific cell-surface proteins, growth factors, wnt/ β -catenin and Notch signaling, and expression of specific microRNAs, such as miR-200 (Kalluri and Weinberg, 2009, Yeh et al., 2009 ; Hay, 1995). The downregulation of E-cadherin levels, a cell adhesion molecule which is commonly expressed in epithelial cells was demonstrated as a critical feature of EMT (Larue and Bellacosa, 2005). E-cadherin can be repressed directly or indirectly by many different transcription factors. Slug, ZEB1/2, E47 and KLF8 can directly repress transcription of E-cadherin by binding to its promoter, while E-cadherin is indirectly inhibited by SIX1 and FOXC2 proteins (Peinado et al., 2007). Recent studies show that EMT can be induced by a single or a combination of signaling pathway multiplexes such as TGF- β , Wnt/ β -catenin, Notch, EGF, FGF and hypoxia via downregulation of the expression of the cell adhesion molecule E-cadherin (Lamouille et al., 2014). The phosphatidylinositol 3' -kinase (PI3K)-Akt signaling pathway (PI3K/Akt) was described as an oncogene and activation of this signaling was shown in many human carcinomas. Recently, this activation was demonstrated as a key feature of EMT, AKT induced EMT which downregulates cell-cell adhesion, changes the cell phenotype, decreases cell-matrix adhesion and induces cell mobility (Larue and Bellacosa, 2005). EMT is divided into three different subtypes based on biological function: type 1 which occurs during implantation, embryogenesis, and organ development; type 2 associated with tissue regeneration and organ fibrosis; and type 3 associated with tumorigenesis and metastasis (Kalluri and Weinberg, 2009).

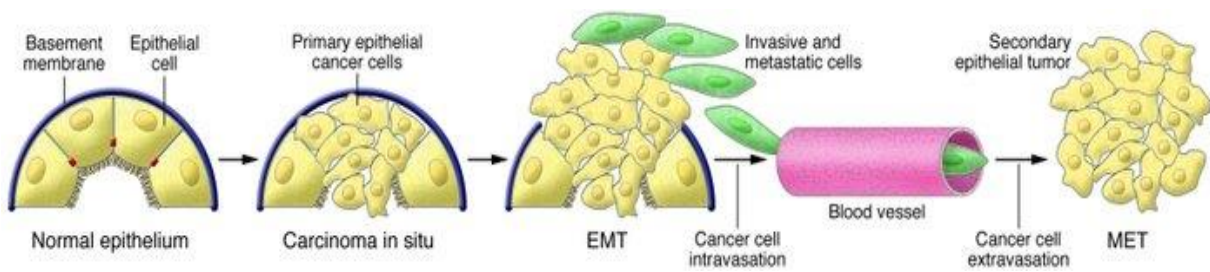


Figure 14. Contribution of EMT to cancer progression. Several stages are needed for the progression of normal epithelium to invasive carcinoma. The later involves the loss of cell polarity and detachment from the basal membrane. There is also a change in the basal membrane composition and an angiogenic switch that facilitates tumor growth. Progression to metastatic cancer also involves EMTs, letting cancer cells access the circulation and exit at a remote site, to form micro- and macro-metastases. Source: (Kalluri and Weinberg, 2009).

In many studies, EMT has provided key understanding of the critical mechanism of cancer progression and more malignant states (Thiery, 2002). The acquisition of morphology of mesenchymal cells with the enhanced expression of its specific markers such as vimentin, FSP1, and desmin showed in studies in mice as well as *in vitro* culture is emerging evidence of the important role of EMT during cancer initiation (Yang and Weinberg, 2008). Recent findings demonstrate that EMT features acquired at an early stage of cancer are closely associated with both invasion and metastasis of cancer cells at a distant site (Thiery, 2002; Kang and Massagué, 2004). A recent report confirms that Twist, an inducer of EMT, downregulates E-cadherin, upregulates vimentin and fibronectin, plays a critical role in circulation, and seed metastases of breast cancer cells (Yang et al., 2004; Yang et al., 2006). Furthermore, Twist is directly regulated by HIF-1 α to promote metastases in response to intratumoral hypoxia (Yang et al., 2008). Importantly, CSCs have been widely accepted as tumor initiating cells via their self-renewal and differentiation. A study on non-tumorigenic mammary cancer epithelial cells induced by expression of Twist or Snail transcription factors, which are two key factors of EMT, showed the generation of CD44⁺/CD24⁻ cell population with enhanced stemness as capacity of *in vitro* mammospheres and *in vivo* tumor formation. Moreover, these CSCs had a high expression of specific mesenchymal cell markers (Mani et al., 2008). Another study also indicated that induction of EMT via activation of the Ras-MAPK pathway was needed to generate breast cancer stem cells. Recently, the acquisition of CSCs and a mesenchymal phenotype induced by EMT via different signaling pathways such as the

PI3K/Akt/mTOR pathway in prostate cancer (Chang et al., 2013) or FOX2 expression in breast cancer (Hollier et al., 2013) was recognized.

EMT, as well as many other kinds of cancer progression, has been linked to gastric cancer. Indeed, downregulation of E-cadherin expression is an important element found in gastric tumor cells. The loss of E-cadherin function is associated with the mutation, deletion or methylation on the CDH1 gene which codes the E-cadherin protein (Guilford et al., 1998, Brooks-Wilson et al., 2004). Furthermore, numerous copy amplifications of genes involved in the EGF, FGF or Akt pathways or upregulation of the WNT signaling pathway also lead to EMT in gastric cancer (Kato, 2005). More recently, TNF- α , a carcinogenic factor in the gastric epithelium produced by *H. pylori*, was recognized as an inducer of EMT in human gastric cancer cell lines (Watanabe et al., 2014). Studies on *H. pylori* infection in gastric cancer have also demonstrated that EMT is promoted via TGF β signaling under hypoxic conditions of gastric cancer cells (Matsuoka et al., 2013) or downregulation of programmed cell death protein (Yu et al., 2014). Moreover, an immunohistochemistry study on human gastric primary tumors indicated the expression of five EMT-related proteins (Snail-1, ZEB-1, E-cadherin, vimentin, and β -catenin) as well as a significant association between expression of CD44, a gastric cancer stem cell marker, and Snail-1, ZEB-1, and E-cadherin expression (Ryu et al., 2012). In a recent study we demonstrated that *H. pylori* infection induced EMT with an upregulation of mesenchymal cell markers including Snail-1, ZEB-1 and vimentin as well as CD44 expression (Bessède et al., 2014), and downregulation of epithelial cell markers such as CK7 and SSP1. Furthermore, our group showed CD44^{high} cells induced by CagA. *H. pylori* infection displayed CSC properties as tumorsphere formation and high tumorigenesis than CD44^{low} in deficient mice (Bessède et al., 2014).

III. STEM CELLS AND CANCER

STEM CELLS

III.1 Normal stem cells

III.1.1 General Introduction

All cells of specific tissues in the body are generated from specific stem cells which are characterized by their capacity to undergo self-renewal and differentiation processes to generate specific cells comprising each organ. Stem cells are known as cells that have the ability to divide asymmetrically to produce two daughter cells, one with a self-renewal capacity, the so-called new stem cell, and the second a progenitor cell which is able to proliferate and differentiate into mature cells but without self-renewal. Self-renewal is the ability of stem cells to generate new stem cells with identical characteristics for proliferation and differentiation and by which the stem cell pool can be maintained. While differentiation is the ability of stem cells to form a heterogeneous offspring of cells, which become more specialized cell types to form specific tissues and organs in the body.

During mammalian development, the zygote and early embryonic cells (2 to 8 cell stage of the morula) have a capacity to proliferate and differentiate into all cell types in the body including the germ line. These cells were defined as “totipotent” as they can generate an entire organism independently (Figure 15). After that, blastocysts are formed via primary cell differentiation processes composed of outer cell layers called the trophoblast, while the “inner cell mass” remains undifferentiated. The cells of the “inner cell mass” within a blastocyst originate from embryonic stem cells (ESCs) which were defined as “pluripotent” based on their ability to generate all cell types of the embryo proper (He et al., 2009). Lastly, “multipotent” adult stem cells are found in multi-cellular organs and can differentiate into tissue-specific cells (Wagers and Weissman, 2004). Many different tissue-specific adult stem cells have been

described, however, the lack of exclusive markers until now has made it difficult to isolate and study characteristics of adult stem cells. The hematopoietic stem cell (HSC) is a typical example of a multipotent adult stem cell with proliferation and differentiation properties to generate differentiated cells into the myeloid and lymphoid lineages in mouse (Spangrude et al., 1988) and human (Baum et al., 1992).

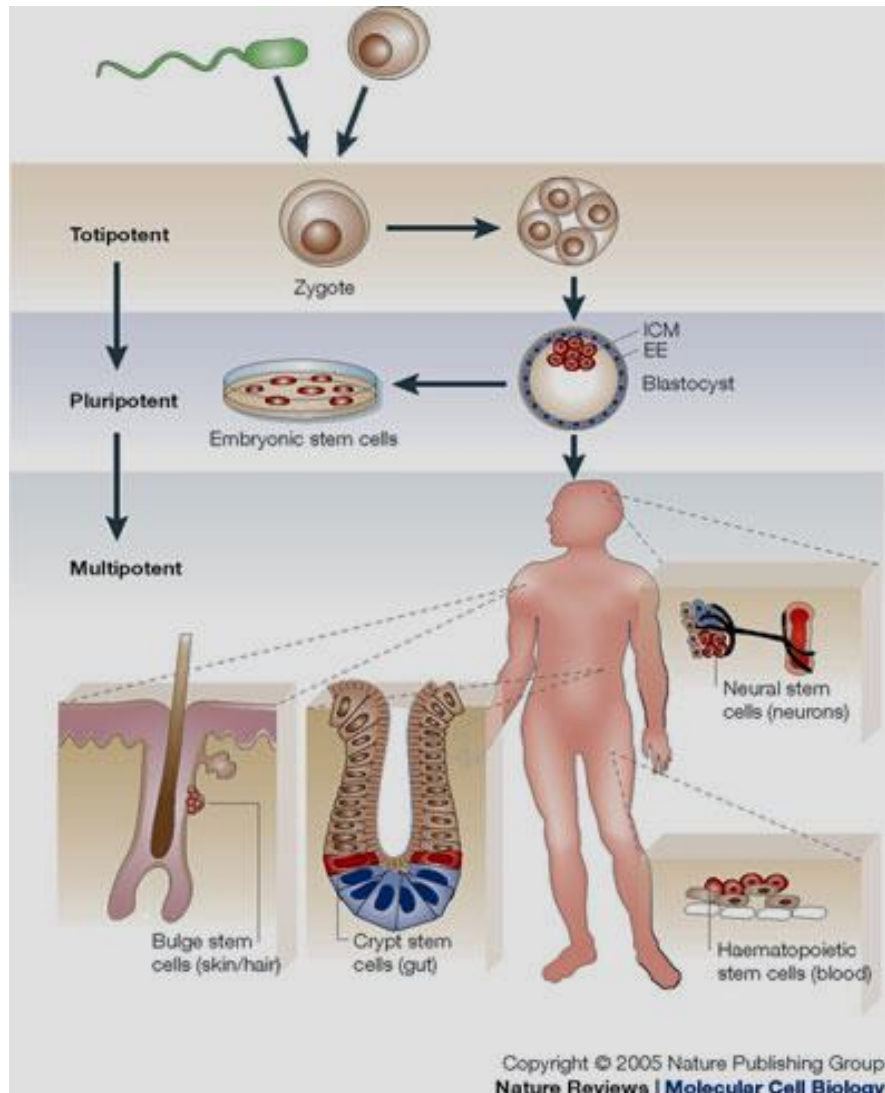


Figure 15. The stem-cell hierarchy

The totipotent zygote divides to form the inner cell mass and the extra-embryonic tissue of the blastocyst. After isolation from the blastocyst *in vitro*, the cells of the ICM can be maintained in culture as pluripotent embryonic stem cell lines. As the embryo develops, the pluripotent stem cells in the ICM suffer a decrease in their lineage potential and generate multipotent stem cells that are tissue-specific and include epidermal, haematopoietic, neural, gastrointestinal, oval and mesenchymal stem cells. Source: (Eckfeldt et al., 2005)

III.1.2 Mechanism of self-renewal of stem cells

Self-renewal is one of most important properties of stem cells, because it is required by many types of stem cells and it is the mechanism by which stem cells generate and perpetuate themselves throughout life (Reya et al., 2001). Self-renewal maintains the undifferentiated state with their multipotency or pluripotency depending on the stem cell types (He et al., 2009). Stem cells are found in different organs, where their self-renewal occurs to maintain a balance with cell differentiation (Reya et al., 2001). However, self-renewal is not only found in stem cells but also in some types of restricted progenitors, even differentiated blood cells such as lymphocytes (He et al., 2009). Cell division is a crucial step in the self-renewal process. However, self-renewal is different from cell division where at least one of the two daughter cells requires properties similar to the mother cell for the subsequent divisions. ESCs are pluripotent stem cells unlimited in their self-renewal and they can differentiate into all cell types in the body. Recent studies have shown that the pluripotency and self-renewal ability of ESCs are regulated by a special transcription mechanism of the oct4, sox2, Nanog genes. These genes co-occupy many target genes which frequently encode transcription factors, some of which play a crucial role in development. Almost all of the promoter regions (more than 90%) bound by two genes, sox2 and oct4, also interact with Nanog to regulate the transcription together (Boyer et al., 2005). A previous study indicated that the activation of TGF β and the Wnt signaling pathway, via the signal transducer SMAD2/3, is necessary to maintain the undifferentiated state or pluripotency in human ESCs (James et al., 2005). Furthermore, key factors of TGF β signaling involved to pluripotency and self-renewal of ESCs were regulated by their own nanog, Oct4 and sox2 genes (Boyer et al., 2005).

In HSCs, some signaling pathways including Wnt, Bmi-1, Notch and Shh that regulate stem cell self-renewal have been studied. Wnt proteins are intercellular signaling molecules which play an important role in the regulation of development in several organisms. The overexpression of β -catenin, a key protein of the Wnt signaling pathway, in long-term culture of HSCs results in an expansion in the pool of transplantable HSCs *in vivo*. Inhibition of Wnt signaling by Axin decreases

proliferation and increases apoptosis of HSCs *in vitro* (Reya et al., 2001). Furthermore, the Bmi-1 oncogene, a member of the Polycomb group ring finger gene family, is shown to be high expressed in HSCs and significantly downregulated during hematopoietic differentiation. The number of HSCs is reduced in Bmi-1 knockout mice, and there is no detectable self-renewal of adult HSCs, indicating a cell autonomous defect in Bmi-1^{-/-} mice. Inactivation of the Bmi-1 gene also increased cell gene expression involving in survival, proliferation such as p16Ink4a and p19Arf, resulted in proliferative inhibition and induction of p53-dependent cell death in Bmi-1^{-/-} mice (Park et al., 2003).

III.1.3 Gastric stem cells

Gastric stem cells have yet to be isolated, but historical studies have established long ago the morphologic characteristics of these cells. Using electron microscopy and ³H-thymidine radio-autography to analyze the renewal of gland cells of the pyloric antrum in mice, Lee and Leblond showed that the gland neck cells located close to the isthmus have characteristics of differentiating cells, whereas the mid-gland cells appears to complete the differentiation. The cells within the gland basis are fully mature. Notably, the highest rate of proliferation is shown in cells located in the gland neck, with lower rates in the mid-gland and gland base. It was thus suggested that the mucous isthmus cells contributed to gland-cell renewal (Lee and Leblond, 1985).

The first evidence of the existence of gastric stem cells was provided by Bjerknes and Cheng. In this study, chemical mutagenesis was used to label random epithelial cells by loss of transgene function in Rosa26-lacZ transgenic mice that express β -galactosidase. Their work described many clones derived from such cells which contained all of the major epithelial cell types, thereby indicating the existence of gastric stem cells in mouse gastric epithelium (Bjerknes and Cheng, 2002).

Gastric progenitor cells were recently reported as rare epithelial cells which are normally quiescent but multiply in response to interferon gamma. *In vivo* lineage tracing experiments showed that villin-1 expressing cells can generate all lineages of the gastric glands. Indeed, these cells are located basally in the stomach epithelium of mouse embryos (Qiao et al., 2007).

Using *in vivo* lineage tracing experiments, Barker *et al.* showed that Lgr5⁺ cells were located at the base of prospective corpus and pyloric glands in the neonatal stomach, whereas these cells were predominantly restricted to the base of mature pyloric glands in the adult stomach. It should be noted that these Lgr5⁺ cells showed the ability of self-renewal, and that they were also responsible for the long-term renewal of the gastric epithelium. Using an *in vitro* culture system, they also showed that single Lgr5⁺ cells efficiently gave rise to long-lived organoids which resemble mature pyloric epithelium (Figure 16). In addition, Lgr5 expression was established as a unique marker of adult stem cells in the distal stomach (Barker *et al.*, 2010).

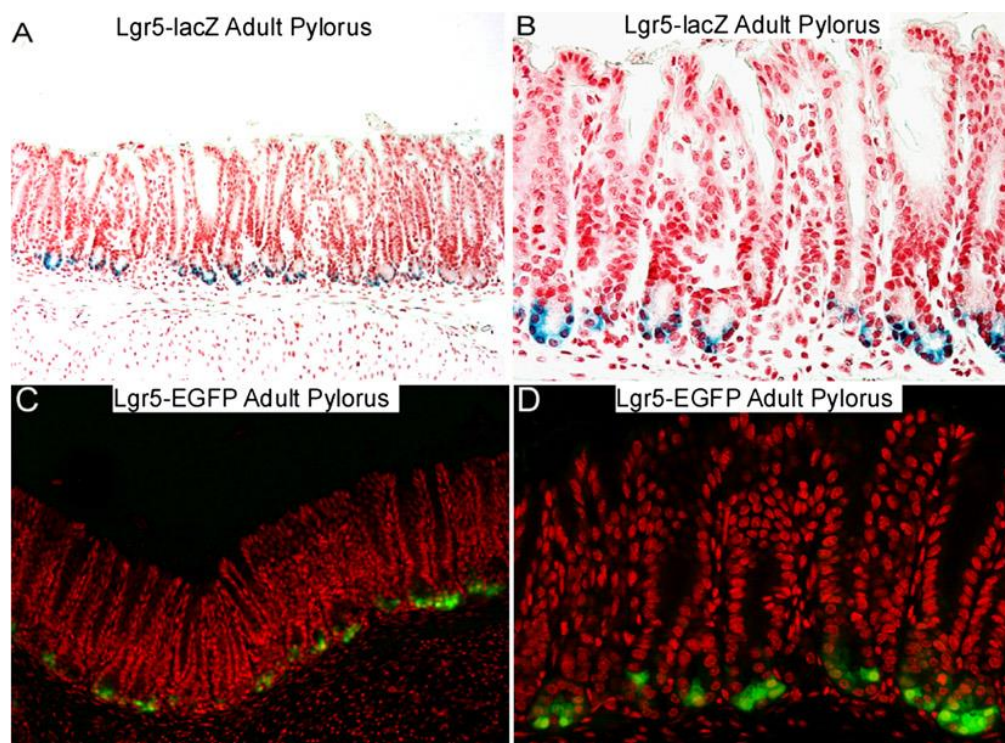


Figure 16. Restricted expression of Lgr5 at the basis of adult pyloric glands

(A and B) Lgr5 expression is restricted to the basis of the pyloric glands in adult Lgr5-lacZ KI mice (A, 103 magnification; B, 203 magnification). (C and D) Confocal images showing Lgr5-EGFP expression at the base of the pyloric glands in adult Lgr5-EGFP-ires-CreERT2 mice (C, 103 magnification; D, 203 magnification).

III.2 Cancer stem cells

III.2.1 Concept of cancer stem cells

Like their normal tissue counterparts, tumors are heterogeneous, consisting of cells with differentiation in morphology and function. For many years, this heterogeneity among cancer cells in the same tumor was explained by a stochastic model, which was based on the notion that all cancers within a tumor mass had the same tumorigenic potential, dependent on genetic and/or epigenetic changes (Figure 17.a).

However, a more recent hypothesis, the so-called hierarchical model, suggests that only a minor subpopulation of cancer cells within a tumor are able to proliferate to form a tumor mass (Figure 17.b). This subpopulation is defined as tumor initiating cells or CSCs.

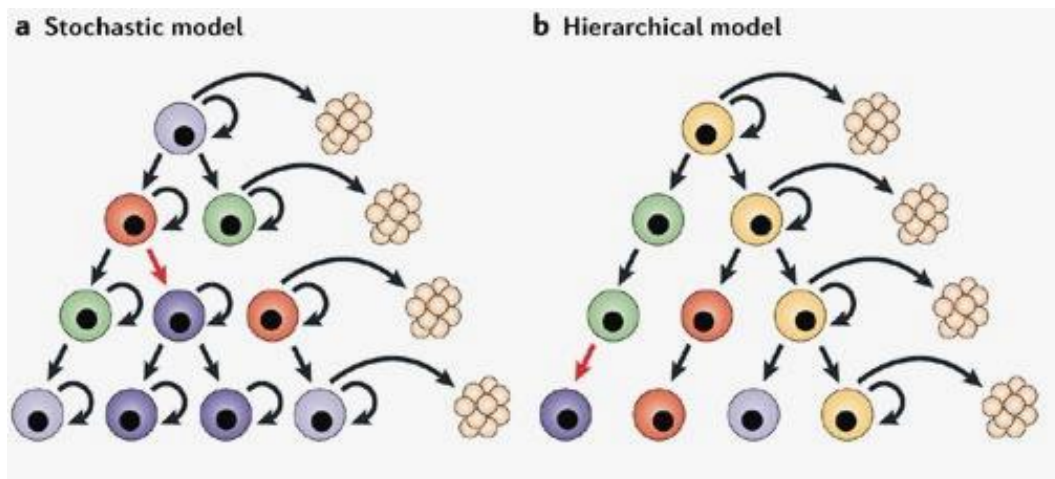


Figure 17. Stochastic and hierarchical model in tumor initiation.

There are two alternative models to explain how tumors initiation and development. The stochastic model (a), in which tumor cells are heterogeneous, but that virtually all of them can function as a tumor-founding cell, although this happens only rarely. The second one is the hierarchical model (b) implies that only a small subpopulation of tumor stem cells can proliferate extensively and sustain the growth and progression of a neoplastic clone. Source: (Vescovi et al., 2006)

CSCs isolated from different tumors possess the same common characteristics including self-renewal, asymmetric division, differentiation into multiple cell types and resistance to chemotherapy. In addition, CSCs are characterized by surface markers and can be isolated from non-tumorigenic cells by means of flow cytometry or other immuno-selection procedures. The concept that tumors contain minor populations with stem cell properties was shown by *in vitro* clonogenic or tumorsphere assays. Furthermore, this subpopulation is identified by its capacity to generate new tumors

through serial transplantations in immunodeficient hosts, reestablishing tumor heterogeneity.

III.2.2 Evidence of cancer stem cells

The first association between cancer and stem cells dates back to the nineteenth century when a histological similarity between tumors and embryonic tissue was shown. This gave rise to the theory that cancers are initiated from cells with properties similar to early embryo cells (Nguyen et al., 2012).

In 1997, John Dick's group identified a hierarchy of stem cells mimicking the normal hierarchy of HSCs, and they were the first to report the prospective isolation of primitive HSCs in acute myeloid leukemia (AML). This report was based on a severely combined immunodeficiency (SCID) mouse model to study the proliferation and self-renewal potential of transplanted human AML cells. In this study, Dick *et al.* suggested that in human AML, a rare subpopulation of cells with a CD34+/CD38- phenotype has the ability to repopulate the entire original disease after serial transplantations but not the CD34+/CD38+ subpopulation. More recent studies have expanded the definition of the leukemic stem cells in AML to the phenotypic CD34+CD38-CD90-IL-3R+CD71-HLADR-CD117- population (Lobo et al., 2007). These reports by Dick *et al.* marked for the beginning of research on CSCs in both hematologic malignancies and solid tumors.

In solid tumors, Al-Hajj et al. first identified CSCs in breast cancer by using a combination of CD44 and CD24 markers in 2003. Since then, CSCs have been isolated from many different solid tumors, such as glioblastoma, lung cancer, liver cancer, prostate cancer, ovarian cancer, clone cancer and gastric cancer. They showed that, within a tumor, cells are heterogeneous and that only a small number of them have the ability of *in vitro* colony and *in vivo* tumor formation. For example, in melanoma, only 1 in 1,000,000 to 1 in 1,000 tumor cells of the total tumor cell population has the capacity to form a new tumor when injected into NOD/SCID mice (Quintana et al., 2008). In the case of AML, the frequency of cells is less than 1 in 10,000 (Bonnet and Dick, 1997).

In gastric cancer, gastric CSCs are identified by analysis of surface marker expression or side population (SP) formation. In 2009, Takaishi *et al.* analyzed the expression of

six potential CSC markers on gastric cancer cell lines and showed that the CD44+ cell population sorted by fluorescent-activated cell sorting (FACS) possessed CSC properties including *in vitro* tumorsphere formation, more resistance to anti-tumor drugs and *in vivo* tumor generation (Takaishi et al., 2009). In addition, based on an analysis of SP formation in five cancer cell lines using Hoechst 33342 staining, Fukuda *et al.* showed SP cells ranging from 0.02±0.001 to 1.93±0.16%. These cells are known to express high quantities of ABC transporter genes such as MDR1 and BCPR1, resistance to cisplatin, 5-fluorouracil or doxorubicin, and *in vivo* tumorigenicity compared to main population cells (Fukuda et al., 2009a).

III.2.2 Origin of cancer stem cells

Many important questions are emerging in the CSC field. For example, do the cells-of-origin for CSCs always begin with normal stem cells which undergo genetic or epigenetic changes to lose control of their cell proliferation? Can progenitor or differentiating cells become stem cells via mutations?

In the case of AML, both leukemic stem cells and their normal stem cells share the same CD34+CD38- phenotype. It is considered that the transformation of the normal HSCs may lead to generate leukemic stem cells. In addition, in the case of B acute lymphoblastic leukemia (B-ALL), based on a Myc-induced mouse model, Sugihara *et al.* found that CSCs high expressed B220 and CD19 markers of B cells. They also showed that the cells-of-origin of CSCs in this model were HSCs (Sugihara et al., 2012).

Studies based on a deficient mouse model, however, revealed that not only HSCs but also their progenitors may be the cells-of-origin of leukemia stem cells. In this model, MOZ-TIF2-transduced progenitor cells induced an *in vivo* AML which could be serially transplanted as well as serially replated *in vitro*. In contrast, a BCR-ABL fusion gene was not able to transform granulocyte-macrophage cells into leukemia stem cells. This showed that hematopoietic progenitors confer leukemic stem cell properties via genetic alterations to some leukemia oncogenes (Huntly et al., 2004).

Current evidence is increasing to confirm that both stem cells and progenitor cells play the role of cells for tumor initiation in many different solid tumors. Lineage tracing is a method developed by Backer *et al.*, which allows the identification of all progeny from a single cell. This is now an essential tool for studying stem/progenitor cell characteristics in adult mammalian tissues. By using this method, crypt stem cells which express the Lgr5+ marker were shown to be intestinal cancer cells. Furthermore, this study revealed that an APC deletion in Lgr5+ stem cells, but not in short-lived transit-amplifying cells, caused adenoma formation throughout the small intestine (Barker *et al.*, 2009).

In addition, by using a BMI1-CreER knock-in mouse model, Sangiorgi and Capecchi found a novel intestinal stem cell which is located in the +4 or +5 position from the base of the crypt, therefore distinct Lg5+ stem cells also acted as the 'cells-of-origin' of intestinal carcinoma via WNT signaling. BMI1 has also been shown to be a marker of intestinal stem cells which processes proliferation, self-renewal capacity and gives rise to all of the differentiated cell lineages of the small intestine epithelium (Sangiorgi and Capecchi, 2008).

In brain cancer, several genetic models were developed to identify 'cells-of-origin' of tumors. These models can be used to activate or inactivate some oncogenes or tumor-suppressor genes in cell populations using cell type specific promoter systems such as Nestin-CreERT2, Adeno-cre, and GFAP-cre. For example, by using an adenovirus expressing *cre* recombinase (either Adeno-cre or Adeno GFAP-cre) to delete Rb/p53, Rb/p53/PTEN or PTEN/p53 in adult subventricular stem cells, Jacques *et al.* suggested that gliomas originates from stem cells bearing PTEN/p53 mutations (Jacques *et al.*, 2010).

In prostate tissue, the differentiating process from basal cells to secretory luminal cells via intermediate phenotypes is induced by circulating androgens. In 1996, Bonkhoff and Remberger described a small number of stem cells in the basal cell layer which generates all epithelial cell types encountered in the normal, hyperplastic, and neoplastic prostate. Accordingly, it was suggested that transformed stem cells which acquire secretory luminal characteristics under androgenic stimulation located in the basal cell layer are cells-of-origin of prostate CSCs (Bonkhoff and Remberger, 1996). Recent reports, however, revealed that distinct stem cells in luminal cellular

compartments are at the origin of prostate tumors due to the loss of PTEN or PI3K inactivation.

III.2.3 Cells-of-origin in gastric cancer

Although the existence of gastric CSCs have been shown in some studies, the origin of these CSCs remains unclear. The understanding the origin of gastric CSCs may be helpful to develop new approaches for treatment or prevention of gastric cancer in humans. Although gastric stem/progenitor cells might seem to be good candidates for gastric CSCs, another possible source of CSCs has recently been described as 'cells-of-origin' of gastric cancer. In 2004, Houghton *et al.* established a *Helicobacter felis*/C57BL/6 mouse model of gastric cancer to evaluate the role of bone marrow–derived cells (BMDCs) in the gastric carcinoma. In this study, they showed that chronic infection of C57BL/6 mice with *H. felis* induced a repopulation of the gland cells with BMDCs which progressed through metaplasia and dysplasia to intraepithelial cancer. Thus, BMDCs are believed to be 'cells-of-origin' of *H. felis*-induced gastric cancer via a transformation of epithelial tissue stem cells. Other more recent studies have revealed that bone marrow–derived endothelial progenitor cells can contribute to cancer progression in glioblastoma, lung adenocarcinoma and squamous cell carcinoma (Avital *et al.*, 2007). Using an *H. pylori*/C57BL/6 mouse model in our laboratory, we confirmed that almost 25% of high-grade dysplastic lesions include cells originating from the bone marrow. Furthermore, the recruitment and accumulation of BMDC in the gastric epithelial mucosa is significantly associated with chronic inflammation, hyperplasia, metaplasia, and dysplasia development (Varon *et al.*, 2012).

IV. IDENTIFICATION OF CANCER STEM CELLS

IV.1 Methods of identification and isolation of cancer stem cells

IV.1.1 Colony formation assays

These assays were developed on the basis of the self-renewal ability of CSCs. In semisolid medium or methylcellulose medium, CSCs can proliferate and differentiate into colonies (Franken et al., 2006). This method was primarily used to analyze the self-renewal and multilineage differentiation of immature hematopoietic cells (Figure 18.II). However, it can be also used to quantify CSCs as well as to assess their proliferation capacity *in vitro*. The limitations of this assay are the variation in preparation of feeder layers and culture conditions between laboratories.

IV.1.2 'Side population' assay

In this method (Figure 18.III), a 'side population' is identified by flow cytometry analysis. These are cells with a high expression of transporter proteins, such as ABCG2, which are able to exclude some dyes such as Hoechst dye, rhodamine or some drugs out of the cells. The activity of transporters found in 'side populations' may explain their resistance to chemotherapies. Hoechst 33342 with its emission at 355 nm is the most common dye used to isolate 'side populations' by flow cytometry. Cells of a 'side population' are negative to dye staining because of dye efflux, while almost all tumor cells are positive and thereby classified as the main population.

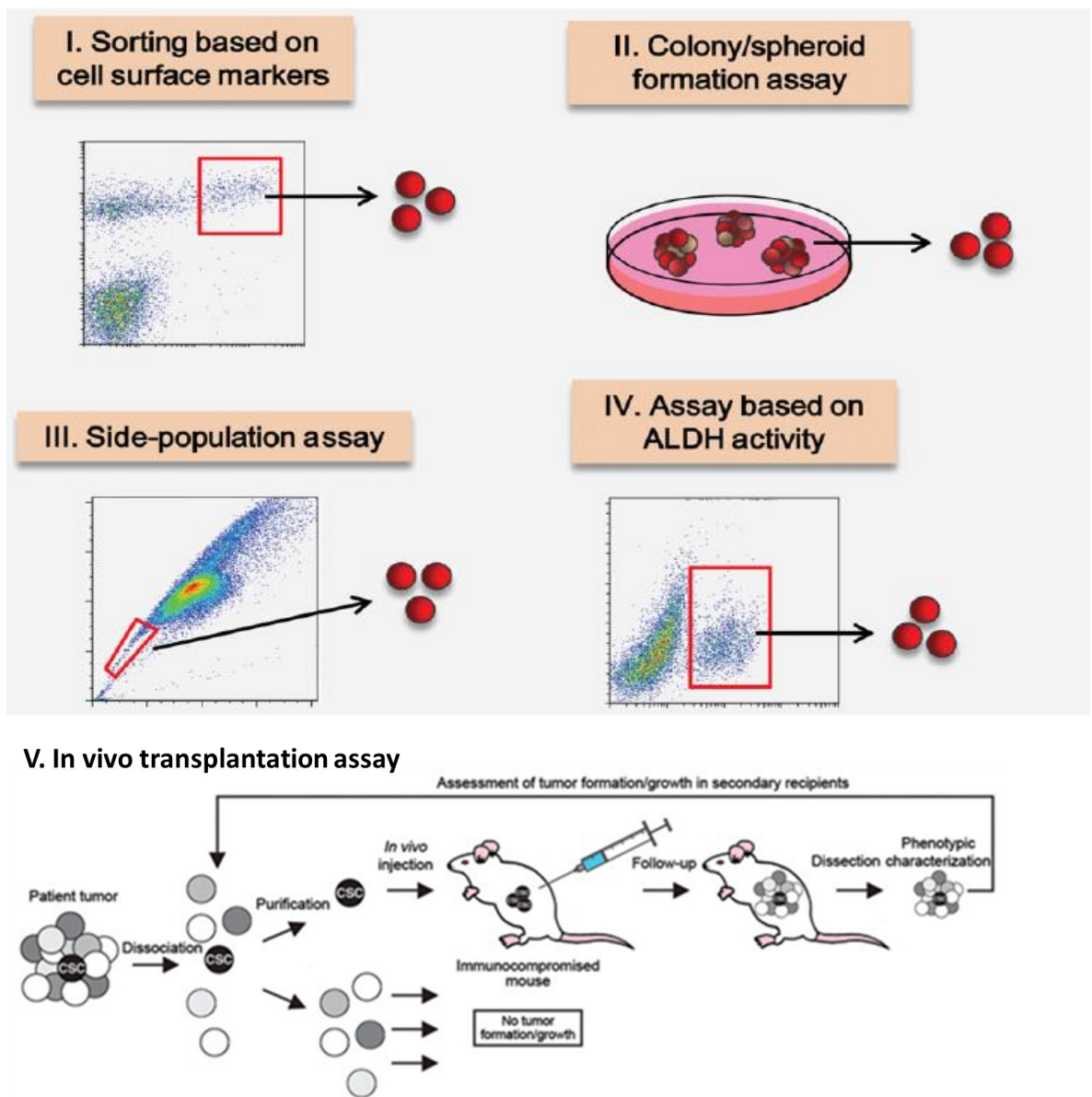


Figure 18. Methods for the identification and enrichment of CSCs.

CSCs can be sorted based on a combination of cell surface markers (I). Their self-renewal activity, allows hematopoietic CSCs to form colonies in methylcellulose medium whereas those for solid tumors form spheroids in serum-free medium under nonadherent conditions (II). The exposure of tumor cells to Hoechst 33342 and irradiation with UV light, followed by cell sorting, permits the isolation of a CSCs enriched cell subpopulation corresponding to a side area (red box) of a flow cytometry plot of Hoechst blue versus red fluorescence (III). The high ALDH activity of CSCs allows their isolation by cell sorting on the basis of their green fluorescence signal when treated with Bodipy-conjugated aminoacetaldehyde (IV). *In vivo* transplantation assay is as the gold standard assay for the study of CSCs (V). Source: (Sugihara and Saya, 2013; Schatton and Frank, 2010)

'Side population' assays are used to isolate CSCs from hepatocellular cancer (Chiba et al., 2006), pancreatic cancer (Wang et al., 2009), ovarian cancer (Rizzo et al., 2011) and gastric cancer (Fukuda et al., 2009). Although this is a simple method, its main problems are caused by the cytotoxic dye, which may have negative effects on the cell viability, sorted afterwards by FACS. In addition, the results of 'side population' isolation also depend on culture conditions and stain conditions, such as the dye concentration and incubation time. Moreover, if there are few 'side populations', it may result in difficulties in analysis. Recent reports showed that 'side population' assays are not suitable for the identification of CSCs in the case of gastrointestinal cancer cell lines such as HT29, HGT101, Caco2 and HRA19a1.1 (Burkert et al., 2008), or are not sufficient for a CSC isolation in multiform glioblastoma (Broadley et al., 2011).

IV.1.3 Tumorsphere assay

Tumorsphere assays were first performed in 1960, to assess and isolate neural stem cells from the mammalian brain. Since then, this assay has been widely used to identify and isolate CSCs from many cancer types such as breast cancer, pancreatic cancer, lung cancer, ovarian cancer and gastric cancer. In this assay, cells are plated and grown in non-adherent conditions and in serum-free culture media supplemented with basic fibroblast growth factor and epidermal growth factor (Vermeulen et al., 2008) (Figure 18.II). Although this is a useful and simple method, it also has some limitations because some quiescent CSCs are not able to form tumorspheres. Cell density is very important to tumorsphere formation. In addition, enzymatic digestion in the early steps or the alteration of growth factors in culture media may affect tumorsphere formation.

IV.1.4 Cancer stem cell isolation based on surface marker expression

CSCs may be separated from other tumor cells based on the expression of some specific surface markers such as CD133, CD44 or CD166. Therefore, these CSCs may be isolated by FACS or magnetic activated cell sorting (MACS) (Figure 18.I).

FACS allows the isolation of cells via fluorochromes in direct or indirect immunofluorescence staining and further separation of cells stained by a multiplex of different markers (Greve et al., 2012). MACS is based on micro-beads linked to a specific monoclonal antibody which allows the enrichment of target cells via binding of their specific antigens to the antibody (Schmitz et al., 1994). Although MACS is simpler than FACS in use, it is not able to isolate cells stained by multiple markers, while the limit of FACS is the difficulty to differentiate and isolate cell subpopulations with similar marker expression. Recently, a series of surface markers was used to differentiate CSCs of different types of human cancers. These markers may be used alone or in combination with one or more other markers for CSC isolation by FACS (Xia, 2014).

IV.1.5 ALDH activity assay

High ALDH activity has been demonstrated as an important characteristic of tumor initiating cells, and is widely used to isolate CSCs in many tumors of different organs. ALDH1 is an enzyme which is able to oxidize aldehydes to carboxylic acids. In this assay, BODIPY-aminoacetaldehyde (BAAA), an ALDH substrate, is added to the cells, and is then converted by intracellular ALDH into fluorescent BODIPY-aminoacetate (BAA-) (Figure 18.IV). DEAB, an ALDH1A specific inhibitor, is used as a negative control. In addition, ALDH expression is also used to identify CSCs by immunohistochemical staining in some types of human cancers, such as endometrioid (Rahadiani et al., 2011) and cervical carcinoma (Yao et al., 2011). Similar to other assays, the ALDH activity assay has certain disadvantages, such as the existence of many ALDH isoforms in the same cell type, and the effect of culture conditions on ALDH expression.

IV.1.6 *In vivo* xenotransplantation models for cancer stem cell identification

Xenotransplantation models are crucial tools for studying cancer biology, particularly for the detection of CSCs which initiate tumors, increase the ability to migrate, and metastasize into many different cancer types as well as the corresponding resistance to chemotherapy and radiation therapy.

In vivo, a limiting-dilution method is very important to show the capacity of CSCs to reconstitute a new tumor when transplanted into immunodeficient mice (Figure 18.V). This method allows CSC detection at a more precise level, and even at a single-cell level. Thus, it also enables the calculation of a CSC ratio in tumors or the tumor's level of differentiation. Currently, *in vivo* xenograft assays are still considered the gold standard in CSC identification. However, more recent studies on the identification of CSCs are typically based on xenotransplantation models of mice with compromised immune system (NOD/SCID) mice. Albeit useful, these systems still have main limits such as the immune response as well as the differences between the murine and human microenvironments. To overcome these limitations in xenotransplantation models, a recent study by Quintana *et al.* revealed that by using IL2 γ null NOD/SCID mice, approximately 25% of unselected melanoma cells generated new tumors compared to 0.1-0.0001% of cells forming tumors when transplanted into NOD/SCID mice. Therefore, genetic modifications in mice used for xenotransplantation assays allow an increase in the detectable capacity of CSCs, which may be similar in some human cancer types (Quintana et al., 2008).

IV.2 Marker of cancer stem cells

Our current understanding of CSC biology shows that CSCs share properties of normal stem cells, such as self renewal, differentiation, and expression of some surface markers and stemness genes. Moreover, the repertoire of CSC surface markers has been identified and these markers are continuously being completed by new studies (Table 1). On other hand, the development of suitable technologies such as FACS or MACS has led to the identification and purification of CSCs from tumor cell populations of both blood and solid tumors based on expression of one or more of these surface markers.

In AML, CD34 and CD38 are two of the first surface markers used to identify a CSC subpopulation. Here, cells corresponding to CSCs have a CD34⁺/CD38⁻ morphology, whereas CD34⁺/CD38⁺ cells do not acquire CSC properties. Further studies on leukemia showed that CD34 may be combined with other markers for the identification of CSC subpopulations of different types. For example, cells with

CD34+/CD10- morphology correspond to CSC subpopulations in ALM, while those with CD34+/CD38-/CD123+ morphology correspond to CSCs of chronic myelogenous leukemia (see Table 1). In addition, Cox *et al.* revealed that in childhood acute lymphoblastic leukemia (ALL), subpopulations of cells expressing CD133 or CD19- were able to self-renew, proliferate, differentiate and engraft serially into NOD/SCID recipient mice (Cox et al., 2009)

Table 1. Surface markers of cancer stem cells

| CSC markers in leukemias (a) | | |
|--|---|--------------------------------|
| Leukemia types | Markers | References |
| Acute myelogenous leukemia (AML) | CD34+/CD38- | Bonnet and Dick, 1997 |
| | CD34+/CD90- | Blair et al., 1997 |
| Acute lymphoblastic leukemia (ALL) | CD34+/CD10- | Cox et al., 2004 |
| Chronic myelogenous leukemia (CML) | CD34+/CD38-/CD123+ | Florian et al., 2006 |
| CSC markers in solid tumors (b) | | |
| Tumor types | Markers | References |
| Breast | ESA+/CD44+/CD24- | Al-Hajj <i>et al.</i> , 2003 |
| | CD24+/CD29+ | Vassilopoulos et al., 2008 |
| | ALDH+/ CD44+/CD24-/lin- | Ginestier <i>et al.</i> , 2007 |
| | CD176+/CD133+ | Lin et al., 2010 |
| | CD44+/CD24 ^{-/low} /ALDH ^{high} | Ricardo et al., 2011 |
| Liver | CD133+ | Ma et al., 2007 |
| | CD133+/CD44+ | Zhu et al., 2010 |
| | CD90+/CD44+ | Yang et al., 2008 |
| | CD90-/CD13+ | Haraguchi et al., 2010 |
| | CD133+ALDH+ | Ma et al., 2008 |
| Prostate cancer | CD44+/alpha2beta1 ^{hi} /CD133+ | Collins et al., 2005 |
| | Lin-/Sca-1+/CD49f ^{high} | Mulholland et al., 2009 |
| | CD44+alpha2beta1 ^{+/high} | Patrawala et al., 2007 |

| | | |
|----------------|--|--|
| | ALDH ^{high} | van den Hoogen et al., 2010 |
| | ALDH7A1+ | van den Hoogen et al., 2011 |
| Colorectal | CD133+ | O'Brien et al., 2007 |
| | ESA ^{high} /CD44+ | Dalerba et al., 2007 |
| | EpCAM ^{high} /CD44 ⁺ /CD166 ⁺ | Dalerba et al., 2007 |
| | CD133+/CD44+ | Haraguchi et al., 2008 |
| | CD133+/CD24+ | Vermeulen et al., 2008 |
| Brain | CD133+ | Singh et al., 2003 |
| | A2B5+CD133- | Ogden et al., 2008 |
| | SSEA-1+ | Son et al., 2009 |
| | ALDH+ | Choi et al., 2014 |
| Pancreatic | CD44+CD24+ESA+ | Li et al., 2007 |
| | CD133+ CXCR4+ | Hermann et al., 2007 |
| | ALDH ^{high} | Kim et al., 2011 |
| Lung | CD133+ | Eramo et al., 2008 |
| | CD44+ | Leung et al., 2010 |
| | ALDH1A1+ | Kim et al., 2011 |
| Ovarian | CD44+/CD117+ | Zhang et al., 2008 |
| | CD133+ | Curley et al., 2009 |
| | CD133+/ALDH+ | Silva et al., 2011; Kryczek et al., 2012 |
| Bladder | Lin-CD44+CK5+CK20- | Chan et al., 2009 |
| | EMA- CD44v6+ | Yang and Chang, 2008 |
| | ALDH1A1+ | Su et al., 2010 |
| Melanoma | CD133+ or CD133+/ABCG2+ | Monzani et al., 2007 |
| Gastric cancer | CD44+ | Takaishi et al., 2009 |
| | CD44V8-10 | Lau et al., 2014 |

In solid tumors, numerous markers used for the identification of CSC are also used to isolate HSCs or mesenchymal cells, such as CD133, CD90, CD166, CD105, CD73, CD117 and CD44. Indeed, other markers such as EpCAM (ESA), CD24, CD49f, SSEA, Nestin, Lin or ABC-G2 and ALDH have also been used. Notably, ALDH, CD44 and CD133 are the three most frequently used markers for the isolation of a large variety of solid tumors. The role of these three markers will be discussed in next

section. Here, we shall discuss the other important markers which are also used to isolate CSCs in solid tumors.

CD24 is a sialoglycoprotein found on mature granulocytes and in many B cells. This protein is also expressed in hematologic malignancies and in many kinds of solid tumors such as breast, stomach, gallbladder, colon, and ovary cancer. In breast cancer, the combination of CD24 with CD29 allowed the identification of CSCs with a CD24⁺/CD29⁺ phenotype (Vassilopoulos et al., 2008). In contrast, other findings showed that in breast CSCs the CD24 protein is absent. For example, CD44⁺/CD24⁻/low/lin⁻ or morphology but not CD44⁺/CD24^{high} + cells (Al-Hajj et al., 2003).

In addition, cells with CD113⁺/CD24⁺ or CD44⁺/CD24⁺/EpCAM⁺ phenotypes are also indicated as subpopulations of CSCs in colorectal cancer (Vermeulen et al., 2008) or pancreatic cancer (Li et al., 2007).

CD49f, otherwise known as integrin alpha-6beta-1, is a member of the integrin protein family. This protein serves as a bridge for cell-cell and cell-extracellular matrix interactions. Expression of the CD49f protein is associated with the regulation of the cell cycle, cell shape, and/or motility (Schaller et al., 1993).

Like CD24, CD49f expression is also used as marker for the isolation of CSC subpopulations from serial solid tumors. CD49f expression in combination with Sca-1 and Lin markers allowed the identification of CSCs with a Lin⁻/Sca-1⁺/CD49⁺ phenotype in prostate cancer (Mulholland et al., 2009). In addition, cells which are positive for both CD24 and CD49 markers have been identified as CSCs in breast cancer (Carrel et al., 1993).

Another common marker of CSC identification is CD90 or Thy1. The expression or absence of CD90 in tumor cells is not only used as a marker for isolating CSCs in leukemias but also in several solid tumors. For example, CD90⁺/CD24⁺ cells respond to CSCs in breast cancer (Cho et al., 2008), whereas cells with the Cd13⁺/90⁻ phenotype were shown to be as subpopulation of CSCs in liver cancer (Haraguchi et al., 2010). Some other markers which are used alone or in combination with other markers for enrichment of CSCs, such as CD117, EpCAM, or ABCG2 have also been reported (Table 1).

IV.3 Aldehyde dehydrogenase

Aldehyde dehydrogenase (ALDH) belongs to the oxidoreductase superfamily, which is represented in all bacteria, plants and animals. One of the most important roles of ALDH is the oxidation of aldehyde to carboxylic acid. Retinoic acid (RA) signaling plays an important role in many physiological processes such as proliferation, differentiation and development. Retinoic acids are converted from retinol by alcohol dehydrogenase (ADH) and ALDH whereas ADH oxidizes retinol to retinaldehyde, which is continuously oxidized to acid retinoic (All-trans retinoic acid or 9-cis retinoic acid) by ALDH. In humans, the main isoform of ALDH, which converts retinaldehyde to RA usually belonging to class 1 including ALDH1A1, ALDH1A2 and ALDH1A3. The generated RA then interacts with the nuclear RA receptor (RAR)/retinoid X receptor (RXR) to form a RA/receptor complex which regulates transcription of many different genes as well as cell differentiation.

Aldehydes are generated from various metabolisms in cells and many of which could interact with intracellular proteins, leading to structural and functional alterations of these proteins (Figure 19). Oxidation of aldehyde groups is imperative in the detoxification process to protect the cell from the harmful effects of aldehydes. However, a number of products formed by this oxidation are very important to the cell biological process, such as RA, an element for cell proliferation and differentiation as well as development, while γ -aminobutyric acid is a significant neurotransmitter (Vasiliou et al., 2000). In addition, ALDH has the ability to interact to some hormones as well as other proteins and to protect the cornea from ultraviolet irradiation (Jackson et al., 2011). Furthermore, ALDH expression has been found in crystalline structures in the mammalian cornea and is emerging evidence for its structural function.

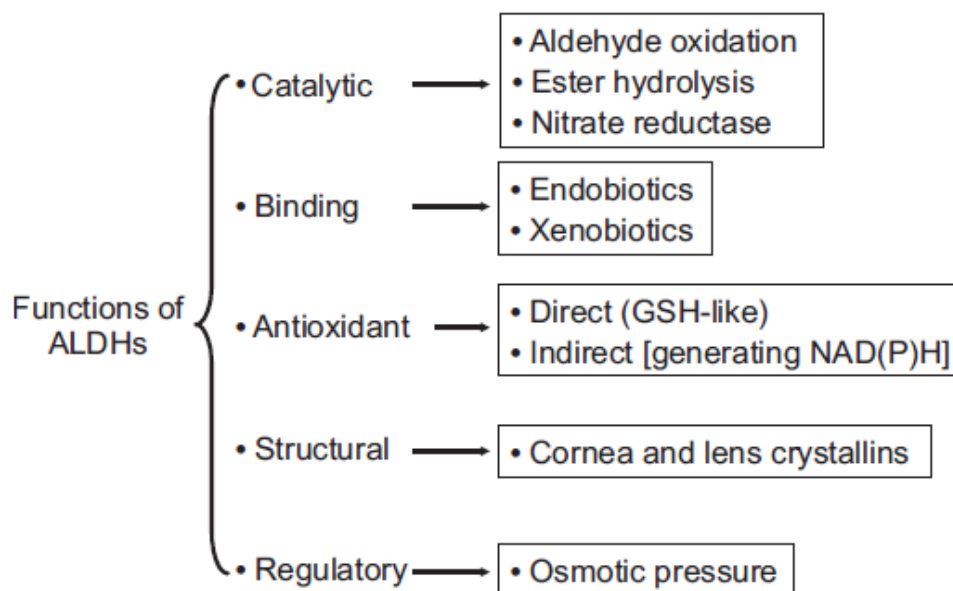


Figure 19. Multiplex function of aldehyde dehydrogenase. Source: Vasiliou et al., 2004

IV.3.1 Human ALDH gene superfamily

As presented above, ALDH genes were found in all three taxa including Archaea, Eubacteria and Eukaryota. A number of genes in the ALDH gene family are species dependent. Following an update of the database on the human ALDH gene superfamily in 2011, the number of ALDH genes changes from 14 in chicken to 25 in zebrafish, and the human genome is comprised of 19 functional protein-coding genes and some protein non-coding pseudogenes belonging to 11 families and 4 subfamilies (Figure 20).

The ALDH1 family consists of six structural genes which code for functional proteins including ALDH1A1, ALDH1A2, ALDH1A3, ALDH1B1, ALDH1L1 and ALDH1L2. ALDH1A1, ALDH1A2 and ALDH1A3 proteins are present in cytosolic and mitochondria in many different tissues in the body, such as the liver, lung, brain and kidney. These proteins have the capacity to catalyze and reject toxic aldehyde from cells. ALDH1A1 is also known to have the ability of high oxidation of both 9-cis and All-trans retinal to their RA forms. In addition, ALDH1A1 proteins are also involved in binding with other molecules, such as androgen, cholesterol and cytosolic thyroid hormone (Vasiliou et al., 2004). ALDH1A2 and ALDH1A3 have been identified as

crucial regulators in the development and differentiation of various tissues, particularly, the brain, liver and lung.

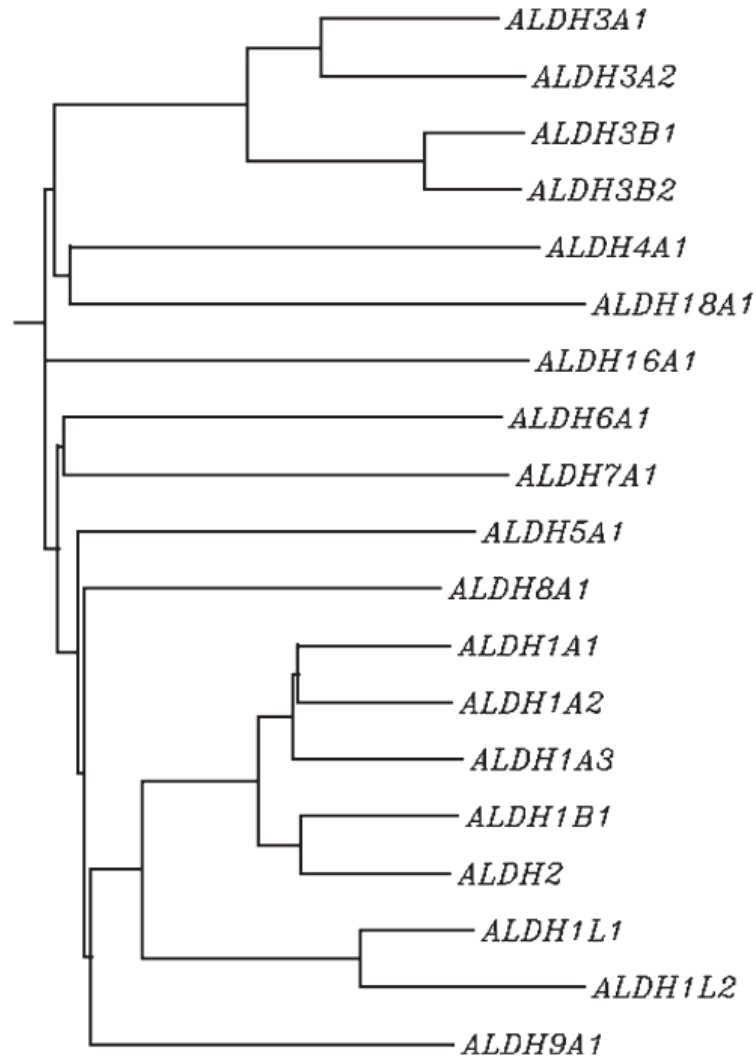


Figure 20. Dendrogram of 19 human aldehyde dehydrogenase genes of the ALDH superfamily.

To avoid additional clusters, alternative splice variants of ALDH genes were not included in the construction of this tree. Source: Vasiliou et al., 2004

The ALDH2 enzyme is expressed in great abundance in mitochondria in the liver and lung. The ALDH2 gene family has polymorphisms, and it has been suggested that various alleles of ALDH2 play an important role in ethanol detoxification. Genetic alterations on ALDH2 genes are associated with Alzheimer's and Parkinson's disease. Notably, ALDH2*2 allele mutations are associated with a high risk of myocardial infarction, and the East Asian population has been identified as carrying a high mutancy rate of this allele. A comparative clinical study on patients with or without a history of alcohol consumption demonstrated that ALDH2*2 is a risk factor

for heavy alcohol consumption (Yao et al., 2011). 4-hydroxy-trans-2-nonenal (4-HNE), a major aldehyde produced from oxidized lipids, is strongly related to stroke disease in humans. A recent finding revealed that ALDH2 can detoxify and reduce the accumulation of this toxin which has been seen as an agent of cerebral injury. Thus, ALDH2 expression may be a potential target for stroke disease prevention (Guo et al., 2013).

The ALDH3 family codes enzymes which play an important role in fatty and peroxidic aldehyde metabolism. High expression of ALDH enzymes is usually found in some tissues such as the cornea, stomach and lung. In addition, the role of ALDH3A1 has been suggested in the prevention of the formation of 4-HNE and the protection of corneal cells from apoptosis. Overexpression of ALDH3 is strongly associated with human hepatocellular carcinomas (Shibuya et al., 1994) and breast cancer (Sládek et al., 2002)

ALDH4 genes code for mitochondrial enzymes which have the ability of converting pyrroline-5-carboxylate to glutamate via oxidation. A genetic deficiency of ALDH4 genes may be related to type II hyperprolinemia, an autosomal recessive disorder caused by Δ^1 -pyrroline-5-carboxylate dehydrogenase accumulation which is coded by the ALDH4 gene (Srivastava et al., 2012).

ALDH5 genes are located on chromosome 6 and code for succinic semialdehyde hydrogenase, a protein which is expressed at its highest levels in the liver, kidney, muscle, heart and brain. A genetic alteration of this gene leads to central nervous system dysfunction (Jakobs et al., 1993).

ALDH6 genes code for methylmalonate semialdehyde dehydrogenase, a mitochondrial enzyme which plays a role in the degradation of valine and pyrimidines. ALDH6 has a high ability for oxidation of All-trans retinaldehyde to form RA. In addition, the ALDH6 enzyme is expressed at high levels in the ventral retina during development (Grün et al., 2000).

The ALDH9 gene family is located on chromosome 1 and codes for gamma-aminobutyraldehyde dehydrogenase enzyme which has a strong activity for oxidation of γ -aminobutyraldehyde and other amino aldehydes derived from polyamines and

choline. ALDH9 is expressed in almost all human organs, with a high level in the early stages of embryonic brain development as well as in adult skeletal muscle, liver, and kidney but low levels in other adult tissues such as the heart, brain and lung (Lin et al., 1996).

ALDH16 genes are present in many species and in various tissues of mammals such as the kidney, heart, lung and bone marrow. A more recent study revealed that a single nucleotide polymorphism of ALDH16 may be associated with gout via interactions with HPRT1, a crucial enzyme participating in uric acid metabolism (Vasiliou et al., 2013).

The ALDH18 family codes for the mitochondrial membrane enzyme which has ability to oxidize lumatic γ -semialdehyde and it is essential in arginine synthesis. Mutations in ALDH18A1 lead to many metabolic disorders as well as neurologic abnormalities, such as hypornithinemia and hypocitrullinemia.

IV.3.2 Role of ALDH in protection of normal and cancer stem cells

Many recent studies have shown a high expression of ALDH enzymes in both stem cells and CSCs. High ALDH activity plays a key role in protecting these cells from cytotoxic agents. In addition, active oxidative species, and particularly hydrogen peroxide (H_2O_2), are known to play an important role in inducing programmed cell death. However, high ALDH activity also enhanced the cell viability of human muscle precursor cells via resistance to a H_2O_2 -mediated cytotoxic effect (Jean et al., 2011).

The first evidence of the role of ALDH in drug resistance was found in a case of leukemic cell lines. It has been suggested that ALDH1 expressed at high levels leads to enhanced resistance to cyclophosphamide. In addition, specific inhibition of ALDH1 by DEAB reduced sensitivity to 4-hydroperoxycyclophosphamide, an active form of cyclophosphamide (Hilton, 1984 ; Moreb et al., 1996).

In breast cancer, a high expression of ALDH and CD44 indicates a CSC population. ALDH^{high}CD44⁺ cells have a significant ability for colony formation and chemoresistance compared to ALDH^{low}CD44⁻ cells. In addition, these CSCs also express a high level of resistance related proteins including glutathione-S-transferase,

checkpoint protein 1/2 and phospho-checkpoint protein 1/2. Interestingly, pre-treatment of this cell population with ALDH inhibitors including DEAB or ATRA clearly increased its sensitivity to doxorubicin, paclitaxel, and radiotherapy while this pre-treatment did not have an effect on ALDH^{low}CD44⁻ cells. Thus inhibition of ALDH expression by agents such as ATRA, DEAB and other inhibitors can be very interesting to decrease drug resistance of CSC populations expressing high levels of ALDH activity (Croker and Allan, 2012). Recently, there has been a growing interest in the combination of ATRA and anti-cancer drugs or other therapy in the treatment of cancer cell populations with high ALDH expression. A phase II clinical trial on non-small-cell lung cancer patients showed that treatment by paclitaxel and cisplatin in combination with ATRA (20 mg/m²/day) increased the response rate (55.8% vs. 25.4%) and progression-free survival (8.9 versus 6 months) compared to the group without ATRA, respectively (Arrieta et al., 2010).

In recent years, growth factor receptors, tyrosine kinase inhibitors (EGFR-TKI), have been used as a potential therapy for growth inhibition of cancer cells. EGFR-TKI may inhibit cell proliferation via blocking activated EGFR in the tyrosine kinase signaling pathway, one of the main pathways observed in different cancers. However, in a recent study, Cheng-Po Huang *et al.* revealed that EGFR-TKI drug resistance of lung cancer cells was associated with high ALDH1A1. In addition, an ALDH1A1 positive cell population shows a 5-6 fold increase in TKI drug-resistant lung cancer cells (Huang et al., 2013).

Inhibiting ALDH activity by RA or DEAB, direct inhibitors of ALDH1A, significantly reduces resistance of these cells to 4-hydroperoxycyclophosphamide, doxorubicin and radiotherapy. These results has been observed on breast, leukemia and lung cancer cells (Croker and Allan, 2012; Moreb et al., 2012).

Although ALDH overexpression has been found in many types of drug resistant tumor cells, one pertinent question is: is ALDH mechanically associated with resistance or is it simply a marker of cells with a drug resistance capacity?

For instance, the most clearly understood mechanism of chemotherapy resistance is associated with ATP-binding cassette (ABC) transport proteins. This superfamily is composed of 49 genes, many of which have been shown to confer chemotherapy resistance via the efflux of drugs from cancer cells (Fletcher et al., 2010). ABC transporters contribute to the protection of normal stem cells from toxic substances

and they also play an important role in multidrug resistance of CSCs (Dean, 2009). It should be noted that, although some of the main proteins of the ABC superfamily are overexpressed in the ALDH^{high}/CD44⁺ stem cell population in breast cancer patients, and drug resistance of this population decreased after treatment with ATRA or DEAB, no change in the drug resistance-related protein expression was shown after treatment. Thus, compared to the ABC transporters, the role of ALDH in chemotherapy resistance is still unclear and merits further study to elucidate the drug resistance mechanism in this cell population. In particular, a study on the relationship between ALDH and ABC transport proteins would be an interesting topic.

IV.3.3 ALDH is a common marker of cancer stem cells

As presented above, RA signaling plays a crucial role in proliferation and differentiation. More recent findings showed that this signaling controls the renewal and differentiation of normal and CSCs in different tissues. Gabriel Ghiaur *et al.* suggested that bone marrow stromal cells not only highly express ALDH1 but also receptors of RA signaling. Inhibition of RA signaling led to the maintenance of self-renewal characteristics of HSCs. Expression of the cytochrome P-450 enzyme Cyp26 allowed the conservation of a low level of RA in the microenvironment as a result of inhibition of cell differentiation.

Breast cancer:

Breast cancer stem cells were first isolated based on the expression of two surface markers CD44 and CD24. In this study, Al-Hajj *et al.* showed that CD44(+)CD24(-/low)Lineage(-) cells correspond to CSCs in breast cancer which induced new tumors in deficient mice with an inoculation of only 100 cells while 2×10^4 CD44+/CD24+ cells failed to form tumors (Al-Hajj *et al.*, 2003). Furthermore, Fillmore and Kuperwasser demonstrated that breast cancer cells with CD44+/CD24- expression showed highly invasive properties, an important step for pulmonary metastasis (Sheridan *et al.*, 2006). One year later, using an ALDEFLUOR assay on normal and malignant breast epithelial cells, Ginestier *et al.* showed that ALDH1 high activity cells contained only 3% to 10% of the total cell populations studied. However, continuous tumorsphere formation and *in vivo* assays suggested that these cells represented stemness

properties including a generation of mammospheres at a high level as well as tumor formation in mice after being xenografted with a small number of cells compared to the ALDH- or unsorted cell population. In this study, 0.1% to 1.2% of the cells were shown overlapping between the ALDH1-positive cell population and the CD44+/CD24-/lin- cell population. Cells with both CD44+/CD24-/lin- and ALDH+ phenotypes were shown to have a high ability of inducing new tumors in mice with only 20 xenografted cells. Nevertheless, 50,000 cells expressed only the CD44+/CD24-/lin- phenotype and could not generate tumors while tumor formation was induced by 1,500 ALDH+/non CD44+/CD24-/lin- cells. This indicates that ALDH expression is more specific for breast cancer stem cells than CD44+/CD24-. Furthermore, the combination of ALDH and CD44/CD24 allowed the identification of the more specific CSC population in breast cancer with the ALDH+/ CD44+/CD24-/lin- phenotype (Ginestier et al., 2007). In addition, a study by Charafe-Jauffret *et al.* in 2009 revealed that cells with high ALDH activity may correspond to the metastatic and aggressive behaviours of inflammatory breast cancer (Huang et al., 2013). It is important to note that the most recent study showed that ALDH1A3 expression had a significantly higher relation with RA signaling than ALDH1A1 and ALDH1A2. Furthermore, a study on knockdown ALDH isoforms using shRNA by Marcato *et al.* showed that ALDH1A3 knockdown but no other isoforms of ALDH led to reduced breast cancers with high ALDH activity. Thus, ALDH1A3 was proposed as a new marker of CSCs in breast cancer (Marcato et al., 2011). Moreover, ALDH1A3 overexpression is thought to be linked to increased tumor growth and metastasis in mice and in breast cancer patients (Marcato et al., 2014).

Colorectal cancers:

Current data suggests that colorectal CSCs may be identified based on the expression of certain surface markers including CD133, CD44, CD166 and ALDH (Malcolm et al., J. Cell Science 2011). In 2007, Dalerba *et al.* first demonstrated that colorectal CSCs represent ESA+/CD44+ phenotypes. In this study, ESA+/CD44+ cells isolated from six human colorectal tumors had the ability to form tumors *in vivo* in immunodeficient mice as well as differentiate in various phenotypes (Dalerba et al., 2007). Based on this study carried out in 2008, Scott J. Dylla *et al.* analyzed the role

of ALDH in colorectal CSCs with the identified phenotype ESA+/CD44+ and showed that ALDH1 was expressed at a significantly higher rate in the colorectal CSC population. In particular, ALDH+/ESA+/CD44+ cells but not ALDH-/ESA+/CD44+ cells induced new tumors in xenografted mice. Thus, ALDH represented a special marker for the identification of colorectal CSCs (Dylla et al., 2008). A more recent study on colon cancer patients also confirmed this role for ALDH (Shenoy et al., 2012).

Prostate cancer:

In 2009, Burger *et al.* were the first to suggest that high ALDH activity may be used as a marker for isolation of murine prostate stem cells. In this investigation, cells with high ALDH activity also showed the coexpression of stemness genes such as CD24, Oct3/4, nestin and prominin and a higher proliferation capacity than cells with low ALDH activity (Burger et al., 2009). A study on primary human prostate tumors and cell lines established by Van Den Hoogen *et al.* in 2010 indicated that prostate cancer cells with high ALDH activity increased colony formation and migration *in vitro* as well as reduced tumorigenicity *in vivo*. Nevertheless, this study also revealed that other ALDH isoforms (not only ALDH1) may correspond to ALDH activity, and ALDH7A1 is thought to be related to the observed high ALDEFLUOR activity in human prostate CSCs while expression of ALDH3A2 and ALDH18A1 were not found in human prostate cancer. Notably, knockdown of ALDH7A1 expression led to an inhibition of colony formation and migratory capacity of human prostate cancer cells *in vitro* as well as the formation of distant bone metastases (van den Hoogen et al., 2011). Thus, ALDH7A1 can be used as a CSC marker in prostate cancer.

Ovarian cancer:

The ovarian cancer cell population was first isolated in 2008, based on expression of the CD44 marker (Zhang et al., 2008). One year later, Baba *et al.* showed that, CD133+ cells purified from ovarian cancer cell lines and/or primary tumors of ovarian cancer patients, formed more tumors in xenografted mice, increased resistance to platinum-based therapy, and generated both CD133+ and CD133- cells. Thus, CD133 expression can be used to identify CSCs in ovarian cancer (Baba et al.,

2009). However, using FACS analysis for multiplex markers, Silvia *et al.* demonstrated that ALDH⁺ cells, like CD133⁺ cells, are able to form more tumorspheres *in vitro* and tumors in deficient mice. In particular, CD133⁺/ALDH⁺ cells represented greater growth than ALDH⁺CD133⁻ and ALDH⁻/CD133⁻ cells. In addition, CD133⁺/ALDH⁺ cells induced tumors in mice, beginning with only 11 cells (Silva *et al.*, 2011).

Interestingly, Kryczek *et al.* also showed that ovarian CSCs can be isolated using different markers. Results of this team confirmed once again that CD133⁺, ALDH⁺ or CD133⁺/ALDH⁺ cells have the same properties as CSCs, shown by their ability to form tumorspheres *in vitro* and their tumorigenic capacity in different mice (Kryczek *et al.*, 2012).

Other cancers:

In 2006, Suetsugu *et al.* were the first to show that CD133 is a marker of hepatocellular carcinoma cells (Suetsugu *et al.*, 2006). However, using dual-color flow cytometry analysis for both CD133 and ALDH expression, Ma *et al.* then showed that almost all ALDH⁺ hepatocellular carcinoma cells express CD133, however, not all CD133⁺ cells are ALDH⁺ cells (Ma *et al.*, 2008). Furthermore, CD133⁺ALDH⁺ sorted cells presented a significantly higher tumorigenicity than the CD133⁺ALDH⁻ or CD133⁻ALDH⁻ cell populations both *in vitro* and *in vivo*. Accordingly, ALDH expression is more specific to hepatocellular CSC populations than the CD133 marker (Ma *et al.*, 2008).

Elevated ALDH activity was used as marker for identification of lung CSCs by Sullivan *et al.* in 2010. In this study, ALDH⁺ cells isolated from lung cancer cell lines and tumor samples exhibited higher colony and tumorigenicity capacities than their ALDH⁻ counterparts. Furthermore, ALDH expression in lung CSCs was associated with *NOTCH3*, an important protein in Notch signaling. Suppression of Notch3 by shRNA or γ -secretase inhibitor resulted in a significant decrease in ALDH⁺ lung cancer cells (Sullivan *et al.*, 2010).

IV.4 CD44 and cancer stem cells

IV.4.1 Structure of CD44

CD44 is a ubiquitous multi-structural and multifunctional class I transmembrane glycoprotein present on the cell surface, it participates in cell-cell interactions, adhesion of the extracellular matrix, proliferation, differentiation and cell migration. CD44 is also described as a receptor of hyaluronic acid and binds this ligand via a lectin-like fold. Furthermore, CD44 is also able to bind to other ligands such as collagen and osteopontin. CD44 is coded by a single gene, which is comprised of two groups of exons. One group consists of exons 1–5 and 16–20 encoding for a standard form of CD44 protein (CD44s). These are constant exons during splicing and are expressed together in all cell types. In contrast, exons 6–15 are variable exons by splicing, which are included within the standard exons and combined with these exons to encode different forms of CD44 variants (CD44v) (Figure 21a and 21b). Isoforms of CD44 are generated via a complex alternative splicing, by which more than 1,000 CD44 variants can be formed.

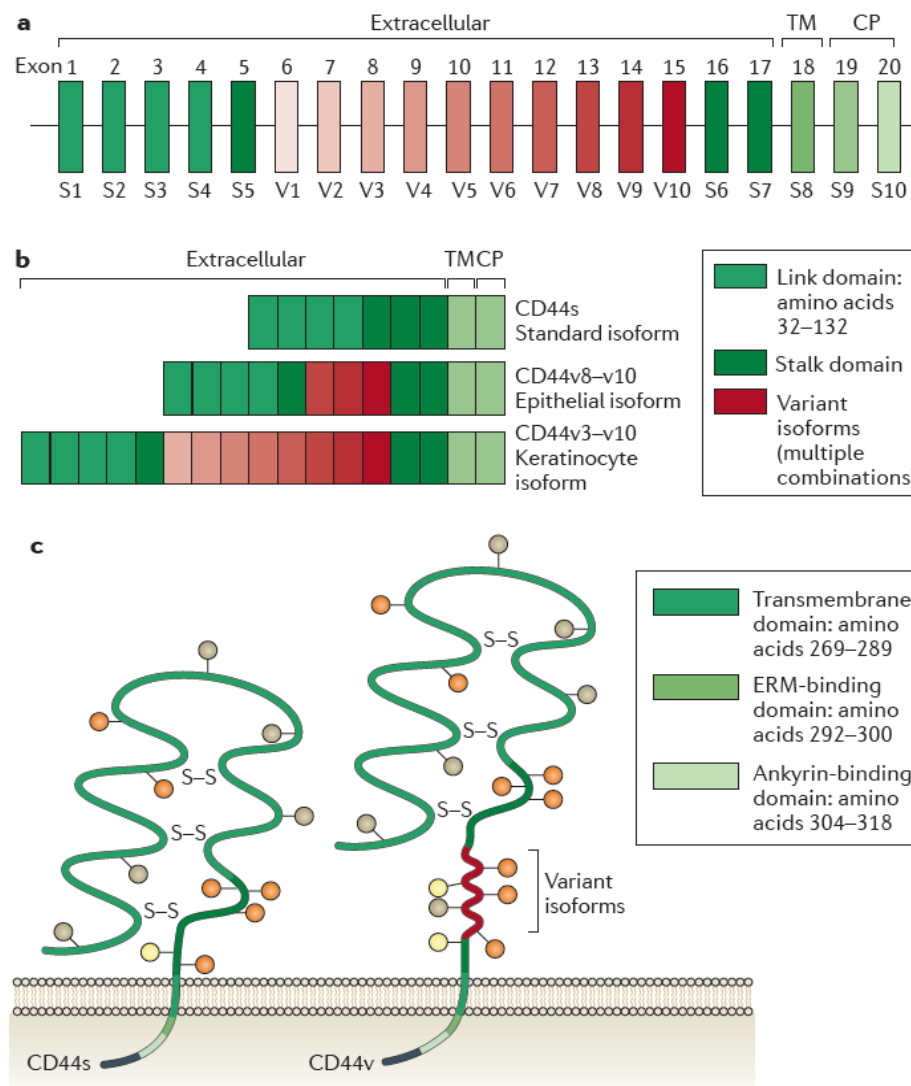


Figure 21: CD44 gene and protein structure.

a) CD44 consists of 20 exons, which include constant exons (green) and variant exons (red) used in variants generated by alternative splicing. **b)** Examples of alternatively spliced CD44 proteins. **c)** CD44 has an extracellular link domain that contains the binding site for hyaluronan, a stalk-like region in the extracellular domain, where the variant exon products (red) are inserted, the transmembrane region, and the cytoplasmic tail, which has binding motifs for cytoskeletal linker proteins, as well as for SRC kinases. Source: (Zöller, 2011)

CD44 is a small molecule with a weight of 85 – 95kDa, which does not include any exon of the variable region (exons 6-15). This single molecule is comprised of different domains: a distal extracellular domain with ligand-binding sites at the N-terminal, a membrane-proximal region, a transmembrane-spanning domain, and a cytoplasmic tail. The N-terminal encoded by exons 1 to 5 is highly conserved between species and is the region which corresponds to hyaluronic acid binding (Figure 21c). The transmembrane domain is a single-pass membrane of glycoproteins encoded by exon 18. This domain consists of a site that could interact with

hexadecanoic acid. The cytoplasmic tail is also a highly conserved region, encoded by part of exon 18 and by exons 19 and 20, and can be phosphorylated as the substrate of protein kinase C. CD44s are expressed in many different tissues such as the lung, liver, pancreas and the central nervous system. However, CD44 expression is principally found in cells of lymphatic hematopoietic origin, thereby it is also called hematopoietic CD44 (Naor et al., 1997) .

Variants of CD44 are restricted in their distribution, and are principally found in epithelial cells. Overexpression of several CD44v isoforms has been associated with poor tumor prognosis and may be related to tumor metastasis. Alternative splicing of variant exons may encode different CD44 molecules with molecular weight ranging from 90 to >220 kDa as well as different capacities to interact with hyaluronic acid. In fact, there are more than 11 CD44v isoforms detected by a specific antibody for the epitope encoded by this exon or by exon-specific polymerase chain reaction. Splicing alternation results in the changes in structure and function between CD44 isoforms which may be specific to tissues. For example, a CD44 isoform consisting of 3 exons (v8-v10) in the variable region is discriminatorily detected on epithelial cells, and also named epithelial CD44 (CD44E). Moreover, another CD44 isoform expressing 8 exons (v3-v10) in this region is found in keratinocytes (Naor et al., 1997). In contrast, no isoforms of the CD44 molecule have been detected in certain types of cells including pancreatic acinar cells and cells of kidney and pancreas tubules (Goodison et al., 1999).

IV.4.2 Role of CD44 in cancer

The CD44 isoform overexpression is significantly associated with tumor progression, tumorigenicity, growth, metastasis and prognosis of many carcinomas in humans. Thus, many publications have shown the important role of CD44s and their different isoforms (CD44v) in the diagnosis and prognosis of some types of human tumors. Binding of CD44 with its ligands such as hyaluronan, chondroitin sulphate, fibronectin, laminin, collagen, and matrigel may induce a production of autocrine growth factors which might play important role in tumor growth (Sneath and Mangham, 1998).

Self-renewal is known to be one of the most important properties of CSCs. This stemness of CSCs may be maintained via an interaction between CD44 proteins and

their ligands such as hyaluronic acid. Knockdown of CD44 by siRNA or antibodies targeting CD44 decreases CD44 expression and the self-renewal capacity of CSCs and induces apoptosis in spheroid cultures and in the mouse xenograft model (Subramaniam et al., 2007; Marangoni et al., 2009).

In a recent study, Hiraga *et al.* used 4-methylumbelliferone (4-MU), an inhibitor of HA synthesis, and demonstrated that 4-MU decreases tumorsphere and osteoclast-like cell formation *in vitro* and inhibits bone metastases *in vivo*. This suggests that CD44 expression in CSCs promotes bone metastasis via an interaction between HA and CD44. In addition, CD44–HA interaction may be a potential target to develop a potential therapy for bone metastases (Hiraga et al., 2013).

The transmembrane glycoprotein CD44 is also known to be a common component of the stem cell niches which regulate stem cell properties including self-renewal and differentiation, tumor progression and metastasis. Niche stromal cells secrete numerous growth factors, some of which play a role in the regulation of stem cell function such as self-renewal and stem cell fate. CD44s and their variants bind these growth factors initiating alternate signaling pathways. For example, CD44v6 binds and presents HGF to c-Met, to form the CD44v6/HGF/c-Met complex and activate c-Met, MEK and ERK signaling to promote CSC migration and invasion. This ability has also been shown for other CD44 variants such as C44v3 and CD44v10, (Williams et al., 2013). In another publication, CD44v6 correlated with a higher proliferative activity and with a stem cell-like phenotype in urothelial carcinoma cell lines (Kuncová et al., 2005). Metastasis is the result of complex interactions between tumor cells and the extracellular matrix as well as normal cells. These interactions depend on cell surface determinants including cell adhesion, extracellular receptor molecules, growth factors, and growth factor receptors. CD44 is seen as an important cell surface determinant and is necessary for metastatic spread occurrence (Sneath and Mangham, 1998). The CD44v6 isoform is expressed at low levels in primary tumors but is enhanced in clonogenic colorectal CSC populations. CD44v6 expression is found in all colorectal CSCs, and it is thought that it initiates colorectal cancer as well as migration and formation of metastatic tumors. Thus, CD44v6 has been proposed as a new marker for colorectal CSCs (Todaro et al., 2014). In contrast, a previous study on

squamocellular tumors suggested that CD44v6 expression is not associated with tumor metastasis and the downregulation of CD44v6 in squamocellular tumors results in malignant transformation (Soukka et al., 1997).

In 2002, Miyake *et al.* measured the expression level of CD44v8-10 and standard CD44 by real time (RT)-PCR in tissue and spontaneously voided urine samples of patients with urothelial cancer and showed that CD44v8-10 is strongly expressed in most urothelial tumor tissues of patients; furthermore, the CD44v8-10/standard CD44 ratio in urothelial cancer was closely associated with tumor progression. The high CD44v8-10/standard CD44 ratio may therefore be used as a novel prognostic marker and indicator in urothelial cancer progression (Miyake et al., 2002).

In addition, a study team revealed that overexpression of CD44v8–10 in bladder cancer cells decreased the cell-binding capacity to hyaluronic acid but not to other extracellular matrix proteins. In contrast, these cells significantly enhanced tumor growth after subcutaneous injection into deficient mice and increased metastasis after orthotopic injection (Muramaki et al., 2004).

The CD44 expression and CD44 variant isoforms confer a selective advantage to resist apoptosis. This role of CD44 is associated with mechanisms including the inhibition of Fas expression, concomitant alterations in caspase 9, caspase 3, Bcl-xl, and Bak, and downregulation of pRb and phosphorylated AKT (Lakshman et al., 2004). In lung cancer, interaction of CD44 with extracellular hyaluronic acid reduces Fas expression. Therefore, Fas-mediated apoptosis and IFN- γ production by autologous cytotoxic lymphocytes are downregulated and resulting in reduced sensitivity of the cells to T lymphocytes-mediated cytotoxicity via the Fas-Fas ligand pathway (Yasuda et al., 2001). Enhanced sensitivity to apoptosis has been shown in CD44 deficient colonic epithelium after activation of caspase 3 in combination alterations in caspase 9 but not caspase 8. Lakshman *et al.* were the first to show that CD44 promoted cell transformation into a malignant phenotype, in conjunction with other anti-apoptotic factors in the colonic epithelium *in vivo* (Lakshman et al., 2005).

Expression of CD44s and their variants in gastric cancer was also reported. A study by Yamaguchi *et al.* in 2002 on 201 cancer tissue samples showed that 47.9%

expressed CD44v6. The expression level of CD44v6 studied in various types of gastric adenocarcinoma showed that it was higher in the intestinal than in the diffuse type, and a significant correlation between CD44v6-positive cells and hematogenous metastasis was also found. Accordingly, CD44v6 may be used as a marker for the prognosis of differentiated type gastric cancers (Yamaguchi et al., 2002).

Other recent studies also suggest that CD44v6 is expressed in gastric adenocarcinoma tissues, and is significantly associated with invasion and lymph node metastasis. A combination of CD44v6, MMP-7 and nuclear Cdx2 may be useful to predict lymph node status in gastric cancer (Okayama et al., 2009; Liu et al., 2005).

The role of CD44v8-10 in gastric cancer was first shown in a study on advanced gastric cancer specimens by western blot analysis and immunohistochemistry. In this study, CD44v8-10 expression was found in the cell membrane, in 33.5% of the cases studied (65/194). Interestingly, CD44v8-10 expression was significantly associated with hematogenous metastasis. Thus, this study suggested that CD44v8-10 may play a role in gastric adenocarcinoma metastasis (Yamaguchi et al., 1995). In addition to CD44v6 and CD44v8-10, expression of the CD44 variant 9 in primary gastric adenocarcinoma at early stage was also shown. The CD44v9-positive group was significantly associated with the recurrence rate of early gastric cancers compared to the CD44v9-negative group. As a result, CD44v9 expression was proposed as a potential marker to predict recurrence in early gastric cancers (Hirata et al., 2013).

IV.4.3 CD44 is a universal marker of cancer stem cells

As previous mentioned, many studies refer to CD44 which is commonly expressed on the cell surface in tumors of different organs. The conclusions from many of these studies suggest that high CD44 expression plays an important role in tumor initiation, migration and metastasis. Experiments using animal models showed that targeting of CD44 by monoclonal antibodies, siRNA or CD44-soluble proteins resulted in a marked reduction of the malignant activities of various tumors (Naor et al., 2002). According to the hierarchy model, CSCs are seen at the origin of tumorigenicity, migration and metastasis. They represent a small proportion of all cancer cells in the tumor mass and may be identified based on the expression of certain surface

markers which are unique for each subpopulation. CD44 was shown as a marker more specific to the CSC subpopulation compared to differentiated cells in many different tumor types. CSCs may be isolated by FACS based on CD44 expression alone or based on a combination of CD44 with other markers like CD133, CD24, CD166 or ALDH.

CD44 expression alone was employed for the identification and isolation of CSCs in cases of head and neck cancer, colorectal cancer and gastric cancer. CD44 positive cells in the cancer cell population have a high ability of tumorsphere formation *in vitro* as well as new tumor formation *in vivo*. Furthermore, to identify cells which are more selective of the CSC subpopulation, the combination of CD44 with one or more different markers was used. CD44 was combined with CD133 to identify the CSC population in colon cancer (Haraguchi et al., 2008) and liver cancer (Zhu et al., 2010). In addition, CD44+/CD24+ cells defined CSCs in pancreatic cancer while CD44+/CD24- cells have been shown to be the tumorigenic cells in breast cancer and retinal cancer. Co-expression of CD44 with other markers such as ESA, CD105, CD166 and ALDH was also used to identify CSC subpopulations in bone sarcomas (Gibbs et al., 2005), colon cancer (Dalerba et al., 2007), and breast cancer (Ricardo et al., 2011).

CD44 was recognized as the first marker for the identification of human gastric CSCs in gastric cancer cell lines by Takaishi *et al.* in 2009. In this study, five of the six gastric cancer cell lines studied had a subpopulation of CD44+ cells, and these cells showed a high capacity of tumorsphere formation *in vitro* and they also induced new tumors when injected into the stomach and skin of deficient mice. In addition, CD44+ cells were shown to be more resistant to chemotherapy and radiation therapy than CD44- cells. Knockdown CD44 by shRNA decreased the ability of tumorsphere formation as well as tumor size in mice (Takaishi et al., 2009). In a more recent study, Lau *et al.* demonstrated that the CD44v8-10 isoform but not CD44s corresponded to gastric CSCs which initiated tumor formation in immunocompromised mice. In addition the CD44v8-10 isoform was found at a lower level in normal tissue than in

malignant tissue (Lau et al., 2014).

IV.5 Role of CD133 in cancer stem cells

CD133 (or prominin-1) was discovered as the target of AC133, a monoclonal antibody which is selectively expressed in CD34+ hematopoietic stem/progenitor cells. CD133 is a plasma membrane glycoprotein with a molecular weight of 120 kD, containing an N-terminal extracellular domain, five transmembrane domains, two large glycosylated extracellular domains, and a cytoplasmic C-terminal domain (Yin et al., 1997; Weigmann et al., 1997) (Figure 22).

Known stemness genes such as Nanog, OCT4, Sox2, BMI1 are upregulated in CD133+ populations in many tumors in brain, lung, liver, and prostate cancers. These genes play a key role in the maintenance of CSC self-renewal, and their inhibition may lead to a loss of stemness properties such as tumorsphere formation, differentiation, increased sensitivity to chemotherapies and a significant downregulation of CD133 expression (Keysar and Jimeno, 2010). The relation of CD133 with growth and self-renewal capacity via the neurotensin/interleukin-8/CXCL1 signaling pathway has been reported. Here, overexpression of IL-8 protein was found in CD133+ cells isolated from both HCC cell lines and primary tumor cells in hepatocellular carcinoma. Furthermore, the enhanced IL-8 secretion in CD133+ cells was shown to increase the self-renewal ability, and promote angiogenesis and tumorigenesis. IL-8 overexpression in CD133+ hepatocellular cells may activate an IL-8-dependent feedback loop which signals using the MAPK pathway (Tang et al., 2012). One of the CSC properties is the high resistance to traditional chemotherapies. Cisplatin treatment of lung cancer cells *in vitro* increased the CD133+ cell population with the co-expression of ABC transporters with a stable cisplatin-resistant phenotype. In addition, CD133+ABCG2+ cells were spared by *in vivo* cisplatin treatment of xenograft tumors originating from primary lung cancer cells (Bertolini et al., 2009). In a similar manner, the radioresistant capability of CD133+ cells increased significantly compared to CD133- cells in the case of brain cancer. Furthermore,

CD133+ cells had an increased expression of BCL-2 and p-ATM proteins compared to CD133- cells in an ionizing radiation (IR)-treated mouse xenograft model. Effects of IR treatment on CD133+ cells increased in combination of debromohymenialdisine, an inhibitor of checkpoint kinases (Chiou et al., 2008). In particular, the use of an anti-human CD133 antibody conjugated with monomethyl auristatin, a potent anti-tumor drug, effectively inhibited the growth and induced apoptosis in hepatocellular and gastric cancer cell lines *in vitro* with IC50 values of 2-7 ng/ml. This result confirms that CD133 is a potential target for future treatment of gastric cancer (Smith et al., 2008). CD133 is primarily used as a surface marker to isolate CSC subpopulations from human brain tumors. A xenograft assay showed that only 100 CD133+ brain tumor cells were able to initiate tumors in NOD-SCID mice, while an injection of 10⁵ CD133- cells did not form new tumors. CD133+ cells also exhibited CSC properties *in vitro* (Singh et al., 2004). CD133 expression is therefore used to identify CSC subpopulations in different solid tumors. Like ALDH and CD44, CD33 may be used alone or in combination with other markers to define CSCs. For example, CD133 combined with ALDH is used to identify tumor-initiating cells in ovarian cancer (Silva et al., 2011) or with CD44 in gallbladder carcinoma (Shi et al., 2010).

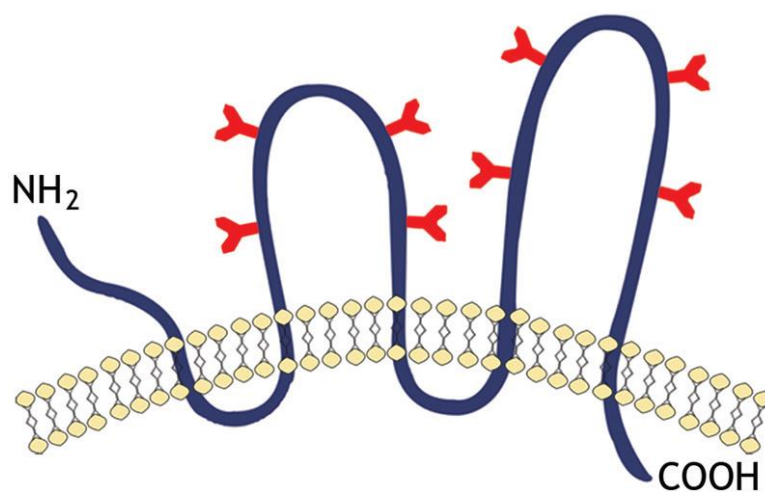


Figure 22. Schematic representation of the transmembrane glycoprotein CD133

In the model proposed by Miraglia *et al.*, CD133 has an extracellular N-terminus, a cytoplasmic C-terminus, 2 small cysteine rich cytoplasmic loops and 2 very large extracellular loops each containing 4 potential sites for N-linked glycosylation. Source: (Irollo and Pirozzi, 2013)

Although CD133 is widely used, some recent reports showed limits of this marker in

the identification of CSC subpopulations. In a study on colon cancer, both CD133+ and CD133- cells shared similar stemness including their tumor–initiating capacity as well as metastasis (Shmelkov et al., 2008). In addition, the limit of CD133 markers in defining CSCs was also shown in a glioma case. CD133+ glioma cells were purified using hCD133-microbeads; no unique glioma CSC subpopulation with self-renewal behaviour was detected compared to CD133- cells (Clément et al., 2009).

V. RETINOIC ACID IN CANCER THERAPY

Vitamin A and all of its active metabolites are collectively called retinoids, which are recognized as essential for most forms of life. It is well accepted that vitamin A plays an important role in controlling cell proliferation and differentiation, embryonic development, and immune function. Notably, the retinoid signaling pathway is often compromised early in tumorigenesis, which indicates that a reduction or an inactivation in the retinoid pathway may be associated with tumor development. Numerous recent studies reported on the retinoid role in cancer treatment, in part because of its capacity to prevent proliferation, induce differentiation, and senescence (De Luca, 1991; Chambon, 1996). In addition, a combination therapy of retinoids and other drugs is likely to successfully regulate the epigenetics as well as classical chemotherapeutic agents. Thus, retinoid research is particularly valuable in both cancer prevention and cancer treatment (Tang and Gudas, 2011). Nowadays, a wide range of animal models and experimental tools have been successfully utilized to clarify the function of retinoids at the cell and molecular levels.

V.1. Retinoid metabolism

V.1.1. Retinoids

All-trans retinoic acid and other active retinoids are derived from liposoluble vitamin A. Many other functions of this vitamin have been identified. Vitamin A has long been known to be absolutely necessary for vision, it acts as a light-sensitive molecule, absorbs light and communicates it to the brain. Besides that, it is crucial for fetal development including bones, lungs, heart, eyes, ears, and growth hormone (Blomhoff and Blomhoff, 2006).

Retinoids are classically described as a group of compounds with similar chemical structures comprising a beta-ionone ring, a polyene side chain and a polar end group. However, it is known that some synthetic forms have dissimilar structures but still show retinoid activity. No animal species has the ability to synthesize vitamin A *de novo*, and the only source of retinoids in most animals is diet-derived. Over 4,000 natural and synthetic molecules related to vitamin A have been reported. Three main active forms of natural retinoids have been extensively studied: All-trans, 9-cis, and 13-cis with All-trans being the predominant physiological form (Figure 23). All-trans retinoic acids can be transformed into different isomers under experimental and physical conditions (Napoli, 1996). Each isomer may cause various effects on the cell biological process via activation of different receptors.

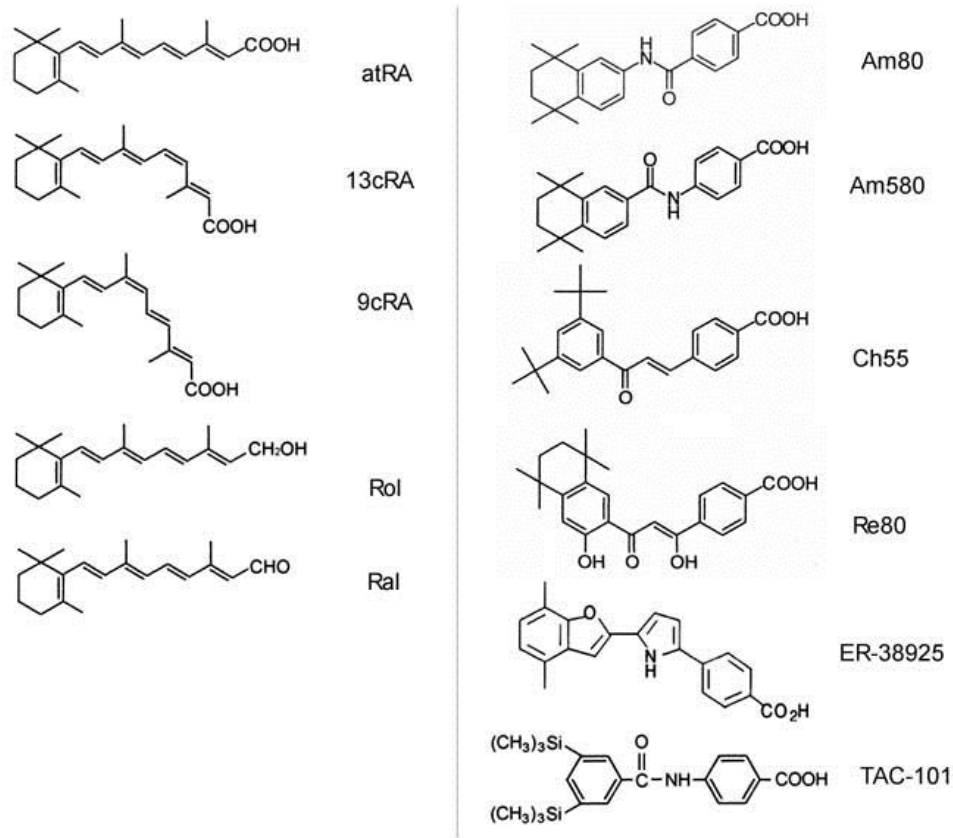


Figure 23. Chemical structures of retinoids used

Left panel: five natural retinoids. atRA: all-trans retinoic acid, 13cRA: 13-cis retinoic acid, 9cRA: 9-cis retinoic acid, Rol: all-trans retinol, Ral: all-trans retinal. Right panel: six synthetic retinoids. Source: (Yoshimura et al., 2003)

V.1.2. Synthesis and degradation of retinoic acids

Synthesis of retinoic acids

Retinol is the major retinoid in blood. It is converted from dietary β -carotene and retinyl ester in the intestine or from retinyl esters stored in the liver. RA is formed in cells from All-trans retinol by a two step oxidation process, which is represented in Figure 24. In mammals, the main circulating retinoid is bound to the retinol-binding protein (RBP). RBP is mainly synthesized in liver cells, and secretion of RBP from the liver is regulated by the availability of retinol. Retinol is then absorbed by target cells via a multi-transmembrane protein STRA6. This protein functions as an RBP receptor. Interestingly, STRA6 mutations have been identified as causes of a complex spectrum of developmental abnormalities and effects on visual function (Rhinn and

Dollé, 2012).

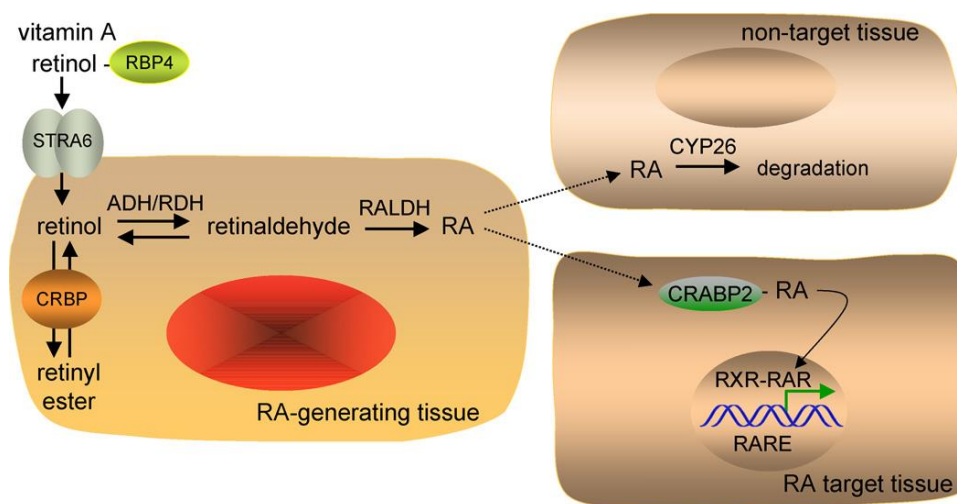


Figure 24. Retinoic acid synthesis and signaling

Retinol is carried in the serum by secreted retinol-binding protein (RBP4). It enters cells by the receptor STRA6, and the cellular retinol-binding protein (CRBP) facilitates its conversion to retinyl esters for storage. In a retinoic acid (RA)-generating tissue, there is a paracrine RA-signaling mechanism (depicted), where retinol is oxidized to retinaldehyde by either alcohol dehydrogenase (ADH) or retinol dehydrogenase (RDH), and retinaldehyde is oxidized to RA by retinaldehyde dehydrogenase (RALDH). RA is then released and taken up by surrounding cells. Cells expressing cytochrome P450 (CYP26) initiate the further oxidation of RA for degradation and excretion and are not RA target cells. Some RA target cells express cellular-RA binding protein (CRABP) that facilitates uptake of RA and transport to the nucleus where RA binds the RA receptor (RAR). The ternary complex of ligand bound-RAR with RXR and a retinoic acid response element (RARE) regulates transcription of RA target genes by altering the binding of corepressors and coactivators. Source: (Duester, 2008)

Oxidation of retinol to retinal:

The first step of RA synthesis is oxidation of retinol into retinaldehyde by retinol dehydrogenase enzymes. These enzymes belong to two families: the cytosolic alcohol dehydrogenases (ADHs) and microsomal short-chain dehydrogenases (SDR). Several members in the ADH family including ADH1, ADH3 and ADH4 all have the capacity of conversion of All-trans retinol into All-trans retinal (Mic et al., 2002; Duester, 2008). However, some of them showed a selective oxidation of retinol isomers. For example, ADH1 is capable of oxidizing 9-cis retinol but not 13-cis retinol, while ADH4 can oxidize all three including All-trans, 9-cis and 13-retinol into their

retinal forms (Martras et al., 2004). Important roles of other members have also been identified. Notably, RDH5 does not play a vital role in RA synthesis but it is important for vision (Lidén and Eriksson, 2006). Indeed, RDH10 is a crucial protein for RA syntheses during embryonic development and its mutations may lead to embryonic lethality (Belyaeva et al., 2008).

Oxidation of retinal to retinoic acid:

The second step of RA synthesis is retinal conversion into RA, mediated by enzymes of the ALDH (also called RALDH) superfamily. In humans, the ALDH superfamily is comprised of 19 genes belonging to 11 families and 4 subfamilies. Three aldehyde dehydrogenases which play an important role in this step are ALDH1A1, ALDH1A2 and ALDH1A3, all belonging to the ALDH1 family. The expression of these aldehyde dehydrogenases shows a high level of tissue specificity compared to ADHs.

ALDH1A1 is highly expressed in the dorsal retina of embryos and in several epithelial tissues and is associated with the metabolism of excess retinol. Furthermore, ALDH1A2 is expressed in numerous different tissues, both embryonic and adult. Studies on ALDH1A2 knockout mouse models suggest that ALDH1A2 plays a role in the production of RA in several cell types during embryonic development (Blomhoff and Blomhoff, 2006). ALDH1A3 contributes to RA synthesis in the eyes and olfactory system. ALDH1A3 is expressed in mouse and chicken retina, ALDH1A3^{-/-} mice have defects in nasal and ocular development and die due to respiratory distress within 10 h of birth, implying that it is important for RA synthesis.

Retinoic acid transport by cellular retinoic acid binding proteins (CRABPs):

CRABPs type I and II (CRABP-I and CRABP-II) have a high affinity for All-trans RA. CRABPs bind to the newly synthesized RAs and transport these molecules into the nucleus to then activate target gene transcription via interaction with their nuclear receptors. In adults, CRABP is expressed ubiquitously, while CRABP-II is only found in several tissues including the skin, ovaries, uterus and choroid plexus. CRABP-I presents RA to metabolising enzymes (CYP26), and CRABP-II delivers RA to RARs

by direct protein-protein interactions. Overexpression of CRABP-I may contribute to RA of cancer cells after combined retinoic acid radiation treatment (Blaese et al., 2003).

The degradation of retinoic acids

The distribution and levels of RA have to be tightly controlled during embryogenesis. Thus, RA catabolism is an essential process to balance for RA synthesis in cells and tissues. RA catabolism is mediated by enzymes of the cytochrome P450 26 subfamily including CYP26A1, CYP26B1 and CYP26C1 which have the capacity to convert RA into more polar metabolites such as 4-hydroxy-RA, 8-hydroxy-RA and 15-hydroxy-RA. Production of hydroxyl-RA results in downregulation of the RA concentration in the periphery of the cells. CYP26 proteins display various expression patterns indicating differential roles for each enzyme in RA catabolism (Rhinn and Dollé, 2012). CYP26a1 was the first CYP26 to be identified, and it is expressed in the rostral-most embryonic epiblast. Expression of all three Cyp26 genes has also been documented during hindbrain development (Sirbu et al., 2005). Genetic alternation of Cyp26 genes may lead to homeotic transformation of vertebrae and misspecification of the rostral hindbrain (Sakai et al., 2001).

V.2. Retinoic acid receptors and their roles

V.2.1. Retinoic acid receptor (RAR)

Chambon *et al.* were the first to identify the retinoic acid alpha receptor (RAR α) belonging to the steroid receptor family (Chambon, 1996). Continuing studies identified other RARs including RAR β and RAR γ . Furthermore, each receptor includes various isoforms by utilizing different promoters or splicing (Leroy et al., 1991). For example, two main isoforms of RAR α are RAR α 1 and RAR α 2, while RAR β has four main isoforms: RAR β 1, RAR β 2 and RAR γ 1 and RAR γ 2. In addition, regulation of expression of these isoforms is not similar during embryonic development (Takeyama et al., 1996). It is now known that regulation of RAR β 2 expression at the translational level involves choosing upstream open reading frames

(uORFs) in the 5'-untranslated region. Reynolds *et al.* showed that each uORF's process in individual functions. For example, in heart and brain tissues, uORF4 plays a crucial role and may be an inhibitor of other ORFs, whereas uORFs2 and uORFs25 play an important role in all other tissues (Reynolds et al., 1996). *In vivo* experiments of RAR α mice or RAR γ null mice have indicated the role of RAR receptors to viable capacity of these mice as well as their effects on normal functions of many organs in the body, whereas knockout or mutated mice of RAR genes exhibited growth deficiency or died *in utero*. This confirms the important role of RAR receptors in the RA signaling pathway during animal development.

V.2.2. Retinoic X receptor (RXR)

RXR was also discovered as a member of the nuclear-receptor superfamily. It is a specific receptor for 9-*cis* retinoic acid but not for other ligands. RXR usually binds to RAR to form a heterodimer complex with high affinity to DNA. However, RXRs can also form homodimers. Similar to RARs, three isotypes of RXR have also been identified: RXR α , RAR β and RAR γ (Chambon, 1996). These isotypes are encoded by different genes and each isotype has various isoforms (Table 2)

Table 2. Isotype of RA receptors

| Retinoic acid and Retinoic X receptors | | | | |
|--|--------------|---------------------------|------------|---|
| Receptors | Isotypes | Major Isoforms | Chromosome | Ligands |
| RAR | RAR α | RAR α 1 and 2 | 17q21.1 | All-trans and 9- <i>cis</i> retinoic acid |
| | RAR β | RAR β 1; 2; 3 and 4 | 3p24 | |
| | RAR γ | RAR γ 1 and 2 | 12q13 | |
| RXR | RXR α | RXR α 1 and 2 | 9q34.3 | 9- <i>cis</i> retinoic acid |
| | RAR β | RAR β 1 and 2 | 6p21.3 | |
| | RAR γ | RAR γ 1 and 2 | 1q22-q23 | |

Source: (Chambon, 1996)

Among three isotypes of RXR, RXR α is known to be the most abundant and it plays an important role during epidermal development. RXR α -null mice exhibited an aberration of epidermal cell proliferation and differentiation leading to a delay in hair follicle growth in adult mice (Li et al., 2001). Another study showed that approximately

50% of RXR β - β - mice died *in utero* or at birth due to a heart abnormality during development (Kastner et al., 1996). The RXR γ isoform also fulfills a role in the RA signaling pathway. A recent study using a RXR γ - γ - mouse model to identify the role of this gene during central nervous system development revealed that RXR γ is important for suppression of S-opsin expression. All mice bearing the RXR γ - γ - genotype highly expressed S-opsin in dorsal cone cells, while this protein was distributed in a few dorsal cone cells in wild-type mice (Roberts et al., 2005).

V.2.3. Role of retinoic acid receptors in gene transcription regulation

Regulation of gene transcription through binding to ligand binding domain – genomic activation

RAs function as ligands of RARs or RXRs. As mentioned above, RXR binds specifically to 9-cis RA, while RAR can bind to both All-trans retinoic acid 9-cis RA and All-trans RA. RA interacts with RAR/RXR heterodimers via binding to the ligand binding domain (LBD). The LBD which comprises a high conserved structure includes a ligand-binding pocket and an activation function (called AF12) controlling the interaction of RARs with co-regulators (Altucci and Gronemeyer, 2001; Rochette-Egly and Germain, 2009) (Figure 25).

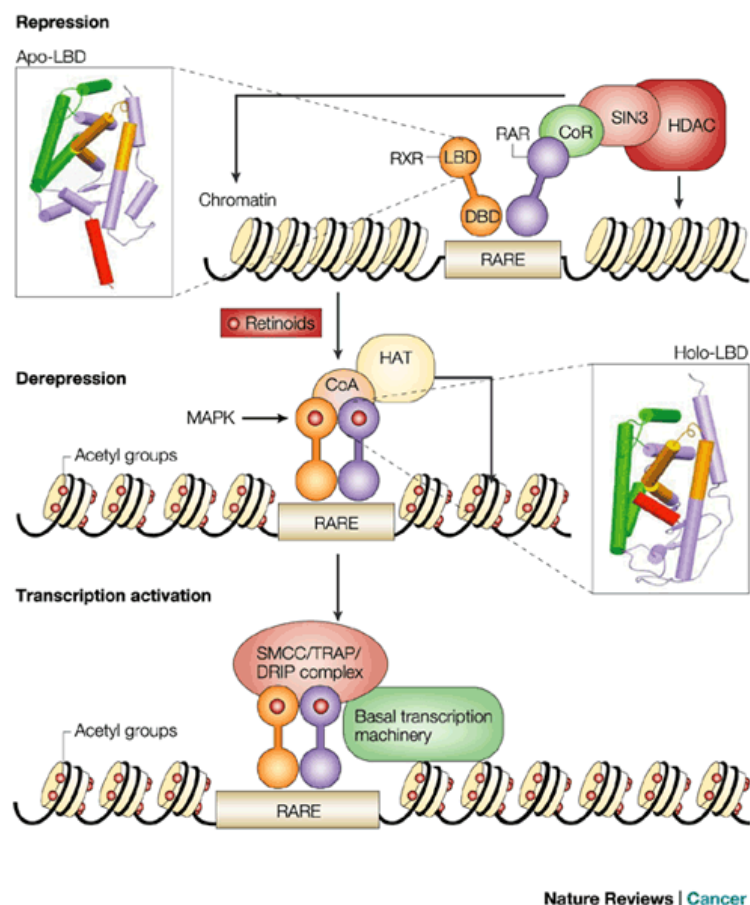
One crucial step in the activation process of RA signaling is the binding of RAR/RXR dimers to DNA sequences which are known as retinoic acid responsible elements (RAREs) or as retinoic X responsible elements (RXREs). RAREs are comprised of a short repeat sequence of the (A/G)G(G/T)TCA or (A/G)G(G/T)(G/T)(G/C)A motif (Rhinn and Dollé, 2012). The direct repeat sequence of RAREs are commonly separated by five (DR5) or two (DR2) nucleotides, while RXREs are typically separated by one nucleotide (DR1) (Blomhoff and Blomhoff, 2006). RAREs are distributed in the promoter structure of numerous target genes corresponding to RA signaling such as RAR β 2, Cyp26A1, CRPB1, CRAPB2 and several homeobox genes (Rochette-Egly and Germain, 2009).

RAR/RXR heterodimers interact with steroid receptor coactivators of the p160 family (such as SRC-1, SRC2, SRC3) or corepressors (such as NCoR, NCoR1, RIP13) to regulate the transcription of target genes. Co-repressors bind RAR/RXR heterodimers

via an Lxxl/Hlxxxl/L motif situated at the C-terminal, while co-activators contain a highly conserved LxxLL motif binding to receptors (Rochette-Egly and Germain, 2009). The interaction of these motifs with DNA promoters of target genes results in an alteration of the chromosomal structure around the binding site.

Co-activators role in recruiting different enzyme activity complexes including histone acetyltransferases (HATs), histone methyl transferases (HMTs), ubiquitinase/deubiquitinases and chromatin-remodelling complexes like SWI/SNF. In contrast, repressors do not bind to enzyme activity complexes but recruit complexes with high molecular weight such as histone deacetylases (HDACs). The contribution of coactivators and corepressors is represented as a “switch” for controlling transcription of target genes. HATs act gene expression through chromatin decondensation at the promotor site of target gene, while HDACs suppress gene expression via chromatin deacetylation (Perissi et al., 2010).

In the absence of RA, co-repressors bind to RAR/RXR receptor complexes leading to deacetylation in the chromatin structure and transcription is inhibited. In contrast, the binding of ligands to RAR/RXR heterodimers results in a conformational change in structure. Thereby, this complex destabilizes interaction with the co-repressor, and allows binding to co-activators in order to activate transcription.



Nature Reviews | Cancer

Figure 25. Mechanisms of transcriptional repression and activation by RAR–RXR.

In the absence of agonists, co-repressor complexes (CoRs) NCoR or SMRT bind to the RAR–RXR heterodimer and link the heterodimer to histone deacetylases (HDACs). HDACs remove acetyl groups from nucleosomal histones, resulting in chromatin condensation and gene silencing. Agonists induce a conformational change that destabilizes the interface with the co-repressor and allows interaction with co-activators (CoAs) of the p160 family. CoAs recruit (or pre-exist in a complex with) histone acetyltransferases (HATs), such as CBP (CREB-binding protein) or p300, whose action induces nucleosomal repulsion and chromatin decondensation. A third multisubunit complex, known as TRAP/DRIP/SMCC may lead to increased frequency of transcription initiation. DBD, DNA-binding domain; RAR, retinoic-acid receptor ; RARE, retinoic-acid response element; RXR, retinoid receptor. Source: (Altucci and Gronemeyer, 2001)

There is increasing evidence that HDAC plays an important role in controlling the transcription of RA-reduced target genes via interaction with the RA receptor complex. The HDAC protein family is comprised of 11 members (HDAC1-11) belonging to three different classes: class I includes HDAC1-3 and HDAC8; class II contains HDAC4–7, HDAC9 and HDAC10; and Class III consists of only member HDAC11. The role of HDACs is to remove acetyl groups on histone proteins to

change the chromosome structure, resulting in a disruption of the interaction of RNA polymerase II with target gene promoters. However, the combination of HDAC and different co-repressors is very important to obtain an epigenetic modification (Perissi et al., 2010).

Non-genomic activation

Recent studies found novel mechanisms of signal transduction via RA receptors to add to the classical mechanisms mentioned above, also called non-genomic effects. It has been shown that RA rapidly activates the p38MAPK/MSK1 or PI3K signaling pathway. Bruck *et al.* revealed that MSK1 phosphorylate RAR α at S369 located LBD, thereby allowing this receptor to bind to common transcription factor TFIIH. And finally, RAR α /TFIIH complexes require the activation of target genes. Indeed, it has also been demonstrated that deregulation of the MAPK/MSK1 signaling pathway in tumors results in a lack of response to RA (Bruck et al., 2009). Activation of p38MAPK in p38MAPK/MSK1 signaling is recognized in fibroblasts, mouse embryocarcinoma, breast cancer and leukemia. Nevertheless, it is also known that RA rapidly activates p42/44MAPK proteins in neuronal cells and Sertoli cells (Al Tanoury et al., 2013) (Figure 26).

Other reports suggest that the presence of RARs in the cytosol or in cell membranes indicates a role in PI3K activation. It is believed that the absence of RA results in the binding of RAR to p85, a regulatory step in the PI3K signaling pathway. In contrast, the binding of ligands to RAR leads to an interaction of this complex with p110, a catalytic subunit of PI3K, hence inducing this pathway activation (Pan et al., 2005; Masiá et al., 2007).

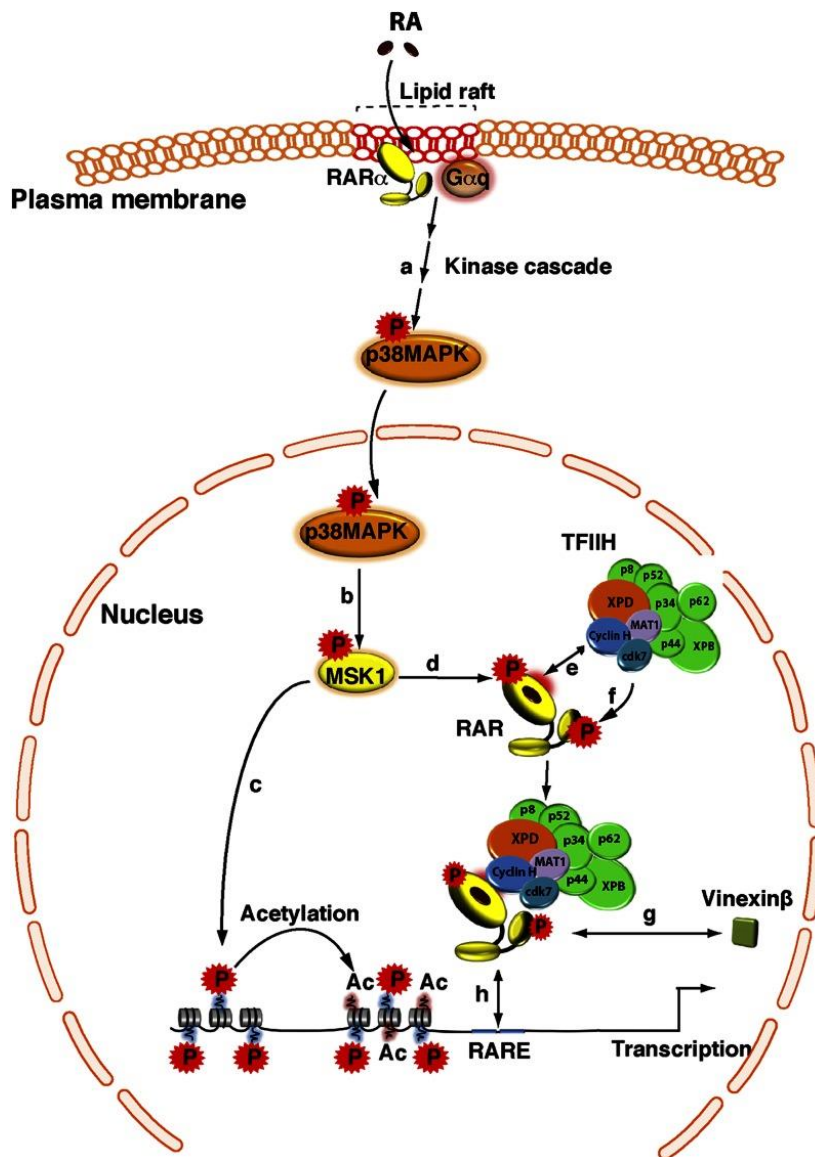


Figure 26. Crosstalk between the RA-activated p38MAPK pathway and the expression of RAR target genes

In response to RA, p38MAPK is activated (a), and then translocates into the nucleus and phosphorylates MSK1 (b). MSK1 phosphorylates histones (c) and RARα (d). Following conformational changes, the cyclin H subunit of the CAK subcomplex of TFIID is recruited to an adjacent domain (e), and forms the RARα/TFIID complex and allows the phosphorylation of the NTD by the cdk7 kinase (f). For the RARγ subtype, phosphorylation of the NTD promotes the dissociation of coregulators, such as vinexinβ (g). Finally, phosphorylated RARα is recruited to response elements located in the promoter of target genes (h). Source: (Al Tanoury et al., 2013)

Target genes are regulated by RA

RA is now known as an ubiquitous signaling molecule affecting the expression of a large number of different target genes in most species. To date, the review of Balmer and Blomhoff in 2002 seems to be the most systematic study on gene groups regulated by RA. Following this study and further data, we know that 532 genes are regulated by RA, and they are classified into four groups according to the level of direct or indirect control by RA. Group 0 (or category 0) includes 133 genes which seem to be regulated indirectly, group 3 (category 3) is comprised of 27 genes regulated directly by RA, groups 1 and 2 (categories 1 and 2) include 372 genes which are between groups 0 and 3 with some evidence of direct regulation but which is not sufficient (Balmer and Blomhoff, 2002). Importantly, 27 genes regulated by RA contain functional binding sites to an RAR/RXR heterodimer and this has been confirmed by experiments (Table 3). A study on mouse embryonic fibroblasts revealed that RA activates the TGF β signaling pathway, and around approximately 1,000 genes were activated (Fadloun et al., 2008). However, in this study it was not possible to identify the genes regulated directly or indirectly by RARs. Another study of this group used chromatin immunoprecipitation in combination with array hybridization in the analysis of binding of 354 target loci to RA receptors and suggested that RAR binds directly to *Ctgf* and TGF β 3 genes (Delacroix et al., 2010). In the most recent studies, several other new RA targets were also identified such as *Grsf1*, *Ror2* and *Prickle 1* involved in antero-posterior patterning and development (Savory et al., 2014), and *G0S2*, known to be a G0/G1 switch gene which plays an important role in regulation of cell cycle and differentiation (Kitareewan et al., 2008, Heckmann et al., 2013). Interestingly, existence of a RARE sequence on the promoter of a *G0S2* gene has been identified and the mutation in this RARE sequence is associated with a decrease in RA binding on the *G0S2* promotor. Consequently, *G0S2* is proposed as a direct target gene for RA (Kitareewan et al., 2008).

Table 3. Target genes that are directly regulated by retinoic acid

| Gene Symbol | Name in reference | Expression change | References |
|-------------------------|----------------------------------|--------------------------|---------------------------|
| ADH1C | ADH3 | Up | Balmer and Blomhoff, 2002 |
| CD38 | CD38 | Up | |
| Cdx1 | Cdx1 | Up | |
| CEBPE | C/EBP epsilon | Up | |
| CRABP2 | CRABP-II | Up | |
| Cryab | α B-crystallin/small HSP | Up | |
| Drd2 | dopamine D2 receptor | Up | |
| Egr1 | Egr-1, zif268, Krox-24 | Up | |
| ETS1 | Ets1, ets-1 | Up | |
| Foxa1 | HNF-3 α | Up | |
| H1F0 | H1 $^{\circ}$ histone, H1 degree | Up | |
| Hoxa1 | ERA-1, Hox-1.6, Hoxa-1 | Up | |
| HOXA4 | hoxa-4 | Up | |
| Hoxb1 | Hoxb-1 | Various | |
| Hoxb4 | Hox-2.6, Hoxb-4 | Up | |
| Hoxd4 | Hox-4.2, Hoxd-4 | Up | |
| HSD17B1 | 17HSD type 1 c | Up | |
| IL2RA | IL-2R α | Up | |
| Pck1 | PEPCK | Up | |
| Pit1^d | Pit-1 | Up | |
| RARA | RAR- α 2 | Up | |
| RARB | RAR β | Up | |
| RARG | RAR γ | Up | |
| Rbp1 | CRBPI | Up | |
| SFTPB | SP-B | Up | |
| Tgm2 | TGase 2 | Up | |
| Ucp1 | ucp, upc-1 | Up | |
| CDX1 | CDX-1 | up | Houle et al., 2000 |
| CDKN1A | p21WAF1/CIP1 | up | Tanaka et al., 2007 |
| Tbx3 | T-box 3 | up | Ballim et al., 2012 |
| GOS2 | G0/G1switch 2 | up | Kitareewan et al., 2008 |
| TGFB3 | TGF- β 3 | up | Delacroix et al., 2010 |
| CTGF | <i>Ctgf</i> | up | Delacroix et al., 2010 |
| F11R | <i>F11r, Jam</i> | up | Savory et al., 2014 |

Furthermore, recent reports have shown that RARs bind to several genes involved in cell cycle and cell transformation such as *Tnfrsf13*, *Ccnd1*, *Nupr1*, *Fgf18*, and *Src* (Delacroix et al., 2010). In addition, Tanoury *et al.* identified approximately 50 RA-directed genes involved in cell adhesion, some of which encode key proteins related to cell adhesion capacity like integrin, cadherin 17, collagens, vitrin, vanin and robos. All genes are downregulated in the absence of RA. In contrast, in the presence of ligands, numerous target genes involved in metabolism signal transduction are upregulated (Al Tanoury et al., 2014). It is interesting to note that F11r, which encodes a junction adhesion molecule A belonging to the adhesion protein family, is an new RA target gene. In addition, electrophoretic mobility shift assay allowed the confirmation that RARs bind directly to DR5 elements in the F11r promotor region (Savory et al., 2014). In particular, CDKN1A (p21WAF1/CIP1), which plays an important role in the regulation of cell cycle and senescence, is also a direct target gene of RA. RA regulates transcription of the P21 gene via the binding of RXR α to the RARE sequence of the P21 promoter (Tanaka et al., 2007).

Notably, numerous RA target genes involved in the regulation of pluripotency and self-renewal of embryonic stem cells (ESCs) have been shown (Giuliano et al., 2005). The 12p13.31 cluster is known to be a cassette including the pluripotent gene Nanog and several markers of ESCs such as CD9, GDF3, Stella and EDR1 (Giuliano et al., 2005; Korkola et al., 2006). RA is known to increase differentiation in ES cells by regulating the expression of Nanog as well as ESC markers. Importantly, Oct4, a key gene for pluripotency is also down-regulated in RA-induced ES cells (Giuliano et al., 2005; Gu et al., 2005). Furthermore, it was shown that knockdown of oct4 using siRNA results in repressed Nanog expression as well as EDR1, GDF3 and Stella expression (Giuliano et al., 2005). Indeed, many different genes involved in pluripotency and self-renewal such as SOX2, POUL5F1, TDGF1 and Lin 28 have also been identified as being downregulated during RA-induced ESC differentiation (Delacroix et al., 2010; Jagtap et al., 2013).

RA regulates signaling pathways during embryonic development

One of the most important roles of RA is its effect on expression of genes in signaling pathways involved in stem cells such as EGF, Notch, Hedgehog, Wnt and NF- κ B. Many different studies showed that RA activates NF- κ B signaling, resulting in differentiation of ESCs (Kang et al., 2007; Huang et al., 2010). It has been further demonstrated that activation of RA-induced NF- κ B signaling results in increased expression of miR-10a and miR-1; microRNAs have an important function during differentiation of ESCs by repressing the expression of self-renewal genes like KLF4 and HDAC1 (Huang et al., 2010; Xie et al., 2011; Xie et al., 2011).

Wnt signaling plays an important role in self-renewal maintenance and differentiation in ESCs and adult stem cells as well as CSCs. Inhibitory effects of RA on the Wnt signaling pathway associated with mouse ESC differentiation has been recognized. It has been shown that inactivation of the Wnt signaling pathway is due to an increased RA-induced expression of secreted frizzled-related protein-2 (Sfrp2) which contains homology domains to the frizzled receptors (Rattner et al., 1997; Aubert et al., 2002). Furthermore, it has also been suggested that β -catenin binds directly to RAR but not to RXR and therefore, RA directly regulates β -catenin–LEF/TCF signaling during ESC differentiation (Easwaran et al., 1999). Interestingly, a recent study by Osei-Sarfo *et al.* revealed that RA inhibits the canonical Wnt signaling pathway but activates non-canonical Wnt signaling pathway during ESC differentiation. RA induced the non-canonical Wnt signaling pathway via increased expression of its receptors (Wnt 5a, Wnt 7a, Fzd2 and Fzd6) and Tcf3 (Osei-Sarfo and Gudas, 2014).

Recent evidence points to the importance of the Notch signaling pathway during embryonic development. Inhibition of Notch signaling pathways by some inhibitors like 6-bromoindirubin-3'-oxime, a glycogen synthase kinase-3 β inhibitor or γ -secretase, efficiently induced differentiation of ESCs into all intestinal cells via activation of molecular markers such as IFABP and ISX in enterocytes, Tff3 in goblet cells, LYZ in Paneth cells, and GAST, SYP and SST in enteroendocrine cells (Ogaki et al., 2013). In addition, motor neuron differentiation from human ESCs has also

been closely related to inhibition of Notch signaling. It has been shown that inactivation of the Notch signaling pathway by a γ -secretase inhibitor results in downregulation of Hes5 expression, which remain neural progenitor cells (Ohtsuka et al., 1999), thereby increasing the differentiation of ESCs into motor neurons (Ben-Shushan et al., 2015).

Similar to the signaling pathways presented above, the Hedgehog signaling pathway maintains an important role during embryonic development. It is known that Hh proteins act as morphogens which control different developmental processes, and hedgehog expression is found in the brain, notochord, and the zone of polarizing activity during embryonic development, (Varjosalo and Taipale, 2008). A study on anterior neuronal differentiation in *Xenopus laevis* embryos suggested that RA acts very early in the primary neurogenesis by inhibiting shh expression, which is proven to be an inhibitory differentiation, and enhancing proliferation in cerebellar cells (Rowitch et al., 1999). Patched 1 (Ptch1), a known receptor of sonic hedgehog, acts as a repressor of the smoothed (Smo) protein. The interaction of shh with Ptch1 results in releasing Smo and activating cell proliferation (Tabata and Kornberg, 1994). Hedgehog inhibition by increasing RA-induced Ptch1 expression has been found. Furthermore, the enhanced Ptch1 expression was implicated in induction of Meis1 expression, a direct RA target gene. This finding is important to develop a clinical cancer therapy (Busch et al., 2014).

V.3. Role of retinoic acid in anticancer treatment

Carcinogenesis is the process of transformation of normal cells into cancer cells. This process includes a series of genetic and epigenetic changes, and thus leads to uncontrolled cell division and formation of a malignant tumor mass. RA can inhibit tumorigenesis as well as tumor growth by interfering with this process via the

activation of apoptosis, cell division inhibition, and induction of senescence and cell differentiation (Figure 27). RA antitumor activity has been widely studied using different models as well as clinical trials for both leukemia and solid tumors. To date, it has gained success in the treatment of leukemia types by RA, and also opens promises in the treatment to numerous solid tumors.

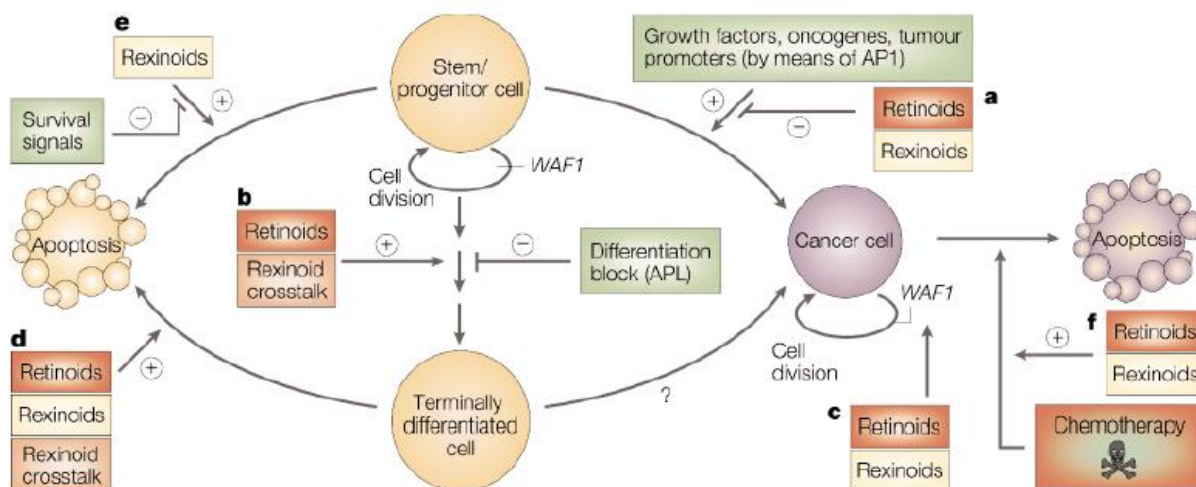


Figure 27. Retinoids and rexinoids can interfere with events leading to tumorigenicity at several levels.

a) In skin, chemical carcinogenesis is blocked at the promotion step, probably because of the anti-AP1 activity of retinoids and rexinoids. b) Retinoids and rexinoids are strong inducers of cell differentiation and might overcome a block in a differentiation pathway. c) Retinoid and rexinoid action is associated with a cell-cycle block in G1, frequently because of the increased expression of WAF1, a direct target gene of retinoid and vitamin D3 receptors. d) In myeloid cells, retinoid and rexinoid action or crosstalk between rexinoids and protein kinase A leads to post-maturation apoptosis. e) Rexinoids can autonomously induce premature cell death and survival and differentiation signals rescue the cells from rexinoid apoptosis. f) Perhaps owing to activation of death receptors and/or their cognate ligands, retinoids and rexinoids - alone or in combination with chemotherapy ('sensitization') - can synergistically induce apoptosis. Source: (Altucci and Gronemeyer, 2001)

V.3.1. RA in acute promyelocytic leukemia

Acute promyelocytic leukemia (APL) is a subtype of AML and represents approximately 5 to 8% of all AML cases. Treatment of the HL-60 cell line, isolated

from a patient with APL, induces cell differentiation at a concentration of 1 nM. Notably, 1 μ M RA was sufficient to cause differentiation of 90% of the HL-60 cells into mature granulocytes (Breitman et al., 1980). Seven years later, Huang et al. used ATRA successfully to obtain complete remission in patients with APL. (Huang et al., 1988). Other clinical trials in APL patients have also confirmed the high efficacy of RA to induce complete remission and to increase the five-year survival rate (Warrell et al., 1991).

In almost all APL cases the chromosomal translocation and/or the fusion of promyelocytic leukemia gene PML (on chromosome 15) and the RAR α gene (on chromosome 17) led to formation of PML-RAR α complex (Grignani et al., 1993). This fusion inhibits the apoptotic pathway, as well as cell differentiation, resulting in the accumulation of immature granulocytes (granulocyte precursors) (Grignani et al., 1993). The binding of ATRA and other RA isoforms to PML-RAR α LBD results in an alteration of the corepressor complex; it also relieves HDAC, triggers the transcription through coactivator complexes and finally, induces cell differentiation (Altucci and Gronemeyer, 2001). Furthermore, RA rapidly induces the cAMP/PKA pathway leading to an accumulation of intracellular cAMPs in APL cells. Subsequently, cAMP activates RAR target genes, followed by an increase in the differentiation of APL cells (Zhao et al., 2004). Indeed, inhibitory effects of RA on APL cells is also associated with the regulation of Start1, tyrosine kinases and MAP signaling (Kambhampati et al., 2004; Gianni et al., 1997) .

However, treatment with RA alone has increased resistance to RA leading to a reduction in the remission rate and relapse after treatment. Therefore, the combination of RA and other drugs is necessary to reduce RA resistance in APL patients. Several drugs such as daunorubicin, ara-C, methotrexate, 6-mecaptoprine (Fenaux et al., 1999) and arsenic trioxide (As₂O₃) (Huang et al., 2012) were combined with ATRA to treat APL patients. Lo-Coco *et al.* showed a two year event-free survival rate reaching 97% in APL patients treated by ATRA-As₂O₃ compared to 86% in the group treated by ATRA-chemotherapy (Lo-Coco et al., 2013). A low dose

of arsenic trioxide activates cell differentiation, while at a high dose, it induces apoptosis (Zhou et al., 2007).

V.3.2. RA in solid tumors

The success of ATRA use to treat APL patients has opened a promise to utilize RA in the treatment of solid cancers. Notably, 13-cis-RA is used in clinical trials for the treatment of skin, head and neck, prostate, non-small-cell lung and cervical cancer, while ATRA and 9-cis RA are used in treatment of thyroid, prostate, breast, renal-cell and squamous cell cancers (Altucci and Gronemeyer, 2001).

In neuroblastoma, 13-cis-RA is effectively used to treat children with high-risk neuroblastoma, increasing the 5 year event-free survival rate and compared to chemotherapy, decreasing the risk of relapse after stem cell transplantation (Matthay et al., 2009). Treatment of patients carrying advanced stage tumors of thyroid cancer by ATRA showed an increase in iodine uptake and cell differentiation compared to before therapy (Zhang et al., 2007). Similar to that, a cell growth inhibitory effect of RA on many other solid tumors such as prostate cancer, lung cancer, and ovarian cancer has been clearly demonstrated in *in vitro* culture and mouse models. In addition, mechanisms by which RA inhibits growth of cancer cells have been also explained clearly such as the induction of apoptosis, cell cycle arrest, senescence and differentiation. Of note, regulation of the differentiation of CSCs is seen as the most important characteristic of RA to develop anticancer therapies. Various studies have shown that RA induces the differentiation of CSCs via the Notch or MAPK signaling pathway in glioblastoma (Ying et al., 2011; Karsy et al., 2010), or by suppressing the wnt/ β -catenin signaling pathway in head and neck carcinoma (Lim et al., 2012). Nevertheless, results of RA treatment in patients with solid tumors have not fulfilled the expectations (Connolly et al., 2013). For breast cancer, evidence of inhibitory effects of RA on breast cancer cell lines in culture have been confirmed. Furthermore, clinical trials have also been carried out in phase II with ATRA (Sutton et al., 1997) or fenretinide, a synthetic retinoid (Modiano et al., 1990) on advanced breast cancer patients; however, no statistically significant difference was shown.

Limits of the effect of RA on these cancers may be explained by epigenetic modifications in DNA molecules or histone proteins and therefore the combination of RA and epigenetic inhibitors which can affect methylation or de-acetylation of target cells, is necessary in future therapeutics (Tang and Gudas, 2011, Schenk et al., 2014).

V.4. Retinoic acid signaling pathway and gastric carcinoma

V.4.1 Modifications of RA signaling in gastric cancer

Alterations in the expression of genes involved in RA signaling have been described in gastric carcinoma. Several early studies showed the change of expression level of genes coding for RAR and RXA in gastric tumor tissues compared to normal tissues. Furthermore, RAR (α , β and γ) and RXR (α , β) were expressed in all normal tissues of the stomach, whereas RAR α was significantly downregulated in intestinal metaplasia, dysplasia and gastric cancer tissues. RAR α and RAR β were also expressed in only 30% of the cancer tissues studied (Jiang et al., 1999). This early finding identified the role of RAR α in gastric tumorigenesis. In another study, Kim *et al.* found that RAR β was decreased in almost all gastric cancer tissues compared to normal tissues. This study suggested in particular that silencing of RAR β in gastric cancer due to overexpression of the HDAC1 protein, an important protein involved in epigenetic changes, may represent a certain role during gastric tumorigenesis (Kim et al., 2004). Indeed, it has been shown that deacetylation of histone H4 is progressively regulated from the early stages to the late stages of gastric tumorigenesis, and is found in almost gastric carcinomas (Tahara, 2002). However, other earlier studies on gastric cancer cell lines showed that the transcriptional inactivation of RAR β due to CpG hypermethylation on the promoter site and its expression could be retrieved by treatment with 5-azacytidine (Hayashi et al., 2001; Oue et al., 2002; Oue et al., 2003).

Interestingly, RAR β promoter hypemethylation is found more frequently in the diffuse type than in the intestinal type of gastric cancer (Oue et al., 2002). CpG hypermethylation in the CRBP1 gene, which plays an important role in transportation of RA from the cytoplasm into the cell nuclei, is also found in gastric cancer cell lines as well as in cancer tissues (Shutoh et al., 2005). Thereby, it seems that the inactivation or downregulation of the expression of genes coding for receptors or other proteins of the RA signaling pathway may be associated with both methylation and deacetylation mechanisms in the chromosomal region containing their promoters, and these epigenetic alterations are useful for prognosis or as novel targets for gastric cancer therapeutics (Duester, 2008; Tahara, 2002).

V.4.2 Role of RA in gastric cancer treatment

Investigation of the inhibitory effect of RA and retinol on gastric cancer was first carried out in the 1990s. In a first clinical study on patients after gastric cancer surgery, Fujii *et al.* showed that the use of vitamin A in combination with auxiliary chemotherapies could decrease the recurrence rate and improve the survival rate compared to the group treated with chemotherapy only. However, the difference between these two groups was not significant (Fujii and Yokomori, 1991). Several *in vitro* analyses carried out later suggested that ATRA and other forms of RA such as 13-trans RA and 9-cis RA inhibited the growth of gastric cancer cell lines (SC-M1, and TSGH9201 cell lines). The role of the Bcl-2 gene in RA-reduced growth arrest was shown. The growth of SC-M1/Bcl-2 cells, which were transfected with a Bcl2-DNA vector, was inhibited when treated with RA compared to SC-M1/neo cells (Chou et al., 2000). It was also found that the treatment of gastric cancer cells with ATRA upregulated the expression of RAR α and induced cell cycle arrest at G0/G1 phase but decreased the S phase (Shyu et al., 1995). In addition, RA also decreased the expression of cyclin A and B1 involving the cell cycle control (Chao et al., 1997). Interestingly, ATRA-induced downregulation of VEGF expression leading to cell cycle arrest at the G0/G1 phase in BGC-823 cells. Apoptosis induction by ATRA was also found on MKN45 and MKN28 gastric cancer cell lines in monolayer culture conditions. However, the apoptosis level was less than 5% (Fang and Xiao, 1998). ATRA treatment on BGC-823 cells (RAR α (+) and RAR β (+)) and MKN45 cells (RAR α

(low) and RAR β (+)) inhibited the activator protein-1 (AP-1) in the BGC-823 cells but not the MKN45 cells. Transfection of the MKN-45 cells with the RAR α -DNA vector resulted in AP-1 downregulation as well as ATRA-induced inhibition of cell proliferation and colony formation. This showed that RAR α and RAR β are necessary mediators in gastric cancer inhibition by ATRA via downregulation of AP1-activity (Wu et al., 2002). In contrast, ATRA and 9-cis RA were able to induce cell growth arrest via upregulation of two protein tyrosine kinases including Eph and Hek5 (Kao et al., 2003). It should be noted that ATRA treatment on the SC-M1 C123 gastric cancer cell line also increased the expression of S100P, a calcium-binding protein involved in drug resistance and metastasis (Shyu et al., 2003). Consequently, RA treatment of cancer cells in combination with S100P targeting may be a promising therapy in the future (Arumugam and Logsdon, 2011). Besides the use of traditional RAs like ATRA and 9-cis RA in growth inhibition of gastric cancer cells, 4-amino-2-trifluoromethyl-phenyl retinate (ATPR), a novel RA analog has also been proposed as a potential growth inhibitor in gastric cancer. Indeed, ATPR (50 μ M) increased the cell number at the subG1 phase in AGS and MKN74 cell lines. In addition, ATPR reduced the Bcl-2/BAX ratio as well as the AP1-activity (Hu et al., 2014).

In summary, many studies have focused on the role of RA in gastric cancer. However, many limitations in the understanding of the mechanism as well as anticancer potential of RA in gastric cancer remained. In the present study, we describe the important role of ATRA in gastric cancer therapeutics via its effects on gastric CSC properties.

PART II. Results

**Article 1 – CD44 and Aldehyde dehydrogenase
are markers of cancer stem cells in intestinal
and diffuse types of non-cardia gastric
carcinoma**

Submitted for publication

CD44 and aldehyde dehydrogenase are markers of cancer stem cells in diffuse and intestinal types primary gastric carcinoma

Phu Hung Nguyen^{1,2}, Lucie Chambonnier^{1,2}, Pierre Dubus^{2,3,4}, Linda Wittkop^{2,5,6}, Geneviève Belleannée⁴, Denis Collet⁴, Isabelle Soubeyran⁷, Serge Evrard⁷, Benoit Rousseau^{2,8}, Nathalie Senant-Dugot^{2,9}, Francis Mégraud^{1,2,4}, Frédéric Mazurier¹⁰, Christine Varon^{1,2}.

1 INSERM, U853, Bordeaux F-33000, France.

2 Université de Bordeaux, Bordeaux F-33000, France.

3 EA 2406, Bordeaux F-33000, France.

4 University Hospital Center of Bordeaux, Bordeaux F-33000, France.

5 INSERM, ISPED, Centre INSERM U897-Epidemiologie- Biostatistique, F-33000 Bordeaux, France.

6 Pôle de Santé Publique, Service d'information Médicale, University Hospital Center of Bordeaux, Bordeaux F-33000, France.

7 Institut Bergonié, Bordeaux F-33000, France.

8 Service Commun des animaleries, animalerie A2, Bordeaux F-33000, France.

9 SFR TransBioMed, Bordeaux F-33000, France.

10 CNRS UMR 7292, GICC LNOx, Tours F-37032, France.

Short title : CD44 and ALDH as gastric cancer stem cells markers

Contact. Dr. Christine Varon, INSERM U853, Université de Bordeaux, 146 rue Leo Saignat, Bordeaux F-33000, France. Email: christine.varon@u-bordeaux.fr. Tel: +33(0)557579575, Fax: +33(0)556514182.

Summary

Gastric adenocarcinoma are heterogeneous, and current classification based mainly on stomach localization and histopathological criteria remain poorly indicative for therapy. This study aimed to identify and characterize biomarkers of cancer stem cells (CSC) in primary intestinal and diffuse variants of non-cardia gastric adenocarcinoma. Mouse xenograft models of patients primary tumors were developed. The expression of eleven CSC markers was studied, and tumorigenic properties of FACS-sorted cells were evaluated *in vitro* and *in vivo*. Results revealed that tumorigenic CSC expressed the cell surface markers ESA, CD133, CD166, CD44 and a high ALDH activity. *In vivo* studies of tumorigenicity in limiting dilutions showed that ALDH⁺ cells formed tumors at a higher frequency than CD44⁺ cells and CD133⁺ cells. In conclusion, CD44 expression and ALDH activity define a small subpopulation of cells containing CSCs, and can be considered as markers of CSC in both intestinal and diffuse variants of non-cardia gastric adenocarcinoma.

Key words. Gastric cancer ; gastric adenocarcinoma; xenograft ; tumorsphere ; cell sorting ; ELDA ; variant ; CD133 ; CD166 ; tumor initiating cell; Aldefluor; side population; *Helicobacter pylori*; signet ring cell carcinoma; tumorsphere; biomarker; human

Introduction

Gastric cancer is the fourth most common cancer in frequency and the third leading cause of cancer mortality in the world. Ninety-five percent of all gastric cancers are gastric adenocarcinomas. They can be divided into 2 subtypes depending on their localization in the stomach: adenocarcinomas of the cardia, whose etiology remains unclear, and non-cardia gastric adenocarcinomas which develop in the body of the stomach. Among the possible etiological origins of non-cardia gastric adenocarcinoma, the main factor is the chronic infection by *Helicobacter pylori*, considered to be responsible for more than 93% of the cases (Gonzalez et al., 2012). Infection with *H. pylori*, classified as a class 1 carcinogen by the WHO in 1994, induces a chronic inflammation evolving over decades from a chronic atrophic gastritis with intestinal metaplasia, to dysplasia and finally adenocarcinoma (IARC'Working'Group, 1994) (Correa and Houghton, 2007) (Bessede et al., 2014a) . Some cases are also related to Lynch syndromes (with microsatellite instability, MSI) and to Epstein Barr Virus (EBV) infection. The classification of gastric adenocarcinomas is based essentially on histological criteria. The Lauren classification system distinguishes 2 main subtypes, the intestinal type which represents the majority of the cases, and the diffuse type (Lauren, 1965). The intestinal type is composed of glands having more or less preserved the glandular organization and differentiation state, or having acquired intestinal characteristics; it is sub-classified into tubular, mucinous or papillary carcinoma in the WHO classification of gastric carcinoma (Flejou, 2011). The diffuse type is characterized as poorly cohesive, composed of isolated cells (often signet ring cells) producing mucins.

These classification systems have little clinical utility, as they cannot orientate patient therapy. Furthermore, there is no specific molecular signature of gastric carcinoma variants with the exception of Her2 positivity which orientates toward Herceptin treatment. As a

consequence, treatment is still based essentially on surgery combined with conventional chemotherapy and/or radiotherapy, and the five-year survival rates remain under 30% in most countries (Luis et al., 2013).

Tumors are heterogeneous, composed of cells which are more or less differentiated and not all proliferative. In 1997, Dick *et al.* described in acute myeloid leukemia an immature subpopulation of cells with the capacity to reproduce the disease after transplantation in NOD/SCID mice, paving the way for the cancer stem cell (CSC) theory (Bonnet and Dick, 1997). Over the last decade, extensive research has focused on the discovery and the characterization of CSCs at the origin of cancers in numerous organs, and it is now believed that cancer is a stem cell disease (Alison et al., 2010) (Clevers, 2011). These CSCs correspond to a subpopulation of cells within the tumor defined by self-renewal and asymmetrical division and differentiation properties, giving rise to more or less differentiated cells composing the tumor mass, and by tumorigenic properties when transplanted in immunodeficient mice *in vivo*. CSCs are able to stay in quiescence under some conditions, to resist conventional chemotherapies or radiotherapies, and later, to be at the origin of metastasis.

The definition of CSCs remains largely operational and is based on functional assays that register self-renewal and asymmetrical division properties, giving rise to tumorsphere formation *in vitro*, and tumor initiation properties *in vivo* (Alison et al., 2010) (Clevers, 2011). Several CSC markers have been characterized in tumors of different organs, including CD133, CD44 and CD24 among those studied (Alison et al., 2010) (Clevers, 2011) (Al-Hajj et al., 2003) (Li et al., 2007) (Collins et al., 2005) (Zhang et al., 2008) (Singh et al., 2004) (O'Brien et al., 2007) (Ricci-Vitiani et al., 2007). More recently, the activity of the aldehyde dehydrogenases (ALDH), intracellular enzymes involved in oxidation of aldehydes and

retinoic acid signaling, also identified CSCs in acute myeloid leukemia (AML) (Cheung et al., 2007) and in solid tumors in the breast (Ginestier et al., 2007), lung (Jiang et al., 2009), colon (Huang et al., 2009)(Huang et al., 2009) and other organs (Ma and Allan, 2011).

In the stomach, their existence has been subject to debate. The first study performed by Takaishi *et al.* on gastric cancer cell lines proposed CD44 as a marker of gastric CSCs, but this marker was expressed in 3 out of 6 gastric cell lines, and confirmation in primary tumors was lacking (Takaishi et al., 2009). Then, the study performed by Rocco *et al.* on 12 human primary cases of gastric adenocarcinoma failed to demonstrate tumor-initiating properties of CD133 and CD44 sorted cells in xenograft assays in both NOD/SCID and nude immunodeficient mice (Rocco et al., 2012).

In addition, a point that need to be addressed concerns the heterogeneity of gastric adenocarcinomas, classified in numerous histological variants depending on the different classification systems, which suggests that markers of gastric CSCs, if they indeed exist, may be different according to the histological variant of gastric carcinoma.

In this study, we aimed to confirm the existence of CSCs and to characterize markers allowing their identification and isolation in human primary non-cardia intestinal and diffuse type gastric adenocarcinomas. The expression of the most commonly studied CSC markers in other solid tumors, ESA, CD133, CD24 and CD44, was evaluated on paired tumor and non-tumor tissues. To overcome the problem of the small size of the human samples which was a limiting factor for the study of tumorigenic properties on FACS-sorted subpopulations of tumor cells, we first developed a strategy to amplify human tumors by xenograft in NSG immunodeficient mice. In order to determine markers of enrichment for CSCs and CSC frequency, tumorigenicity of FACS-sorted cell subpopulations from these mouse-adapted human primary gastric carcinoma cases of both intestinal and diffuse histological types was

then evaluated in both *in vitro* tumorsphere assays and *in vivo* xenograft experiments in extreme limiting dilution assays. To study in greater depth the characterization of gastric CSCs and find more specific markers, the expression of CD10, CD49f, CD166, CD90, CD73, CD105, and ALDH activity were studied and the tumorigenic properties of these cell subpopulations were evaluated in both intestinal and diffuse type cases. In conclusion, our findings demonstrated that CD133, CD44 and ALDH are markers of CSC enrichment in primary non-cardia gastric adenocarcinomas of both intestinal and diffuse types, and that ALDH activity is more specific than CD44 and CD133 expression in isolating gastric CSCs.

Results

Establishment of a mouse model of primary xenografts of non-cardia diffuse and intestinal type gastric adenocarcinomas from patients

Fresh gastric tissue samples were collected by pathologists upon surgical resection from consenting patients who underwent gastrectomy for non-cardia gastric adenocarcinoma at the University Hospital Center and the Bergonié Regional Cancer Center in Bordeaux, France. Paired non-tumor gastric tissue samples distant from the tumor site were also collected.

After pathological analyses and classification of the tumor type, only cases of non-cardia gastric adenocarcinoma were retained for the study (Supplementary Table 1). Among these 37 cases, the median age was 72 years (interquartile range: 56-79), 59.5% were males and 54.1% did not receive preoperative chemotherapy. Approximately half of the tumors were tubular and one third were poorly cohesive according to the WHO and Lauren classifications of gastric cancers. More than half were high grade (51.4%), highly penetrant (T4 = 51.3%) with lymph node invasion (N1-4 = 67.6%) and at stages 3 and 4 (51.4%). Small pieces of fresh

tumor and non-tumor adjacent tissues were subcutaneously xenografted in NSG immunodeficient mice (3 to 10 mice per case). When the tumor size was sufficient, pieces of tissues were dissociated using collagenase/hyaluronidase and dissociated cells were also xenografted by subcutaneous or intraperitoneal injection, and analyzed by flow cytometry for the expression of ESA, an epithelial marker, in combination with CD24, CD133 and CD44 as putative CSC markers, and 7-AAD to exclude dead cells (Figure 1A).

Xenografts of the tissue samples were carried out within 3-5 hours following gastrectomy. Concerning all of the cases where non-tumor tissues were xenografted in NSG mice, no tumor developed before 10 months. Among the 37 tumor cases xenografted in mice, only 8 cases led to the growth of a secondary tumor; 7 were of intestinal type and 1 was of diffuse type according to the Lauren classification (Table 1). There was no statistically significant association between the development of a tumor after xenografting and the following characteristics: gender, age of the patient, the preoperative treatment, WHO and Lauren classifications of gastric tumor histological type, grade, TNM classification and stage (Table 1 and Table 2). These secondary tumors were used for serial transplantation (until passage 4) in NSG mice and histopathological and flow cytometry analyses were performed.

In these 8 cases, tumors reached a tumor size of 500 mm^3 16.6 ± 3.4 weeks after the first passage (P) (P1) in mice, after 10.9 ± 5.9 weeks at P2, and after 10.6 ± 6.9 to 7.2 ± 0.8 weeks at P3 to P5 (Figure 1B). One case GC42, of mucinous histological type according to the WHO classification, was excluded after P2 because tumors appeared slowly and were full of mucus with very few tumor cells inside, rendering its study impossible (Figure 1B). Histopathological analyses confirmed that the tumors obtained in the mice between P1 and P5 remained similar to the respective primary tumor of the patients for all cases (Figure 1C) except one, GC07 which appeared to dedifferentiate after P2 and was excluded (data not shown).

Evaluation of the expression of CD24, CD133 and CD44 cell surface markers on the patients' gastric tissues and tumor xenografts

The expression of CD24, CD133 and CD44 was evaluated by flow cytometry in live (7-AAD negative) ESA positive epithelial cells (ESA negative non-epithelial cells from the microenvironment were excluded) dissociated from freshly collected paired non-tumor and tumor gastric tissue samples from 7 cases. In cells from non-tumor gastric tissue, CD24 and CD133 expression was high, CD24 being expressed in $65\pm 17\%$ of the cells and CD133 in $44\pm 17\%$ of the cells. CD44 was expressed only in $10\pm 9\%$ of cells. In cells from paired tumors of these patients, the expression of CD24, CD133 and CD44 was significantly higher compared to non-tumor cells, CD24 being expressed in most of the tumor cells ($90\pm 8\%$), CD133 in near than $\frac{3}{4}$ of the tumor cells ($71\pm 17\%$), and CD44 in about $\frac{1}{4}$ of the tumor cells ($27\pm 17\%$) (Figure 2A). The percentages of tumor cells expressing these markers were evaluated on serial xenograft from P1 to P4 of the 6 primary cases. The expression of ESA, CD24, CD133 and CD44 remained similar, CD44 being the marker expressed in the smallest proportion of cells after each tumor passage in mice (Figure 2B).

These results were confirmed by immunohistochemistry analyses of the expression of CD44 on patient's non-tumor and tumor tissues and on the corresponding P2-3 xenograft for the 6 primary cases studied (5 intestinal: GC04, GC10, GC35, GC40, GC44 and 1 diffuse: GC06) (Figure 2C). In the non-tumor area, CD44 was expressed at a low level, preferentially in cells in the isthmus region of gastric glands in area of gastritis, as previously reported (Bessede et al., 2014b). In patient's tumors, CD44 was expressed in a mosaic pattern in some tumor cells but not all, most of the time at the periphery of the tumor islets for the intestinal type tumors. A similar pattern of CD44 expression was observed in corresponding xenografts for each

case, confirming that the cellular heterogeneity of the primary tumor was reproduced in the serial xenografts.

Gastric cancer cells expressing CD133 and CD44 have tumorigenic CSC properties

In order to determine the percentage of cells expressing CD44 inside the CD24⁺ and the CD133⁺ tumor cells subpopulations, respectively, single stainings or combined stainings (7-AAD + ESA-FITC + CD24-PE or CD133-PE + CD44-APC) were performed on freshly dissociated cells from P2-P3 xenografts of 4 intestinal cases (GC04, GC10, GC40, GC44) and 1 diffuse case (GC06). Results revealed that CD24⁺CD44⁺ cells and CD133⁺CD44⁺ cells represented between 3 and 14% of tumor cells depending on the case. Most of the CD44⁺ cells expressed CD24 and CD133 (81±12% and 88±7%, respectively) and represented a small subpopulation inside the CD24⁺ and the CD133⁺ tumor cells (23±8% and 19±7%, respectively) (Figure 3A).

To evaluate the tumorigenic properties of cells expressing CD133 and CD44, freshly dissociated cells from P2-P3 tumor xenografts of 2 intestinal cases (GC04 and GC10) and 1 diffuse case (GC06) were sorted by FACS based on the expression of CD133 and CD44 on 7-AAD-ESA⁺ cells (Figure 3B) and submitted to *in vitro* tumorsphere assays and *in vivo* xenografts in extreme limiting dilution assays (ELDA). For all cases, both CD133⁺ and CD44⁺ cells formed significantly more tumorspheres after 10 days of *in vitro* culture than their CD133⁻ and CD44⁻ respective counterparts (Figure 3C). The number of tumorspheres obtained was higher in all cases with the CD44⁺ cells compared to the CD133⁺ cells, suggesting that the CD44⁺ cell subpopulation contained the higher number of CSCs.

Xenografts in mice were performed from 10,000 to 30 cells per injection and per mouse . Carcinoma initiating cell frequencies with 95% confidence intervals were estimated by limiting dilution analyses (Bonnetfoix et al., 2001) (Bonnetfoix et al., 1996) (Hu and Smyth,

2009) and are expressed in 1/stem cell frequency. Concerning the 3 cases studied, tumors developed at a statistically significant higher frequency in ESA+CD133+ and ESA+CD44+ positive cells than in respective ESA+CD133- and ESA+CD44- cells. The observed CSC frequency was between 1/105 to 1/1911 ESA+CD133+ cells versus 1/781 to 1/66876 ESA+CD133- cells, and between 1/29 to 1/1020 ESA+CD44+ cells versus 1/568 to 1/28963 ESA+CD44- cells (Table 3 and Table 4). As for *in vitro* tumorsphere assays, GC10 displayed the highest *in vivo* tumorigenic capacity and GC04 the lowest. These results confirmed that CSCs express CD133 and CD44 and that CD44 is more specific than CD133 for the isolation of CSCs in non-cardia gastric adenocarcinomas of both intestinal and diffuse types. However, because all CD44+ do not have CSC properties, CSCs may represent a subpopulation inside the ESA+CD133+CD44+ cells.

ALDH is a more specific marker of gastric CSCs than CD44

In order to better characterize CSCs from non-cardia intestinal and diffuse type gastric carcinomas, we used flow cytometry to measure the expression of 7 additional putative markers of CSCs described in carcinomas of other organs, CD10, CD49f, CD73, CD166, CD90, CD105 and the activity of ALDH in 5 cases of primary gastric tumor xenografts (4 intestinal cases, GC04, GC06, GC10, GC35, GC40; 1 diffuse case, GC06) and 5 gastric cancer cell lines (3 intestinal, MKN74, MKN7, NCI87; 2 diffuse, AGS, MKN45). CD10 was negative except for 2 of the 10 cases studied. CD49f was expressed in more than 80% of the cells, similarly to ESA, in both primary cases and cell lines. For the other markers, the expression pattern was more homogeneous in primary cases than in the gastric cancer cell lines which exhibited more heterogeneity, being either highly positive or highly negative (Figure 4A). In primary cases, ESA and CD49f were the most highly expressed, followed by CD90 expressed in nearly half of the cells, then CD73 in more than a third of the cells with

the exception of one case. CD166 was expressed in $21\pm 13\%$ of the cells. CD105 expression and ALDH activity were detected in only $9\pm 6\%$ and $8\pm 5\%$ of the cells, respectively, in these 5 primary cases (Figure 4A).

Flow cytometry experiments of CD44 co-staining with either CD73, CD166, CD90, or CD105 or detection of ALDH activity were performed, and the percentage of cells positive for each marker inside the CD44⁺ subpopulation and conversely were determined (Figure 4B). Results revealed that CD166 and CD44 were co-expressed and detected the same tumor cell subpopulation. CD73 was expressed in a high percentage of CD44⁺ cells as well as in CD44⁻ cells. CD90⁺ and CD105⁺ cells were in equal amounts in CD44⁺ and CD44⁻ cells. Interestingly, most of the ALDH⁺ cells expressed CD44, and the ALDH⁺CD44⁺ cells represented less than half of the CD44⁺ cells (Figure 4B).

To evaluate the tumorigenic properties of the cells expressing or not CD73, CD166, CD90, CD105 and ALDH activity, FACS-sorted cells from primary cases (GC04, GC06 and GC10) were submitted to tumorsphere assays. For the 3 cases, sorted-cells forming tumorspheres were essentially ALDH⁺ and CD166⁺, and to a lower extent CD73⁺, CD90⁻ and CD105⁻. We confirmed the high tumorsphere capacity of ALDH⁺ cells on both MKN45 and MKN74 cell lines. Xenografts in mice were then performed as previously described with cells freshly collected from P2-P3 xenografts of primary cases and cell lines after cell sorting by FACS on ALDH activity, , including 2 intestinal cases (GC10 and MKN74) and 2 diffuse cases (GC06 and MKN45) according to the ELDA method to determine the frequency of CSCs in each engrafted subpopulation. For all cases studied excepted MKN45, ALDH⁺ cells led to the development of tumors at a significantly higher frequency than the respective ALDH⁻ cells, ranging between 1/38 to 1/273 for ALDH⁺ cells versus 1/368 to 1/21208 ALDH⁻ cells (Table 5). For the GC10 primary intestinal case and the GC06 primary diffuse case, the CSC frequencies were higher in ALDH⁺ cells (1/38 and 1/273, respectively) than in CD133⁺

(1/105 and 1/1658, respectively) and CD44⁺ cells (1/49 and 1/352, respectively) (Table 3 and Table 4).

The expression of ALDH1, the main isoform of ALDH enzymes, was confirmed by immunohistochemistry with CD44 and Ki67 on tissues from tumor xenografts from the GC04, GC06, GC10 and MKN45 cases (Figure 5A). As expected, ALDH1 was expressed at a lower level than CD44 in all cases, except for case GC10 for which ALDH was expressed in the whole tumor. This discrepancy for case GC10 with the result obtained with the ALDEFUOR assay could be explained by a reduced activity of ALDH in spite of a high expression of ALDH1 detected by immunohistochemistry. In addition, ALDH1 was also expressed at a lower level than Ki67 in all cases, suggesting that not only ALDH⁺ but also ALDH⁻ cells have proliferation properties, but those of ALDH⁻ must be very limited as they cannot initiate new tumors *in vivo* and *in vitro* (Figure 4D and Table 5).

The expression of CD44 and ALDH activity were analyzed on tumorsphere development of MKN45 cells *in vitro* over time. In young, small tumorspheres (5 day culture), most of the tumor cells were positive for both CD44 expression and ALDH activity, and excluded Hoechst 33342 stain. When tumorspheres became bigger (after 10 and 15 days), only a proportion of cells inside the tumorsphere remained CD44⁺ALDH⁺, corresponding to CSC, with the appearance of CD44⁺ALDH⁻ cells incorporating the Hoechst 33342 stain, corresponding to more differentiated cells (Figure 5B). Verapamil treatment, known to inhibit drug efflux systems, restored Hoechst 33342 incorporation and staining in ALDH⁺ cells. This result suggests that CD44⁺ALDH⁺ cells may correspond to cells of the so called side population previously proposed as CSCs in gastric cell lines by Fukuda *et al.* (Fukuda et al., 2009) (Supplementary Figure 1). These results confirmed that ALDH is a more selective marker than CD133 and CD44 for the identification and isolation of CSCs in intestinal and diffuse variants of non-cardia gastric adenocarcinomas.

Discussion

In this study, we aimed to characterize cell surface markers of gastric CSCs in non-cardia intestinal and diffuse type gastric adenocarcinomas according to the Lauren classification criteria for gastric carcinoma. Currently, these classification systems have limited clinical use, as they cannot be used to orientate patient therapy. Until very recently, there was no specific molecular signature of diffuse and intestinal carcinomas allowing guided and personalized therapy, with the exception of Her2 expression found in approximately 25% of the intestinal cases offering the possibility of molecular-targeted therapy similar to that used for Her2+ breast cancer. Last year, the Cancer Genome Atlas Research Network and the group of Wang *et al.* published a molecular characterization of gastric carcinomas based on the study of 295 cases and 100 cases, respectively (TCGARN, 2014) (Wang et al., 2014) . Both studies led to a classification of gastric carcinomas into four main subtypes according to their molecular profiles of mutations and amplification : the group enriched in EBV+ tumors (frequent PIK3CA mutations, extreme DNA hypermethylation), the group of MSI tumors characterized by elevated mutation rates and hypermethylation, the group of genomically stable tumors enriched for the diffuse histological variants (drivers mutations included regulators of cytoskeleton and cell junctions including CDH1 mutations and newly described RHOA mutations found in 15% of the cases), and the group of tumors with chromosomal instability (marked aneuploidy and focal amplification of receptor tyrosine kinases) with an elevated frequency in the cardia (TCGARN, 2014)(Wang et al., 2014) . These studies were performed without distinguishing between cardia and non-cardia gastric adenocarcinomas. The identification of molecular markers of CSCs at the protein level in these different variants could be useful to distinguish subtypes of gastric carcinomas which may allow further orientation toward a more personalized therapy.

Another important point that could be taken into consideration to orientate therapy is the origin of the CSCs. As Houghton and our group reported, the cells from non-cardia gastric carcinoma linked to *Helicobacter* infection may be of a different nature; originating from the transformation of a local epithelial stem cell or originating from the transformation of a bone-marrow (BM) derived stem cell (Houghton et al., 2004) (Varon et al., 2012) (Bessede et al., 2014a) . Taking advantage of the mouse model of gastric carcinogenesis experimentally induced by a chronic *H. pylori* infection which enables a one year recapitulation of the cascade of histological lesions observed after more than 60 years of infection in humans, we were able to show that chronic infection in old mice led to BM derived cell (BMDC) recruitment and homing within the gastric mucosa (Varon et al., 2012) (Ferrand et al., 2011a) (Ferrand et al., 2011b). BMDC recruitment theoretically overcomes local epithelial stem cell failure of tissue repair but, in the context of chronic infection and inflammation, an altered differentiation occurs leading to metaplasia and dysplasia which are finally comprised of BMDCs in nearly one quarter of the cases; it suggests that gastric carcinoma may originate from both local epithelial stem cells and, to a lesser extent, BMDCs. In this model, high grade dysplastic lesions were comprised of CD44+ cells, regardless of their BMDCs or local origin (Varon et al., 2012). In human and mouse gastric mucosa, CD44 is not detected in healthy gastric mucosa or in very few cells at the isthmus level of the gastric glands in the corpus, where stem cells are localized (Bessede et al., 2014b) (Bessede et al., 2014a). These CD44+ stem/progenitor cells expand from the isthmus towards the base of the unit in metaplastic and dysplastic areas induced in response to chronic *H. pylori* infection (Bessede et al., 2014b) (Khurana et al., 2013). We showed that *H. pylori* infection is responsible for the emergence of CD44+ cells possessing CSC-like properties, and that it occurs via an epithelial-mesenchymal-like transition (Bessede et al., 2014b) (Bessede et al., 2014a) (Baud et al., 2013). CD44 is a targetable molecule and very recently, it was reported that its inhibition by

peptide inhibitors in mouse and Mongolian gerbil models of *H. pylori*-induced gastric carcinogenesis resulted in the inhibition of *H. pylori*-induced proliferation and chronic atrophic gastritis (Khurana et al., 2013) (Bertaux-Skeirik et al., 2015).

In the present study we show that CD44 was expressed in all primary cases of gastric carcinoma studied, independently of their diffuse or intestinal histological classification. CD44 was always expressed at a higher level in tumor cells than in paired normal non-tumor tissue. Experiments by FACS of ESA+CD44+ and ESA+CD44- cells followed by *in vitro* tumorsphere assays and xenografts in extreme limiting dilutions in immunodeficient mice revealed that CD44 was a marker of enrichment of CSCs in all primary cases studied. These results suggest that CD44 can be considered as a robust marker of CSCs independently of the histopathological classification of the gastric tumors.

CD44 is a cell surface transmembrane glycoprotein encoded by a gene composed of 20 exons. In addition to the standard isoform, CD44s, numerous splicing variants composed of additional exons exist. The variants CD44v6, CD44v9 and the epithelial variant CD44v8-10 have been reported in gastric carcinoma (Yasui et al., 1998) (Chen et al., 2004) (Lau et al., 2014) (da Cunha et al., 2010).

Contrarily to the situation in colon cancer in which CD133+ cells containing colon CSCs represent a small and rare subpopulation within tumor cells, we demonstrated that CD133 was a marker of enrichment of gastric CSCs, but less specific than CD44, as it is expressed in at least 50% of the gastric cancer cells (detected with the same antibodies and staining procedures for flow cytometry described by others in colon cancer (O'Brien et al., 2007) (Ricci-Vitiani et al., 2007)).

Interestingly, flow cytometry analyses of co-staining with CD44 and *in vitro* tumorsphere assays showed that CD166 was coexpressed with CD44 and, as a consequence, CD166+ cells presented the same tumorigenic properties as CD44+ cells *in vitro*. Similar analyses led to the

conclusion that the gastric CSC phenotype corresponds to ESA+, CD24+, CD133+, CD73+, CD90-, CD105-, CD166+, CD44+ and ALDH+ activity. Finally, in all of the primary cases studied, cells with ALDH+ activity displayed the highest tumorigenic properties both *in vitro* and *in vivo*, with an estimated tumor initiating cell frequency superior to that of CD44+ and CD133+.

Some studies suggest that CD44 and ALDH could be considered as targetable molecules in therapy, as inhibition by small interfering RNA strategies can lead to reduced tumorigenic capacities in xenograft models of primary colon carcinoma and melanoma (Luo et al., 2012) (Du et al., 2008). The ALDEFLUOR assay used to isolate CSCs in liquid and solid tumors detects the activity of several isoforms of ALDH (Marcato et al., 2011). Among them, the main isoforms expressed in tumors are retinaldehyde dehydrogenases ALDH1A1 and ALDH1A3, responsible for the oxidation of retinal to retinoic acid and, to a lesser extent, ALDH3A1 (Marcato et al., 2011) (Ma and Allan, 2011). They can metabolize and detoxify chemotherapeutic agents such as cyclophosphamide in hematopoietic stem cells, and their level of expression was shown to be predictive of response to treatment in breast cancer (Magni et al., 1996) (Sladek et al., 2002). In this study, we show that CD44+ALDH+ cells did not incorporate the vital DNA dye Hoechst 33342, instead the CD44+ALDH- cells incorporated it, suggesting that ALDH+ cells may correspond to the side population of cells with CSC properties described by Fukuda *et al.* in gastric cancer cell lines (Fukuda et al., 2009). The ability of ALDH+ cells to efflux Hoechst 33342 was reversed by verapamil treatment, an inhibitor of efflux pumps such as the ATP-binding cassette (ABC) transporter family member ABCG2, suggesting that these cells could be associated with chemotherapy resistance as proposed by others (Magni et al., 1996) (Sladek et al., 2002) (Nishikawa et al., 2013) (Raha et al., 2014). These findings implicate that ALDH isozymes can be considered

not only as biomarkers of CSCs but also as putative targets to inhibit tumor growth and to overcome resistance in cancer therapy.

It is of importance to note that in this study, mouse adapted xenografts from patient's primary tumors always remained heterogeneous and composed of subpopulations of tumor cells expressing ESA, CD24, CD133 and CD44 similarly to the patients' situation, while gastric cancer cell lines were found to be negative for CD133 and either positive or negative for CD44 and ALDH. These results strengthen the importance and the necessity to perform the characterization of CSCs on models as close as possible to the patients' situation, as is the case with these mouse models of primary tumor xenografts, and not only on *in vitro* cancer cell lines.

Results of this study demonstrate that gastric CSC co-express ESA, CD133, CD44, CD166 and ALDH, CD44 expression and ALDH activity being the most specific markers of enrichment of CSCs in both diffuse and intestinal variants of non-cardia gastric adenocarcinoma. This finding led to the hypothesis that a common treatment strategy for non-cardia gastric carcinoma may be considered, focusing on CD44⁺ALDH⁺ CSCs independently of the diffuse versus intestinal histological classification of the tumor.

Experimental procedures

Ethics Statement:

Studies on fresh tumors from primary gastric adenocarcinoma cases were performed in agreement with the Direction for Clinical Research and the Tumor and Cell Bank of the Haut-Leveque Hospital of the University Hospital Center of Bordeaux and of the Bergonié Institute of Bordeaux. Fresh tumors samples were collected from gastric surgical wastes from patients who underwent gastrectomy for distant non-cardia gastric adenocarcinoma and for who

informed consent was obtained. Activities of conservation and preparation of elements of human origin are declared at the French Ministry of Research (reference number DC-2008-412).

Mouse xenografts

Animal experiments with non obese diabetous/severe combined immunodeficiency /interleukin-2R γ null (NSG) immunodeficient mice housed under germ-free conditions were performed in level 2 animal facilities of the University of Bordeaux, in accordance with national institutional guidelines and with the agreement of the local Ethic Committee on Animal Experiments CEEA50 of Bordeaux (agreement number 50120151-A) and the French Committee of Genetic Engineering (approval number 4608). Samples of tumor and paired non-tumor tissues were collected from patients specimen and transported in medium composed of DMEM 4.5 g/l with 20% FBS, 50 IU/ml of penicillin and 50 μ g/ml of streptomycin, 50 μ g/ml of vancomycin and 15 μ g/ml amphotericin B. Samples were minced in small pieces of 2 mm x 2 mm size, and were subcutaneously transplanted into the right dorsal flank of 7-week-old male NSG mice under 2.5 % isoflurane anesthesia (Belamont, Cournon, France). Alternatively, cells were dissociated by collagenase IV and hyaluronidase (all from Sigma, Saint-Quentin Fallavier, France) after mechanical mincing as previously described (O'Brien et al., 2007) and resuspended in 100 μ L of 7 mg/mL ice-cold Matrigel (BD Biosciences, Le Pont de Claix, France) for subcutaneous injection. The tumor size was monitored with callipers once a week, and tumor volume was estimated as $(D^2 \times d)/2$, where D is the large diameter and d is the small diameter of the tumor as previously described (Bessede et al., 2014b). At the end of the experiments (until 10 months post-engraftment for the primary xenograft) and when tumor reached $\sim 500 \text{ mm}^3$, mice were sacrificed by cervical dislocation and tumors immediately harvested and processed for further analyses. Secondary

tumors were amplified subcutaneously in mice by serial transplantation of small pieces of tumor bulk, or by injection of tumor cells resuspended in matrigel.

For xenograft experiments in limiting dilution assay, 10,000 to 30 FACS-sorted cells were suspended in ice cold Matrigel and subcutaneously injected in NSG mice, and tumor size was recorded twice a week.

Histology and immunohistochemistry

Tissue sections 3 μ m thickness were prepared from formalin-fixed paraffin-embedded tissues (PET) and submitted to standard Hematoxylin/Eosin/Safran (HES) (all from Sigma) staining and immunohistochemistry protocols with primary mouse monoclonal anti- human CD44 antibodies 1:100 (G44-26, BD), mouse monoclonal anti- human ALDH1 antibodies 1:300 (clone 44/ALDH, BD), mouse monoclonal anti-Ki67 antibodies 1:75 (DAKO, Les Ulis, France) all for 30 min at room temperature, followed by 30 min incubation at room temperature with anti-mouse Labelled Polymer-HRP DAKO Envision Systems (DAKO). Immunolabeling was revealed by 10 min incubation in liquid substrate-diaminobenzidine-chromogen (DAKO) at room temperature. Slides were counterstained with hematoxylin, dehydrated and mounted with Eukitt-mounting medium (Labonord, Templemars, France). Histology was examined by an expert pathologist (P. Dubus). Images of the staining of each marker were recorded on the same field on serial tissue sections using light microscopy and a x20 objective.

Gastric cancer cell lines culture

Gastric cancer cell lines were cultured in DMEM/F12 media for AGS cells and in RPMI1640 media for MKN45, MKN74, NCI87 and MKN28 cells supplemented with 10% heat-inactivated fetal bovine serum (FBS), 50 IU/ml of penicillin and 50 μ g/ml of streptomycin (all

from Invitrogen, Cergy-Pontoise, France) at 37°C in the presence of 5% CO₂ as previously described (Bessede et al., 2014b).

Statistical analysis

Quantification values represent the means of three or more experiments as indicated \pm standard deviation (SD). Statistics were performed using the non-parametric Kruskal-Wallis and Mann-Whitney U tests on SPSS16.0F software (SPSS Inc., Chicago, IL, USA).

Regarding patients' characteristics: Qualitative variables were described using numbers (and percentages), and quantitative variables were described using medians (and interquartile ranges [IQRs]). The Mann–Whitney U test was used to compare quantitative variables between groups of graft tumor development. The Fisher exact test was used to compare qualitative variables between groups of graft tumor development. Analyses were performed using SAS® 9.3 (SAS Institute, Inc., Cary, NC). Furthermore, limiting dilution analyses were performed (Bonnefoix et al., 2001) (Bonnefoix et al., 1996) using the “limdil” function of the R-package “StatMod” (Hu and Smyth, 2009). Carcinoma initiating cell frequencies with 95% confidence intervals were estimated and are expressed in 1/stem cell frequency. Further, gastric cancer-initiating cell frequencies were compared between groups (e.g. presence or absence of a specific marker such as CD133) using likelihood ratio tests.

Flow cytometry analysis

Cells were dissociated from tumors freshly collected from mice after mechanical mincing with a scalpel and incubation in a solution of 1 mg/ml collagenase I and 0.2 mg/ml hyaluronidase in PBS (all from Sigma) for 1 h at 37°C with shaking. Single cells were collected using a 70 μ m filter (BD). Red blood cells were removed from cell suspension by

incubating in a solution containing 2 mM KHCO₃, 0.1 mM EDTA and 170 mM NH₄Cl for 8 min at 4°C, then cells were centrifuged for 3 min at 1,200 rpm.

For flow cytometry analyses, 100,000 cells in 100 µL PBS 0.5% bovine serum albumin (BSA) (Sigma) and 2 mM EDTA per condition were stained with 3-5 µL of primary fluorescent-labelled antibodies including ESA-FITC (Stem Cell Technologies, Grenoble, France), CD10-PE, CD24-PE, CD73-PE, CD49f-PE, CD105-PE, CD166-PE, CD90-PECy5, CD44-PE or CD44-APC (all from BD) and CD133-PE (MACS Miltenyi Biotec, Paris, France) for 20 min at 4°C. Cells were rinsed twice with PBS containing 0.5% bovine serum albumin, 2 mM EDTA and 50 µg/ml 7-amino actinomycin D (7-AAD) (BD) before being analysed in a FACS Canto II flow cytometry system. The ALDEFLUOR Kit (Stem Cell Technologies) was used to detect ALDH activity according to the manufacturer's instructions. Flow cytometry was performed using a BD FACSCanto II instrument and DIVA software (BD).

For FACS cell sorting, 5 to 10 million cells were collected from gastric tumors or cancer cell lines and stained with primary fluorescent-labelled antibodies or ALDEFLUOR reagent and 7-AAD as described above and were sorted using FACS BDaria (BD) on 7-AAD negative cells.

Tumorsphere assay

1,000 FACS-sorted cells were plated in non-adherent 24 well plates previously coated with a 10 % polyHEMA solution in 95 % ethanol (v/v) (Sigma), in serum-free DMEM-F12 Glutamax media supplemented with 20 ng/ml human EGF, 20 ng/ml basic-FGF, 5 µg/ml insulin, 0.3 % glucose, 50 IU/ml of penicillin (all from Sigma) (Bessede et al., 2014b). It is important to note that, for the tumorsphere culture of cells from primary tumors, the media was supplemented with 5% FBS for the first 2 days of culture to maintain cell viability, and

was then replaced by serum-free media. After 7 days, the number of spheroids per well was counted under a light inverted microscope using a $\times 20$ objective.

Immunofluorescence

Tumorspheres collected from culture plates were centrifuged at 600 g for 5 min, then washed with PBS. Live tumorspheres were directly stained with mouse anti-CD44-PE antibodies 1:50 (BD) and ALDEFUOR reagent 1:50 in 500 μ l ALDEFUOR buffer during 20 min at 37°C. Tumorspheres were rinsed by centrifugation in ALDEFUOR buffer, incubated in 100 μ l ALDEFUOR buffer containing Hoechst 33342 10 μ g/ml (Sigma) during 30 min to stain cell nucleus, then mounted on glass slides with coverslips prior to direct fluorescent imaging. Efflux proteins were inactivated by incubating tumorspheres in ALDEFUOR buffer containing verapamil 20 μ M (Sigma) during 10 min at 37°C before staining with Hoechst 33342. Fluorescent imaging was performed with an Eclipse 50i epi-fluorescence microscope (Nikon, Champigny sur Marne, France) equipped with Nis Element acquisition software and a x40 (numerical aperture, 1.3) oil immersion objective.

Authors contributions

- Phu Hung Nguyen, animal experiments, tumorsphere assays, flow cytometry analyses, FACS cell sorting, immunofluorescence analyses,
- Frédéric Mazurier, study concept and design, development of dissociation protocol of primary tumors and xenograft assays in NSG mice, flow cytometry and FACS analyses,
- Lucie Chambonnier, animal care and animal experiments, flow cytometry and FACS analyses, tissue processing, histology and immunohistochemistry experiments,
- Pierre Dubus, study design, histopathological analyses of primary tumors and tumor xenografts,

- Linda Wittkop, mathematical and statistical analyses,
- Geneviève Belleannée, Denis Collet, Isabelle Soubeyran and Serge Evrard, collection of patient's informed consent, collection of human tissue samples from consenting patients who underwent gastrectomy, histopathological analyses,
- Benoit Rousseau, animal care and animal experiments,
- Nathalie Senant-Dugot, technical assistance for tissue processing and histology,
- Francis Mégraud, study concept and design, general supervision of the project,
- Christine Varon, study concept and design, animal experiments, flow cytometry and FACS analyses, histological experiments and analyses, writing of the manuscript.

Acknowledgments

We thank Marie-Edith Lafon (CNRS UMR 5234, University of Bordeaux) and technicians from the Service de Pathologie des Tumeurs (Haut-Leveque Hospital, University Hospital Center of Bordeaux) for molecular analyses on tumor tissues, Pierre Costet (Animal Facilities, University of Bordeaux), Vincent Pitard and Santiago Gonzalez (Flow Cytometry and FACS Platform, University of Bordeaux), Alban Giese (Experimental pathology platform of the Canceropole GSO and SIRIC BRIO, University of Bordeaux) and Lucie Benejat (INSERM U853) for technical assistance, and the French 'Association pour la Recherche contre le Cancer' (grant number 8412). This project was supported by SIRIC BRIO (Site de Recherche Intégrée sur le Cancer – Bordeaux Recherche Intégrée Oncologie) (grant INCa-DGOS-Inserm 6046). We thank the 'Institut National du Cancer' (grant 07/3D1616/IABC-23-12/NC-NG and grant 2014-152), the 'Conseil Regional d'Aquitaine' (grant number 20071301017 and 20081302203), the French National Society for Gastroenterology, and the Canceropole Grand Sud-Ouest (grant 2010-08-canceropole GSO-Université Bordeaux 2) for financial support.

Conflict of interest

All authors declare no conflict of interest.

References

- Al-Hajj, M., Wicha, M.S., Benito-Hernandez, A., Morrison, S.J., and Clarke, M.F. (2003). Prospective identification of tumorigenic breast cancer cells. *Proceedings of the National Academy of Sciences of the United States of America* *100*, 3983-3988.
- Alison, M.R., Islam, S., and Wright, N.A. (2010). Stem cells in cancer: instigators and propagators? *Journal of cell science* *123*, 2357-2368.
- Baud, J., Varon, C., Chabas, S., Chambonnier, L., Darfeuille, F., and Staedel, C. (2013). *Helicobacter pylori* initiates a mesenchymal transition through ZEB1 in gastric epithelial cells. *PLoS one* *8*, e60315.
- Bertaux-Skeirik, N., Feng, R., Schumacher, M.A., Li, J., Mahe, M.M., Engevik, A.C., Javier, J.E., Peek, R.M., Jr., Ottemann, K., Orian-Rousseau, V., *et al.* (2015). CD44 Plays a Functional Role in *Helicobacter pylori*-induced Epithelial Cell Proliferation. *PLoS pathogens* *11*, e1004663.
- Bessede, E., Dubus, P., Megraud, F., and Varon, C. (2014a). *Helicobacter pylori* infection and stem cells at the origin of gastric cancer. *Oncogene*.
- Bessede, E., Staedel, C., Acuna Amador, L.A., Nguyen, P.H., Chambonnier, L., Hatakeyama, M., Belleanne, G., Megraud, F., and Varon, C. (2014b). *Helicobacter pylori* generates cells with cancer stem cell properties via epithelial-mesenchymal transition-like changes. *Oncogene* *33*, 4123-4131.
- Bonnefoix, T., Bonnefoix, P., Callanan, M., Verdiel, P., and Sotto, J.J. (2001). Graphical representation of a generalized linear model-based statistical test estimating the fit of the single-hit Poisson model to limiting dilution assays. *J Immunol* *167*, 5725-5730.
- Bonnefoix, T., Bonnefoix, P., Verdiel, P., and Sotto, J.J. (1996). Fitting limiting dilution experiments with generalized linear models results in a test of the single-hit Poisson assumption. *Journal of immunological methods* *194*, 113-119.
- Bonnet, D., and Dick, J.E. (1997). Human acute myeloid leukemia is organized as a hierarchy that originates from a primitive hematopoietic cell. *Nature medicine* *3*, 730-737.
- Chen, J.Q., Zhan, W.H., He, Y.L., Peng, J.S., Wang, J.P., Cai, S.R., and Ma, J.P. (2004). Expression of heparanase gene, CD44v6, MMP-7 and nm23 protein and their relationship with the invasion and metastasis of gastric carcinomas. *World J Gastroenterol* *10*, 776-782.
- Cheung, A.M., Wan, T.S., Leung, J.C., Chan, L.Y., Huang, H., Kwong, Y.L., Liang, R., and Leung, A.Y. (2007). Aldehyde dehydrogenase activity in leukemic blasts defines a subgroup of acute myeloid leukemia with adverse prognosis and superior NOD/SCID engrafting potential. *Leukemia* *21*, 1423-1430.
- Clevers, H. (2011). The cancer stem cell: premises, promises and challenges. *Nature medicine* *17*, 313-319.
- Collins, A.T., Berry, P.A., Hyde, C., Stower, M.J., and Maitland, N.J. (2005). Prospective identification of tumorigenic prostate cancer stem cells. *Cancer research* *65*, 10946-10951.
- Correa, P., and Houghton, J. (2007). Carcinogenesis of *Helicobacter pylori*. *Gastroenterology* *133*, 659-672.
- da Cunha, C.B., Oliveira, C., Wen, X., Gomes, B., Sousa, S., Suriano, G., Grellier, M., Huntsman, D.G., Carneiro, F., Granja, P.L., *et al.* (2010). De novo expression of CD44

variants in sporadic and hereditary gastric cancer. *Laboratory investigation; a journal of technical methods and pathology* 90, 1604-1614.

Du, L., Wang, H., He, L., Zhang, J., Ni, B., Wang, X., Jin, H., Cahuzac, N., Mehrpour, M., Lu, Y., *et al.* (2008). CD44 is of functional importance for colorectal cancer stem cells. *Clin Cancer Res* 14, 6751-6760.

Ferrand, J., Lehours, P., Schmid-Alliana, A., Megraud, F., and Varon, C. (2011a). *Helicobacter pylori* infection of gastrointestinal epithelial cells in vitro induces mesenchymal stem cell migration through an NF-kappaB-dependent pathway. *PloS one* 6, e29007.

Ferrand, J., Noel, D., Lehours, P., Prochazkova-Carlotti, M., Chambonnier, L., Menard, A., Megraud, F., and Varon, C. (2011b). Human bone marrow-derived stem cells acquire epithelial characteristics through fusion with gastrointestinal epithelial cells. *PloS one* 6, e19569.

Flejou, J.F. (2011). [WHO Classification of digestive tumors: the fourth edition]. *Annales de pathologie* 31, S27-31.

Fukuda, K., Saikawa, Y., Ohashi, M., Kumagai, K., Kitajima, M., Okano, H., Matsuzaki, Y., and Kitagawa, Y. (2009). Tumor initiating potential of side population cells in human gastric cancer. *International journal of oncology* 34, 1201-1207.

Ginestier, C., Hur, M.H., Charafe-Jauffret, E., Monville, F., Dutcher, J., Brown, M., Jacquemier, J., Viens, P., Kleer, C.G., Liu, S., *et al.* (2007). ALDH1 is a marker of normal and malignant human mammary stem cells and a predictor of poor clinical outcome. *Cell stem cell* 1, 555-567.

Gonzalez, C.A., Megraud, F., Buissonniere, A., Lujan Barroso, L., Agudo, A., Duell, E.J., Boutron-Ruault, M.C., Clavel-Chapelon, F., Palli, D., Krogh, V., *et al.* (2012). *Helicobacter pylori* infection assessed by ELISA and by immunoblot and noncardia gastric cancer risk in a prospective study: the Eurgast-EPIC project. *Ann Oncol* 23, 1320-1324.

Houghton, J., Stoicov, C., Nomura, S., Rogers, A.B., Carlson, J., Li, H., Cai, X., Fox, J.G., Goldenring, J.R., and Wang, T.C. (2004). Gastric cancer originating from bone marrow-derived cells. *Science (New York, NY)* 306, 1568-1571.

Hu, Y., and Smyth, G.K. (2009). ELDA: extreme limiting dilution analysis for comparing depleted and enriched populations in stem cell and other assays. *Journal of immunological methods* 347, 70-78.

Huang, E.H., Hynes, M.J., Zhang, T., Ginestier, C., Dontu, G., Appelman, H., Fields, J.Z., Wicha, M.S., and Boman, B.M. (2009). Aldehyde dehydrogenase 1 is a marker for normal and malignant human colonic stem cells (SC) and tracks SC overpopulation during colon tumorigenesis. *Cancer research* 69, 3382-3389.

IARC Working Group (1994). Schistosomes, liver flukes and *Helicobacter pylori*: Views and expert opinion of IARC Working Group on the evaluation of carcinogenic risks to humans. 61, 177-240. Lyon, IARC Monographs. International Agency for research on Cancer.

Jiang, F., Qiu, Q., Khanna, A., Todd, N.W., Deepak, J., Xing, L., Wang, H., Liu, Z., Su, Y., Stass, S.A., *et al.* (2009). Aldehyde dehydrogenase 1 is a tumor stem cell-associated marker in lung cancer. *Mol Cancer Res* 7, 330-338.

Khurana, S.S., Riehl, T.E., Moore, B.D., Fassan, M., Rugge, M., Romero-Gallo, J., Noto, J., Peek, R.M., Jr., Stenson, W.F., and Mills, J.C. (2013). The hyaluronic acid receptor CD44 coordinates normal and metaplastic gastric epithelial progenitor cell proliferation. *The Journal of biological chemistry* 288, 16085-16097.

Lau, W.M., Teng, E., Chong, H.S., Lopez, K.A., Tay, A.Y., Salto-Tellez, M., Shabbir, A., So, J.B., and Chan, S.L. (2014). CD44v8-10 is a cancer-specific marker for gastric cancer stem cells. *Cancer research* 74, 2630-2641.

Lauren, P. (1965). The Two Histological Main Types of Gastric Carcinoma: Diffuse and So-Called Intestinal-Type Carcinoma. an Attempt at a Histo-Clinical Classification. *Acta pathologica et microbiologica Scandinavica* 64, 31-49.

Li, C., Heidt, D.G., Dalerba, P., Burant, C.F., Zhang, L., Adsay, V., Wicha, M., Clarke, M.F., and Simeone, D.M. (2007). Identification of pancreatic cancer stem cells. *Cancer research* 67, 1030-1037.

Luis, M., Tavares, A., Carvalho, L.S., Lara-Santos, L., Araujo, A., and de Mello, R.A. (2013). Personalizing therapies for gastric cancer: molecular mechanisms and novel targeted therapies. *World J Gastroenterol* 19, 6383-6397.

Luo, Y., Dallaglio, K., Chen, Y., Robinson, W.A., Robinson, S.E., McCarter, M.D., Wang, J., Gonzalez, R., Thompson, D.C., Norris, D.A., *et al.* (2012). ALDH1A isozymes are markers of human melanoma stem cells and potential therapeutic targets. *Stem cells (Dayton, Ohio)* 30, 2100-2113.

Ma, I., and Allan, A.L. (2011). The role of human aldehyde dehydrogenase in normal and cancer stem cells. *Stem cell reviews* 7, 292-306.

Magni, M., Shammah, S., Schiro, R., Mellado, W., Dalla-Favera, R., and Gianni, A.M. (1996). Induction of cyclophosphamide-resistance by aldehyde-dehydrogenase gene transfer. *Blood* 87, 1097-1103.

Marcato, P., Dean, C.A., Giacomantonio, C.A., and Lee, P.W. (2011). Aldehyde dehydrogenase: its role as a cancer stem cell marker comes down to the specific isoform. *Cell cycle (Georgetown, Tex)* 10, 1378-1384.

Nishikawa, S., Konno, M., Hamabe, A., Hasegawa, S., Kano, Y., Ohta, K., Fukusumi, T., Sakai, D., Kudo, T., Haraguchi, N., *et al.* (2013). Aldehyde dehydrogenase high gastric cancer stem cells are resistant to chemotherapy. *International journal of oncology* 42, 1437-1442.

O'Brien, C.A., Pollett, A., Gallinger, S., and Dick, J.E. (2007). A human colon cancer cell capable of initiating tumour growth in immunodeficient mice. *Nature* 445, 106-110.

Raha, D., Wilson, T.R., Peng, J., Peterson, D., Yue, P., Evangelista, M., Wilson, C., Merchant, M., and Settleman, J. (2014). The cancer stem cell marker aldehyde dehydrogenase is required to maintain a drug-tolerant tumor cell subpopulation. *Cancer research* 74, 3579-3590.

Ricci-Vitiani, L., Lombardi, D.G., Pilozzi, E., Biffoni, M., Todaro, M., Peschle, C., and De Maria, R. (2007). Identification and expansion of human colon-cancer-initiating cells. *Nature* 445, 111-115.

Rocco, A., Liguori, E., Pirozzi, G., Tirino, V., Compare, D., Franco, R., Tatangelo, F., Palaia, R., D'Armiento, F.P., Pollastrone, G., *et al.* (2012). CD133 and CD44 cell surface markers do not identify cancer stem cells in primary human gastric tumors. *Journal of cellular physiology* 227, 2686-2693.

Singh, S.K., Hawkins, C., Clarke, I.D., Squire, J.A., Bayani, J., Hide, T., Henkelman, R.M., Cusimano, M.D., and Dirks, P.B. (2004). Identification of human brain tumour initiating cells. *Nature* 432, 396-401.

Sladek, N.E., Kollander, R., Sreerama, L., and Kiang, D.T. (2002). Cellular levels of aldehyde dehydrogenases (ALDH1A1 and ALDH3A1) as predictors of therapeutic responses to cyclophosphamide-based chemotherapy of breast cancer: a retrospective study. *Rational individualization of oxazaphosphorine-based cancer chemotherapeutic regimens. Cancer chemotherapy and pharmacology* 49, 309-321.

Takaishi, S., Okumura, T., Tu, S., Wang, S.S., Shibata, W., Vigneshwaran, R., Gordon, S.A., Shimada, Y., and Wang, T.C. (2009). Identification of gastric cancer stem cells using the cell surface marker CD44. *Stem cells (Dayton, Ohio)* 27, 1006-1020.

TCGARN (2014). Comprehensive molecular characterization of gastric adenocarcinoma. *Nature* 513, 202-209.

Varon, C., Dubus, P., Mazurier, F., Asencio, C., Chambonnier, L., Ferrand, J., Giese, A., Senant-Dugot, N., Carlotti, M., and Megraud, F. (2012). Helicobacter pylori infection recruits bone marrow-derived cells that participate in gastric preneoplasia in mice. *Gastroenterology* 142, 281-291.

Wang, K., Yuen, S.T., Xu, J., Lee, S.P., Yan, H.H., Shi, S.T., Siu, H.C., Deng, S., Chu, K.M., Law, S., *et al.* (2014). Whole-genome sequencing and comprehensive molecular profiling identify new driver mutations in gastric cancer. *Nature genetics* 46, 573-582.

Yasui, W., Kudo, Y., Naka, K., Fujimoto, J., Ue, T., Yokozaki, H., and Tahara, E. (1998). Expression of CD44 containing variant exon 9 (CD44v9) in gastric adenomas and adenocarcinomas: relation to the proliferation and progression. *International journal of oncology* 12, 1253-1258.

Zhang, S., Balch, C., Chan, M.W., Lai, H.C., Matei, D., Schilder, J.M., Yan, P.S., Huang, T.H., and Nephew, K.P. (2008). Identification and characterization of ovarian cancer-initiating cells from primary human tumors. *Cancer research* 68, 4311-4320.

Figure Legends

Figure 1. Establishment of mouse xenograft models using primary tumors from patients with non-cardia gastric adenocarcinoma.

A. Schematic representation of the strategy used to collect, analyze and xenograft in NSG immunodeficient mice primary tumors collected from patients who underwent gastrectomy for non-cardia gastric carcinoma. Only 8 cases among the 37 cases xenografted led to the development of serially subcutaneously transplantable tumors in mice. At each passage by serial transplantation in mice (P), histology and flow cytometry analyses for the expression of some cell surface markers were performed respectively on tissue samples and on cells freshly dissociated by enzymatic procedures. Cell sorting by FACS of subpopulations positive or negative for the expression of ESA, CD133 and CD44 were performed on cells freshly dissociated from tumors after passage (P) 2 (P2) in mice for *in vitro* tumorsphere assays and *in vivo* xenograft following the ELDA method.

B. Number of weeks after subcutaneous tumor bulk xenograft to reach a tumor size of 500 mm³ after serial transplantation in mice (from P1 to P5). Histograms represent the mean ± SD

for each case, and numbers the global mean \pm SEM of all cases. $1 < n < 12$ mice xenografted per passage and per case.

C. Representative images of HES staining of primary tumors from patients and corresponding P2-P3 xenografts. Scale bars, 50 μ m.

Figure 2. Expression of CD24, CD133 and CD44 on gastric epithelial cells from patients and gastric tumor xenografts.

The percentage of cells expressing CD24, CD133 and CD44 was determined by flow cytometry analyses on stained cells after dissociation by enzymatic procedure from freshly collected specimens.

A. Flow cytometry analyses were performed on 7-AAD-ESA+ live gastric epithelial cells dissociated from paired non-tumor (healthy) and tumor gastric mucosa samples from patients' gastrectomy specimens ($n=7$). Bars, median. * $P < 0.05$.

B. Histograms represent the cumulated results of the percentages of positive cells determined for each marker in serial xenografts. Results indicate that the percentage of cells expressing the different markers remained stable in serial xenografts from P1 to P4, high for ESA ($>80\%$), relatively high or at an intermediate level for CD24 and CD133 (58-81% and 47-64%, respectively), and always less than a third of total cells for CD44 (21-32%). Note: CD24 and CD44 expression were not evaluated on GC06 P1.

n , number of tumors analysed per passage in mice and per case. P1, $1 < n < 3$; P2-4, $3 < n < 17$.

C. Representative images of CD44 detection by immunohistochemistry on paired tumor and non-tumor distant mucosa from the patient and corresponding P2-P3 tumor xenografts in mice. Scale bars, 50 μ m.

Figure 3. Tumorigenic properties of CD133+ and CD44+ cell subpopulations from primary gastric tumor xenografts.

Cells freshly dissociated from P2-P4 tumor xenografts of primary cases (GC04, GC06, GC10, GC40, GC44) were stained with anti-ESA-FITC antibodies with either anti-CD24-PE or anti-CD133-PE antibodies, anti-CD44-APC antibodies and 7-AAD (to exclude 7-AAD+ dead cells) for 4-color flow cytometry analyses.

A. Representative dot-plot analyses of CD24 or CD133 with CD44 and determination of the percentages of ESA, CD24, CD133 and CD44 positives cells and of double-positive cells, as well as the percentages of PE/ CD24+ or CD133+ cells into the APC/CD44+ subpopulation and conversely (3<n<6 per condition and per case). Data represent the mean \pm SEM.

B. 7-AAD-ESA+ tumor cells were sorted by FACS on the expression of CD44 or CD133, and the positive and negative subpopulations of sorted-cells were submitted to the *in vitro* tumorsphere assays and to *in vivo* ELDA xenografts (Table 3 and Table 4). Representative images of cell sorting by FACS and phase contrast microscopy of tumorspheres formed by CD44+ and CD133+ cells or single CD44- and CD133- cells after 10 days of culture of cells seeded at 1,000 cells per well in non-adherent 24 well plates. Scale bars, 50 μ m.

C. Quantification of the number of tumorspheres described in **B** for the indicated cases (n=8 per condition). Data represent the mean \pm SEM. * $P<0.05$.

Figure 4. Analyses of ESA, CD44, CD10, CD49f, CD73 CD166, CD90, CD105 cell surface markers expression and ALDH activity on cells from primary gastric tumor xenografts and cancer cell lines and of their tumorigenic properties.

A. The percentages of cells expressing ESA, CD44, CD10, CD49f, CD73 CD166, CD90, CD105 and ALDH activity were determined by flow cytometry analyses on 7-AAD- cells

from 5 P2-P4 primary tumor xenografts cases (GC04, GC06, GC10, GC40 and GC44) and 5 gastric cancer cell lines (AGS, MKN28, MKN45, MKN74 and NCI87). Bars, median.

B. Representative dot-plot analyses of CD73, CD166, CD90 and CD105 stained with PE-labeled antibodies and of ALDH activity determined by ALDEFLUOR in combination with anti-CD44-APC antibodies on GC10 cells.

C. Quantification of the percentages of positive cells for each marker into the APC/CD44+ subpopulation and conversely in the 5 primary cases. Bars, median.

D. Quantification of the number of tumorspheres formed by FACS-sorted positive and negative cells for each marker after 5 to 10 days of culture of cells seeded at 1000 cells per well in non-adherent 24 well plates for the indicated cases and cell lines (n=8 per condition). Results represent the mean \pm SEM. * $P < 0.05$ for all cases studied. # $P < 0.05$ only for 2 out of 3 cases studied. Representative images of flow cytometry analyses of ALDH activity determined by the fluorescent ALDEFLUOR assay and of the tumorspheres obtained with ALDH+ FACS-sorted cells by phase contrast microscopy. Scale bars, 50 μ m.

Figure 5. Detection of cells expressing CD44 and ALDH in gastric tumors tissues *in vivo* and in tumorspheres *in vitro*.

A. Representative images of immunohistochemistry staining of CD44, ALDH and Ki67 on serial tissue sections of tumor xenografts of GC04 and GC10 intestinal type gastric carcinoma cases and on GC06 and MKN45 diffuse type gastric carcinoma cases. Bars, 50 μ m.

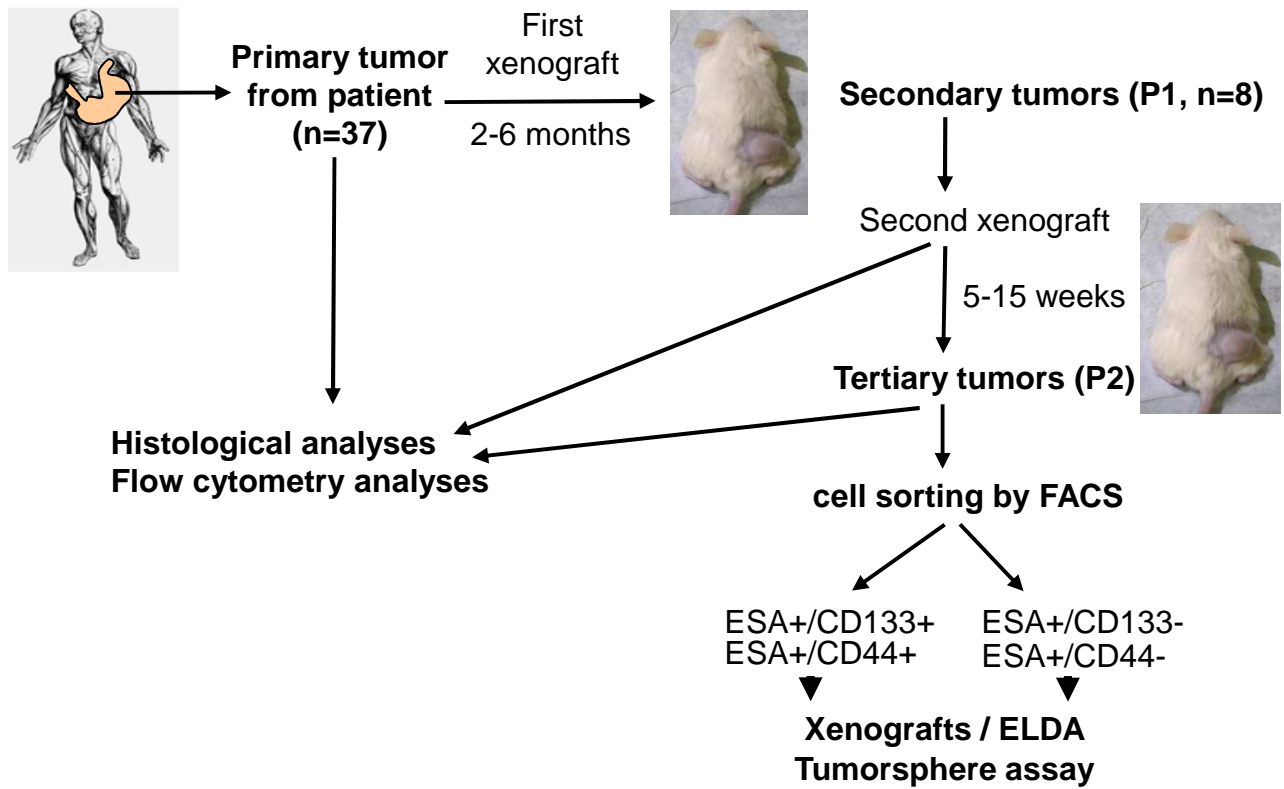
B. Representative images of fluorescent imaging of CD44 stained with anti-CD44-PE antibodies (in red), ALDH activity detected by ALDEFLUOR reagent (in green), and nuclei staining with Hoechst 33342 (in blue) on MKN45 tumorspheres formed after 5, 10 and 15 days. Small tumorspheres are composed essentially of CD44+ALDH+Hoechst- cells, and

medium (10 days) and big (15 days) size tumorspheres of both CD44+ALDH+Hoechst- and CD44+ALDH-Hoechst+ cells. Bars, 10 μ m.

C. Representative dot-plot analysis of CD44 expression and ALDH activity of 15 days MKN45 tumorspheres by flow cytometry showing CD44+ALDH+ and CD44+ALDH- cells. Values represent the percentages of positive cells in each dot-plot quarter.

Figure 1

A



B

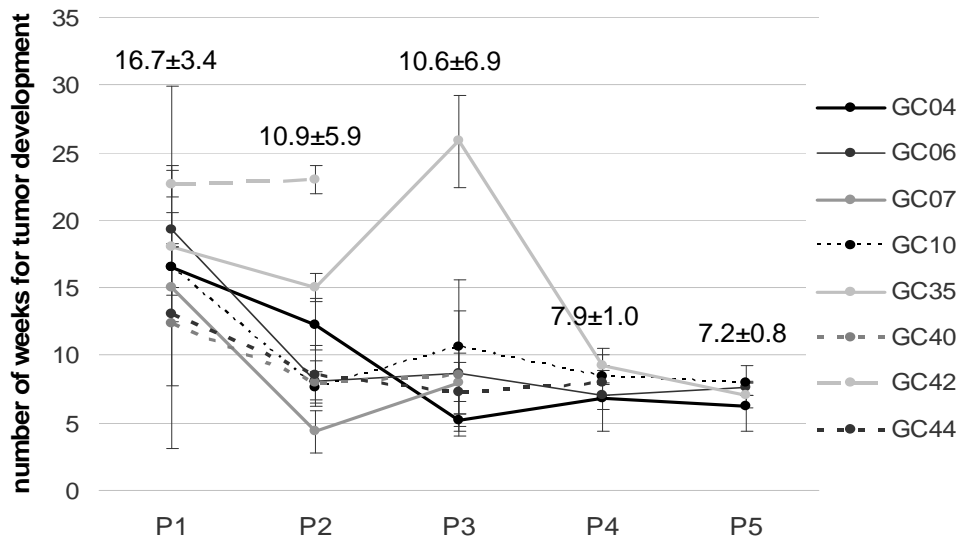


Figure 1

C

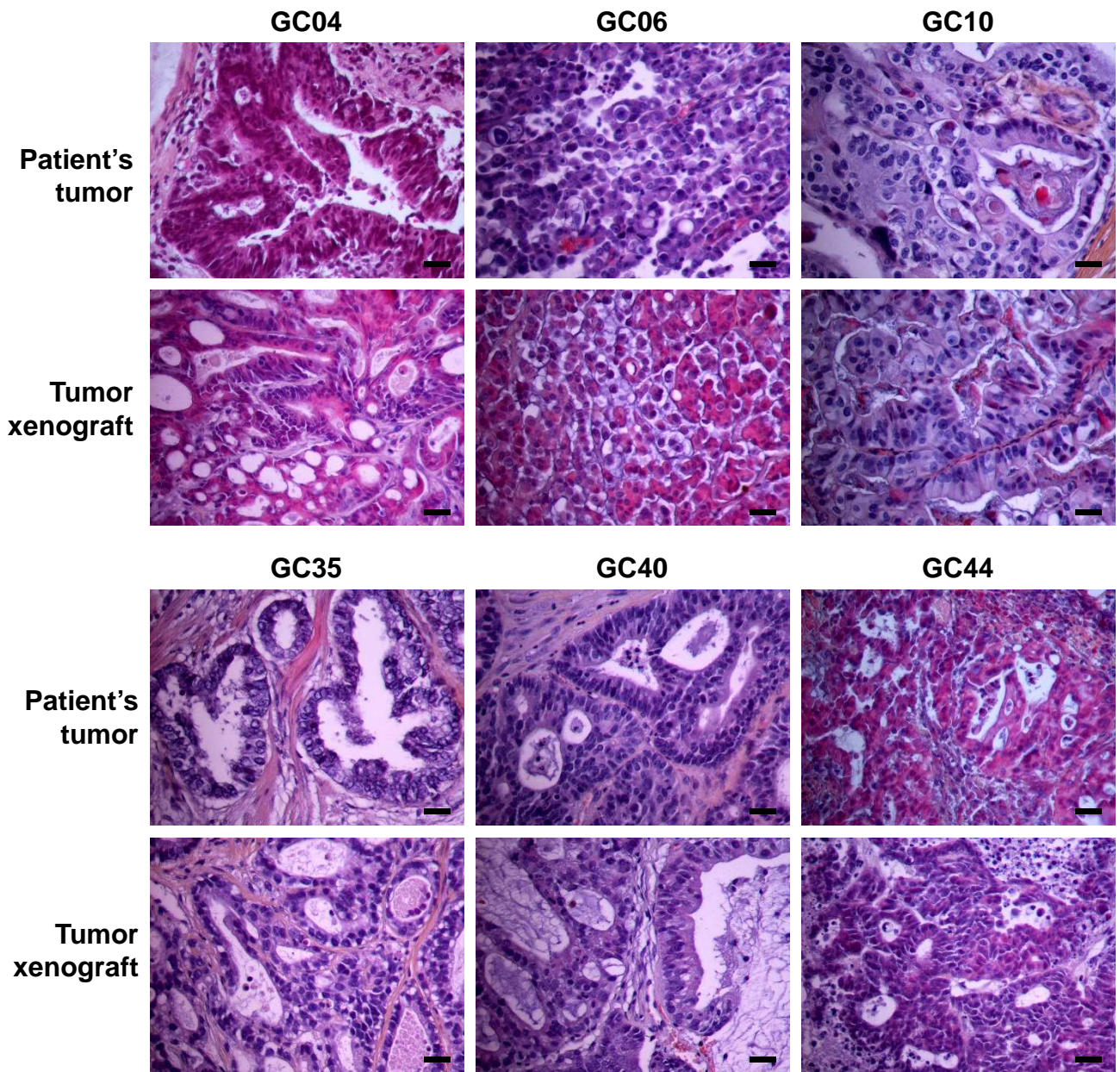
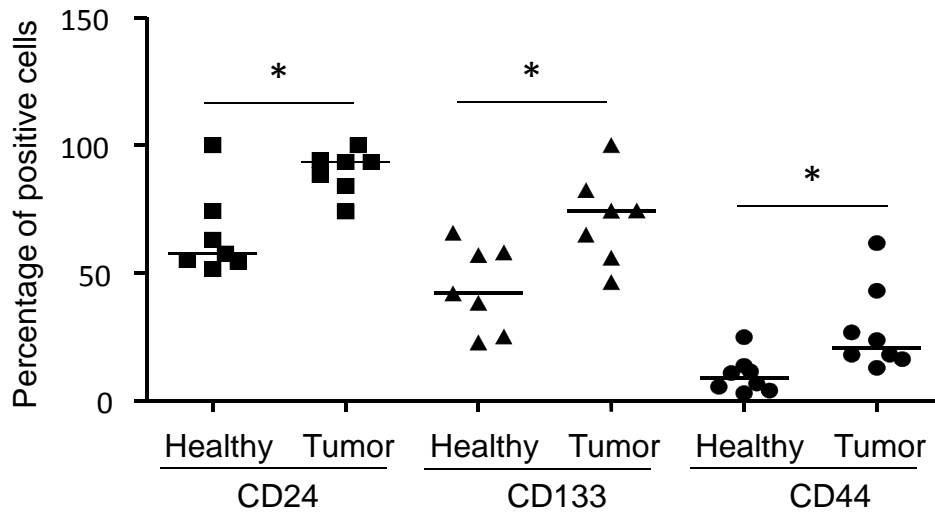


Figure 2

A



B

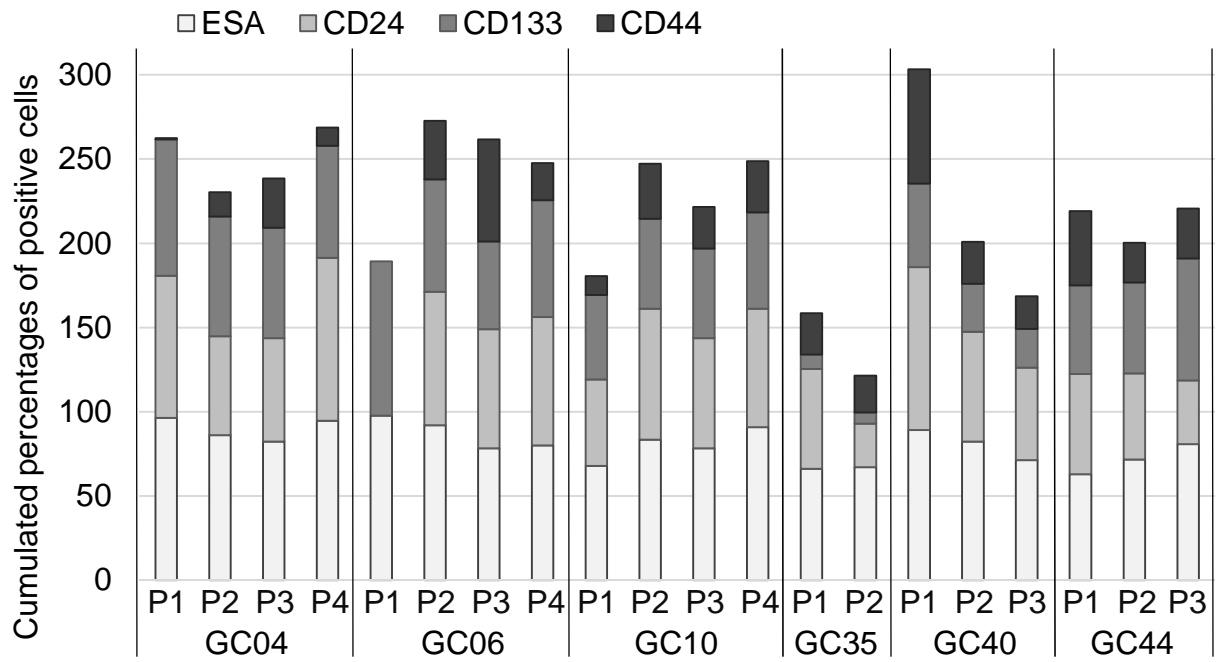


Figure 2

C

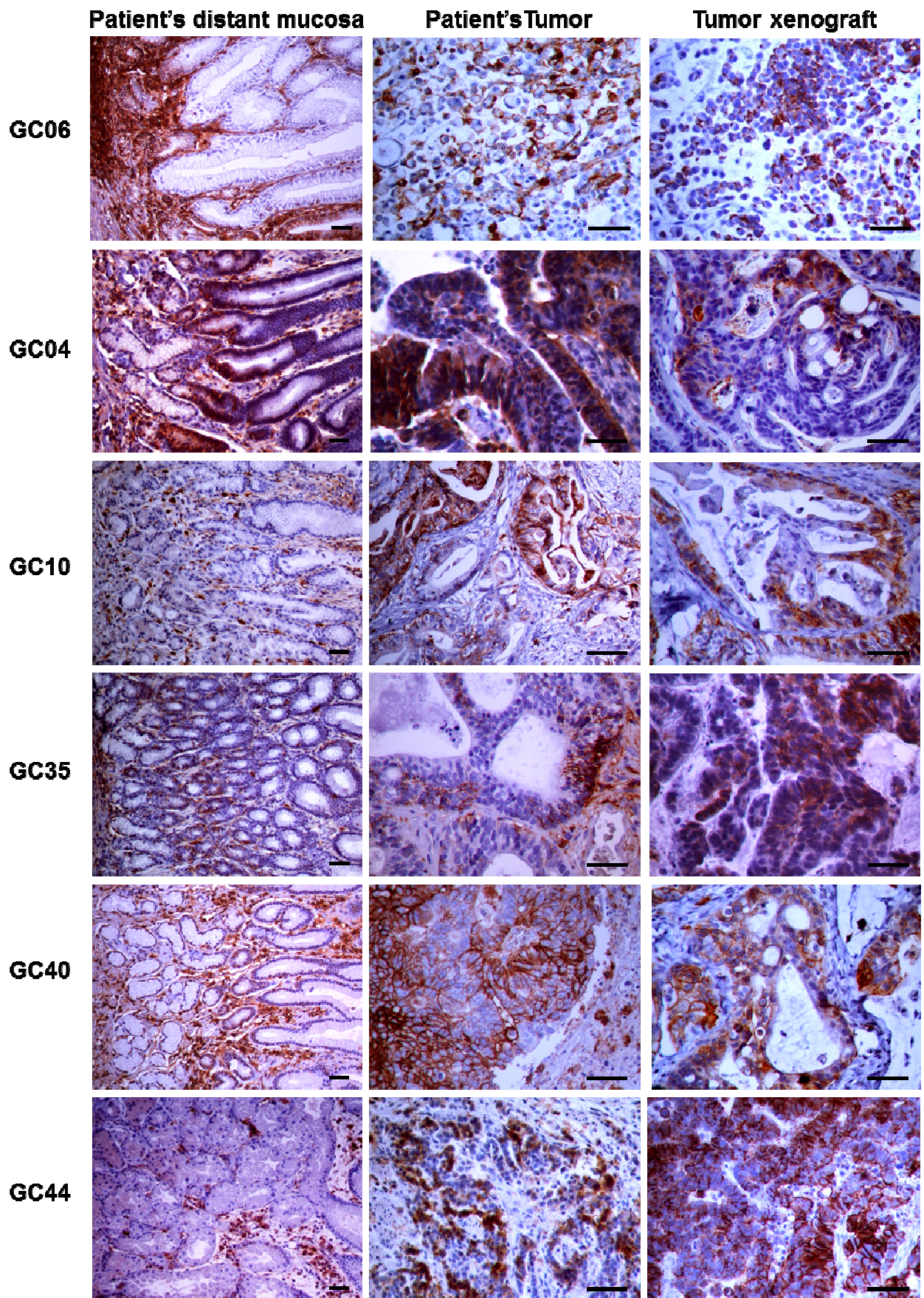
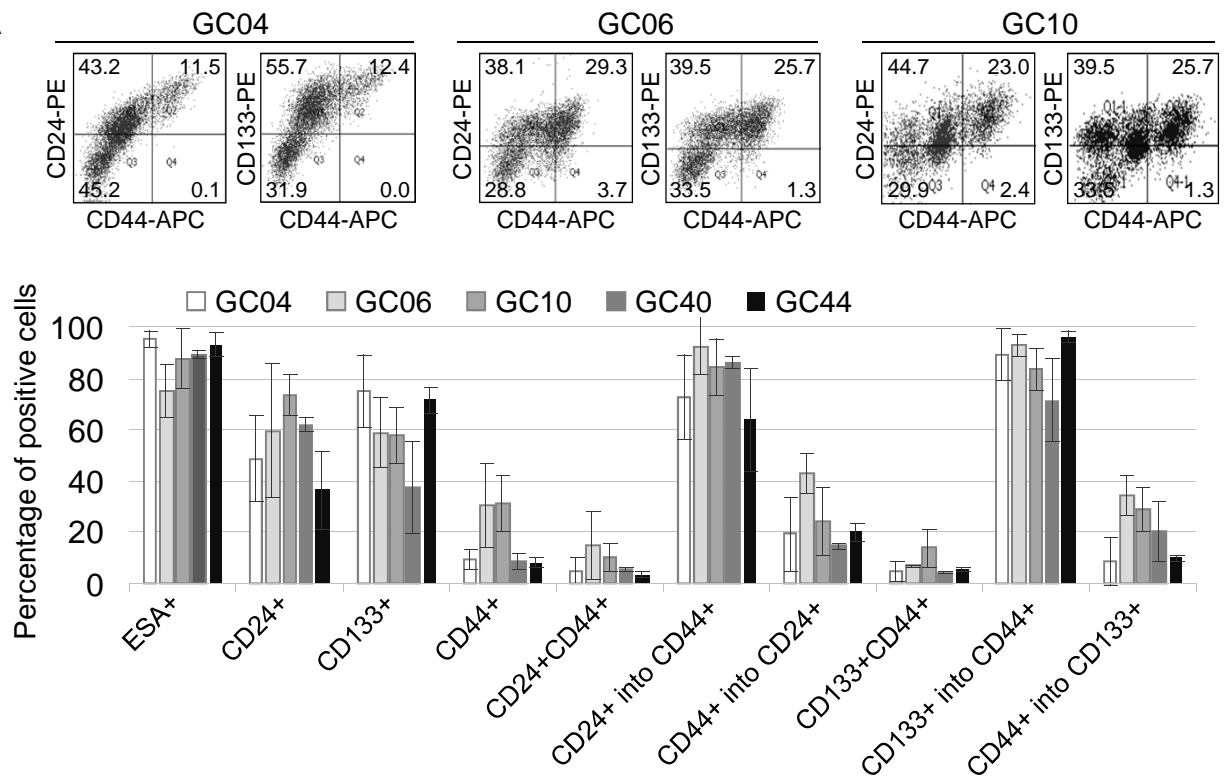
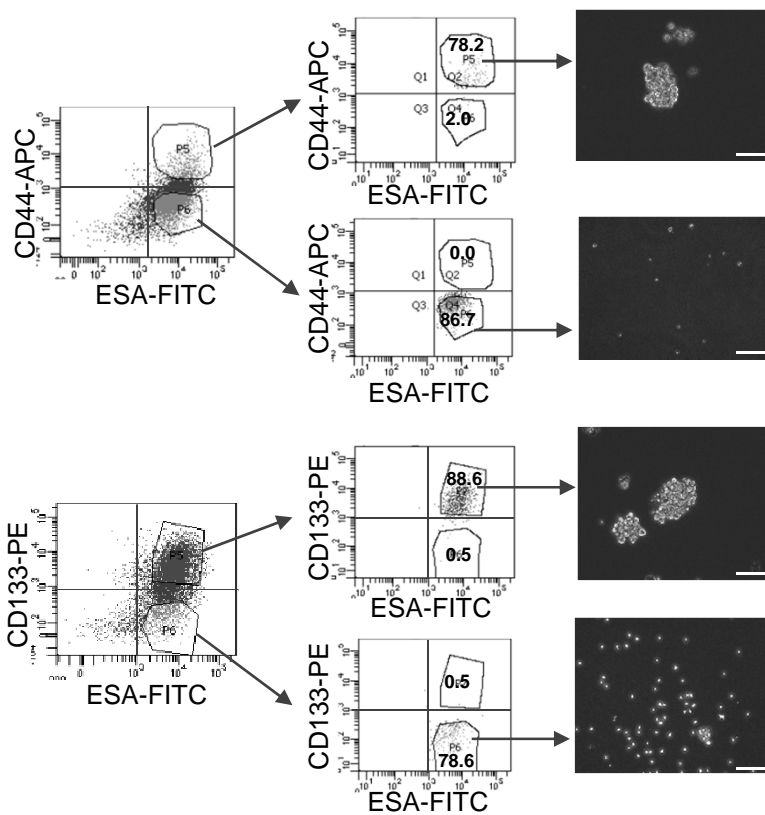


Figure 3

A



B



C

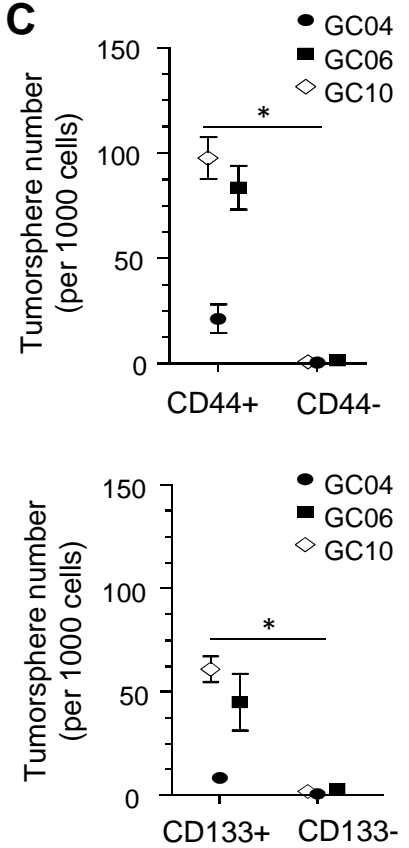
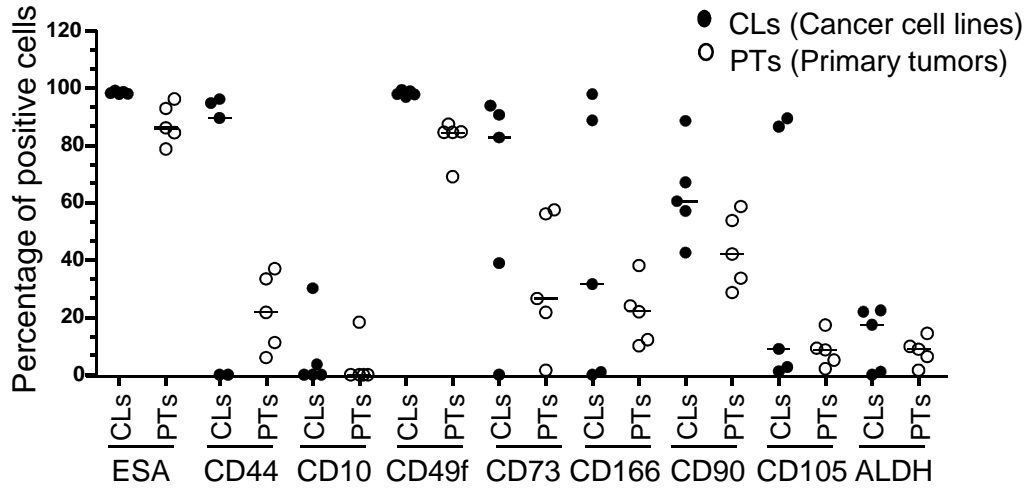
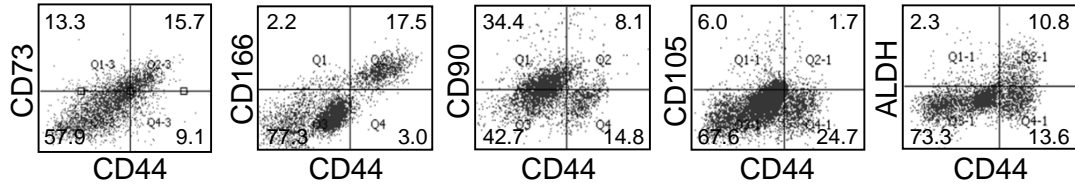


Figure 4

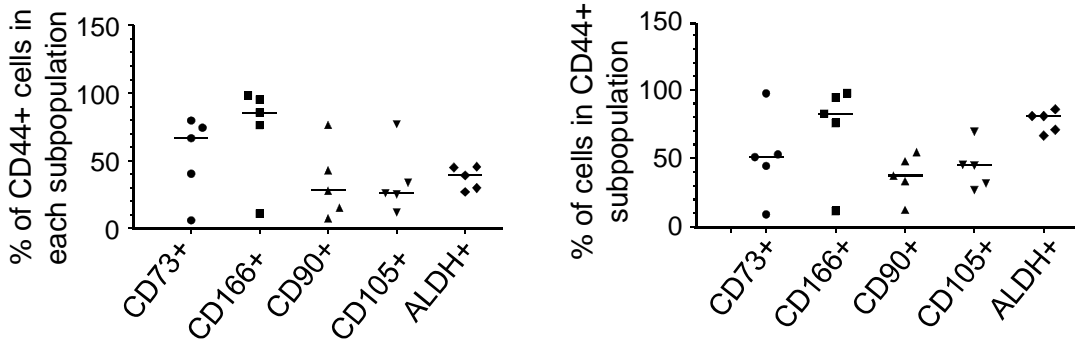
A



B



C



D

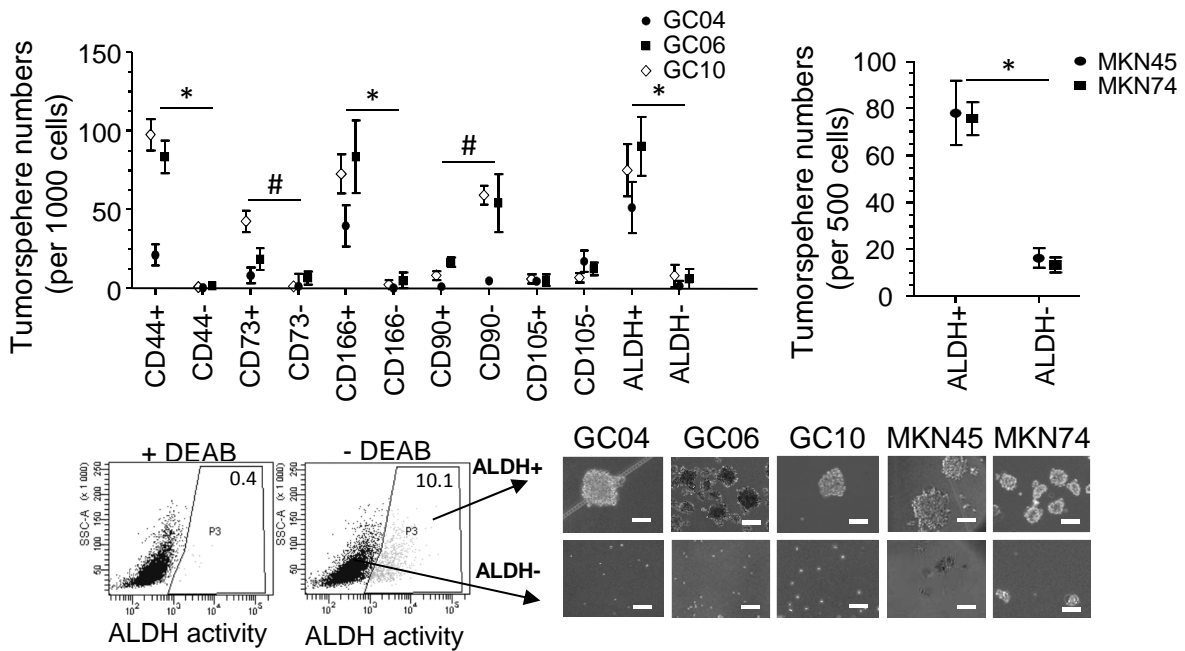


Figure 5

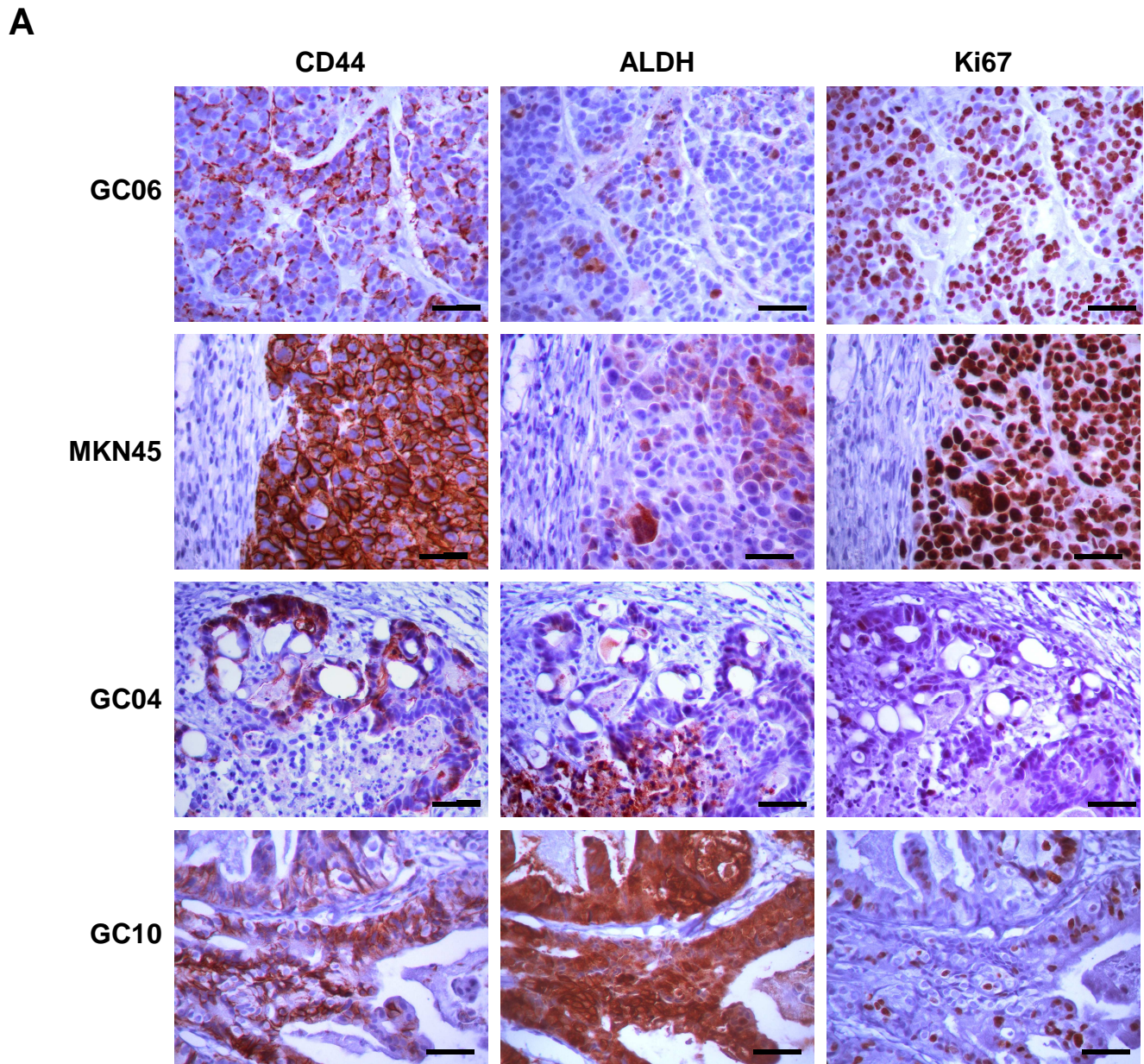


Figure 5

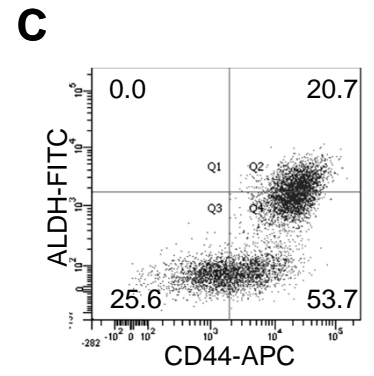
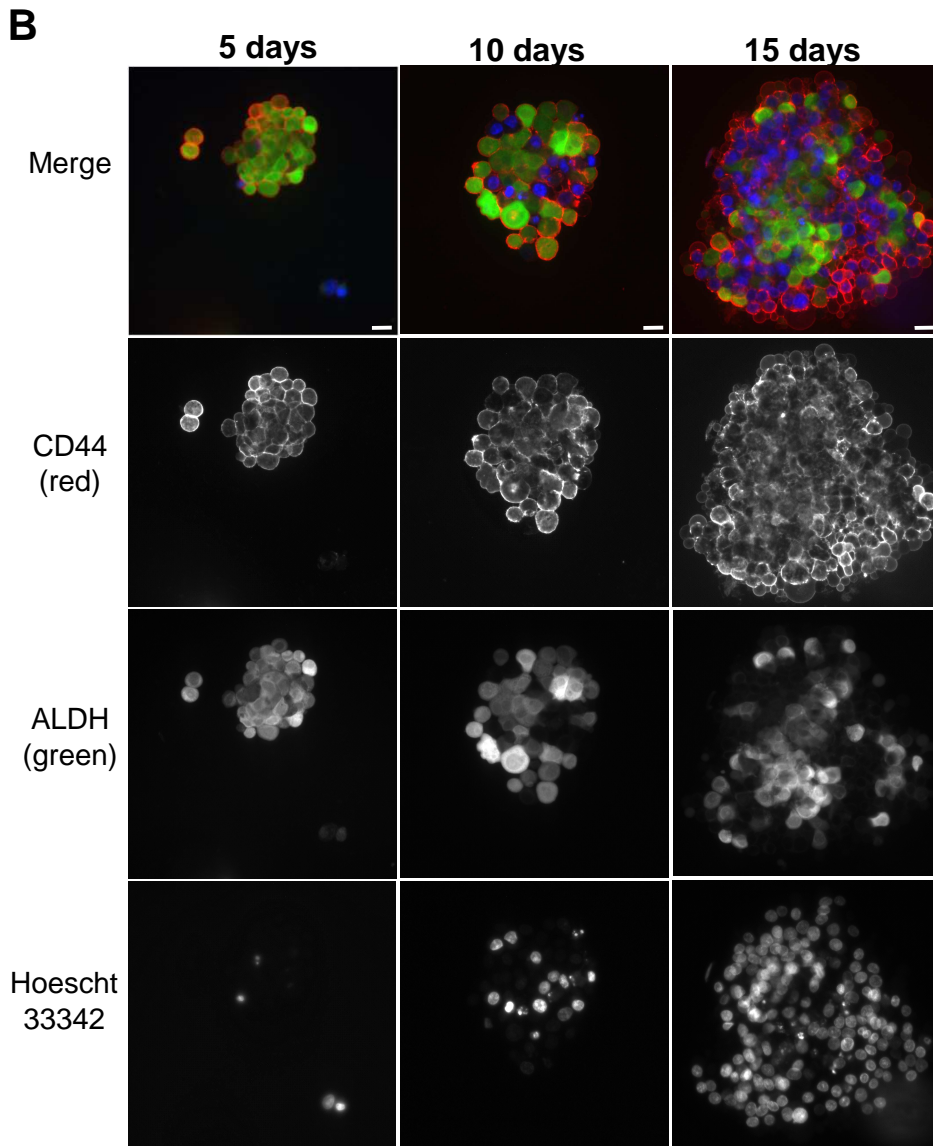


Table 1: Age according to Graft tumor development

| | | Graft tumor | | Total | <i>P</i> |
|------------|---------------|-------------|-----|-------|----------|
| | | No | Yes | | |
| age | N | 29 | 8 | 37 | |
| | median | 69 | 75 | 72 | 0.5185 |
| | Q1 | 51 | 68 | 56 | |
| | Q3 | 79 | 80 | 79 | |
| | mean | 65 | 69 | 66 | |
| | std | 18 | 19 | 18 | |
| | min | 21 | 25 | 21 | |
| | max | 87 | 83 | 87 | |

Table 2: Qualitative variables according to graft tumor development

| | Graft tumour | | | | TOTAL | | P |
|------------------------------|--------------|------|-----|------|-------|------|--------|
| | No | | Yes | | N | % | |
| | N | % | N | % | | | |
| Total | 29 | 100 | 8 | 100 | 37 | 100 | |
| Gender | 19 | 65.5 | 3 | 37.5 | 22 | 59.5 | 0.2281 |
| male | | | | | | | |
| female | 10 | 34.5 | 5 | 62.5 | 15 | 40.5 | |
| Pre OP chemotherapy | 17 | 58.6 | 3 | 37.5 | 20 | 54.1 | 0.4283 |
| No | | | | | | | |
| Yes | 12 | 41.4 | 5 | 62.5 | 17 | 45.9 | |
| WHO stage | 13 | 44.8 | 5 | 62.5 | 18 | 48.6 | 0.2872 |
| tubular | | | | | | | |
| mucinos | 1 | 3.4 | 1 | 12.5 | 2 | 5.4 | |
| poorly cohesive | 12 | 41.4 | 1 | 12.5 | 13 | 35.1 | |
| mixed | 2 | 6.9 | | | 2 | 5.4 | |
| other variants | 1 | 3.4 | 1 | 12.5 | 2 | 5.4 | |
| Grading | 12 | 41.4 | 6 | 75.0 | 18 | 48.6 | 0.1245 |
| BG | | | | | | | |
| HG | 17 | 58.6 | 2 | 25.0 | 19 | 51.4 | |
| Lauren classification | 14 | 48.3 | 7 | 87.5 | 21 | 56.8 | 0.1784 |
| intestinal | | | | | | | |
| diffuse | 13 | 44.8 | 1 | 12.5 | 14 | 37.8 | |
| mixed | 2 | 6.9 | | | 2 | 5.4 | |
| TNM (T) | | | 1 | 12.5 | 1 | 2.7 | 0.1740 |
| T1a | | | | | | | |
| T1b | 3 | 10.3 | 1 | 12.5 | 4 | 10.8 | |
| T3 | 10 | 34.5 | 3 | 37.5 | 13 | 35.1 | |
| T4a | 15 | 51.7 | 2 | 25.0 | 17 | 45.9 | |
| T4b | 1 | 3.4 | 1 | 12.5 | 2 | 5.4 | |
| TNM (N) | 9 | 31.0 | 3 | 37.5 | 12 | 32.4 | 0.6547 |
| N0 | | | | | | | |
| N1 | 3 | 10.3 | 2 | 25.0 | 5 | 13.5 | |
| N2 | 5 | 17.2 | 2 | 25.0 | 7 | 18.9 | |
| N3a | 8 | 27.6 | 1 | 12.5 | 9 | 24.3 | |
| N3b | 4 | 13.8 | | | 4 | 10.8 | |
| TNM (M) | 17 | 58.6 | 7 | 87.5 | 24 | 64.9 | 0.2164 |
| No | | | | | | | |
| Yes | 12 | 41.4 | 1 | 12.5 | 13 | 35.1 | |
| stage grouping | 1 | 3.4 | 1 | 12.5 | 2 | 5.4 | 0.1778 |
| IA | | | | | | | |
| IB | 1 | 3.4 | 1 | 12.5 | 2 | 5.4 | |
| IIA | 6 | 20.7 | 1 | 12.5 | 7 | 18.9 | |
| IIB | 2 | 6.9 | 2 | 25.0 | 4 | 10.8 | |
| IIIA | 2 | 6.9 | | | 2 | 5.4 | |
| IIIB | 2 | 6.9 | 2 | 25.0 | 4 | 10.8 | |
| IIIC | 3 | 10.3 | | | 3 | 8.1 | |
| IV | 12 | 41.4 | 1 | 12.5 | 13 | 35.1 | |

Table 3: Gastric cancer-initiating cell frequencies for the marker CD133

| CASE | Marker | Number of tumours/number of transplanted mice | | | | | | Gastric cancer-initiating cell frequencies (95% Confidence intervals) | Test for difference in stem cell frequencies between CD133+ and CD133 negative cells | |
|------|------------|---|-------|-------|------|------|-----|---|--|-------------|
| | | number of cells transplanted cells | | | | | | | | |
| | | 10 000 | 3 000 | 1 000 | 300 | 100 | 30 | | | |
| 1* | ESA+CD133+ | 5/5 | 5/5 | 4/10 | 1/9 | 0/10 | | 1/1658 | (1/3071-1/895) | $P=0.0001$ |
| 1* | ESA+CD133- | 2/2 | 0/5 | 0/10 | 0/10 | 0/10 | | 1/19065 | (1/70548-1/2153) | |
| 2 | ESA+CD133+ | 5/5 | 4/5 | 1/5 | 2/5 | 0/5 | | 1/1911 | (1/4019-1/908) | $P<10^{-4}$ |
| 2 | ESA+CD133- | 1/5 | 0/5 | 0/5 | 0/5 | 0/5 | | 1/66876 | (1/467214-1/9573) | |
| 3 | ESA+CD133+ | | | | 4/4 | 3/5 | 1/6 | 1/105 | (1/229-1/48.5) | $P=0.0057$ |
| 3 | ESA+CD133- | | | | 2/4 | 0/5 | 0/6 | 1/781 | (1/3030-1/202) | |

Case 1, GC06; case 2, GC04; case 3, GC10. *There was complete data separation, thus estimates may not be reliable. Further, the single-hit assumption that one cell is sufficient for a positive response may not be true.

Table 4: Gastric cancer-initiating cell frequencies for the marker CD44

| CASE | Marker | Number of tumours/number of transplanted mice | | | | | | Gastric cancer-initiating cell frequencies (95% Confidence intervals) | Test for difference in stem cell frequencies between CD44+ and CD44 negative cells | |
|------|-----------|---|-------|-------|-------|-------|------|---|--|-------------|
| | | number of cells transplanted cells | | | | | | | | |
| | | 10 000 | 3 000 | 1 000 | 300 | 100 | 30 | | | |
| 1 | ESA+CD44+ | 8/8 | | 9/10 | 6/10 | 2/5 | | 1/352 | (1/625-1/198) | $P=0.0012$ |
| 1 | ESA+CD44- | 4/4 | | 4/8 | 1/8 | 0/5 | | 1/1688 | (1/3913-1/728) | |
| 2 | ESA+CD44+ | 5/5 | 5/5 | 8/15 | 4/15 | 2/10 | | 1/1020 | (1/1670-1/623) | $P<10^{-4}$ |
| 2 | ESA+CD44- | 2/5 | 0/4 | 0/5 | 0/5 | | | 1/28963 | (1/113477-1/7392) | |
| 3* | ESA+CD44+ | | | 15/15 | 15/15 | 19/20 | 7/10 | 1/29 | (1/50-1/17) | $P<10^{-4}$ |
| 3* | ESA+CD44- | | | 5/5 | 2/5 | 0/5 | | 1/568 | (1/1202-1/268) | |

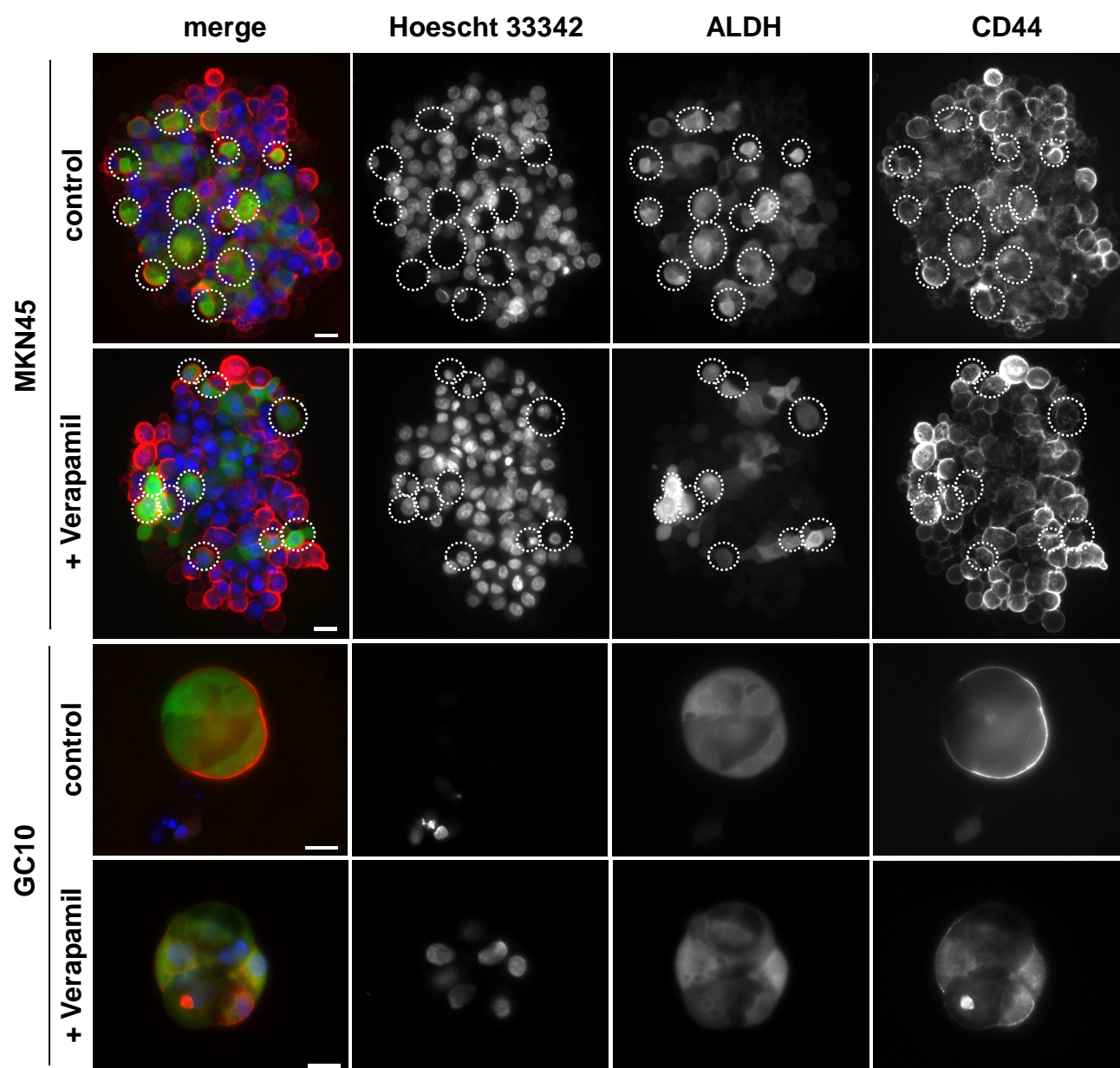
Case 1, GC06; case 2, GC04; case 3, GC10. * There was complete data separation, thus estimates may not be reliable.

Table 5: Gastric cancer-initiating cell frequencies for the marker ALDH

| CASE | Marker | Number of tumours/number of transplanted mice | | | | | | Gastric cancer-initiating cell frequencies (95% Confidence intervals) | Test for difference in stem cell frequencies between ALDH+ and ALDH- cells | |
|------|--------|---|-------|-------|-----|-----|-----|---|--|------------|
| | | number of cells transplanted cells | | | | | | | | |
| | | 10 000 | 3 000 | 1 000 | 300 | 100 | 30 | | | |
| 1* | ALDH+ | | | | 2/2 | | 5/5 | 2/5 | 1/38 (1/89-1/16) | $P=0.0002$ |
| 1* | ALDH- | | | | 2/3 | | 0/5 | 0/5 | 1/613 (1/2348-1/160) | |
| 2* | ALDH+ | | 6/6 | | 5/6 | | | | 1/167 (1/454-1/62) | $P=0.2145$ |
| 2* | ALDH- | | 6/6 | | 3/6 | | | | 1/427 (1/1284-1/142) | |
| 3 | ALDH+ | | | 5/5 | 5/5 | 3/5 | 2/5 | 1/80 (1/174-1/37) | $P=0.0042$ | |
| 3 | ALDH- | | | 4/5 | 3/5 | 2/5 | 1/5 | 1/368 (1/782-1/173) | | |
| 4* | ALDH+ | 6/6 | 5/6 | | 5/6 | | | 1/273 (1/763-1/98) | $P<10^{-4}$ | |
| 4* | ALDH- | 5/6 | 1/6 | | 0/6 | | | 1/21208 (1/64690-1/6953) | | |

Case 1, GC06; case 2, MKN45; case 3, GC10; case 4, MKN74. * There was complete data separation, thus estimates may not be reliable. Further, the single-hit assumption that one cell is sufficient for a positive response may not be true.

Supplementary Figure 1



Supplementary Table 1: Description of patient characteristics

| Characteristics | N | % |
|------------------------------|----|-----------|
| Gender | | |
| male | 22 | (59.5) |
| female | 15 | (40.5) |
| Age (years) | 72 | (56; 79) |
| pre OP chemotherapy | . | |
| No | 20 | (54.1) |
| Yes | 17 | (45.9) |
| WHO stade | . | |
| tubular | 18 | (48.6) |
| mucinos | 2 | (5.4) |
| poorly cohesive | 13 | (35.1) |
| mixed | 2 | (5.4) |
| other variants | 2 | (5.4) |
| Grading | . | |
| BG | 18 | (48.6) |
| HG | 19 | (51.4) |
| Lauren classification | . | |
| intestinal | 21 | (56.8) |
| diffuse | 14 | (37.8) |
| mixed | 2 | (5.4) |
| TNM (T) | . | |
| T1a | 1 | (2.7) |
| T1b | 4 | (10.8) |
| T3 | 13 | (35.1) |
| T4a | 17 | (45.9) |
| T4b | 2 | (5.4) |
| TNM (N) | . | |
| N0 | 12 | (32.4) |
| N1 | 5 | (13.5) |
| N2 | 7 | (18.9) |
| N3a | 9 | (24.3) |
| N3b | 4 | (10.8) |
| TNM (M) | . | |
| No | 24 | (64.9) |
| Yes | 13 | (35.1) |
| stage grouping | . | |
| IA | 2 | (5.4) |
| IB | 2 | (5.4) |
| IIA | 7 | (18.9) |
| IIB | 4 | (10.8) |
| IIIA | 2 | (5.4) |
| IIIB | 4 | (10.8) |
| IIIC | 3 | (8.1) |
| IV | 13 | (35.1) |

Supplementary Figure legend.

Supplementary Figure 1. ALDH positive cells in gastric tumorspheres have drug efflux properties.

Representative images of fluorescent imaging of CD44 stained with anti-CD44-PE antibodies (in red), ALDH activity detected by ALDEFLUOR reagent (in green), and nuclei staining with Hoechst 33342 (in blue) on 12 days MKN45 tumorspheres and on 5 days GC10 tumorspheres. Tumorspheres were treated or not (control) with verapamil 10 min before the staining procedure. Dotted circles point out ALDH⁺ cells without or with Hoechst 33342 staining of the nuclei in controls and after verapamil treatment, respectively. Bars, 10 μ m.

Article 2 – All-trans retinoic acid targets cancer stem cells and inhibits tumor growth in gastric carcinoma

Manuscript in preparation

All-trans retinoic acid targets cancer stem cells in gastric carcinoma and inhibits tumor growth

Phu Hung Nguyen^{1,2}, Cathy Staedel^{2,3}, Lucie Chambonnier^{1,2}, Pierre Dubus^{2,4,5}, Edith Chevret^{2,4}, Xavier Gauthereau^{2,6}, H el ene B œuf^{2,6}, Benoit Rousseau^{2,7}, Murielle Fevre^{2,7}, Isabelle Soubeyran⁸, Genevi eve Belleann e⁹, Serge Evrard¹⁰, Denis Collet¹¹, Francis M egraud^{1,2,5}, Christine Varon^{1,2}.

1 INSERM, U853, F-33000 Bordeaux, France

2 University of Bordeaux, F-33000 Bordeaux, France

3 INSERM, U869, ARNA Laboratory, F-33000 Bordeaux, France

4 EA2406, University of Bordeaux, F-33000 Bordeaux, France

5 University Hospital Center, F-33000 Bordeaux, France

6 UMR CNRS 5164 CIRID, F-33000 Bordeaux, France

7 Service Commun des Animaleries, University of Bordeaux, F-33000 Bordeaux, France

8 Department of Biopathology, Institut Bergoni e, F-33000 Bordeaux, France

9 Department of Histopathology of Tumors, Haut-Leveque Hospital, F-33000 Bordeaux, France

10 Department of Digestive Oncology, Institut Bergoni e, F-33000 Bordeaux, France

11 Department of Digestive Surgery, Haut-Leveque Hospital, F-33000, Bordeaux, France

Contact. Dr. Christine Varon, INSERM U853, Universit e de Bordeaux, 146 rue Leo Saignat, Bordeaux F-33076, France. Email: christine.varon@u-bordeaux.fr.

Summary (292 word)

Gastric carcinoma, one of the leading causes of cancer-related death worldwide. This cancer, most of the time metastatic, remains treated essentially by surgery with conventional chemotherapy, and is of poor prognosis. The existence of cancer stem cells (CSC) expressing CD44 and a high aldehyde dehydrogenase (ALDH) activity was recently demonstrated in gastric carcinoma, which has opened new perspectives to develop targeted therapy. In this study, we evaluated the effects of all-trans-retinoic acid (ATRA) on the self-renewal and tumorigenic properties of gastric CSC from cancer cell lines and from patient's derived primary tumors, *in vitro* in conventional 2D culture and in 3D culture system where only CSC form tumorspheres, and *in vivo* in mouse xenografts models where only CSC can initiate a new tumor. In these models, ATRA induced an inhibition of both the formation and the growth of tumorspheres *in vitro*. This was associated to a blockade of the cell cycle through the upregulation of cyclin dependant kinase (CDK) inhibitors P21, P27, P53, P16 and the downregulation of actors of cell cycle progression, cyclins A2, B1, D1, E1, Cdc25C, CDK2, E2F1 and PCNA3. Most interestingly, ATRA also markedly down-regulated the expression of the CSC markers CD44 and ALDH as well as stemness genes such as Klf4 and Sox2 in tumorspheres. Surprisingly, ATRA treatment of tumor xenografts *in vivo* was sufficient to block tumor growth and to induce tumor regression after 2 weeks of treatment, but was insufficient to prevent tumor relapse after several weeks. However, the percentage of CD44, ALDH, Ki67 and PCNA positive cells in resting tumor contingents was drastically decreased. In conclusion, ATRA appears as a potent strategy to target and inhibit gastric CSC to efficiently inhibit tumor growth in gastric carcinoma of both the intestinal and the diffuse type.

Key words. Gastric cancer, ALDH, CD44, primary tumor, xenograft, cell cycle, tumorsphere

Introduction

Gastric cancer is currently the third leading cause of death by cancer in the world. Gastric adenocarcinoma which constitute the majority of the cases are heterogeneous, being classified in numerous histological variants depending on the WHO classification (1). The Lauren's classification system distinguishes mainly the diffuse and the intestinal subtypes based on histological criteria (2). Gastric adenocarcinomas are also classified based on their localization in the stomach, those of the cardia having a different etiological origin than those of the corpus and the antrum which are related to infection with *Helicobacter pylori*. Chronic infection with *H. pylori*, classified as a class 1 carcinogen by the WHO in 1994, is considered to be responsible for more than 93% of non-cardia gastric carcinoma (3) (4). This cancer, most of the time metastatic because it is detected too late, has a poor prognosis. Current treatment continues to be essentially based on surgery combined with conventional chemotherapy. However, chemoresistance of cancer cells leading to recurrence following treatment is a major problem. In recent years, many studies have shown that tumors are heterogeneous, containing a subpopulation of cells at the origin of tumor growth, the so-called cancer stem cells (CSC), which are now considered to be the cells to target to eradicate cancer. These cells are characterized by self-renewal and asymmetrical division properties, being at the origin of the more or less differentiated cells composing the tumor mass. CSCs have been shown to be more resistant to treatments than the more differentiated cells composing the tumor mass, and are therefore at the origin of cancer recurrence after treatment. This chemoresistance mechanism was shown to be associated with the expression of drug efflux systems, such as ABC transporter proteins, as well as a high aldehyde dehydrogenase (ALDH) activity (5) (6) (7). Some of the ALDH isoforms are retinaldehyde dehydrogenase which convert retinal derived from vitamin A into active All-trans- and cis9-retinoic acids (RA). RAs play a key role during development and in adult, they control

homeostasis in some tissues by regulating the self-renewal and differentiation properties of stem cells. Concerning cancer treatment, retinoic therapy with All-trans retinoic acid (ATRA) was introduced in the late 1980s into the therapy of acute promyelocytic leukemia (APL), and radically changed the management and the outcome of this disease. In APL patients, ATRA induces an inhibition of proliferation and the differentiation of leukemia cells, leading to a complete remission in the majority of cases when administered in combination with light chemotherapy and/or arsenic trioxide (8). The success of ATRA-based differentiation therapy to treat APL patients has opened the perspective to utilize RA in the treatment of solid tumors. Currently, 13-cis RA is used in clinical trials for the treatment of skin, head and neck, prostate, non-small-cell lung and cervical carcinoma, while ATRA and 9-cis RA are used in treatment of thyroid, prostate, breast, and squamous cell cancer (9). Indeed ATRA-induced differentiation was considered as the most important mechanism of action of RA in cancer treatment, recent studies revealed that ATRA also regulated CSCs properties in glioblastoma and head and neck carcinoma via the regulation of Notch and Wnt/ β -catenin pathway (10)(11).

Concerning gastric cancer, the existence of CSCs was first reported in gastric cancer cell lines and more recently in primary human gastric adenocarcinoma cases. Gastric CSCs were essentially characterized by the expression of the cell surface marker CD44, as well as by a high ALDH activity (12)(13)(7)(14) (15) (16).

The purpose of the present report was to evaluate the effect of ATRA treatment on self-renewal and tumorigenic properties of CSCs from gastric cancer cell lines and from primary tumors of intestinal and diffuse variants of non-cardia gastric adenocarcinoma. The effects of ATRA treatment were evaluated on the tumorigenic properties of gastric CSCs by *in vitro* tumorsphere assays and by *in vivo* xenografts in immunodeficient mice. The effects of ATRA

on proliferation, cell cycle progression and apoptosis were evaluated *in vitro*. Finally the expression of the cell cycle and CSCs and stemness markers were evaluated in response to ATRA treatment *in vitro* and confirmed *in vivo* on tumor xenografts.

Results

1. Optimization of cell culture conditions for studying the anti-proliferative effects of ATRA

The human gastric adenocarcinoma MKN45 and MKN74 cell lines, of diffuse and intestinal histological types respectively, were grown in monolayers with or without fetal calf serum in the culture medium, and the effects of increasing ATRA concentrations were evaluated on cell growth after 48 h of treatment (Fig. 1). Fig. 1A shows that ATRA efficiently inhibited the growth of both cell lines in a dose-dependent manner under serum-free conditions, whereas the presence of serum totally prevented its effect in MKN74 cells and notably diminished it in MKN45 cells. Indeed, a dose of 5 μ M, which was totally inefficient in the presence of serum in MKN74 cells, reduced cell growth by 60% under serum-free conditions. To further assess the hampering action of serum on ATRA effects on gastric adenocarcinoma cells, we grew six different cell lines (MKN45 and AGS of diffuse type; NCI-87, MKN7, MKN74 and MKN28 of intestinal type) in monolayers with or without 5 μ M ATRA, in the presence of increasing serum concentrations in the culture media. For each of the six cell lines tested, the serum prevented ATRA-induced inhibition of cell growth in a concentration-dependent manner (Supplementary Fig. S1). Some cell lines such as MKN7, MKN74 and MKN28 responded to ATRA only under conditions of total serum deprivation. With a growth inhibition of 70 %,

the diffuse type MKN45 and the intestinal type MKN74 cell lines appeared to be the most sensitive to ATRA under serum-free conditions.

We then wondered whether the difference in sensitivity of these cell lines to ATRA was related to their basal levels of retinoic acid (RA) signaling pathway components in the presence or in the absence of serum. Therefore, we analyzed the expression levels of the ATRA transporters, cellular RA binding protein (CRABP) 1 and CRABP2; the RA receptors RAR- α , - β , - γ and RXR- α , - β , - γ ; and the cytochrome P450 hydrolase CYP26A1 which mediates ATRA degradation, in two diffuse (MKN45 and AGS) and two intestinal type (MKN74 and MKN28) gastric cancer cell lines. Only RAR- γ , RXR- α and RXR- β were expressed at a substantial level (at least 1/10 of the housekeeping genes) in every cell line, with CRABP2 in MKN74, MKN28 and AGS but not in MKN45 cells (Supplementary Table S2 and data not shown). The changes in the expression of these components were therefore determined par reverse transcription quantitative polymerase chain reaction (RT-qPCR) in the presence or in the absence of serum. Table S2 shows that the RAR- γ and RXR- β receptors were upregulated upon serum removal in all cell lines, by 2.5 to almost 5 fold in MKN45 and MKN74 cells with a concomitant upregulation of RXR- α by 2.5 to 3.4 fold. The CRABP2 transporter was also enhanced by 3.4 fold in MKN74 cells under the same conditions. In MKN28 and AGS cells, the serum removal enhanced only RAR- γ and RXR- β expression. Thus, the enhanced expressions of these RA receptors upon serum deprivation likely contributed to sensitize cell lines to ATRA treatment. MKN45 and MKN74 cell lines which harbor the highest expression of RA components and are sensitive to ATRA treatment upon serum deprivation, were therefore chosen for further studies on the mechanisms of action of ATRA on gastric adenocarcinoma cells.

In addition to its inhibitory effect on cell growth upon serum deprivation, ATRA also affected the cell morphology (Fig. 1B). MKN45 cells became rounded, clumpy and loosely adherent to the cell support, whereas MKN74 cells, usually typical adherent epithelial cells with a polygonal shape, became elongated and fibroblast-shaped.

To clarify the mechanism by which ATRA inhibited cell growth under serum-free conditions, we performed a cell cycle DNA analysis by flow cytometry (Fig. 1C). In the presence of increasing concentrations of ATRA, the proportion of cells in the G0/G1 phase progressively increased to the detriment of the proportion of cells in the S and G2/M phases. The proportion of sub-G1 cells, indicating the number of dead cells, remained virtually unaffected in both cell lines. The combination of these results indicated that ATRA inhibited gastric carcinoma cell growth by blocking cell cycle progression at the G1/S transition rather than by inducing cell death.

2. ATRA inhibits the formation of tumorspheres in tridimensional cultures of human gastric carcinoma cell lines and primary cases

We previously reported a tridimensional (3D) culture system in serum-free media to evaluate the tumorigenic properties of gastric cancer cells from cell lines and from primary tumors of patients (15). These 3D culture conditions, allowing the formation from a single growing cell of a spheroid of compact cells floating in the culture medium, are considered to be closer to physiological conditions than monolayer culture. In addition, they reveal the CSC-like population of cells possessing these tumorigenic properties inside the cell line or the primary tumor (15, 16)(12). Taking into account the fact that ATRA is efficient under serum-free conditions, we evaluated the effects of ATRA treatment on tumorsphere formation and growth of MKN45 and MKN74 cell lines (Supplementary Fig. S2 and Fig. 2A). Addition of ATRA to the culture medium at the time of plating cells prevented the formation of

tumorspheres recorded after 5 days, in a dose-dependent manner (Fig. 2A-B). The number of tumorspheres was inversely correlated with the ATRA doses, suggesting that ATRA reduced the number of CSC-like cells (Fig. 2B). This parameter was particularly affected in MKN74 cells with concentrations as low as 1 μ M ATRA, with a 3 fold decrease in the number of tumorspheres compared to the control DMSO-treated cultures.

To assess whether the ability of ATRA to interfere with the CSC properties of established cell lines could be applicable to primary human gastric adenocarcinoma, carcinoma cells were isolated from freshly collected tumors of human primary cases xenografted in mouse models, and submitted to the *in vitro* tumorsphere assay in the presence of increasing ATRA concentrations (Fig. 2C). GC04 and GC10 are intestinal type gastric adenocarcinomas, whereas GC06 is a diffuse type gastric adenocarcinoma. Carcinoma cells isolated from these primary tumors formed tumorspheres, indeed at a lower extent than gastric cancer cell lines (Fig. 2C). As in the established cell lines, ATRA similarly prevented the growth of tumorspheres of all primary cases in a dose-dependent manner, the 80% inhibitory concentration being 5 μ M ATRA. This result confirmed the ability of ATRA to interfere with the CSC properties in either primary or established gastric carcinoma cell culture.

We then evaluated whether ATRA could also inhibit the growth of tumorspheres, once they are formed. MKN45 cells were grown as tumorspheres for 5 days, before the addition of increasing ATRA concentrations. Both the kinetics and the images in Fig. 2D showed that the number of tumorspheres declined in the presence of ATRA in a time- and dose-dependent manner. A similar experiment performed on MKN74 cells confirmed this result for the dose of 5 μ M ATRA applied for 10 days on tumorsphere cultures (Fig. 2D right). In addition to the number of tumorspheres (Fig. 2B) which corresponds to the number of CSC-like cells, we also evaluated the size of the tumorspheres (Fig. 2E) which corresponds to the self-renewal

and proliferation properties of the CSC-like cells. At a dose of 5 μM which efficiently reduced the tumorsphere number in both cell lines, the size of tumorspheres was also significantly reduced by 2 and 10 fold in MKN45 and MKN74 cells, respectively (Fig. 2E). This suggested that the proliferative capacities of the residual CSC-like cells were also hindered by ATRA. All combined, these results showed that ATRA interferes with the capacity of gastric carcinoma cells to grow as tumorspheres, thereby unveiling the particular efficiency of this drug to target cells with CSC-like properties within the carcinoma cell population.

3. ATRA represses the expression of cell cycle-driving genes

To get further insight into the mechanisms by which ATRA hinders the growth and self-renewal properties of CSC-like cells in tumorspheres in 3D culture, we performed a cell cycle DNA analysis by flow cytometry on MKN45 and MKN74 tumorspheres after 48 h of ATRA treatment at 5 μM . In MKN45 cells, ATRA increased the proportion of cells in the G0/G1 phase to the detriment of cells in the S and G2/M phases (Fig. 3A), while enhancing the percentage of dead cells in sub-G1 (Fig. 3B). In MKN74 cells, ATRA increased the proportion of cells in the G2/M phase (Fig. 3A) without affecting the percentage of sub-G1 cells (Fig. 3B). These results indicated that ATRA blocked the cell cycle progression in both cell lines, at the G1/S or the G2/M transition with a moderate or null effect on cell death, depending on the cell line.

Using RT-qPCR and immunofluorescence, we analyzed the expression of some cell cycle regulators in response to 5 μM ATRA for 2 or 5 days. MKN45 responded to ATRA by a marked increase in the expression of the cyclin-dependent kinase (CDK) inhibitor (CDKI) p21, p27 and the growth arrest and DNA damage inducible protein GADD45A, as well as by a moderate increase in the tumor suppressor p53 (Fig. 3C). These changes were visible as

early as the second day of treatment and declined thereafter. Notably, the expression of cyclins A2, B1, D1 and E1 as well as CDK2, the phosphatase Cdc25c, the transcription factor E2F1 and the regulator of DNA replication PCNA3 were significantly down-regulated in both gastric cancer cell lines studied. Immunofluorescent analyses of MKN45 tumorspheres after day 5 clearly revealed a higher proportion of p21- and p53- stained cell nuclei and a reduced proportion of PCNA positive cells after ATRA treatment compared to control (Fig. 3D). In MKN74 tumorspheres, no variation in p53 expression was observed after ATRA treatment but p21, p27, p16 (not expressed in MKN45) and GADD45A were overexpressed. In addition, the expression of cyclins A2, B1, D1 and E1 as well as CDK2, Cdc25c, E2F1 and PCNA3 was clearly decreased in ATRA-treated MKN74 tumorspheres as for MKN45, excepted for cyclin E1 whose expression was not modified upon ATRA treatment. Immunofluorescent analyses of MKN74 tumorspheres after day 5 confirmed a higher proportion of p21 positive cells and a reduced proportion of PCNA positive cells after ATRA treatment (Fig. 3D). These combined results indicated that ATRA blocks cell cycle progression by enhancing the expression of various CDKIs, mainly P21 and P27 in both cell lines, and P53 in MKN45 cells and P16 in MKN74 cells. These results are in agreement with the cell cycle arrest detected by flow cytometry in G0/G1 phase for MKN45 and in G2/M phase for MKN74.

The increased proportion of sub-G1 cells after ATRA treatment of MKN45 cells (Fig. 3B) suggested that the drug may also trigger apoptosis. We therefore analyzed the expression of the programmed cell death protein 4 (PDCD4) involved in the programmed cell death (Supplementary Fig. S3). RT-qPCR data on PDCD4 expression showed that PDCD4 was up-regulated after ATRA treatment in both MKN45 and MKN74 tumorspheres, confirming the pro-apoptotic effect of ATRA which remained discrete and significant only in MKN45 cell line as shown by flow cytometry experiments (Fig. 3B).

4. ATRA represses the expression of CSC markers

Lastly, we analyzed the expression of the CSC markers CD44 and ALDH1A1 in MKN45 tumorspheres after 48 h and 5 days of ATRA treatment. RTqPCR experiments revealed that ATRA decreased the expression of CD44 and ALDH1A1 in MKN45 after 48 h of ATRA treatment (Fig. 4A). These results were confirmed at the protein level by flow cytometry analyses revealing that the percentage of cells expressing CD44 and ALDH decreased significantly and progressively from 48 h to 5 days of ATRA treatment (Fig. 4B-C). Similar results were observed in MKN74 cells after 48 h of ATRA treatment (Supplementary Fig. S4). In MKN45 tumorspheres, ~50% and ~35% of cells expressed the membrane receptor CD44 and the cytoplasmic ALDH enzyme, respectively, as shown both by flow cytometry (Fig. 4B) and by fluorescent imaging (Fig. 4C), while the percentage of CD44+ MKN74 cells was very low (Fig. 4B) and null for ALDH (data not shown). These results indicated that in both cell lines ATRA reduced the number of CSC-like cells.

5. ATRA induces inhibition of tumor growth in a mouse xenograft model

In order to evaluate the tumorigenic properties of the cells in resting tumorspheres after 10 days of ATRA treatment, ATRA-treated MKN74 tumorspheres were subcutaneously injected into the dorsal flank of immunodeficient NSG mice to follow tumor growth. Only control DMSO treated tumorspheres led to tumor growth, and not ATRA treated ones (Supplementary Fig. S5), confirming that a 10 days *in vitro* ATRA treatment led to the disappearance of tumorigenic CSC.

We then determined whether ATRA would be effective in inhibiting the growth of primary tumors from gastric adenocarcinoma cases *in vivo*. Therefore, we performed xenograft experiments with cells from GC06 and GC10 primary cases of gastric adenocarcinoma and

with MKN45 and MKN74 cell lines. After 10 to 21 days post-injection, when the tumor size reached 100 mm³, 3.3 or 33 μmol/kg ATRA in DMSO, or DMSO alone as control, were subcutaneously injected at the tumor periphery for 15 consecutive days. The size of the tumor was measured periodically after the first injection. At day 15 post-treatment, the mice were euthanized and the residual tumors were removed, weighed and processed for histology.

While the DMSO-treated tumor xenografts continued to actively grow during the two weeks of treatment, the ATRA-treated ones at 33 μmol/kg were noticeably inhibited. Indeed no effect was observed at 3.3 μmol/kg, whether they were derived from cell lines or a human primary adenocarcinoma, as shown by the tumor weight at 15 days post-treatment (Fig. 5A-B). These results were confirmed in a second round of experiments (Fig. 5C). The ATRA anti-tumor effect was particularly visible in the GCO6 and GC10 primary tumors, as shown by the tumor size evolution over time, in which ATRA seemed to be effective as early as after 3 days of treatment (Fig. 5C). In one set of mice in which we let the tumor xenografts grow without treatment after the two-week ATRA treatment at 33 μmol/kg, we noticed that tumors relapsed after 35 days for MKN74 and GC06 tumors, 28 day for MKN45, and after 14 days for GC10 (Fig. 5C). This suggests that although the daily ATRA treatment for two weeks drastically reduced the tumor mass, it was insufficient to eliminate all of the CSCs and eradicate carcinoma.

The histological analysis of the residual tumors after the 33 μmoles/kg ATRA treatment revealed that for the 2 primary cases studied, GC06 and GC10, only small foci of resting tumor cells were detected within the stroma of the resting tumor, contrarily to gastric cancer cell lines for which larger area of resting tumor cells were detected (Fig. 6A). Immunohistochemical analyses of control and ATRA treated tumors showed that the percentage of cells expressing CD44 and ALDH, which contain the CSC, was strongly

reduced until 5 fold in resting tumors after ATRA treatment compared to control for all cases studied (excepted for MKN74 which does not express ALDH1A) (Fig. 6). The percentage of proliferating cells expressing Ki67 and PCNA markers of DNA replication was also strongly reduced, particularly in primary tumors for which it decreased from ~60% in control tumors to less than 10% in ATRA treated tumors. In addition, the percentage of apoptotic cells expressing clived-caspase 3, which was very low in control tumors (with a tumor size ≤ 500 mm³), was significantly increased in all cases and once again in a more important manner for the two primary cases studied compared to the two cancer cell lines (Fig. 6). These results confirmed those obtained *in vitro* with tumorspheres, ie. that ATRA targeted CSC to inhibit the expression of the CSC markers CD44 and ALDH as well as their self-renewal and proliferation properties and increased apoptosis, leading to a blockade of tumor growth and to tumor regression.

Discussion

In the present study, we evaluated the effects of ATRA on the proliferation and tumorigenic properties of human gastric cancer cells using three different models including an *in vitro* monolayer culture (2D), *in vitro* tumorsphere assay under non-adherent culture conditions (3D) and *in vivo* mouse models of xenograft of gastric cancer cell lines and primary tumors of both the diffuse and the intestinal histological subtypes. Under 2D culture conditions, ATRA induced a dose-dependent anti-proliferative effect and cell cycle arrest under serum-free culture conditions, in which the RAR γ , RXR α and RXR β transcription factors of RA were highly expressed in the five gastric cancer cell lines studied. We previously developed a tumorsphere assay under 3D culture conditions in serum free media, to study the functional property of CSCs to self-renew and form tumorspheres under these conditions (15). This 3D

culture system constitutes a better model which bridges the gap between *in vitro* experiments under conventional 2D culture conditions and pre-clinical *in vivo* assays for the evaluation of the therapeutic efficiency of anticancer drugs (17). In this model, pre-treatment with ATRA reduced the number of developing tumorspheres from gastric cancer cell lines and primary tumors in a dose-dependent manner. In addition, post-treatment of tumorspheres already formed with ATRA led to a decrease in both tumorsphere number and size over time. The breaking down of tumorsphere structure during ATRA treatment finally resulted in the disappearance of some tumorspheres. Furthermore, mice which were xenografted with ATRA-pretreated tumorspheres showed no new tumor formation. As with 2D culture conditions, ATRA induced a cell cycle blockade in tumorspheres. ATRA-induced inhibition of transcription of cyclin genes leading to cell cycle arrest was previously reported in some gastric cancer cell lines in 2D culture *in vitro* (18) (19). In this study, ATRA induced an upregulation of the cell cycle inhibitors P21, P27 and GADD45, with an additional P53 and/or P16 upregulation depending on the case studied. Key players of the cell cycle progression in G1/S and G2/M phases, including cyclins A1, B1, D1, E1, the phosphatase Cdc25C which control CDK/cyclin activity and the kinase CDK2, were concomitantly strongly downregulated, as well as the transcription factor E2F1 which controls G1/S transition, and the protein PCNA necessary for DNA replication in S phase. P21 is a master regulator of cell cycle progression via the inhibition of CDK and E2F1 activity and indirectly the expression of target genes involved in cell cycle progression such as CCNB1, CDC25C, CDC2 and CHECK1, but also via its interaction and inhibition of PCNA activity leading to DNA replication arrest (20) (21). P21 is regulated in p53-dependent and p53-independent ways, and the promoter of the P21 gene CDKN1A contains a RA responsive element (RARE) recognized by an RXR receptor, indicating that P21 can be directly regulated by ATRA (22). Although P21 is a potent inhibitor of cell proliferation, it is also one of the main inducers of

senescence and an inhibitor of apoptosis in numerous systems, which may counteract its tumor-suppressor activity (20). In this study, a discrete pro-apoptotic effect was detected in cancer cell lines or primary tumors after treatment by ATRA, attested by PDCD4 overexpression and detection of sub-G1 cells by flow cytometry in tumorspheres, and by the detection of the activated cleaved form of Caspase 3 on resting tumors post-treatment with ATRA, particularly in primary tumors. Thus, ATRA not only inhibited cell cycle progression through the regulation of the expression of members of the CIP/KIP family and CDK/cyclins but also positively regulated pro-apoptotic genes and induced caspase activation, leading to gastric cancer cell apoptosis. These results combined suggest that ATRA targets the self-renewal properties of CSCs to prevent the development and the growth of tumorspheres, but also affect their survival potential leading to tumor regression.

More interestingly, we showed that ATRA also downregulated the expression of the CSC markers CD44 and ALDH in tumorspheres, as well as some stemness marker genes like Klf4 and Sox2, and upregulated the expression of the gastric differentiation marker MUC5AC. The connection between the regulation by ATRA of the expression of cell cycle regulators and CSC markers remains to be elucidated. We previously reported that inducing an epithelial-mesenchymal transition (EMT) in gastric epithelial cell lines can generate cells expressing CD44, possessing CSC-like properties and forming tumorspheres (15), as reported by others in breast cancer (23)(24). A recent study revealed that the loss of P21 led to an EMT in breast cancer cells, while P21 overexpression inhibited mamospheres formation and CSC markers expression as a result of EMT inhibition (25). In addition, interaction of P21 and ZEB1 resulting in EMT inhibition was also reported (26). Further studies will determine whether P21 induction by ATRA is linked to the ATRA-induced downregulation of CSC marker expression.

Altogether, these results indicate that ATRA targets gastric CSCs and their stem cell properties, affecting their self-renewal, survival, asymmetrical division and tumorigenic properties *in vitro*.

These effects were confirmed *in vivo* in mouse models of xenograft from gastric cancer cell lines and primary tumors. In these models, a 2 week ATRA treatment by daily peritumoral injection led to an efficient blockade of tumor growth in all cases studied. This effect was particularly impressive in some cases engrafted with primary tumors, for which the tumors initially formed before starting the treatment fully regressed to become macroscopically undetectable after ATRA treatment. The percentage of cells expressing CD44 and ALDH corresponding to CSCs was strongly reduced in resting tumor cells after ATRA treatment, confirming the *in vitro* observations that ATRA targets CSCs and inhibit CSC self-renewal properties. This was associated with a strong decrease in Ki67 and PCNA positivity, two biomarkers of DNA replication which are closely associated with high grade malignancy and metastasis in gastric cancer (27) (28), suggesting that ATRA could efficiently control gastric cancer progression. However, a 2 weeks ATRA treatment was not sufficient to fully eradicate cancer cells, as post-treatment relapses were observed for all cases after 14 to 28 days. Further studies are necessary to evaluate the consequences on tumor growth and relapse post-ATRA treatment over a longer period and in combination with conventional chemotherapy drugs.

In conclusion, we have shown and confirmed in three complementary models including 2D and 3D *in vitro* culture systems and *in vivo* primary tumor xenografts in mice that ATRA is a potent inhibitor of gastric cancer cell growth and tumorigenic properties. Most importantly, our study reports for the first time that ATRA not only targets the expression of cell cycle regulators to inhibit cell cycle progression and tumorigenesis of gastric carcinoma cells, but also targets CSCs and the expression of stemness genes and CSC markers controlling their

self-renewal and tumorigenic properties, such as CD44 and ALDH1. This study unveils the potential usefulness of ATRA in addition to current chemotherapy to target CSC for the treatment of gastric adenocarcinoma.

Material and Methods

Cell culture. The gastric epithelial cell lines AGS, MKN45, MKN74, NCI87, MKN7 and MKN28 were cultured in DMEM/F12 media for AGS or RPMI1640 media for the others, with glutamax, 10% heat-inactivated fetal bovine serum (FBS), 50 IU/ml of penicillin and 50 µg/ml of streptomycin (all from Invitrogen, Cergy-Pontoise, France), at 37°C in a humidified 5% CO₂ atmosphere, as previously described (15)(29).

Reagent and ATRA treatment procedure. All-trans retinoic acid (Sigma, Saint-Quentin Fallaviers, France) was solubilized in 100% dimethyl sulfoxic acid (DMSO) at a stock concentration of 10 mM and kept at -20°C up to 2 months. Cells were cultured *in vitro* with or without ATRA from 1 to 10 µM added in the culture media; the same volume of DMSO was used for the control conditions.

Cell viability. Cell viability was evaluated using the MTT (3-(4, 5-dimethylthiazol-2-yl)-2, 5-diphenyl tetrazolium bromide) bioassay (Sigma). 10,000 cells were seeded in 96-well plate (n=5 for each experimental condition) and cultured under conditions containing a concentration of FBS from 0 to 20%. After 24 h, cells were treated with ATRA with 1 to 10 µM ATRA or the corresponding volumes of DMSO for 48 h. Next, culture media was replaced by 100 µl of fresh media containing 20 µl of MTT reagent (5 mg/ml in PBS) and incubated at 37°C and 5% CO₂ for 4 h. Subsequently, the MTT solution was replaced with 100 µl of DMSO supplemented with 12 µl of Sorenson buffer (0.1 M NaCl, 0.1 M glycine,

pH10.5) and incubated at 37°C for 15 min. The optical density of each culture well was measured at 570 nm by a spectrophotometer (SPECTROstar^{Nano}, BMG LABTECH, Champigny sur Marne, France).

Tumorsphere culture and treatment. 100 or 10,000 cells were seeded in non-adherent 96 or 6-well culture plates previously coated with a 10% polyHEMA solution (Sigma) in 95% (v/v) ethanol and dried overnight at 56°C, in serum-free DMEM-F12 Glutamax medium supplemented with 20 ng/ml of EGF, 20 ng/ml of basic-FGF, 0.3% glucose, 5 µg/ml of insulin, 50 IU/ml of penicillin (all from Invitrogen and Sigma) and cultured at 37°C in a humidified 5% CO₂ atmosphere. Cells were cultured with ATRA or DMSO and tumorsphere number was evaluated after 5 days. In other experiments, tumorspheres formed after 5 days of culture were treated with ATRA or DMSO and images were recorded every 7 days until 3 weeks post-treatment. Images were recorded using a NIKON TE2000 inverted light microscope using a 20x objective, and the number and/or size of tumorspheres of each well was quantified using NIS-BR software (Nikon, Champigny sur Marne, France).

Cell cycle and apoptosis analyses. Cells from monolayer culture or tumorspheres after 48 h treatment with ATRA or DMSO were recovered and dissociated into single cells by trypsination. Single cells were fixed in 70% ethanol for 2 h on ice and were then rinsed with PBS by centrifuge at 400 g for 5 min. The supernatant was removed, cells were stained with a solution of 0.1 % sodium citrate (w/v), 0.1 % Triton X-100 (v/v), 50 µg/ml of propidium iodide and incubated at 4°C for 1 h. The percentages of cells in each phase of the cell cycle and of apoptotic cells in sub-G1 were determined on 30,000 cells using a BD FACSCanto II instrument and DIVA software as previously described (30).

Flow cytometry. Cells were recovered and 100,000 cells per condition were stained with anti- human CD44-APC antibodies 1:25 (clone G44-26, BD Biosciences, Le Pont de Claix,

France) in PBS containing 0,5% bovine serum albumin (BSA) and 2 mM EDTA for 20 min at 4°C. The ALDEFLUOR Kit (StemCell Technologies, Grenoble, France) was used to detect ALDH activity according to the manufacturer's instructions. Flow cytometry was performed using a BD FACSCanto II instrument and DIVA software (BD).

Immunofluorescence. Tumorspheres were fixed in 4% paraformaldehyde for 10 min and attracted to glass slides by cytopspin at 500 g for 5 min, permeabilized in 0.5% Triton X-100 solution for 15 min at room temperature and blocked in blocking solution containing 1% BSA and 2 % FBS in tris-buffered saline (TBS) for 30 min. After washing with PBS, tumorspheres were incubated with primary antibodies, including mouse monoclonal anti-human P53 antibodies 1:100 (BD), mouse monoclonal anti-human PCNA antibodies 1:50 (Merck Millipore, Molsheim, France), and mouse monoclonal anti-human P21 antibodies 1:200 (BD) for 30 min, and then incubated with Alexa Fluor® 488 Goat Anti-Mouse IgG secondary antibodies 1:350 (Molecular Probes, Thermo Fischer Scientific, Illkirch, France). F-actin was labeled with Alexa Fluor® 568 phalloidin 1:350 and DAPI 1:10,000 was used for nuclear DNA stain (Molecular Probes). To stain viable tumorspheres directly to detect ALDH activity, tumorspheres were incubated with anti-CD44-PE antibodies or ALDEFLUOR reagent as described for flow cytometry analyses above. After washing with the buffer, tumorspheres were recovered in buffer containing Hoechst 33342 compound (Molecular Probes, Invitrogen) for nuclear staining. Images were fast captured using Olympus fluorescent microscopy.

RNA extraction and quantitative RT-PCR. Total cellular RNAs were extracted using Trizol reagent (Invitrogen) according to the manufacturer's protocol and quantified by their absorbance at 260 nm using a NanoDrop spectrophotometer (NanoDrop Technologies, FisherSciences, Illkirch, France). RNA quality was analyzed on a 2100 Bioanalyzer (Agilent

Technologies, Les Ulis, France). One μg of total RNAs was retro-transcribed in 20 μl using the Quantitect Reverse Transcription (RT) kit (Qiagen, Courtaboeuf, France), according to the manufacturer's recommendations. Quantitative PCR was performed on 0.3 μl of the RT reaction mixture, using the SYBR Green qPCR master mix (Promega, Charbonnières-les-Bains, France) and specific primers at 0.3 μM (listed in Table S1). Real-time PCRs were run on a Rotor-Gene cycler (Qiagen). Gene expressions were normalized relative to both housekeeping genes, HPRT1 and TBP, using the comparative Ct method.

Histology and immunohistochemistry (IHC)

Tissue sections 3 μm thick were prepared from formalin-fixed paraffin-embedded tissues (PET) and submitted to standard IHC protocols with primary mouse monoclonal antibodies including anti-human CD44 1:100 (G44-26, BD), anti-human ALDH1 antibodies 1:400 (clone 44/ALDH, BD), anti-human Ki67 antibodies 1:100 (DAKO, Les Ulis, France), anti-human PCNA antibodies 1:50 (Merck Millipore), and mouse monoclonal anti-human cleaved caspase 3 antibodies 1:50 (BD), all for 1 h at room temperature, followed by 30 min incubation at room temperature with anti-mouse labelled polymer-HRP DAKO Envision Systems (DAKO). Immunolabeling was revealed by a 10 min incubation in liquid substrate-diaminobenzidine-chromogen (DAKO) at room temperature. Slides were counterstained with hematoxylin, dehydrated and mounted with Eukitt-mounting medium (Labonord, Templemars, France). Images of the staining of each marker were recorded on the same region on serial tissue sections using light microscopy and a 40x objective on a Nikon TE2000 microscope using NIS-BR software (Nikon).

Ethic Statement. Approval was obtained from the French Committee of Genetic Engineering (approval number 4608) and the local Central Animal Facility Committee at the University of Bordeaux before initiation of the study. All animal experiments were performed in level 2

animal facilities of the University of Bordeaux, in accordance with national institutional guidelines and with the agreement of the local Ethic Committee on Animal Experiments CEEA50 of Bordeaux (agreement number 50120151-A). Studies on primary tumors from human gastric adenocarcinoma cases were performed in agreement with the Direction for Clinical Research and the Tumor and Cell Bank of the Haut-Leveque Hospital of the University Hospital Center and the Bergonié Institute of Bordeaux. Fresh tumor samples were collected from gastric surgical wastes from consenting patients (written consent) who underwent gastrectomy for non-cardia gastric adenocarcinoma. Activities of conservation and preparation of elements of human origin were declared at the French Ministry of Research (reference DC-2008-412).

In vivo xenograft experiments. 10,000 cells from gastric cancer cell lines MKN45 and MKN74 and from human primary gastric tumors GC06 and GC10 were suspended in DMEM/Matrigel (BD Biosciences) at a 1:2 ratio in a total volume of 100 μ l and subcutaneously injected on the dorsal side of each flank of 7-week-old non-obese diabetous/severe combined immunodeficiency/interleukin-2Rag γ null (NSG) mice. Tumors were measured using a caliper twice a week and tumor volumes were calculated according to the $L \times W \times W / 2$ formula. Fifty μ L volumes of DMSO (control group) or ATRA solution at a dose of 3.3 or 33 μ mol/kg per mouse were subcutaneously injected at the periphery of the tumor. Treatment started when tumor volumes reached 100 mm^3 . ATRA treatment was administered daily for 15 days. Mice were euthanized after the 15 day treatment, or when tumors in the control and recurrence groups reached 500 mm^3 . Tumors were then collected, fixed in a 3.7 % formaldehyde solution and embedded in paraffin following standard procedures for immunohistochemical studies.

Statistical analysis

Quantification values represent the mean of three or more experiments as indicated \pm standard deviation (SD). Statistics were performed using Mann-Whitney U tests on SPSS16.0F software (SPSS Inc., Chicago, IL, USA).

Acknowledgments

We thank Vincent Pitard and Santiago Gonzalez (Flow Cytometry and FACS Platform, University of Bordeaux), Lamia Azzi-Martin and Jacky Ferrer (EA2406, University of Bordeaux) and Armelle Ménard (INSERM U853) for technical assistance and helpful advices. This project was supported by SIRIC BRIO (Site de Recherche Intégrée sur le Cancer – Bordeaux Recherche Intégrée Oncologie) (grant INCa-DGOS-Inserm 6046). We thank the French ‘Association pour la Recherche contre le Cancer’ (grant number 8412), the ‘Institut National du Cancer’ (grant 07/3D1616/IABC-23-12/NC-NG and grant 2014-152), the ‘Conseil Regional d’Aquitaine’ (grant number 20071301017 and 20081302203) and the French National Society for Gastroenterology for financial support.

Conflict of interest

All authors declare to have no conflict of interest.

Figure legends

Figure 1. Effect of fetal bovine serum (FBS) on retinoic acid (RA)-induced growth inhibition of gastric carcinoma cell lines.

A. MKN45 and MKN74 cells were cultured in media supplemented with 10 % or no FBS. After 24 h of culture, cells were treated with ATRA at 1-10 μ M or DMSO (control). After 48 h of treatment, cell viability was determined by MTT assays (n = 5). *P<0.05.

B. Representative images of cellular morphology and growth inhibition of MKN45 and MKN74 cells after 1 and 5 μ M ATRA treatment in serum-free media for 48 h. Scale bars, 50 μ m.

C. Flow cytometry analyses of apoptosis and cell cycle of MKN45 and MKN74 cells after 48 h of treatment with 5 μ M ATRA or DMSO (control). Values are mean \pm SD (n = 3 per condition).

Figure 2. Inhibitory effect of ATRA on formation and growth of tumorspheres.

A-B. MKN45 or MKN74 cells were cultured in 3D and submitted to the tumorsphere assay with DMSO (control) or 1-10 μ M ATRA. The number of tumorspheres was counted on day 5 of culture. Representative images of tumorspheres (**A**) and quantification of the number of tumorspheres formed by 100 seeded cells per well (**B**) after 5 days. Scale bars = 50 μ m. Data represent the mean \pm SD (n=8). **C.** The same experiment was performed on GC04, GC06 and GC10 primary tumors. 500 cells were seeded per well, and tumorsphere numbers were counted on day 7 of culture (n=8).

D-E. Tumorspheres at day 5 of culture were treated with ATRA at 1-10 μ M as indicated. The number of tumorspheres was counted every 7 days for 3 weeks for MKN45, and at day 10 of treatment for MKN74 (**D**). Representative images of tumorspheres at day 5 before treatment and at day 10 after treatment are shown (**D**).

Data represent the mean tumorsphere number (**B-D**) and size (**E**) \pm SD (n=8). *P<0.05 versus control.

Figure 3. ATRA induced cell cycle arrest of tumorspheres

Tumorspheres at day 5 of culture were treated with 5 μ M ATRA for 48 h. **A-B**. Cells were stained with propidium iodide (PI) solution and the percentage of cells in each phase of the cell cycle (**A**) and apoptotic cells in sub-G1 (**B**) were determined by flow cytometry analyses (n=5). Values are mean \pm SD (n=3 per condition).

C. Expression of genes controlling cell cycle progression were analyzed by RT-qPCR.

D. Immunofluorescence analyses on fixed tumorspheres stained with anti-P21, anti-P53, anti-PCNA antibodies in green, phalloidin to detect F-actin in red and Hoechst 33342 stain to detect nuclei in blue. Scale bars, 20 μ m.

Figure 4. ATRA inhibited the expression of cancer stem cell markers in gastric tumorspheres

Tumorspheres of MKN45 at day 5 of culture were treated with 5 μ M ATRA or DMSO for 2 to 5 days. **A**. After 48 h of treatment, total cellular RNAs were extracted and the expression of CD44, ALDH, Klf4, Sox2 stemness genes and Muc5AC gastric differentiation marker were analysed by RT-qPCR. Data represent the mean \pm SD (n=5). *P<0.05 versus control.

B-C. Cells from tumorspheres of MKN45 and MKN74 cell lines after 2 or 5 days of ATRA treatment were stained with anti-CD44-APC and ADEFUOR reagent and analyzed by flow cytometry. Representative dot-plot images of flow cytometry analyses. Values and histograms indicate the mean \pm SD of positive cells (n=5). * P<0.05.

D. Expression of CD44 and ALDH activity were confirmed by immunofluorescence on fresh MKN45 tumorspheres after 5 days of treatment with ATRA. Tumorspheres were stained

directly with anti-CD44-PE (in red), ALDEFLUOR reagent (in green) and Hoechst 33342 stain (in blue). Scale bars = 50 μm .

Figure 5. Analysis of the inhibitory effect of ATRA on formation and relapse of gastric tumors in a xenograft model

10,000 cells from MKN45 and KMN74 cancer cell lines and GC06 and GC10 primary tumors were xenografted into NSG mice (n=10 per group). DMSO (control) or 3.3 or 33 $\mu\text{mol/kg}$ ATRA was injected subcutaneously at the tumor periphery when their volume reached 100 mm^3 . The treatment was repeated daily for 15 days. Tumor size was recorded every 3 days.

A. Tumor weight was measured at day 15 of treatment. Data represent the mean of tumor weight \pm SD (n=5 per condition).

B. One representative example with GC06 of the difference in tumor size between DMSO (control) and 33 $\mu\text{mol/kg}$ ATRA treated tumors.

C. In another experiment, tumor xenografts were daily treated with DMSO or 33 $\mu\text{mol/kg}$ ATRA. After 15 days, treatment was stopped, DMSO-treated controls were sacrificed and the tumor growth in ATRA-treated group was measured every week until recurrence occurred and reached 500 mm^3 (5<n<10 mice per condition). Data represent the mean of tumor volume \pm SD.

Figure 6. Effect of ATRA treatment on the expression of CD44, ALDH, Ki67, PCNA and clived Caspase3 detected by IHC on tumor xenografts after ATRA treatment.

IHC analyses on paraffin embedded tissue sections of MKN45, MKN74, GC06 and GC10 tumor xenografts after DMSO or 33 $\mu\text{mol/kg}$ ATRA -treatment for 15 days.

(A) CD44 (membrane staining), ALDH1A (cytoplasm diffuse staining), Ki67 and PCNA3 (nuclear staining) and cleaved caspase3 (detection of apoptotic cells and bodies) are stained in brown, with hematoxylin counterstaining. Scale bars, 50 μ m.

(B) Relative quantification of the percentage of positive cells for each indicated marker (3<n <5 per condition and per case). Data represent the mean \pm SD. *P<0.05 versus respective control.

References

1. Flejou JF. [WHO Classification of digestive tumors: the fourth edition]. *Annales de pathologie* 2011;31(5 Suppl):S27-31.
2. Lauren P. The Two Histological Main Types of Gastric Carcinoma: Diffuse and So-Called Intestinal-Type Carcinoma. an Attempt at a Histo-Clinical Classification. *Acta Pathologica et Microbiologica Scandinavica* 1965;64:31-49.
3. Gonzalez CA, Megraud F, Buissonniere A, *et al.* Helicobacter pylori infection assessed by ELISA and by immunoblot and noncardia gastric cancer risk in a prospective study: the Eurgast-EPIC project. *Ann Oncol* 2012;23(5):1320-4.
4. IARC'Working'Group. Schistosomes, liver flukes and *Helicobacter pylori*:Views and expert opinion of IARC Working Group on the evaluation of carcinogenic risks to humans. 1994;61:177-240. Lyon, IARC Monographs. International Agency for research on Cancer.
5. Sreerama L, Sladek NE. Cellular levels of class 1 and class 3 aldehyde dehydrogenases and certain other drug-metabolizing enzymes in human breast malignancies. *Clin Cancer Res* 1997;3(11):1901-14.
6. Abdullah LN, Chow EK. Mechanisms of chemoresistance in cancer stem cells. *Clinical and translational medicine* 2013;2(1):3.
7. Nishikawa S, Konno M, Hamabe A, *et al.* Aldehyde dehydrogenase high gastric cancer stem cells are resistant to chemotherapy. *International journal of oncology* 2013;42(4):1437-42.
8. Schenk T, Stengel S, Zelent A. Unlocking the potential of retinoic acid in anticancer therapy. *British journal of cancer* 2014;111(11):2039-45.
9. Connolly RM, Nguyen NK, Sukumar S. Molecular pathways: current role and future directions of the retinoic acid pathway in cancer prevention and treatment. *Clin Cancer Res* 2013;19(7):1651-9.
10. Ying M, Wang S, Sang Y, *et al.* Regulation of glioblastoma stem cells by retinoic acid: role for Notch pathway inhibition. *Oncogene* 2011;30(31):3454-67.
11. Lim YC, Kang HJ, Kim YS, Choi EC. All-trans-retinoic acid inhibits growth of head and neck cancer stem cells by suppression of Wnt/beta-catenin pathway. *Eur J Cancer* 2012;48(17):3310-8.
12. Takaishi S, Okumura T, Tu S, *et al.* Identification of gastric cancer stem cells using the cell surface marker CD44. *Stem cells (Dayton, Ohio)* 2009;27(5):1006-20.
13. Lau WM, Teng E, Chong HS, *et al.* CD44v8-10 is a cancer-specific marker for gastric cancer stem cells. *Cancer research* 2014;74(9):2630-41.

14. Chen W, Zhang X, Chu C, *et al.* Identification of CD44⁺ cancer stem cells in human gastric cancer. *Hepato-gastroenterology* 2013;60(124):949-54.
15. Bessede E, Staedel C, Acuna Amador LA, *et al.* Helicobacter pylori generates cells with cancer stem cell properties via epithelial-mesenchymal transition-like changes. *Oncogene* 2013;33(32):4123-31.
16. Bessede E, Dubus P, Megraud F, Varon C. Helicobacter pylori infection and stem cells at the origin of gastric cancer. *Oncogene* 2014.
17. Shin CS, Kwak B, Han B, Park K. Development of an in vitro 3D tumor model to study therapeutic efficiency of an anticancer drug. *Molecular pharmaceutics* 2013;10(6):2167-75.
18. Shyu RY, Jiang SY, Huang SL, *et al.* Growth regulation by all-trans-retinoic acid and retinoic acid receptor messenger ribonucleic acids expression in gastric cancer cells. *Eur J Cancer* 1995;31A(2):237-43.
19. Chao TY, Jiang SY, Shyu RY, Yeh MY, Chu TM. All-trans retinoic acid decreases susceptibility of a gastric cancer cell line to lymphokine-activated killer cytotoxicity. *British journal of cancer* 1997;75(9):1284-90.
20. Abbas T, Dutta A. p21 in cancer: intricate networks and multiple activities. *Nature reviews* 2009;9(6):400-14.
21. Waga S, Hannon GJ, Beach D, Stillman B. The p21 inhibitor of cyclin-dependent kinases controls DNA replication by interaction with PCNA. *Nature* 1994;369(6481):574-8.
22. Tanaka T, Suh KS, Lo AM, De Luca LM. p21WAF1/CIP1 is a common transcriptional target of retinoid receptors: pleiotropic regulatory mechanism through retinoic acid receptor (RAR)/retinoid X receptor (RXR) heterodimer and RXR/RXR homodimer. *The Journal of biological chemistry* 2007;282(41):29987-97.
23. Mani SA, Guo W, Liao MJ, *et al.* The epithelial-mesenchymal transition generates cells with properties of stem cells. *Cell* 2008;133(4):704-15.
24. Morel AP, Lievre M, Thomas C, Hinkal G, Ansieau S, Puisieux A. Generation of breast cancer stem cells through epithelial-mesenchymal transition. *PloS one* 2008;3(8):e2888.
25. Liu M, Casimiro MC, Wang C, *et al.* p21CIP1 attenuates Ras- and c-Myc-dependent breast tumor epithelial mesenchymal transition and cancer stem cell-like gene expression in vivo. *Proceedings of the National Academy of Sciences of the United States of America* 2009;106(45):19035-9.
26. Li XL, Hara T, Choi Y, *et al.* A p21-ZEB1 complex inhibits epithelial-mesenchymal transition through the microRNA 183-96-182 cluster. *Molecular and cellular biology* 2014;34(3):533-50.
27. Czyzewska J, Guzinska-Ustymowicz K, Lebelt A, Zalewski B, Kemon A. Evaluation of proliferating markers Ki-67, PCNA in gastric cancers. *Roczniki Akademii Medycznej w Bialymstoku (1995)* 2004;49 Suppl 1:64-6.
28. Isozaki H, Okajima K, Ichinona T, *et al.* Significance of proliferating cell nuclear antigen (PCNA) expression in gastric cancer in relation to lymph node metastasis. *Journal of surgical oncology* 1996;61(2):106-10.
29. Baud J, Varon C, Chabas S, Chambonnier L, Darfeuille F, Staedel C. Helicobacter pylori initiates a mesenchymal transition through ZEB1 in gastric epithelial cells. *PloS one* 2013;8(4):e60315.
30. Varon C, Mocan I, Mihi B, *et al.* Helicobacter pullorum cytolethal distending toxin targets vinculin and cortactin and triggers formation of lamellipodia in intestinal epithelial cells. *The Journal of infectious diseases* 2013;209(4):588-99.

Supplementary Figures

Figure S1. Effect of fetal bovine serum (FBS) on ATRA-induced inhibition of proliferation of gastric cancer cell lines. 10,000 cells of MKN45, MKN74, AGS, NCI87, MKN7 and MKN28 cell lines were seeded in 96 well plates and cultured in media containing 10% FBS. After 24h of culture, culture media was replaced by fresh media containing varying concentration of FBS (0-20%), and cells were treated with 5 μ M ATRA or DMSO (control) for 48h. The cell viability was recorded after MTT assays (n = 5). *P<0.05 versus control.

Figure S2. Formation and growth of tumorspheres from gastric cancer cell lines of diffuse type (MKN45) and intestinal type (MKN74). MKN45 or MKN74 cells were cultured in the serum-free media and under non-adherent culture conditions for the tumorsphere assay. Representative images of tumorsphere formation were recorded daily during 12 days. Scale bars, 20 μ m.

Figure S3. Effect of ATRA on the expression of PDCD4 determined by quantitative RT-PCR on tumorspheres of gastric cancer cell lines. Tumorspheres obtained from MKN45 and MKN74 cells after 5 days of culture were treated with 5 μ M ATRA or DMSO for 2 to 5 days. After 48 h and 5 days of treatment, total cellular RNAs were extracted and the expression of the pro-apoptotic PDCD4 marker was analyzed by RT-qPCR. Data represent the mean \pm SD (n=5). *P<0.05 versus control.

Figure S4. ATRA inhibited the expression of cancer stem cell markers in gastric tumorspheres. Tumorspheres obtained from MKN74 cells after 5 days of culture were treated with 5 μ M ATRA or DMSO during 48 h. **A.** After 48 h of treatment, total cellular

RNAs were extracted and the expression of CD44, ALDH, Klf4, Sox2 and Muc5AC was analyzed by RT-qPCR. Data represent the mean \pm SD (n=5). *P<0.05 versus control.

B-C. Flow cytometry analyses of CD44 expression on cells dissociated from tumorspheres after a 2 day treatment. Representative dot-plot images represent flow cytometry analyses. Values and histograms indicate the mean \pm SD of positive cells (n=5). * P<0.05.

Figure S5. Analysis of the tumorigenic properties of *in vitro* ATRA-treated tumorspheres after xenograft in mice. Tumorspheres obtained from MKN74 or AGS cells after 5 days were treated with 5 μ M ATRA for 10 days. 100 tumorspheres collected from ATRA treated or control (DMSO) wells were injected into NGS mice (n=10 per condition). Tumor formation was recorded after 1 to 2 months post-xenograft.

Figure S6. Capacity of tumorsphere formation of cells isolated from ATRA-treated tumor xenografts. 3,000 cells from MKN45 or MKN74 tumors, collected after treatment with 33 μ mol/kg ATRA or DMSO for 15 days, were cultured in serum-free media under non-adherent culture conditions and submitted to the tumorsphere assay. The number of tumorsphere per 3.000 cells seeded per well (n=8 wells per case) was counted after 10 days. Data represent the mean \pm SD (n=3 mice analyzed per condition). *P<0.05 versus control.

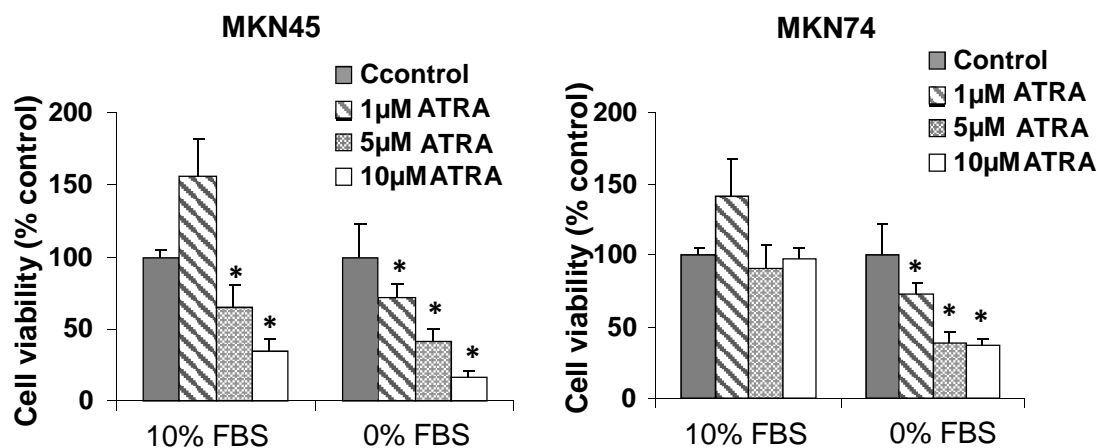
Supplementary Tables

Table S1. List of primers used for RT-qPCR analyses.

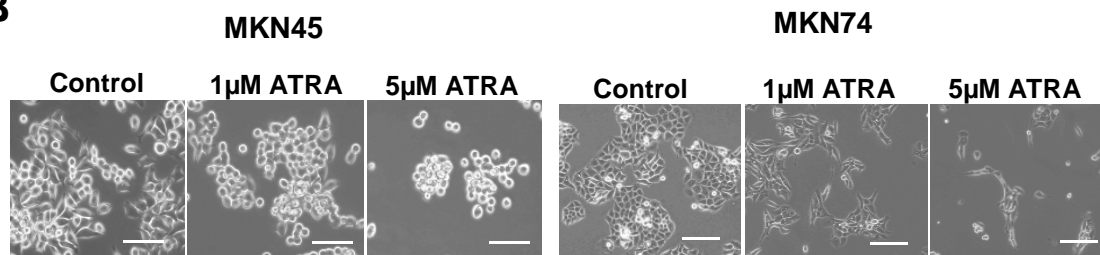
Table S2. Fold changes in the expression of components of the retinoic acid signaling pathway upon serum deprivation. MKN45, MKN74, AGS and MKN28 cells were cultured in media with 10 or no fetal bovine serum. After 48h of culture, total cellular RNAs were extracted, and their transcription level was analyzed by RT-qPCR.

Figure 1

A



B



C

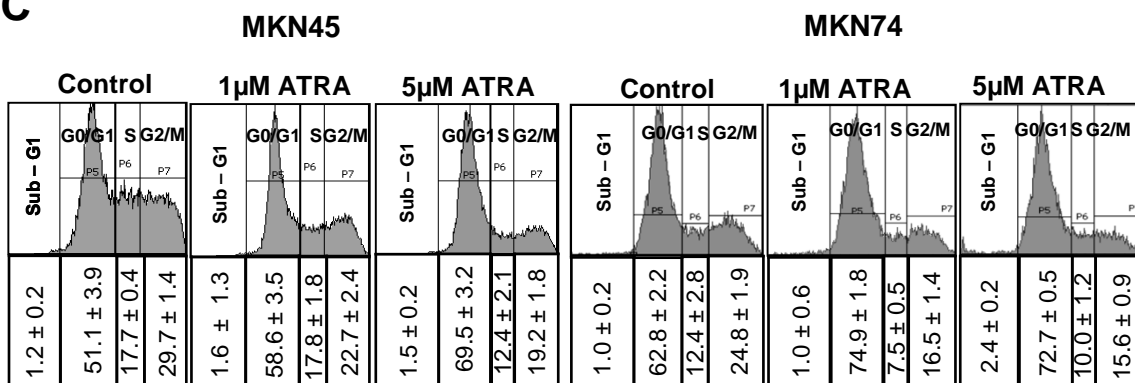


Figure 2

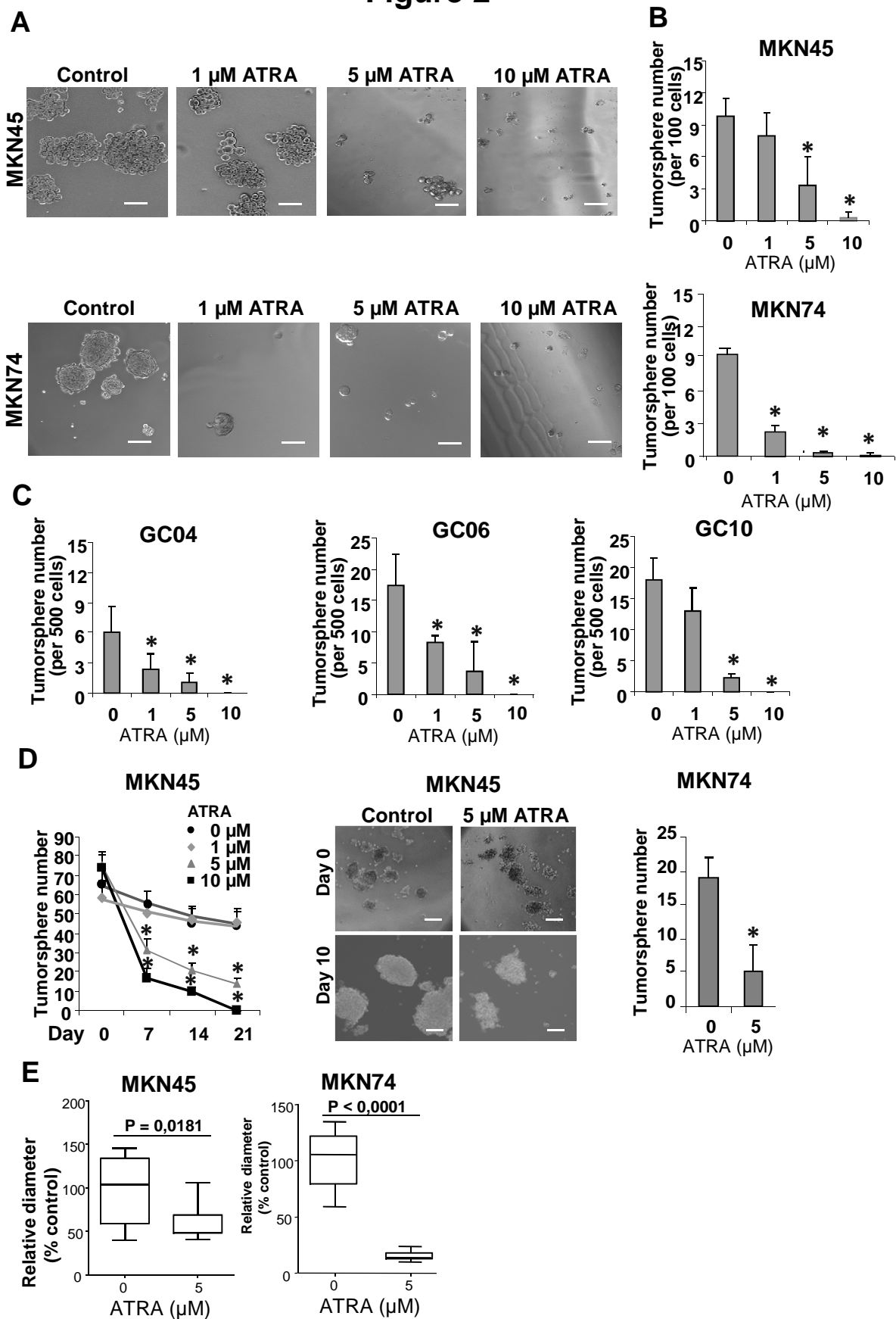


Figure 3

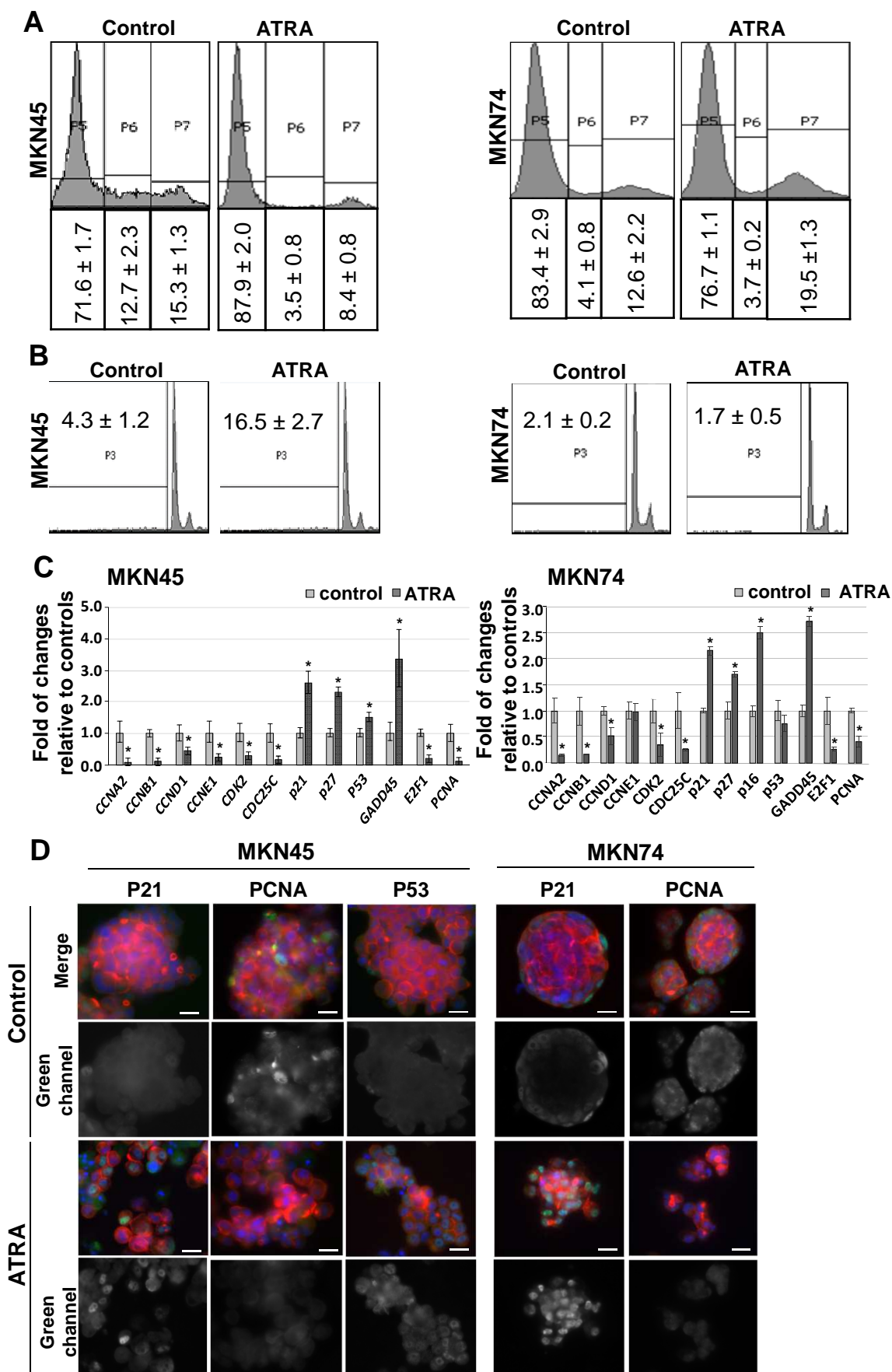


Figure 4

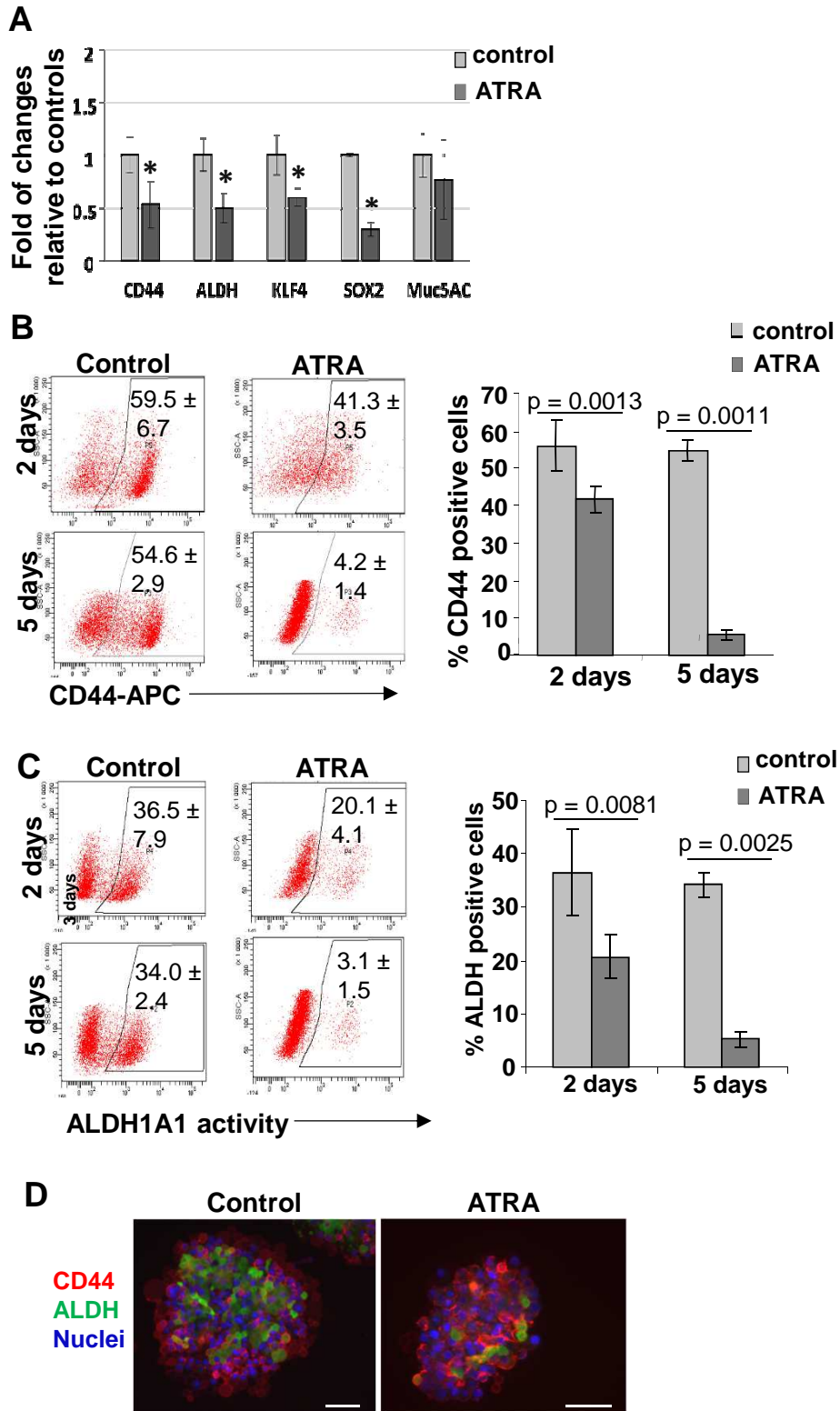


Figure 5

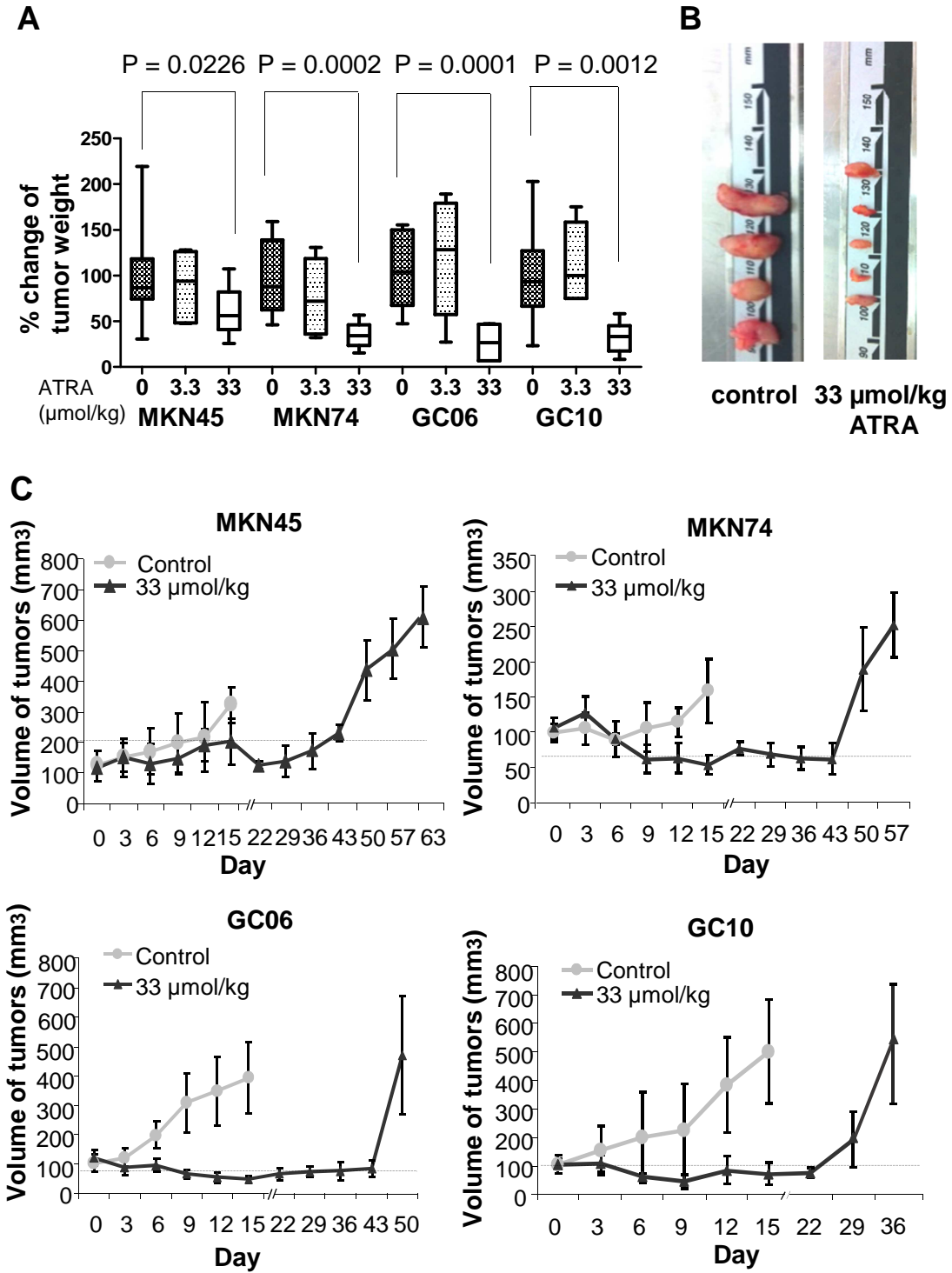
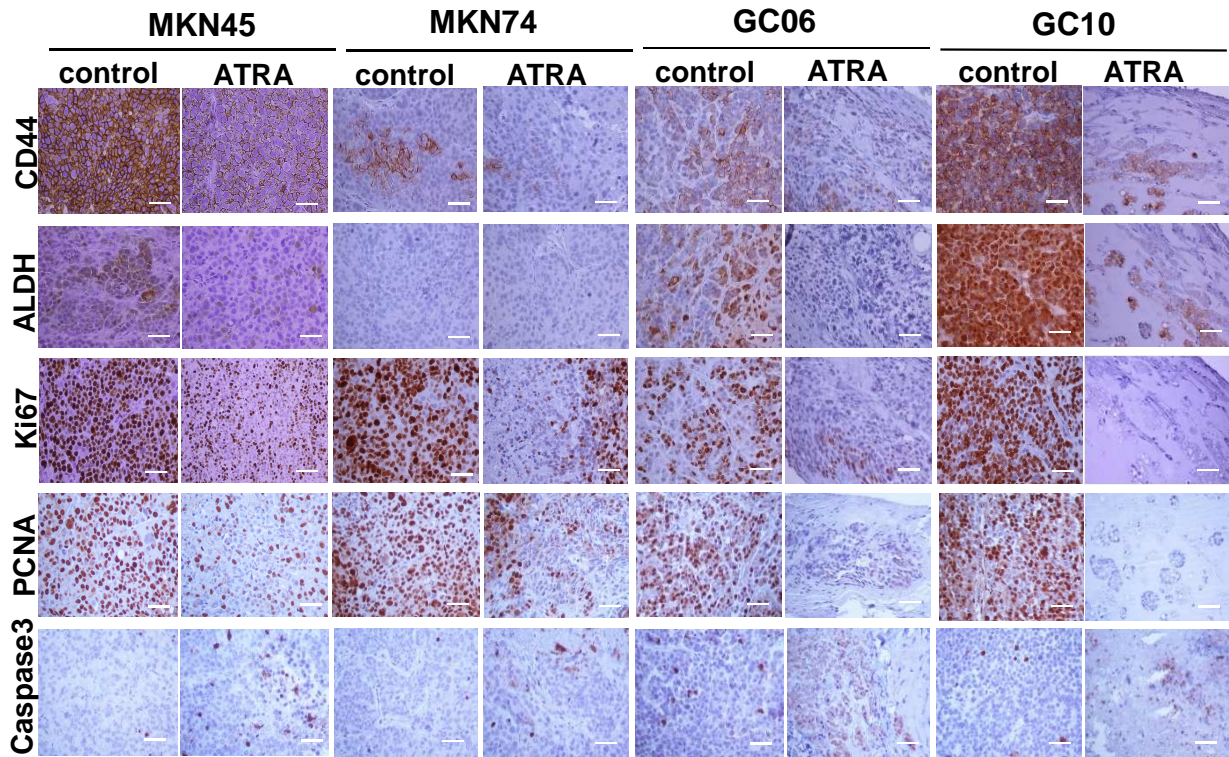
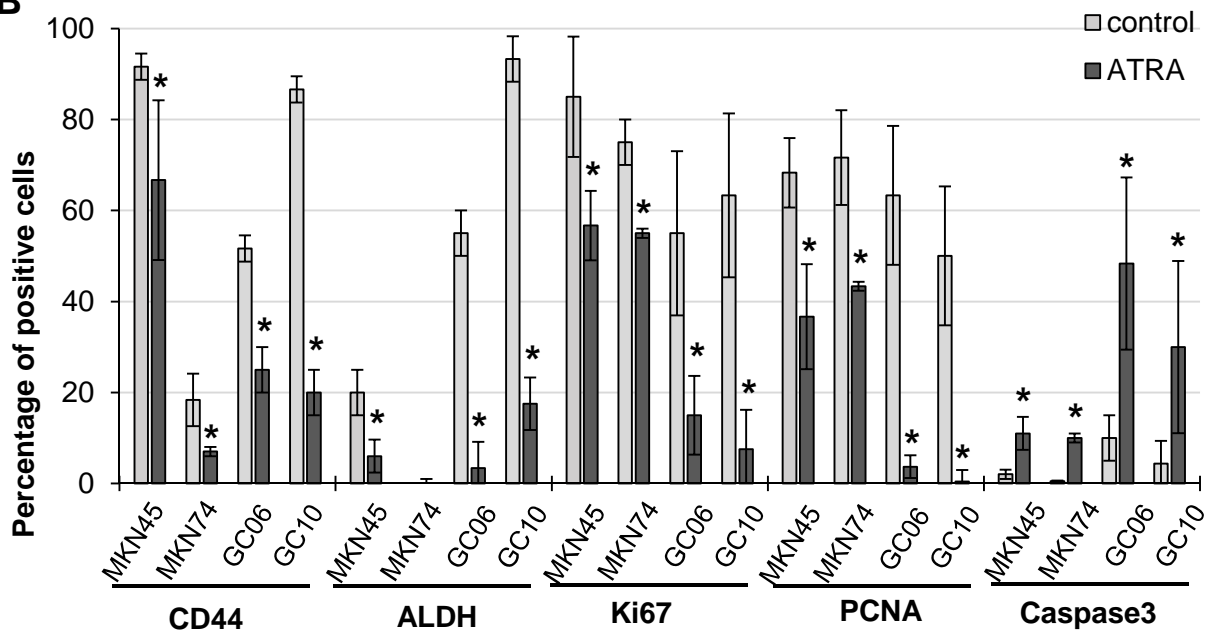


Figure 6

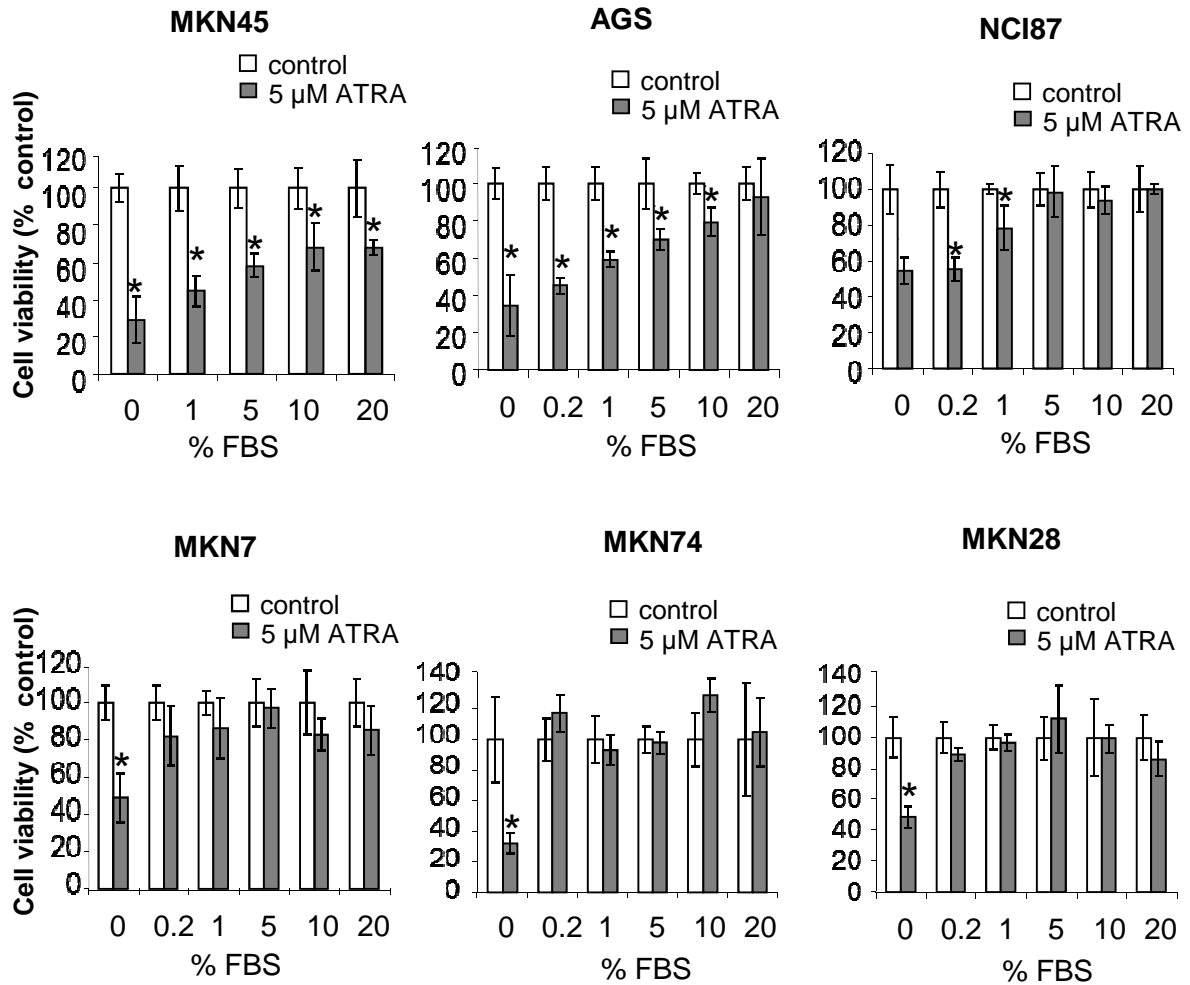
A



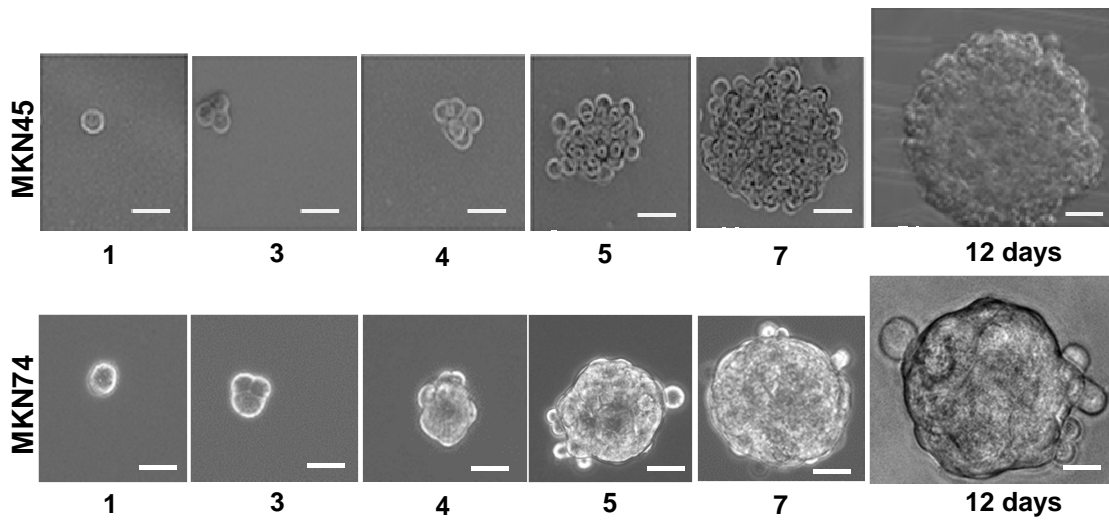
B



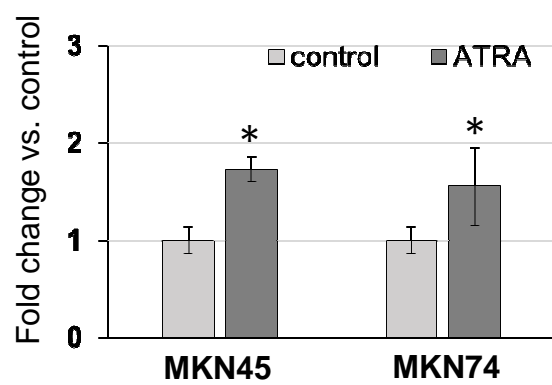
Supplementary Figure S1



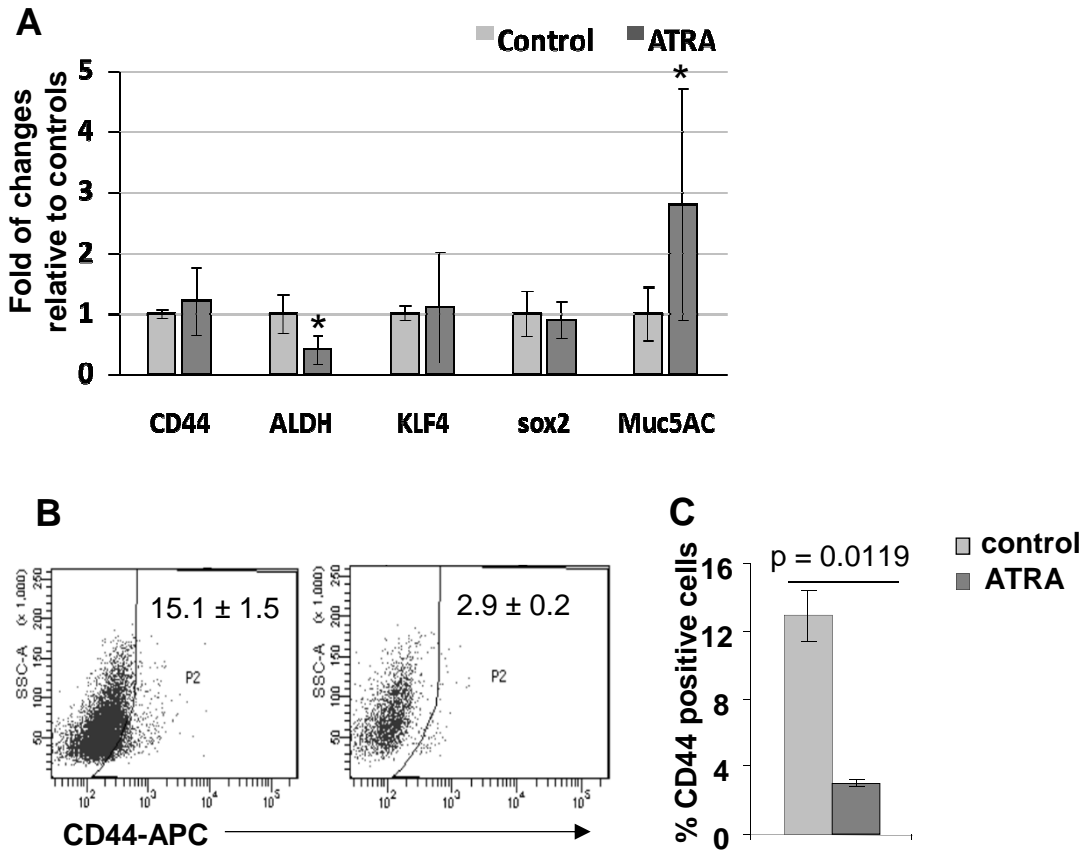
Supplementary Figure S2



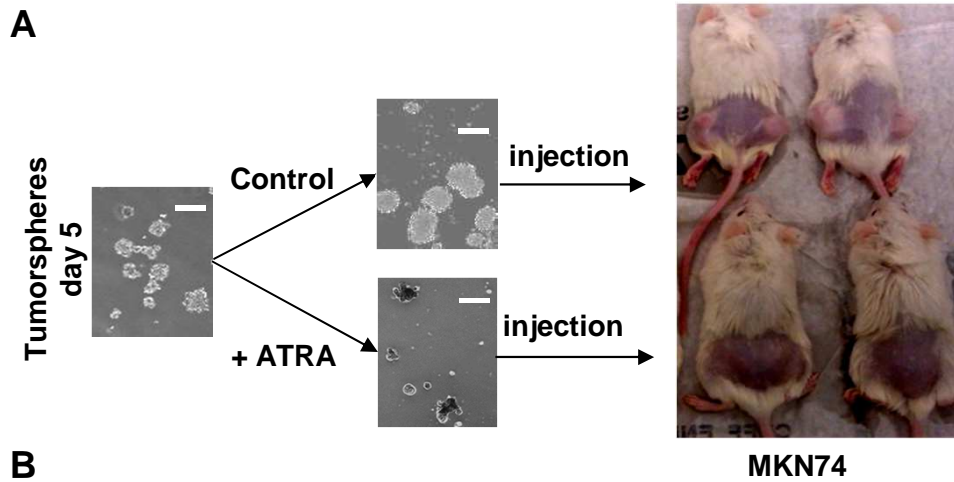
Supplementary Figure S3



Supplementary Figure S4



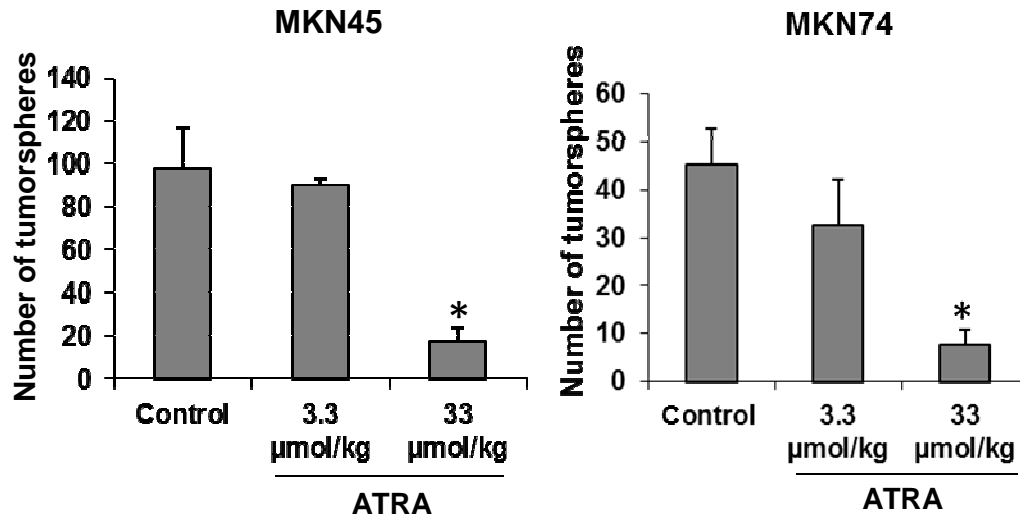
Supplementary Figure S5



B

| Cell lines | <i>In vitro</i> treatment | Tumors/ injection |
|--------------|---------------------------|----------------------|
| MKN74 | Control | 10/10 |
| | 5 μ M ATRA | 0/10 |
| AGS | Control | 5/5 |
| | 5 μ M ATRA | 0/10 |

Supplementary Figure S6



Supplementary Table S1: List of primers used for quantitative RT-PCR analyses.

| Name | Sequences | References | |
|--------------|---------------------------------|-------------------------|-----------------------|
| TBP | F: 5'-tgcacaggagccaagagtgaa | (Bièche et al., 2003) | |
| | R: 5-cacatcacagctccccacca | | |
| P53 | F: 5'-gttccgagagctgaatgagg | (Mizuno et al., 2009) | |
| | R: 5'-ttatggcgggaggtagactg | | |
| p27kip | F: 5'-gccctcccagctctcta | | |
| | R: 5'-tcaaaactcccccaagcacctc | | |
| CYP26A | F: 5'-tttgaggacacgaaaccac | (Zaitseva et al., 2007) | |
| | R: 5'-cagcatgaatcggtcaggat | | |
| CRBP1 | F: 5'-tagagatgagagtggaaggtgtggt | | |
| | R: 5'-ggggtggctggacattttg | | |
| RAR α | F: 5'-cagagcagcagttctgaagagata | | |
| | R: 5'-gacacgtgtacaccatgttctct | | |
| RAR β | F: 5'-gtcaccgagataagaactgtgta | | |
| | R: 5'-actcagctgtcatttcatagctctc | | |
| RAR γ | F: 5'-ctgtatcatcaacaaggtgacca | | (Kaiser et al., 2005) |
| | R: 5'-tggatgatgagcttcttaactgag | | |
| RXR α | F: 5'-tgcttcgtgtaagcaagtacataag | | |
| | R: 5'-cttttatggatctgtcatcctctc | | |
| RXR β | F: 5'-ccagagtctcttttacactcacc | | |
| | R: 5'-tcttagtcaacctgggaaagtacag | | |
| RXR γ | F: 5'-gatctagaggcagattcctgactaa | | |
| | R: 5'-catgtttactcgtcagttcatgttc | | |

Supplementary Table S2: Fold changes in the expression of components of the RA signaling pathway upon serum deprivation

| Cell lines | RA transporter | RA Receptors | | |
|--------------|-----------------|-----------------|-----------------|-----------------|
| | CRABP2 | RAR- γ | RXR- α | RXR- β |
| MKN45 | | 2.68 \pm 1.54 | 2.52 \pm 1.44 | 4.28 \pm 2.47 |
| MKN74 | 3.42 \pm 1.28 | 4.87 \pm 1.85 | 3.40 \pm 1.32 | 3.03 \pm 1.15 |
| MKN28 | 1.03 \pm 0.06 | 4.67 \pm 0.26 | 1.05 \pm 0.07 | 1.84 \pm 0.18 |
| AGS | 0.68 \pm 0.12 | 2.15 \pm 0.38 | 0.96 \pm 0.17 | 1.48 \pm 0.24 |

PART III. DISCUSSION AND PERSPECTIVES

Discussion and perspectives

1. Characterization of CSC markers in gastric carcinoma

Recent findings show that CSC represent a subpopulation of cells within tumors which are responsible for tumor growth and metastasis to other organs. CSC identification is extremely valuable for new therapy development targeting CSCs instead of conventional chemotherapy which has led to drug resistance and tumor recurrence after treatment. One of the most currently and frequently used methods to identify CSCs is based on the expression of cell surface markers. However, cell surface markers expressed by CSCs are often not the same depending on cancer types and organs. Indeed, CSCs of the same cancer type may originate from cells having acquired distinct mutations, which may explain the differences in the CSC cell surface marker patterns of expression of these tumors (Visvader, 2011). In particular, in a tumor mass a heterogeneity of CSC with many subpopulations may exist which are able to self renew (Tang, 2012; Magee et al., 2012). Therefore, the use of a unique marker is not enough to identify all CSCs in a tumor type and finding more CSC markers as well as a combination of CSC markers appears to be necessary for that. For example, four markers including CD44, CD133, and ALDH1A1 were used to identify CSCs in lung cancer, and a combination of CD133 with CD44, CD166 or CD24 was used to isolate colorectal CSCs (Table 1 of introduction).

In gastric cancer, CD44 was recently described as a unique cell surface marker used to isolate CSCs in gastric cancer cell lines (Takaishi et al., 2009). In this study, we developed an *in vitro* tumorsphere assay and mouse xenograft models of gastric cancer cell lines and more importantly of primary tumors collected from patients who underwent gastrectomy for gastric carcinoma, to study the tumorigenic properties of subpopulations of cells and to identify CSCs. Using these models, we first demonstrated that CD133 and CD44 are two enrichment markers allowing the isolation of CSCs from human primary non-cardia gastric adenocarcinoma of both the

diffuse and the intestinal histological subtypes according to the Lauren classification. We determined the frequency of the tumor initiating cells within each subpopulation of cells engrafted in mice using limiting dilution assays, and we showed that CD44+ cells contained the highest frequency of tumorigenic CSCs (Nguyen et al., submitted).

Furthermore, in order to find new CSC markers to better characterize gastric CSCs, we analyzed the expression of 11 potential cell surface markers which have been used to isolate CSCs in other cancer types. We looked for markers only expressed in CSC populations which represent a small fraction of cancer cells; indeed, certain markers expressed at a higher rate may be found in both CSCs and non-CSCs. Results obtained from flow cytometry analyses enabled the separation of the 11 putative CSC markers into four categories based on their expression level (Figure 28). These results showed a heterogeneity in the gastric cancer cell population. Furthermore, based on these data on marker expression, we focused on five markers that were expressed in less than 50% of the cells in all cases studied, including CD90, CD73, CD166, CD105 and ALDH. Among them, CD105 and ALDH were expressed at a lower level compared to the others (Figure 28). In addition, we used CD44 as a known-standard CSC marker to assess its expression in subpopulations of cells which express the other putative markers. This allowed us to estimate the CSC rate in each cell population where CD44+ cells are seen as CSCs. Interestingly, Kryczek *et al.* used CD133 and CD44 as known-ovarian CSC markers to demonstrate that ALDH was a new CSC marker in ovarian cancers (Kryczek et al., 2012). Our results show that CD166 is a new candidate for a gastric CSC marker because CD166 and CD44 were expressed at a similarly low level within the tumor cell population, and were co-expressed, detecting the same subpopulation of cells with tumorigenic properties. Some previous studies suggested that CD166 is a marker of intestinal CSCs (Levin et al., 2010; Dalerba et al., 2007). More importantly, here we show that ALDH expression is limited in the CD44+ population and almost all ALDH+ cells co-expressed CD44, representing a subpopulation within the CD44+ population of cells with tumorigenic properties (Nguyen et al., submitted). Therefore, we focused on ALDH.

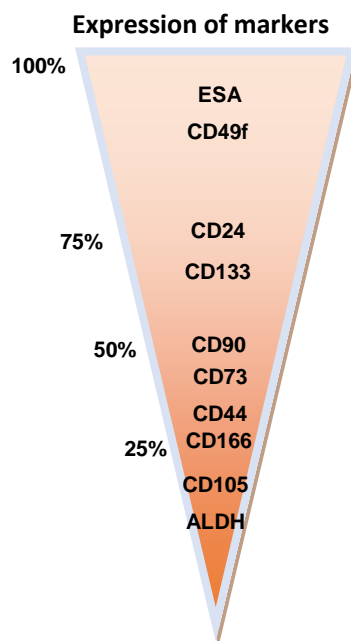


Figure 28. Expression level of putative CSC markers in human primary non-cardia gastric carcinoma.

2. ALDH as a specific marker of CSCs in human gastric carcinoma

ALDH plays a key role in the oxidation of aldehyde to carboxylic acids. This process is very important to protect the cells from the harmful effects of aldehydes. ALDH expression is commonly found in CSCs in many different cancer types. In recent years, ALDH1A1 activity has been reported as a universal CSC marker because of its expression allowing identification of both CSCs and normal stem cells (Ma and Allan, 2011). Interestingly, further studies showed that CSC may be identified by the expression of special isoforms of ALDH. For example, ALDH1A3 but not ALDH1A1 identifies CSC populations in breast cancer (Marcato et al., 2011) and ALDH7A1 in prostate cancer (van den Hoogen et al., 2011).

In addition, in breast cancer ALDH activity was initially reported as a more specific marker than CD44+/CD24- expression (Ginestier et al., 2007), and in colorectal cancer ALDH+/ESA+/CD44+ cells but not ALDH-/ ESA+/CD44+ cells induced new tumor formation in xenografted mice (Dylla et al., 2008).

In the present study and as previously mentioned, we identified ALDH as a potentially more specific marker of gastric CSCs based on its expression with CD44.

In order to confirm that the ALDH activity detected in a low proportion of cells allowed the identification of CSCs, tumorsphere assays with FACS sorted cells were performed. We showed that ALDH+ cells had a high capacity to self renew and form tumorspheres *in vitro*. In contrast, although CD105 was also expressed at a low level (in less than 25% of the cells), CD105+ cells did not present a high ability to form tumorspheres. In addition, *in vivo* assays of tumor xenografts with FACS sorted cells in limiting dilution assays demonstrated that ALDH+ subpopulations of cancer cells contained a significantly higher frequency of gastric CSCs than CD44+ and CD133+ subpopulations (Figure 29).

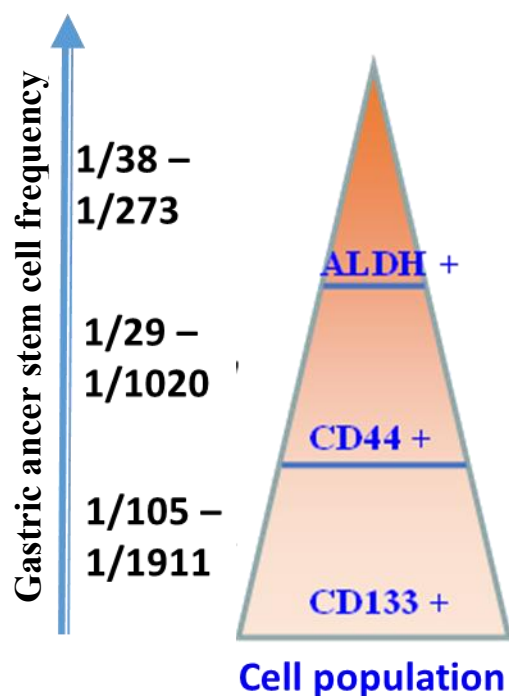


Figure 29. CSC frequency determined by the capacity of FACS sorted cancer cells to initiate a new tumor in mouse xenograft experiments in limiting dilution assays.

This is considered as a key criterion to assess the specificity of a marker to select cells with CSC properties (Magee et al., 2012). Furthermore, we highlighted that the higher specificity of ALDH to detect CSCs compared to CD44 was also due to the property of ALDH+ cells to exclude Hoechst 33342 dye while ALDH-/CD44+ cells did not. Dye efflux capacity has been related to a high level expression of ABC transporter proteins, especially ABCG2, and it was used to identify SP cells with stem cell properties in both normal and tumor tissues (Golebiewska et al., 2011). In gastric cancer, the Hoechst 33342 efflux property was used to isolate SP cells with CSC properties from gastric cancer cell lines by Fukuda *et al.* in 2009 (Fukuda et al., 2009).

In summary, our results combined to those of others highlight that ALDH can be considered as a new marker of CSCs, more specific than CD44, in human non-cardia gastric carcinomas of both the intestinal and the diffuse types. Therefore, we focused on ALDH to understand its putative function in controlling gastric CSC homeostasis. Some of the ALDH isoforms of retinaldehyde dehydrogenase convert retinal derived from vitamin A into active All-trans- and cis 9- retinoic acids (RA). RAs play a key role during development; in adults, it controls homeostasis in many tissues by regulating the self-renewal and differentiation properties of stem cells. In cancer, retinoic therapy with All-trans retinoic acid (ATRA) was included in therapy for acute promyelocytic leukemia (APL) in the late 1980s, and radically changed the management and the outcome of this disease. In APL patients, ATRA induces an inhibition of proliferation and the differentiation of leukemia cells, leading to a complete remission in the majority of cases when administered in combination with light chemotherapy and/or arsenic trioxide (Schenk et al., 2014).

In the second part of our work, we developed an ATRA therapy targeting gastric CSCs.

3. Determination of the culture conditions to assess the inhibitory effect of ATRA on the growth of gastric cancer cells

In this part of our research, we assessed the inhibitory effect of ATRA in three different and complementary models including 2D monolayer cultures, 3D non-adherent cultures in the tumorsphere assay, and *in vivo* xenografts in NSG mice.

Almost all current *in vitro* studies using ATRA or other drugs as anti-tumor agents are carried out under 2D culture conditions containing 10% FBS. FBS is an essential supplement which increases viability and growth of human and animal cells *in vitro*. However, the presence of FBS may also bear some disadvantages such as changes in cell characteristics leading to changes in response to drugs (Fernando et al., 2006). Furthermore, other aspects involved in serum use in cell culture including ethical and safety considerations have been previously mentioned (Even et al., 2006). Therefore, developing serum free media is necessary for basic research, clinical application, and particularly for stem cell research (Merten, 2002; Mohamed et al., 2014). In our preliminary experiments, we found that almost all cell lines studied were not sensitive to ATRA in media supplemented with 10% FBS. However, surprisingly, when we assessed the effect of ATRA on tumorsphere formation of gastric cancer cells in tumorsphere assays which were performed in 3D non-adherent cultures in serum free media, we found that all of the cell lines studied were very sensitive to ATRA. Thus, we proposed that the presence of serum in 2D culture media may inhibit the response of gastric cancer cells to ATRA. To answer this question, the effect of ATRA on the growth of 6 gastric cancer cell lines was assessed in the absence or presence of increasing concentrations of ATRA. As expected, decreasing concentrations of FBS led to a sensitization of cells to ATRA and to an ATRA-induced inhibition of cell proliferation. On the other hand, we checked the effect of other supplements composing the tumorsphere assay culture media, including EGF, bFGF and Insulin, on ATRA induced inhibition of proliferation in serum free media, but no significant contribution was found (data not shown). These data allowed us to confirm that the presence of serum in culture media prevented ATRA-induced inhibition of gastric

cancer cell growth. Furthermore, expression assays of 9 genes controlling the RA signalling pathway showed that the responsiveness of cells to ATRA in serum-free media was closely associated with an increased expression of RAR γ , and a lack of expression of RAR α and RAR β or at very low level. This suggested, for the first time, that RAR γ could be considered as an important receptor mediating the inhibitory effects of ATRA on the growth of gastric cancer cells. However, it is necessary to confirm the effects of ATRA on gene expression at the protein level. In addition, a study on the molecular mechanisms that serum exerts on the modulation of RA signalling and cell response to ATRA at the epigenetic level should also be carried out.

We also showed by quantitative RT-PCR, flow cytometry, immunofluorescence and immunohistochemistry analyses that the expression of CD44 in MKN74 cancer cells was higher in serum-free cultures, both 2D and 3D, and *in vivo* but not in 2D culture with 10% serum. This suggests that the presence of serum in culture media may lead to changes in the cancer cell phenotype, and that 3D culture in serum-free media is closer to the *in vivo* situation than conventional 2D culture with serum. Furthermore, the identification of the FBS components which induce the silencing of the cell response to ATRA may contribute to a better understanding of the resistance mechanism involved in RA therapy which is observed in clinical trials on many different cancer types (Ying et al., 2011; Gallagher, 2002; Freemantle et al., 2003).

4. ATRA targets gastric CSCs

The discovery of CSCs in AML and then in many different solid tumors led to a new approach of cancer treatment. CSCs which generate all cells composing the tumor mass constitute an ideal target for new target therapies, in order to eradicate CSCs to prevent tumor recurrence after treatment. RAs, and particularly ATRA, were widely used in clinical treatment of APL patients based on their property to induce cancer cell differentiation (Breitman et al., 1980). In this work, we were the first to propose an

evaluation of the effects of ATRA specifically on CSCs in gastric cancer. For this purpose, we developed an ATRA treatment on a 3D culture model of gastric tumorspheres which are formed from cells with CSC properties (Takaishi et al., 2009c) (Liu et al., 2013; Bessède et al., 2013). Furthermore, xenograft models were also used to confirm the inhibitory effect of ATRA treatment on tumorigenic properties of gastric CSCs *in vivo*. Our first results showed that ATRA inhibited the growth and caused a cell cycle arrest of cells in gastric tumorspheres. Cell cycle regulation is closely related to cyclins (cyclin A, B, C, D, E) and cyclin-dependent kinases (CDKs). The activation of CDKs by binding to cyclin leads to phosphorylation of retinoblastoma proteins to release E2F from the E2F/DP1/Rb complex. E2F then stimulates the expression of numerous target genes and finally cell entry into the next cell cycle phase. Aberrations in the expression of cyclins have been found in a variety of tumors (MacLachlan et al., 1995). Among them, cyclin D1 and cyclin E which are key regulators to progress from G1 into S phase, were commonly overexpressed in tumors and particularly in tumor cases bearing mutations of the P53 tumor suppressor gene (Diehl, 2002 ; Lindahl et al., 2004a). A recent study of 43 gastric cancer patients revealed that cyclin D1 was expressed in 73% of the cases and was significantly higher than in patients with non-neoplastic mucosa (Arici et al., 2009). Similar to cyclin D1, overexpression of cyclin E was also commonly found in gastric cancer patients and significantly associated with a poor prognosis (Lindahl et al., 2004).

In the present study, ATRA treatment of tumorspheres led to the downregulation of transcription of several genes encoding cyclin A2, cyclin B1, cyclin D1 and cyclin E1 (from 3 to 11 fold). In particular, E2F1 which regulates the expression of genes involved in the cell cycle progression, such as cyclin A, cyclin E1 and PCNA (Bracken et al., 2004), was drastically reduced (by 7 fold). Furthermore, transcription of other genes controlling the cell cycle, cell growth and DNA replication such as CDK2, CDC25C and PCNA (Nilsson and Hoffmann, 2000) (Maga and Hubscher, 2003), were also inhibited by ATRA. It is important to highlight PCNA, which is recognized as a processivity factor of DNA polymerase delta (Kelman, 1997) and plays a crucial role

in DNA replication. Sakakura *et al.* showed that PCNA expression is essential for the growth of gastric tumors and treatment of gastric cancer cell lines with oligonucleotides which target mRNA on the PCNA gene, leading to inhibition of cell proliferation (Sakakura *et al.*, 1994). In this study, the significant decrease in PCNA in gastric cancer cells treated with ATRA was also confirmed at the protein level by immunofluorescence on gastric tumorspheres and by IHC on tumor xenografts. These results suggested that PCNA may be a potent target of ATRA for anti-tumor therapy.

More interestingly, we showed that expression of genes coding for CDK inhibitor proteins (CDKIs) including P21, P16, P27 and P53 were significantly downregulated in ATRA-treated tumorspheres compared to controls. CDKIs are negative regulators of the cell cycle via the inhibition of CDK activity. Genetic disorders in genes encoding these proteins may lead to the loss of control of the cell cycle and finally stimulate tumorigenesis (Hirama and Koeffler, 1995) (MacLachlan *et al.*, 1995). Among these CDKIs, the function of P21 has been extensively studied. Beside of its direct inhibition of CDK activity (CDK1 and CDK2), P21 is also able to inactivate other important proteins involved in DNA synthesis and repair such as PCNA (Abbas and Dutta, 2009). Thus, it is possible that PCNA is not only downregulated by ATRA but also inactivated via its interaction with P21 which is significantly upregulated in ATRA-treated tumorspheres.

Another important aspect of the/our study concerns the inhibitory effects of ATRA on CSCs. We found that ATRA was a powerful agent for the inhibition of the expression of genes controlling self renewal of stem cells such as Sox2 and KLF4 (Fong *et al.*, 2008; Nakatake *et al.*, 2006), as well as the CSC markers, CD44 and ALDH1A1, identified in the first part of the study. In particular, our results showed that ATRA treatment of gastric cancer cells led to a significant reduction in the number of cells expressing the gastric CSC marker CD44 in all of the cases and models studied (in 2D and 3D culture and in tumor xenografts). Some studies have also shown that ATRA induces the differentiation of glioblastoma cells, shown by the downregulation

of the expression of the glioblastoma CSC marker CD133 (Ying et al., 2011) and the differentiation of head and neck CSCs, shown by the downregulation of CD44 (Lim et al., 2012). More interestingly, cells expressing ALDH activity which was identified as a special marker of CSCs for both intestinal and diffuse type gastric carcinoma in the first part of our work, were significantly reduced in number after ATRA treatment both *in vitro* and *in vivo*. Known as a hallmark for identifying CSCs in many different cancer types (Marcato et al., 2011), ALDH activity was therefore used to assess the level of tumor differentiation based on the changes in the number of ALDH+ cells after treatment with drugs targeting CSCs. Elevated ALDH activity is not only used as a marker for the isolation of CSCs but is also associated with chemoresistance of tumor cells (Januchowski et al., 2013). In contrast to conventional chemotherapy which led to increasing anti-drug ALDH+ CSCs after treatment (Dylla et al., 2008), our study suggests that ATRA treatment of gastric cancer cells significantly reduces the number of ALDH+ cells in tumorspheres as well as in tumor xenografts. The inhibitory effects of ATRA on ALDH activity was also reported previously in head and neck CSCs (Bertrand et al., 2014) and breast CSCs (Ginestier et al., 2009). Furthermore, ATRA-induced reduction of ALDH activity was also shown to increase the sensitivity of cancer cells to chemotherapy and radiotherapy (Crocker and Allan, 2012) (Bertrand et al., 2014). Thus, ALDH can be considered both a marker of CSCs and a potent target for new therapy targeting CSCs expressing ALDH activity (Luo et al., 2012).

To assess the global effects of ATRA on signalling pathways of gastric cancer cells, we also used an RT2 Profiler PCR Array (Qiagen) to analyze the expression of 84 genes linked to CSCs in tumorspheres of the MKN45 cell line. Surprisingly, we found that ATRA affected the expression (≥ 2 fold) of 44/84 genes studied (data not shown). Among them, genes involved in the Notch signalling pathway including Jag1, Notch1 and Notch2 were significantly downregulated, as reported previously in glioblastoma by others (Ying et al., 2011). In addition, the ID1 gene (DNA-binding protein inhibitor ID-1 or Inhibitor of differentiation/DNA binding) which is associated with several elements of tumor progression such as the growth, cell survival, self renewal capacity and differentiation of stem cells and CSCs (Strait et al., 2002) was also inhibited (by 5

fold) by ATRA. More interestingly, DNMT1 (DNA (cytosine-5) methyltransferase 1) and HDAC1 (histone deacetylase 1), two key genes controlling epigenetic modification and associated with epithelial-mesenchymal transition/EMT (Giudice et al., 2013), were significantly downregulated by ATRA. We therefore hypothesize that ATRA-induced inhibition of DNMT1 and HDAC1 expression activates the transcription of ATRA target genes such as P21, P53, P16 and P27 resulting in cell cycle and growth arrest as well as cell differentiation.

Overall, our results show that ATRA targets CSCs and inhibits tumor growth via activating or inhibiting the expression of several genes involved in cell cycle control, DNA synthesis and repair, self renewal of CSCs, epigenetic alterations and the Notch signalling pathway.

5. New CSC markers and combined therapies of ATRA with other anti-cancer drugs in gastric cancer treatment.

To date, we have identified CD44 and ALDH as two main markers which may be used for the identification of gastric CSCs. However, not all primary tumor cases or gastric cancer cell lines always express these markers. Therefore, finding new CSC cell surface markers is necessary to detect CSCs in different gastric tumors. Our recent results from the RT2 Profiler PCR Arrays analyses show that MUC1 which was proposed as a new cell surface marker for CSCs in pancreatic cancer (Curry et al., 2013) and which is overexpressed in gastric cancer (Utsunomiya et al., 1998) is also significantly inhibited by ATRA, like CD44 and ALDH. A further study will determine whether MUC1 can be a new candidate as a CSC marker in gastric cancer.

In order to propose new ATRA-based therapies to target CSCs in gastric cancer, the combination of ATRA with other anti-cancer drugs is essential. Current approaches often include the combination of ATRA with other chemotherapy agents such as 5-fluoro-uracil (5-FU), arsenic trioxide, daunorubicin and paclitaxel, which have shown a

significant improvement in tumor growth inhibition (Huang et al., 2012) (Karmakar et al., 2008). However, these drugs are highly toxic and therefore secondary effects during treatment are a problem which need to be considered. We hypothesize that therapies combining ATRA with other anti-cancer drugs which also target CSCs such as metformin (Hirsch et al., 2009), salinomycin, sulforaphan or curcumin (Gupta et al., 2009), could be less toxic and well tolerated.

A recent review of the role of ATRA in cancer treatment showed that the non-response or resistance to ATRA treatment may involve epigenetic alterations in cancer cells (Schenk et al., 2014). Our results demonstrate that ATRA inhibits DNMT1 and HDAC1 (data not shown), which may be related to ATRA-induced gastric cancer inhibition. Therefore, inhibitory effects of ATRA on the growth of gastric cancer cells may be enhanced if these cells are treated by ATRA in combination with specific inhibitors of HDAC1 or DNMT1.

Finally, results of RT2 Profiler PCR Array analyses on tumorsphere expression of genes related to CSCs, show that, although ATRA inhibits the proliferation of gastric cancer cells, it increases the expression of genes responsible for drug efflux and resistance including ABCG5 and ABCG2 (3.9 and 4.7 fold). Thus, gastric cancer treatment with ATRA together with drugs inhibiting these drug-efflux transporters such as Verapamil should also be considered in future studies.

PART IV. REFERENCES

References

- Abbas, T., and Dutta, A. (2009). p21 in cancer: intricate networks and multiple activities. *Nat. Rev. Cancer* 9, 400–414.
- Altucci, L., and Gronemeyer, H. (2001). The promise of retinoids to fight against cancer. *Nat. Rev. Cancer* 1, 181–193.
- Arici, D.S., Tuncer, E., Ozer, H., Simek, G., and Koyuncu, A. (2009). Expression of retinoblastoma and cyclin D1 in gastric carcinoma. *Neoplasma* 56, 63–67.
- Arrieta, O., González-De la Rosa, C.H., Aréchaga-Ocampo, E., Villanueva-Rodríguez, G., Cerón-Lizárraga, T.L., Martínez-Barrera, L., Vázquez-Manríquez, M.E., Ríos-Trejo, M.A., Alvarez-Avitia, M.A., Hernández-Pedro, N., et al. (2010). Randomized phase II trial of All-trans-retinoic acid with chemotherapy based on paclitaxel and cisplatin as first-line treatment in patients with advanced non-small-cell lung cancer. *J. Clin. Oncol. Off. J. Am. Soc. Clin. Oncol.* 28, 3463–3471.
- Arumugam, T., and Logsdon, C.D. (2011). S100P: a novel therapeutic target for cancer. *Amino Acids* 41, 893–899.
- Atherton, J.C., Cao, P., Peek, R.M., Jr, Tummuru, M.K., Blaser, M.J., and Cover, T.L. (1995). Mosaicism in vacuolating cytotoxin alleles of *Helicobacter pylori*. Association of specific vacA types with cytotoxin production and peptic ulceration. *J. Biol. Chem.* 270, 17771–17777.
- Atherton, J.C., Peek, R.M., Jr, Tham, K.T., Cover, T.L., and Blaser, M.J. (1997). Clinical and pathological importance of heterogeneity in vacA, the vacuolating cytotoxin gene of *Helicobacter pylori*. *Gastroenterology* 112, 92–99.
- Aubert, J., Dunstan, H., Chambers, I., and Smith, A. (2002). Functional gene screening in embryonic stem cells implicates Wnt antagonism in neural differentiation. *Nat. Biotechnol.* 20, 1240–1245.
- Avital, I., Moreira, A.L., Klimstra, D.S., Leversha, M., Papadopoulos, E.B., Brennan, M., and Downey, R.J. (2007). Donor-derived human bone marrow cells contribute to solid organ cancers developing after bone marrow transplantation. *Stem Cells Dayt. Ohio* 25, 2903–2909.
- Baba, T., Convery, P.A., Matsumura, N., Whitaker, R.S., Kondoh, E., Perry, T., Huang, Z., Bentley, R.C., Mori, S., Fujii, S., et al. (2009). Epigenetic regulation of CD133 and tumorigenicity of CD133+ ovarian cancer cells. *Oncogene* 28, 209–218.
- Baccarelli, A., Hou, L., Chen, J., Lissowska, J., El-Omar, E.M., Grillo, P., Giacomini, S.M., Yaeger, M., Bernig, T., Zatonski, W., et al. (2006). Mannose-binding lectin-2 genetic variation and stomach cancer risk. *Int. J. Cancer J. Int. Cancer* 119, 1970–1975.
- Backert, S., and Clyne, M. (2011). Pathogenesis of *Helicobacter pylori* infection. *Helicobacter* 16 Suppl 1, 19–25.
- Backert, S., Ziska, E., Brinkmann, V., Zimny-Arndt, U., Fauconnier, A., Jungblut, P.R., Naumann, M., and Meyer, T.F. (2000). Translocation of the *Helicobacter pylori* CagA protein in gastric epithelial cells by a type IV secretion apparatus. *Cell. Microbiol.* 2, 155–164.
- Ballim, R.D., Mendelsohn, C., Papaioannou, V.E., and Prince, S. (2012). The ulnar-mammary

syndrome gene, *Tbx3*, is a direct target of the retinoic acid signaling pathway, which regulates its expression during mouse limb development. *Mol. Biol. Cell* 23, 2362–2372.

- Balmer, J.E., and Blomhoff, R. (2002). Gene expression regulation by retinoic acid. *J. Lipid Res.* 43, 1773–1808.
- Barker, N., Ridgway, R.A., van Es, J.H., van de Wetering, M., Begthel, H., van den Born, M., Danenberg, E., Clarke, A.R., Sansom, O.J., and Clevers, H. (2009). Crypt stem cells as the cells-of-origin of intestinal cancer. *Nature* 457, 608–611.
- Barker, N., Huch, M., Kujala, P., van de Wetering, M., Snippert, H.J., van Es, J.H., Sato, T., Stange, D.E., Begthel, H., van den Born, M., et al. (2010). *Lgr5(+ve)* stem cells drive self-renewal in the stomach and build long-lived gastric units in vitro. *Cell Stem Cell* 6, 25–36.
- Basso, D., Zambon, C.-F., Letley, D.P., Stranges, A., Marchet, A., Rhead, J.L., Schiavon, S., Guariso, G., Ceroti, M., Nitti, D., et al. (2008). Clinical relevance of *Helicobacter pylori* *cagA* and *vacA* gene polymorphisms. *Gastroenterology* 135, 91–99.
- Baum, C.M., Weissman, I.L., Tsukamoto, A.S., Buckle, A.M., and Peault, B. (1992). Isolation of a candidate human hematopoietic stem-cell population. *Proc. Natl. Acad. Sci. U. S. A.* 89, 2804–2808.
- Belyaeva, O.V., Johnson, M.P., and Kedishvili, N.Y. (2008). Kinetic analysis of human enzyme RDH10 defines the characteristics of a physiologically relevant retinol dehydrogenase. *J. Biol. Chem.* 283, 20299–20308.
- Bertolini, G., Roz, L., Perego, P., Tortoreto, M., Fontanella, E., Gatti, L., Pratesi, G., Fabbri, A., Andriani, F., Tinelli, S., et al. (2009). Highly tumorigenic lung cancer CD133+ cells display stem-like features and are spared by cisplatin treatment. *Proc. Natl. Acad. Sci. U. S. A.* 106, 16281–16286.
- Bertrand, G., Maalouf, M., Boivin, A., Battiston-Montagne, P., Beuve, M., Levy, A., Jalade, P., Fournier, C., Ardail, D., Magné, N., et al. (2014). Targeting head and neck cancer stem cells to overcome resistance to photon and carbon ion radiation. *Stem Cell Rev.* 10, 114–126.
- Bessède, E., Stadel, C., Acuña Amador, L.A., Nguyen, P.H., Chambonnier, L., Hatakeyama, M., Belleannée, G., Mégraud, F., and Varon, C. (2014). *Helicobacter pylori* generates cells with cancer stem cell properties via epithelial-mesenchymal transition-like changes. *Oncogene* 33, 4123–4131.
- Bjerknes, M., and Cheng, H. (2002). Multipotential stem cells in adult mouse gastric epithelium. *Am. J. Physiol. Gastrointest. Liver Physiol.* 283, G767–G777.
- Blaese, M.A., Santo-Hoeltje, L., and Rodemann, H.P. (2003). CRABP I expression and the mediation of the sensitivity of human tumour cells to retinoic acid and irradiation. *Int. J. Radiat. Biol.* 79, 981–991.
- Blair, A., Hogge, D.E., Ailles, L.E., Lansdorp, P.M., and Sutherland, H.J. (1997). Lack of expression of Thy-1 (CD90) on acute myeloid leukemia cells with long-term proliferative ability in vitro and in vivo. *Blood* 89, 3104–3112.
- Blaser, M.J., Perez-Perez, G.I., Kleanthous, H., Cover, T.L., Peek, R.M., Chyou, P.H., Stemmermann, G.N., and Nomura, A. (1995). Infection with *Helicobacter pylori* strains possessing *cagA* is associated with an increased risk of developing adenocarcinoma of the stomach. *Cancer Res.* 55, 2111–2115.
- Blomhoff, R., and Blomhoff, H.K. (2006). Overview of retinoid metabolism and function. *J.*

Neurobiol. 66, 606–630.

Bonkhoff, H., and Remberger, K. (1996). Differentiation pathways and histogenetic aspects of normal and abnormal prostatic growth: a stem cell model. *Prostate* 28, 98–106.

Bonnet, D., and Dick, J.E. (1997). Human acute myeloid leukemia is organized as a hierarchy that originates from a primitive hematopoietic cell. *Nat. Med.* 3, 730–737.

Borggreffe, T., and Oswald, F. (2009). The Notch signaling pathway: transcriptional regulation at Notch target genes. *Cell. Mol. Life Sci. CMLS* 66, 1631–1646.

Bourzac, K.M., and Guillemin, K. (2005). Helicobacter pylori-host cell interactions mediated by type IV secretion. *Cell. Microbiol.* 7, 911–919.

Boyer, L.A., Lee, T.I., Cole, M.F., Johnstone, S.E., Levine, S.S., Zucker, J.P., Guenther, M.G., Kumar, R.M., Murray, H.L., Jenner, R.G., et al. (2005). Core transcriptional regulatory circuitry in human embryonic stem cells. *Cell* 122, 947–956.

Bracken, A.P., Ciro, M., Cocito, A., and Helin, K. (2004). E2F target genes: unraveling the biology. *Trends Biochem. Sci.* 29, 409–417.

Bray, S.J. (2006). Notch signalling: a simple pathway becomes complex. *Nat. Rev. Mol. Cell Biol.* 7, 678–689.

Breast Cancer Linkage Consortium (1999). Cancer risks in BRCA2 mutation carriers. *J. Natl. Cancer Inst.* 91, 1310–1316.

Breitman, T.R., Selonick, S.E., and Collins, S.J. (1980). Induction of differentiation of the human promyelocytic leukemia cell line (HL-60) by retinoic acid. *Proc. Natl. Acad. Sci. U. S. A.* 77, 2936–2940.

Broadley, K.W.R., Hunn, M.K., Farrand, K.J., Price, K.M., Grasso, C., Miller, R.J., Hermans, I.F., and McConnell, M.J. (2011). Side population is not necessary or sufficient for a cancer stem cell phenotype in glioblastoma multiforme. *Stem Cells Dayt. Ohio* 29, 452–461.

Brooks-Wilson, A.R., Kaurah, P., Suriano, G., Leach, S., Senz, J., Grehan, N., Butterfield, Y.S.N., Jeyes, J., Schinas, J., Bacani, J., et al. (2004). Germline E-cadherin mutations in hereditary diffuse gastric cancer: assessment of 42 new families and review of genetic screening criteria. *J. Med. Genet.* 41, 508–517.

Bruck, N., Vitoux, D., Ferry, C., Duong, V., Bauer, A., de Thé, H., and Rochette-Egly, C. (2009). A coordinated phosphorylation cascade initiated by p38MAPK/MSK1 directs RARalpha to target promoters. *EMBO J.* 28, 34–47.

Burger, P.E., Gupta, R., Xiong, X., Ontiveros, C.S., Salm, S.N., Moscatelli, D., and Wilson, E.L. (2009). High aldehyde dehydrogenase activity: a novel functional marker of murine prostate stem/progenitor cells. *Stem Cells Dayt. Ohio* 27, 2220–2228.

Burkert, J., Otto, W.R., and Wright, N.A. (2008). Side populations of gastrointestinal cancers are not enriched in stem cells. *J. Pathol.* 214, 564–573.

Busch, A.M., Galimberti, F., Nehls, K.E., Roengvoraphoj, M., Sekula, D., Li, B., Guo, Y., Drenzo, J., Fiering, S.N., Spinella, M.J., et al. (2014). All-trans-retinoic acid antagonizes the Hedgehog pathway by inducing patched. *Cancer Biol. Ther.* 15, 463–472.

Carneiro, F., Oliveira, C., Suriano, G., and Seruca, R. (2008). Molecular pathology of familial gastric cancer, with an emphasis on hereditary diffuse gastric cancer. *J. Clin. Pathol.* 61, 25–30.

- Carrel, T., Pasic, M., Vogt, P., von Segesser, L., Linka, A., Ritter, M., Jenni, R., and Turina, M. (1993). Retrograde ascending aortic dissection: a diagnostic and therapeutic challenge. *Eur. J. Cardio-Thorac. Surg. Off. J. Eur. Assoc. Cardio-Thorac. Surg.* 7, 146–150; discussion 151–152.
- Chambers, M.G., Pyburn, T.M., González-Rivera, C., Collier, S.E., Eli, I., Yip, C.K., Takizawa, Y., Lacy, D.B., Cover, T.L., and Ohi, M.D. (2013). Structural analysis of the oligomeric states of *Helicobacter pylori* VacA toxin. *J. Mol. Biol.* 425, 524–535.
- Chambon, P. (1996). A decade of molecular biology of retinoic acid receptors. *FASEB J. Off. Publ. Fed. Am. Soc. Exp. Biol.* 10, 940–954.
- Chan, K.S., Espinosa, I., Chao, M., Wong, D., Ailles, L., Diehn, M., Gill, H., Presti, J., Chang, H.Y., van de Rijn, M., et al. (2009). Identification, molecular characterization, clinical prognosis, and therapeutic targeting of human bladder tumor-initiating cells. *Proc. Natl. Acad. Sci. U. S. A.* 106, 14016–14021.
- Chang, L., Graham, P.H., Hao, J., Ni, J., Bucci, J., Cozzi, P.J., Kearsley, J.H., and Li, Y. (2013). Acquisition of epithelial-mesenchymal transition and cancer stem cell phenotypes is associated with activation of the PI3K/Akt/mTOR pathway in prostate cancer radioresistance. *Cell Death Dis.* 4, e875.
- Chao, T.Y., Jiang, S.Y., Shyu, R.Y., Yeh, M.Y., and Chu, T.M. (1997). All-trans retinoic acid decreases susceptibility of a gastric cancer cell line to lymphokine-activated killer cytotoxicity. *Br. J. Cancer* 75, 1284–1290.
- Cheng, T. (2004). Cell cycle inhibitors in normal and tumor stem cells. *Oncogene* 23, 7256–7266.
- Chiba, T., Kita, K., Zheng, Y.-W., Yokosuka, O., Saisho, H., Iwama, A., Nakauchi, H., and Taniguchi, H. (2006). Side population purified from hepatocellular carcinoma cells harbors cancer stem cell-like properties. *Hepatology* 44, 240–251.
- Chiou, S.-H., Kao, C.-L., Chen, Y.-W., Chien, C.-S., Hung, S.-C., Lo, J.-F., Chen, Y.-J., Ku, H.-H., Hsu, M.-T., and Wong, T.-T. (2008). Identification of CD133-positive radioresistant cells in atypical teratoid/rhabdoid tumor. *PloS One* 3, e2090.
- Cho, R.W., Wang, X., Diehn, M., Shedden, K., Chen, G.Y., Sherlock, G., Gurney, A., Lewicki, J., and Clarke, M.F. (2008). Isolation and molecular characterization of cancer stem cells in MMTV-Wnt-1 murine breast tumors. *Stem Cells* 26, 364–371.
- Choi, S.A., Lee, J.Y., Phi, J.H., Wang, K.-C., Park, C.-K., Park, S.-H., and Kim, S.-K. (2014). Identification of brain tumour initiating cells using the stem cell marker aldehyde dehydrogenase. *Eur. J. Cancer Oxf. Engl.* 50, 137–149.
- Chou, H.K., Chen, S.L., Hsu, C.T., Chao, Y.C., and Tsao, Y.P. (2000). Bcl-2 accelerates retinoic acid-induced growth arrest and recovery in human gastric cancer cells. *Biochem. J.* 348 Pt 2, 473–479.
- Clément, V., Dutoit, V., Marino, D., Dietrich, P.-Y., and Radovanovic, I. (2009). Limits of CD133 as a marker of glioma self-renewing cells. *Int. J. Cancer J. Int. Cancer* 125, 244–248.
- Lo-Coco, F., Avvisati, G., Vignetti, M., Thiede, C., Orlando, S.M., Iacobelli, S., Ferrara, F., Fazi, P., Cicconi, L., Di Bona, E., et al. (2013). Retinoic acid and arsenic trioxide for acute promyelocytic leukemia. *N. Engl. J. Med.* 369, 111–121.
- Cohen, B., Shimizu, M., Izrailit, J., Ng, N.F.L., Buchman, Y., Pan, J.G., Dering, J., and Reedijk, M. (2010). Cyclin D1 is a direct target of JAG1-mediated Notch signaling in breast cancer. *Breast*

Cancer Res. Treat. *123*, 113–124.

- Collins, A.T., Berry, P.A., Hyde, C., Stower, M.J., and Maitland, N.J. (2005). Prospective identification of tumorigenic prostate cancer stem cells. *Cancer Res.* *65*, 10946–10951.
- Connolly, R.M., Nguyen, N.K., and Sukumar, S. (2013). Molecular pathways: current role and future directions of the retinoic acid pathway in cancer prevention and treatment. *Clin. Cancer Res. Off. J. Am. Assoc. Cancer Res.* *19*, 1651–1659.
- Correa, P. (1992). Human gastric carcinogenesis: a multistep and multifactorial process--First American Cancer Society Award Lecture on Cancer Epidemiology and Prevention. *Cancer Res.* *52*, 6735–6740.
- Corso, G., Velho, S., Paredes, J., Pedrazzani, C., Martins, D., Milanezi, F., Pascale, V., Vindigni, C., Pinheiro, H., Leite, M., et al. (2011). Oncogenic mutations in gastric cancer with microsatellite instability. *Eur. J. Cancer Oxf. Engl. 1990* *47*, 443–451.
- Cover, T.L. (1996). The vacuolating cytotoxin of *Helicobacter pylori*. *Mol. Microbiol.* *20*, 241–246.
- Cox, C.V., Evely, R.S., Oakhill, A., Pamphilon, D.H., Goulden, N.J., and Blair, A. (2004). Characterization of acute lymphoblastic leukemia progenitor cells. *Blood* *104*, 2919–2925.
- Cox, C.V., Diamanti, P., Evely, R.S., Kearns, P.R., and Blair, A. (2009). Expression of CD133 on leukemia-initiating cells in childhood ALL. *Blood* *113*, 3287–3296.
- Crocker, A.K., and Allan, A.L. (2012). Inhibition of aldehyde dehydrogenase (ALDH) activity reduces chemotherapy and radiation resistance of stem-like ALDHhiCD44⁺ human breast cancer cells. *Breast Cancer Res. Treat.* *133*, 75–87.
- Curley, M.D., Therrien, V.A., Cummings, C.L., Sergeant, P.A., Koulouris, C.R., Friel, A.M., Roberts, D.J., Seiden, M.V., Scadden, D.T., Rueda, B.R., et al. (2009). CD133 expression defines a tumor initiating cell population in primary human ovarian cancer. *Stem Cells Dayt. Ohio* *27*, 2875–2883.
- Curry, J.M., Thompson, K.J., Rao, S.G., Besmer, D.M., Murphy, A.M., Grdzlishvili, V.Z., Ahrens, W.A., McKillop, I.H., Sindram, D., Iannitti, D.A., et al. (2013). The use of a novel MUC1 antibody to identify cancer stem cells and circulating MUC1 in mice and patients with pancreatic cancer. *J. Surg. Oncol.* *107*, 713–722.
- Dalerba, P., Dylla, S.J., Park, I.-K., Liu, R., Wang, X., Cho, R.W., Hoey, T., Gurney, A., Huang, E.H., Simeone, D.M., et al. (2007). Phenotypic characterization of human colorectal cancer stem cells. *Proc. Natl. Acad. Sci. U. S. A.* *104*, 10158–10163.
- Delacroix, L., Moutier, E., Altobelli, G., Legras, S., Poch, O., Choukrallah, M.-A., Bertin, I., Jost, B., and Davidson, I. (2010). Cell-specific interaction of retinoic acid receptors with target genes in mouse embryonic fibroblasts and embryonic stem cells. *Mol. Cell. Biol.* *30*, 231–244.
- Diehl, J.A. (2002). Cycling to cancer with cyclin D1. *Cancer Biol. Ther.* *1*, 226–231.
- Van Doorn, L.J., Figueiredo, C., Mégraud, F., Pena, S., Midolo, P., Queiroz, D.M., Carneiro, F., Vanderborght, B., Pegado, M.D., Sanna, R., et al. (1999). Geographic distribution of vacA allelic types of *Helicobacter pylori*. *Gastroenterology* *116*, 823–830.
- Dudley, A.T., and Tabin, C.J. (2003). Deconstructing phosphatases in limb development. *Nat. Cell Biol.* *5*, 499–501.
- Duester, G. (2008). Retinoic acid synthesis and signaling during early organogenesis. *Cell* *134*, 921–931.

- Dylla, S.J., Beviglia, L., Park, I.-K., Chartier, C., Raval, J., Ngan, L., Pickell, K., Aguilar, J., Lazetic, S., Smith-Berdan, S., et al. (2008a). Colorectal cancer stem cells are enriched in xenogeneic tumors following chemotherapy. *PloS One* 3, e2428.
- Easwaran, V., Pishvaian, M., Salimuddin, null, and Byers, S. (1999). Cross-regulation of beta-catenin-LEF/TCF and retinoid signaling pathways. *Curr. Biol. CB* 9, 1415–1418.
- Ebert, M.P.A., Fei, G., Kahmann, S., Müller, O., Yu, J., Sung, J.J.Y., and Malfertheiner, P. (2002). Increased beta-catenin mRNA levels and mutational alterations of the APC and beta-catenin gene are present in intestinal-type gastric cancer. *Carcinogenesis* 23, 87–91.
- Eckfeldt, C.E., Mendenhall, E.M., and Verfaillie, C.M. (2005). The molecular repertoire of the “almighty” stem cell. *Nat. Rev. Mol. Cell Biol.* 6, 726–737.
- Edgren, G., Hjalgrim, H., Rostgaard, K., Norda, R., Wikman, A., Melbye, M., and Nyrén, O. (2010). Risk of gastric cancer and peptic ulcers in relation to ABO blood type: a cohort study. *Am. J. Epidemiol.* 172, 1280–1285.
- Efstratiadis, A., Szabolcs, M., and Klinakis, A. (2007). Notch, Myc and breast cancer. *Cell Cycle Georget. Tex* 6, 418–429.
- El-Omar, E.M., Carrington, M., Chow, W.H., McColl, K.E., Bream, J.H., Young, H.A., Herrera, J., Lissowska, J., Yuan, C.C., Rothman, N., et al. (2000). Interleukin-1 polymorphisms associated with increased risk of gastric cancer. *Nature* 404, 398–402.
- El-Zimaity, H.M.T., Ota, H., Graham, D.Y., Akamatsu, T., and Katsuyama, T. (2002). Patterns of gastric atrophy in intestinal type gastric carcinoma. *Cancer* 94, 1428–1436.
- Eramo, A., Lotti, F., Sette, G., Pillozzi, E., Biffoni, M., Di Virgilio, A., Conticello, C., Ruco, L., Peschle, C., and De Maria, R. (2008). Identification and expansion of the tumorigenic lung cancer stem cell population. *Cell Death Differ.* 15, 504–514.
- Even, M.S., Sandusky, C.B., and Barnard, N.D. (2006). Serum-free hybridoma culture: ethical, scientific and safety considerations. *Trends Biotechnol.* 24, 105–108.
- Everett, S.M., and Axon, A.T. (1998). Early gastric cancer: disease or pseudo-disease? *Lancet* 351, 1350–1352.
- Fadloun, A., Kobi, D., Delacroix, L., Dembélé, D., Michel, I., Lardenois, A., Tisserand, J., Losson, R., Mengus, G., and Davidson, I. (2008). Retinoic acid induces TGFbeta-dependent autocrine fibroblast growth. *Oncogene* 27, 477–489.
- Fang, J.Y., and Xiao, S.D. (1998). Effect of trans-retinoic acid and folic acid on apoptosis in human gastric cancer cell lines MKN-45 and MKN-28. *J. Gastroenterol.* 33, 656–661.
- Fang, D.-C., Luo, Y.-H., Yang, S.-M., Li, X.-A., Ling, X.-L., and Fang, L. (2002). Mutation analysis of APC gene in gastric cancer with microsatellite instability. *World J. Gastroenterol. WJG* 8, 787–791.
- Fenaux, P., Chastang, C., Chevret, S., Sanz, M., Dombret, H., Archimbaud, E., Fey, M., Rayon, C., Huguet, F., Sotto, J.J., et al. (1999). A randomized comparison of all transretinoic acid (ATRA) followed by chemotherapy and ATRA plus chemotherapy and the role of maintenance therapy in newly diagnosed acute promyelocytic leukemia. The European APL Group. *Blood* 94, 1192–1200.
- Fernando, A., Glaysher, S., Conroy, M., Pekalski, M., Smith, J., Knight, L.A., Di Nicolantonio, F., and Cree, I.A. (2006). Effect of culture conditions on the chemosensitivity of ovarian cancer

cell lines. *Anticancer. Drugs* 17, 913–919.

- Fischer, W., Buhrdorf, R., Gerland, E., and Haas, R. (2001). Outer membrane targeting of passenger proteins by the vacuolating cytotoxin autotransporter of *Helicobacter pylori*. *Infect. Immun.* 69, 6769–6775.
- Fitzgerald, R.C., Hardwick, R., Huntsman, D., Carneiro, F., Guilford, P., Blair, V., Chung, D.C., Norton, J., Ragnanath, K., Van Krieken, J.H., et al. (2010). Hereditary diffuse gastric cancer: updated consensus guidelines for clinical management and directions for future research. *J. Med. Genet.* 47, 436–444.
- Fiúza, U.-M., and Arias, A.M. (2007). Cell and molecular biology of Notch. *J. Endocrinol.* 194, 459–474.
- Fletcher, J.I., Haber, M., Henderson, M.J., and Norris, M.D. (2010). ABC transporters in cancer: more than just drug efflux pumps. *Nat. Rev. Cancer* 10, 147–156.
- Fong, H., Hohenstein, K.A., and Donovan, P.J. (2008). Regulation of self-renewal and pluripotency by Sox2 in human embryonic stem cells. *Stem Cells Dayt. Ohio* 26, 1931–1938.
- Forman, D., and Burley, V.J. (2006). Gastric cancer: global pattern of the disease and an overview of environmental risk factors. *Best Pract. Res. Clin. Gastroenterol.* 20, 633–649.
- Fox, J.G., and Wang, T.C. (2007). Inflammation, atrophy, and gastric cancer. *J. Clin. Invest.* 117, 60–69.
- Franco, A.T., Israel, D.A., Washington, M.K., Krishna, U., Fox, J.G., Rogers, A.B., Neish, A.S., Collier-Hyams, L., Perez-Perez, G.I., Hatakeyama, M., et al. (2005). Activation of beta-catenin by carcinogenic *Helicobacter pylori*. *Proc. Natl. Acad. Sci. U. S. A.* 102, 10646–10651.
- Franken, N.A.P., Rodermond, H.M., Stap, J., Haveman, J., and van Bree, C. (2006). Clonogenic assay of cells in vitro. *Nat. Protoc.* 1, 2315–2319.
- Freemantle, S.J., Spinella, M.J., and Dmitrovsky, E. (2003). Retinoids in cancer therapy and chemoprevention: promise meets resistance. *Oncogene* 22, 7305–7315.
- Friedenson, B. (2005). BRCA1 and BRCA2 pathways and the risk of cancers other than breast or ovarian. *MedGenMed Medscape Gen. Med.* 7, 60.
- Fujii, T., and Yokomori, T. (1991). [A clinical study of vitamin A concerning auxiliary chemotherapies after operation of gastric cancer]. *Gan To Kagaku Ryoho* 18, 265–269.
- Fukuda, K., Saikawa, Y., Ohashi, M., Kumagai, K., Kitajima, M., Okano, H., Matsuzaki, Y., and Kitagawa, Y. (2009). Tumor initiating potential of side population cells in human gastric cancer. *Int. J. Oncol.* 34, 1201–1207.
- Galizia, G., Lieto, E., Orditura, M., Castellano, P., Mura, A.L., Imperatore, V., Pinto, M., Zamboli, A., De Vita, F., and Ferraraccio, F. (2007). Epidermal growth factor receptor (EGFR) expression is associated with a worse prognosis in gastric cancer patients undergoing curative surgery. *World J. Surg.* 31, 1458–1468.
- Gallagher, R.E. (2002). Retinoic acid resistance in acute promyelocytic leukemia. *Leukemia* 16, 1940–1958.
- Gangwer, K.A., Shaffer, C.L., Suerbaum, S., Lacy, D.B., Cover, T.L., and Bordenstein, S.R. (2010). Molecular evolution of the *Helicobacter pylori* vacuolating toxin gene vacA. *J. Bacteriol.* 192, 6126–6135.

- Gencer, S., Şen, G., Doğusoy, G., Belli, A.K., Paksoy, M., and Yazicioğlu, M.B.I. (2010). β -Catenin-independent noncanonical Wnt pathway might be induced in gastric cancers. *Turk. J. Gastroenterol. Off. J. Turk. Soc. Gastroenterol.* 21, 224–230.
- Gianni, M., Terao, M., Fortino, I., LiCalzi, M., Viggiano, V., Barbui, T., Rambaldi, A., and Garattini, E. (1997). Stat1 is induced and activated by all-trans retinoic acid in acute promyelocytic leukemia cells. *Blood* 89, 1001–1012.
- Gibbs, C.P., Kukekov, V.G., Reith, J.D., Tchigrinova, O., Suslov, O.N., Scott, E.W., Ghivizzani, S.C., Ignatova, T.N., and Steindler, D.A. (2005). Stem-like cells in bone sarcomas: implications for tumorigenesis. *Neoplasia N. Y. N* 7, 967–976.
- Ginestier, C., Hur, M.H., Charafe-Jauffret, E., Monville, F., Dutcher, J., Brown, M., Jacquemier, J., Viens, P., Kleer, C.G., Liu, S., et al. (2007). ALDH1 is a marker of normal and malignant human mammary stem cells and a predictor of poor clinical outcome. *Cell Stem Cell* 1, 555–567.
- Ginestier, C., Wicinski, J., Cervera, N., Monville, F., Finetti, P., Bertucci, F., Wicha, M.S., Birnbaum, D., and Charafe-Jauffret, E. (2009). Retinoid signaling regulates breast cancer stem cell differentiation. *Cell Cycle Georget. Tex* 8, 3297–3302.
- Giudice, F.S., Pinto, D.S., Nör, J.E., Squarize, C.H., and Castilho, R.M. (2013). Inhibition of histone deacetylase impacts cancer stem cells and induces epithelial-mesenchyme transition of head and neck cancer. *PloS One* 8, e58672.
- Giuliano, C.J., Kerley-Hamilton, J.S., Bee, T., Freemantle, S.J., Manickaratnam, R., Dmitrovsky, E., and Spinella, M.J. (2005). Retinoic acid represses a cassette of candidate pluripotency chromosome 12p genes during induced loss of human embryonal carcinoma tumorigenicity. *Biochim. Biophys. Acta* 1731, 48–56.
- Gnad, T., Feoktistova, M., Leverkus, M., Lendeckel, U., and Naumann, M. (2010). Helicobacter pylori-induced activation of beta-catenin involves low density lipoprotein receptor-related protein 6 and Dishevelled. *Mol. Cancer* 9, 31.
- Golebiewska, A., Brons, N.H.C., Bjerkvig, R., and Niclou, S.P. (2011). Critical appraisal of the side population assay in stem cell and cancer stem cell research. *Cell Stem Cell* 8, 136–147.
- Goodison, S., Urquidi, V., and Tarin, D. (1999). CD44 cell adhesion molecules. *Mol. Pathol. MP* 52, 189–196.
- Greve, B., Kelsch, R., Spaniol, K., Eich, H.T., and Götte, M. (2012). Flow cytometry in cancer stem cell analysis and separation. *Cytom. Part J. Int. Soc. Anal. Cytol.* 81, 284–293.
- Gridley, T. (2007). Notch signaling in vascular development and physiology. *Dev. Camb. Engl.* 134, 2709–2718.
- Grignani, F., Ferrucci, P.F., Testa, U., Talamo, G., Fagioli, M., Alcalay, M., Mencarelli, A., Grignani, F., Peschle, C., and Nicoletti, I. (1993). The acute promyelocytic leukemia-specific PML-RAR alpha fusion protein inhibits differentiation and promotes survival of myeloid precursor cells. *Cell* 74, 423–431.
- Grün, F., Hirose, Y., Kawauchi, S., Ogura, T., and Umesono, K. (2000). Aldehyde dehydrogenase 6, a cytosolic retinaldehyde dehydrogenase prominently expressed in sensory neuroepithelia during development. *J. Biol. Chem.* 275, 41210–41218.
- Gu, P., LeMenuet, D., Chung, A.C.-K., Mancini, M., Wheeler, D.A., and Cooney, A.J. (2005). Orphan nuclear receptor GCNF is required for the repression of pluripotency genes during

retinoic acid-induced embryonic stem cell differentiation. *Mol. Cell. Biol.* 25, 8507–8519.

- Guilford, P., Hopkins, J., Harraway, J., McLeod, M., McLeod, N., Harawira, P., Taite, H., Scoular, R., Miller, A., and Reeve, A.E. (1998). E-cadherin germline mutations in familial gastric cancer. *Nature* 392, 402–405.
- Guo, J.-M., Liu, A.-J., Zang, P., Dong, W.-Z., Ying, L., Wang, W., Xu, P., Song, X.-R., Cai, J., Zhang, S.-Q., et al. (2013). ALDH2 protects against stroke by clearing 4-HNE. *Cell Res.* 23, 915–930.
- Gupta, P.B., Onder, T.T., Jiang, G., Tao, K., Kuperwasser, C., Weinberg, R.A., and Lander, E.S. (2009). Identification of selective inhibitors of cancer stem cells by high-throughput screening. *Cell* 138, 645–659.
- Al-Hajj, M., Wicha, M.S., Benito-Hernandez, A., Morrison, S.J., and Clarke, M.F. (2003a). Prospective identification of tumorigenic breast cancer cells. *Proc. Natl. Acad. Sci. U. S. A.* 100, 3983–3988.
- Hamashima, C., Shibuya, D., Yamazaki, H., Inoue, K., Fukao, A., Saito, H., and Sobue, T. (2008). The Japanese guidelines for gastric cancer screening. *Jpn. J. Clin. Oncol.* 38, 259–267.
- Haraguchi, N., Ohkuma, M., Sakashita, H., Matsuzaki, S., Tanaka, F., Mimori, K., Kamohara, Y., Inoue, H., and Mori, M. (2008a). CD133+CD44+ population efficiently enriches colon cancer initiating cells. *Ann. Surg. Oncol.* 15, 2927–2933.
- Haraguchi, N., Ishii, H., Mimori, K., Tanaka, F., Ohkuma, M., Kim, H.M., Akita, H., Takiuchi, D., Hatano, H., Nagano, H., et al. (2010). CD13 is a therapeutic target in human liver cancer stem cells. *J. Clin. Invest.* 120, 3326–3339.
- Hashimoto, Y., Akiyama, Y., Otsubo, T., Shimada, S., and Yuasa, Y. (2010). Involvement of epigenetically silenced microRNA-181c in gastric carcinogenesis. *Carcinogenesis* 31, 777–784.
- Hatakeyama, M. (2004). Oncogenic mechanisms of the *Helicobacter pylori* CagA protein. *Nat. Rev. Cancer* 4, 688–694.
- Hattori, Y., Odagiri, H., Nakatani, H., Miyagawa, K., Naito, K., Sakamoto, H., Katoh, O., Yoshida, T., Sugimura, T., and Terada, M. (1990). K-sam, an amplified gene in stomach cancer, is a member of the heparin-binding growth factor receptor genes. *Proc. Natl. Acad. Sci. U. S. A.* 87, 5983–5987.
- Hay, E.D. (1995). An overview of epithelio-mesenchymal transformation. *Acta Anat. (Basel)* 154, 8–20.
- Hayashi, K., Yokozaki, H., Goodison, S., Oue, N., Suzuki, T., Lotan, R., Yasui, W., and Tahara, E. (2001). Inactivation of retinoic acid receptor beta by promoter CpG hypermethylation in gastric cancer. *Differ. Res. Biol. Divers.* 68, 13–21.
- He, S., Nakada, D., and Morrison, S.J. (2009). Mechanisms of stem cell self-renewal. *Annu. Rev. Cell Dev. Biol.* 25, 377–406.
- Heckmann, B.L., Zhang, X., Xie, X., and Liu, J. (2013). The G0/G1 switch gene 2 (G0S2): regulating metabolism and beyond. *Biochim. Biophys. Acta* 1831, 276–281.
- Henson, D.E., Dittus, C., Younes, M., Nguyen, H., and Albores-Saavedra, J. (2004). Differential trends in the intestinal and diffuse types of gastric carcinoma in the United States, 1973-2000: increase in the signet ring cell type. *Arch. Pathol. Lab. Med.* 128, 765–770.

- Hermann, P.C., Huber, S.L., Herrler, T., Aicher, A., Ellwart, J.W., Guba, M., Bruns, C.J., and Heeschen, C. (2007). Distinct populations of cancer stem cells determine tumor growth and metastatic activity in human pancreatic cancer. *Cell Stem Cell* 1, 313–323.
- Hilton, J. (1984). Role of aldehyde dehydrogenase in cyclophosphamide-resistant L1210 leukemia. *Cancer Res.* 44, 5156–5160.
- Hiraga, T., Ito, S., and Nakamura, H. (2013). Cancer stem-like cell marker CD44 promotes bone metastases by enhancing tumorigenicity, cell motility, and hyaluronan production. *Cancer Res.* 73, 4112–4122.
- Hirama, T., and Koeffler, H.P. (1995). Role of the cyclin-dependent kinase inhibitors in the development of cancer. *Blood* 86, 841–854.
- Hirata, K., Suzuki, H., Imaeda, H., Matsuzaki, J., Tsugawa, H., Nagano, O., Asakura, K., Saya, H., and Hibi, T. (2013). CD44 variant 9 expression in primary early gastric cancer as a predictive marker for recurrence. *Br. J. Cancer* 109, 379–386.
- Hirsch, H.A., Iliopoulos, D., Tsihchlis, P.N., and Struhl, K. (2009). Metformin selectively targets cancer stem cells, and acts together with chemotherapy to block tumor growth and prolong remission. *Cancer Res.* 69, 7507–7511.
- Hisamichi, S., and Sugawara, N. (1984). Mass screening for gastric cancer by X-ray examination. *Jpn. J. Clin. Oncol.* 14, 211–223.
- Hodkinson, P.S., Mackinnon, A., and Sethi, T. (2008). Targeting growth factors in lung cancer. *Chest* 133, 1209–1216.
- Hollier, B.G., Tinnirello, A.A., Werden, S.J., Evans, K.W., Taube, J.H., Sarkar, T.R., Sphyris, N., Shariati, M., Kumar, S.V., Battula, V.L., et al. (2013). FOXC2 expression links epithelial-mesenchymal transition and stem cell properties in breast cancer. *Cancer Res.* 73, 1981–1992.
- Van den Hoogen, C., van der Horst, G., Cheung, H., Buijs, J.T., Lippitt, J.M., Guzmán-Ramírez, N., Hamdy, F.C., Eaton, C.L., Thalmann, G.N., Cecchini, M.G., et al. (2010). High aldehyde dehydrogenase activity identifies tumor-initiating and metastasis-initiating cells in human prostate cancer. *Cancer Res.* 70, 5163–5173.
- Van den Hoogen, C., van der Horst, G., Cheung, H., Buijs, J.T., Pelger, R.C.M., and van der Pluijm, G. (2011a). The aldehyde dehydrogenase enzyme 7A1 is functionally involved in prostate cancer bone metastasis. *Clin. Exp. Metastasis* 28, 615–625.
- Houghton, J., Stoicov, C., Nomura, S., Rogers, A.B., Carlson, J., Li, H., Cai, X., Fox, J.G., Goldenring, J.R., and Wang, T.C. (2004). Gastric cancer originating from bone marrow-derived cells. *Science* 306, 1568–1571.
- Houle, M., Prinos, P., Iulianella, A., Bouchard, N., and Lohnes, D. (2000). Retinoic acid regulation of Cdx1: an indirect mechanism for retinoids and vertebral specification. *Mol. Cell. Biol.* 20, 6579–6586.
- Hsu, K.-W., Hsieh, R.-H., Huang, K.-H., Fen-Yau Li, A., Chi, C.-W., Wang, T.-Y., Tseng, M.-J., Wu, K.-J., and Yeh, T.-S. (2012). Activation of the Notch1/STAT3/Twist signaling axis promotes gastric cancer progression. *Carcinogenesis* 33, 1459–1467.
- Hu, B., El Hajj, N., Sittler, S., Lammert, N., Barnes, R., and Meloni-Ehrig, A. (2012). Gastric cancer: Classification, histology and application of molecular pathology. *J. Gastrointest. Oncol.* 3, 251–261.

- Hu, K.-W., Pan, X.-H., Chen, F.-H., Qin, R., Wu, L.-M., Zhu, H.-G., Wu, F.-R., Ge, J.-F., Han, W.-X., Yin, C.-L., et al. (2014). A novel retinoic acid analog, 4-amino-2-trifluoromethyl-phenyl retinate, inhibits gastric cancer cell growth. *Int. J. Mol. Med.* *33*, 415–422.
- Huang, C.-P., Tsai, M.-F., Chang, T.-H., Tang, W.-C., Chen, S.-Y., Lai, H.-H., Lin, T.-Y., Yang, J.C.-H., Yang, P.-C., Shih, J.-Y., et al. (2013). ALDH-positive lung cancer stem cells confer resistance to epidermal growth factor receptor tyrosine kinase inhibitors. *Cancer Lett.* *328*, 144–151.
- Huang, H., Xie, C., Sun, X., Ritchie, R.P., Zhang, J., and Chen, Y.E. (2010). miR-10a contributes to retinoid acid-induced smooth muscle cell differentiation. *J. Biol. Chem.* *285*, 9383–9389.
- Huang, H., Qin, Y., Xu, R., You, X., Teng, R., Yang, L., Xu, M., and Liu, H. (2012). Combination therapy with arsenic trioxide, all-trans retinoic acid, and chemotherapy in acute promyelocytic leukemia patients with various relapse risks. *Leuk. Res.* *36*, 841–845.
- Huang, J.Q., Zheng, G.F., Sumanac, K., Irvine, E.J., and Hunt, R.H. (2003). Meta-analysis of the relationship between cagA seropositivity and gastric cancer. *Gastroenterology* *125*, 1636–1644.
- Huang, M.E., Ye, Y.C., Chen, S.R., Chai, J.R., Lu, J.X., Zhao, L., Gu, L.J., and Wang, Z.Y. (1988). Use of all-trans retinoic acid in the treatment of acute promyelocytic leukemia. *Blood* *72*, 567–572.
- Huntly, B.J.P., Shigematsu, H., Deguchi, K., Lee, B.H., Mizuno, S., Duclos, N., Rowan, R., Amaral, S., Curley, D., Williams, I.R., et al. (2004). MOZ-TIF2, but not BCR-ABL, confers properties of leukemic stem cells to committed murine hematopoietic progenitors. *Cancer Cell* *6*, 587–596.
- Irollo, E., and Pirozzi, G. (2013). CD133: to be or not to be, is this the real question? *Am. J. Transl. Res.* *5*, 563–581.
- Jackson, B., Brocker, C., Thompson, D.C., Black, W., Vasiliou, K., Nebert, D.W., and Vasiliou, V. (2011). Update on the aldehyde dehydrogenase gene (ALDH) superfamily. *Hum. Genomics* *5*, 283–303.
- Jacques, T.S., Swales, A., Brzozowski, M.J., Henriquez, N.V., Linehan, J.M., Mirzadeh, Z., O’Malley, C., Naumann, H., Alvarez-Buylla, A., and Brandner, S. (2010). Combinations of genetic mutations in the adult neural stem cell compartment determine brain tumour phenotypes. *EMBO J.* *29*, 222–235.
- Jagtap, S., Meganathan, K., Wagh, V., Natarajan, K., Hescheler, J., and Sachinidis, A. (2013). All-trans retinoic acid and basic fibroblast growth factor synergistically direct pluripotent human embryonic stem cells to extraembryonic lineages. *Stem Cell Res.* *10*, 228–240.
- Jakobs, C., Jaeken, J., and Gibson, K.M. (1993). Inherited disorders of GABA metabolism. *J. Inherit. Metab. Dis.* *16*, 704–715.
- James, D., Levine, A.J., Besser, D., and Hemmati-Brivanlou, A. (2005). TGFbeta/activin/nodal signaling is necessary for the maintenance of pluripotency in human embryonic stem cells. *Dev. Camb. Engl.* *132*, 1273–1282.
- Jang, J.H., Shin, K.H., and Park, J.G. (2001). Mutations in fibroblast growth factor receptor 2 and fibroblast growth factor receptor 3 genes associated with human gastric and colorectal cancers. *Cancer Res.* *61*, 3541–3543.
- Januchowski, R., Wojtowicz, K., and Zabel, M. (2013). The role of aldehyde dehydrogenase (ALDH)

- in cancer drug resistance. *Biomed. Pharmacother. Bioméd. Pharmacothérapie* 67, 669–680.
- Japanese Gastric Cancer Association (2011). Japanese classification of gastric carcinoma: 3rd English edition. *Gastric Cancer Off. J. Int. Gastric Cancer Assoc. Jpn. Gastric Cancer Assoc.* 14, 101–112.
- Jean, E., Laoudj-Chenivesse, D., Notarnicola, C., Rouger, K., Serratrice, N., Bonnieu, A., Gay, S., Bacou, F., Duret, C., and Carnac, G. (2011). Aldehyde dehydrogenase activity promotes survival of human muscle precursor cells. *J. Cell. Mol. Med.* 15, 119–133.
- Jemal, A., Bray, F., Center, M.M., Ferlay, J., Ward, E., and Forman, D. (2011). Global cancer statistics. *CA. Cancer J. Clin.* 61, 69–90.
- Jiang, S.Y., Shen, S.R., Shyu, R.Y., Yu, J.C., Harn, H.J., Yeh, M.Y., Lee, M.M., and Chang, Y.C. (1999). Expression of nuclear retinoid receptors in normal, premalignant and malignant gastric tissues determined by in situ hybridization. *Br. J. Cancer* 80, 206–214.
- Jyotheeswaran, S., Shah, A.N., Jin, H.O., Potter, G.D., Ona, F.V., and Chey, W.Y. (1998). Prevalence of *Helicobacter pylori* in peptic ulcer patients in greater Rochester, NY: is empirical triple therapy justified? *Am. J. Gastroenterol.* 93, 574–578.
- Kalluri, R., and Weinberg, R.A. (2009). The basics of epithelial-mesenchymal transition. *J. Clin. Invest.* 119, 1420–1428.
- Kambhampati, S., Verma, A., Li, Y., Parmar, S., Sassano, A., and Plataniias, L.C. (2004). Signalling pathways activated by all-trans-retinoic acid in acute promyelocytic leukemia cells. *Leuk. Lymphoma* 45, 2175–2185.
- Kang, Y., and Massagué, J. (2004). Epithelial-mesenchymal transitions: twist in development and metastasis. *Cell* 118, 277–279.
- Kang, H., An, H.-J., Song, J.-Y., Kim, T.-H., Heo, J.-H., Ahn, D.-H., and Kim, G. (2012). Notch3 and Jagged2 contribute to gastric cancer development and to glandular differentiation associated with MUC2 and MUC5AC expression. *Histopathology* 61, 576–586.
- Kang, H.-B., Kim, Y.-E., Kwon, H.-J., Sok, D.-E., and Lee, Y. (2007). Enhancement of NF-kappaB expression and activity upon differentiation of human embryonic stem cell line SNUhES3. *Stem Cells Dev.* 16, 615–623.
- Kao, H.-W., Chen, H.-C., Wu, C.-W., and Lin, W.-C. (2003). Tyrosine-kinase expression profiles in human gastric cancer cell lines and their modulations with retinoic acids. *Br. J. Cancer* 88, 1058–1064.
- Karmakar, S., Banik, N.L., and Ray, S.K. (2008). Combination of all-trans retinoic acid and paclitaxel-induced differentiation and apoptosis in human glioblastoma U87MG xenografts in nude mice. *Cancer* 112, 596–607.
- Karsy, M., Albert, L., Tobias, M.E., Murali, R., and Jhanwar-Uniyal, M. (2010). All-trans retinoic acid modulates cancer stem cells of glioblastoma multiforme in an MAPK-dependent manner. *Anticancer Res.* 30, 4915–4920.
- Kastner, P., Mark, M., Leid, M., Gansmuller, A., Chin, W., Grondona, J.M., Décimo, D., Krezel, W., Dierich, A., and Chambon, P. (1996). Abnormal spermatogenesis in RXR beta mutant mice. *Genes Dev.* 10, 80–92.
- Katoh, M. (2005). Epithelial-mesenchymal transition in gastric cancer (Review). *Int. J. Oncol.* 27, 1677–1683.

- Katoh, M., and Katoh, M. (2006). FGF signaling network in the gastrointestinal tract (review). *Int. J. Oncol.* *29*, 163–168.
- Kelman, Z. (1997). PCNA: structure, functions and interactions. *Oncogene* *14*, 629–640.
- Keysar, S.B., and Jimeno, A. (2010). More than markers: biological significance of cancer stem cell-defining molecules. *Mol. Cancer Ther.* *9*, 2450–2457.
- Kim, T.-H., and Shivdasani, R.A. (2011). Notch signaling in stomach epithelial stem cell homeostasis. *J. Exp. Med.* *208*, 677–688.
- Kim, H.J., Chang, W.K., Kim, M.K., Lee, S.S., and Choi, B.Y. (2002). Dietary factors and gastric cancer in Korea: a case-control study. *Int. J. Cancer J. Int. Cancer* *97*, 531–535.
- Kim, J., Kim, N., Park, J.H., Chang, H., Kim, J.Y., Lee, D.H., Kim, J.M., Kim, J.S., and Jung, H.C. (2013). The Effect of *Helicobacter pylori* on Epidermal Growth Factor Receptor-Induced Signal Transduction and the Preventive Effect of Celecoxib in Gastric Cancer Cells. *Gut Liver* *7*, 552–559.
- Kim, J.-H., Choi, Y.-K., Kwon, H.-J., Yang, H.-K., Choi, J.-H., and Kim, D.-Y. (2004). Downregulation of gelsolin and retinoic acid receptor beta expression in gastric cancer tissues through histone deacetylase 1. *J. Gastroenterol. Hepatol.* *19*, 218–224.
- Kim, M.P., Fleming, J.B., Wang, H., Abbruzzese, J.L., Choi, W., Kopetz, S., McConkey, D.J., Evans, D.B., and Gallick, G.E. (2011). ALDH activity selectively defines an enhanced tumor-initiating cell population relative to CD133 expression in human pancreatic adenocarcinoma. *PLoS One* *6*, e20636.
- Kim, M.S., Kim, S.S., Ahn, C.H., Yoo, N.J., and Lee, S.H. (2009). Frameshift mutations of Wnt pathway genes *AXIN2* and *TCF7L2* in gastric carcinomas with high microsatellite instability. *Hum. Pathol.* *40*, 58–64.
- Kitareewan, S., Blumen, S., Sekula, D., Bissonnette, R.P., Lamph, W.W., Cui, Q., Gallagher, R., and Dmitrovsky, E. (2008). *G0S2* is an all-trans-retinoic acid target gene. *Int. J. Oncol.* *33*, 397–404.
- Knights, V., and Cook, S.J. (2010). De-regulated FGF receptors as therapeutic targets in cancer. *Pharmacol. Ther.* *125*, 105–117.
- Korkola, J.E., Houldsworth, J., Chadalavada, R.S.V., Olshen, A.B., Dobrzynski, D., Reuter, V.E., Bosl, G.J., and Chaganti, R.S.K. (2006). Down-regulation of stem cell genes, including those in a 200-kb gene cluster at 12p13.31, is associated with in vivo differentiation of human male germ cell tumors. *Cancer Res.* *66*, 820–827.
- Kryczek, I., Liu, S., Roh, M., Vatan, L., Szeliga, W., Wei, S., Banerjee, M., Mao, Y., Kotarski, J., Wicha, M.S., et al. (201c). Expression of aldehyde dehydrogenase and CD133 defines ovarian cancer stem cells. *Int. J. Cancer J. Int. Cancer* *130*, 29–39.
- Kunath, T., Saba-El-Leil, M.K., Almousaillekh, M., Wray, J., Meloche, S., and Smith, A. (2007). FGF stimulation of the Erk1/2 signalling cascade triggers transition of pluripotent embryonic stem cells from self-renewal to lineage commitment. *Dev. Camb. Engl.* *134*, 2895–2902.
- Kuncová, J., Kostrouch, Z., Viale, M., Revoltella, R., and Mandys, V. (2005). Expression of CD44v6 correlates with cell proliferation and cellular atypia in urothelial carcinoma cell lines 5637 and HT1197. *Folia Biol. (Praha)* *51*, 3–11.
- Kurayoshi, M., Oue, N., Yamamoto, H., Kishida, M., Inoue, A., Asahara, T., Yasui, W., and Kikuchi,

- A. (2006). Expression of Wnt-5a is correlated with aggressiveness of gastric cancer by stimulating cell migration and invasion. *Cancer Res.* 66, 10439–10448.
- Kusters, J.G., van Vliet, A.H.M., and Kuipers, E.J. (2006). Pathogenesis of *Helicobacter pylori* infection. *Clin. Microbiol. Rev.* 19, 449–490.
- Lacy, B.E., and Rosemore, J. (2001). *Helicobacter pylori*: ulcers and more: the beginning of an era. *J. Nutr.* 131, 2789S – 2793S.
- Lakshman, M., Subramaniam, V., Rubenthiran, U., and Jothy, S. (2004). CD44 promotes resistance to apoptosis in human colon cancer cells. *Exp. Mol. Pathol.* 77, 18–25.
- Lakshman, M., Subramaniam, V., Wong, S., and Jothy, S. (2005). CD44 promotes resistance to apoptosis in murine colonic epithelium. *J. Cell. Physiol.* 203, 583–588.
- Lamouille, S., Xu, J., and Derynck, R. (2014). Molecular mechanisms of epithelial-mesenchymal transition. *Nat. Rev. Mol. Cell Biol.* 15, 178–196.
- Larsson, S.C., Bergkvist, L., Näslund, I., Rutegård, J., and Wolk, A. (2007). Vitamin A, retinol, and carotenoids and the risk of gastric cancer: a prospective cohort study. *Am. J. Clin. Nutr.* 85, 497–503.
- Larue, L., and Bellacosa, A. (2005). Epithelial-mesenchymal transition in development and cancer: role of phosphatidylinositol 3' kinase/AKT pathways. *Oncogene* 24, 7443–7454.
- Lau, W.M., Teng, E., Chong, H.S., Lopez, K.A.P., Tay, A.Y.L., Salto-Tellez, M., Shabbir, A., So, J.B.Y., and Chan, S.L. (2014). CD44v8-10 is a cancer-specific marker for gastric cancer stem cells. *Cancer Res.* 74, 2630–2641.
- LAUREN, P. (1965). THE TWO HISTOLOGICAL MAIN TYPES OF GASTRIC CARCINOMA: DIFFUSE AND SO-CALLED INTESTINAL-TYPE CARCINOMA. AN ATTEMPT AT A HISTO-CLINICAL CLASSIFICATION. *Acta Pathol. Microbiol. Scand.* 64, 31–49.
- Lee, E.R., and Leblond, C.P. (1985). Dynamic histology of the antral epithelium in the mouse stomach: IV. Ultrastructure and renewal of gland cells. *Am. J. Anat.* 172, 241–259.
- Leroy, P., Krust, A., Zelent, A., Mendelsohn, C., Garnier, J.M., Kastner, P., Dierich, A., and Chambon, P. (1991). Multiple isoforms of the mouse retinoic acid receptor alpha are generated by alternative splicing and differential induction by retinoic acid. *EMBO J.* 10, 59–69.
- Leung, E.L.-H., Fiscus, R.R., Tung, J.W., Tin, V.P.-C., Cheng, L.C., Sihoe, A.D.-L., Fink, L.M., Ma, Y., and Wong, M.P. (2010). Non-small cell lung cancer cells expressing CD44 are enriched for stem cell-like properties. *PLoS One* 5, e14062.
- Levin, T.G., Powell, A.E., Davies, P.S., Silk, A.D., Dismuke, A.D., Anderson, E.C., Swain, J.R., and Wong, M.H. (2010). Characterization of the intestinal cancer stem cell marker CD166 in the human and mouse gastrointestinal tract. *Gastroenterology* 139, 2072–2082.e5.
- Li, C., Heidt, D.G., Dalerba, P., Burant, C.F., Zhang, L., Adsay, V., Wicha, M., Clarke, M.F., and Simeone, D.M. (2007). Identification of pancreatic cancer stem cells. *Cancer Res.* 67, 1030–1037.
- Li, G.-G., Li, L., Li, C., Ye, L.-Y., Li, X.-W., Liu, D.-R., Bao, Q., Zheng, Y.-X., Xiang, D.-P., Chen, L., et al. (2013). Influence of up-regulation of Notch ligand DLL4 on biological behaviors of human gastric cancer cells. *World J. Gastroenterol.* WJG 19, 4486–4494.
- Li, M., Chiba, H., Warot, X., Messaddeq, N., Gérard, C., Chambon, P., and Metzger, D. (2001). RXR-alpha ablation in skin keratinocytes results in alopecia and epidermal alterations. *Dev.*

Camb. Engl. 128, 675–688.

- Lidén, M., and Eriksson, U. (2006). Understanding retinol metabolism: structure and function of retinol dehydrogenases. *J. Biol. Chem.* 281, 13001–13004.
- Lim, Y.C., Kang, H.J., Kim, Y.S., and Choi, E.C. (2012). All-trans-retinoic acid inhibits growth of head and neck cancer stem cells by suppression of Wnt/ β -catenin pathway. *Eur. J. Cancer Oxf. Engl.* 1990 48, 3310–3318.
- Lin, S.W., Chen, J.C., Hsu, L.C., Hsieh, C.L., and Yoshida, A. (1996). Human gamma-aminobutyraldehyde dehydrogenase (ALDH9): cDNA sequence, genomic organization, polymorphism, chromosomal localization, and tissue expression. *Genomics* 34, 376–380.
- Lin, W.-M., Karsten, U., Goletz, S., Cheng, R.-C., and Cao, Y. (2010). Co-expression of CD173 (H2) and CD174 (Lewis Y) with CD44 suggests that fucosylated histo-blood group antigens are markers of breast cancer-initiating cells. *Virchows Arch. Int. J. Pathol.* 456, 403–409.
- Lindahl, T., Landberg, G., Ahlgren, J., Nordgren, H., Norberg, T., Klaar, S., Holmberg, L., and Bergh, J. (2004a). Overexpression of cyclin E protein is associated with specific mutation types in the p53 gene and poor survival in human breast cancer. *Carcinogenesis* 25, 375–380.
- Lindahl, T., Landberg, G., Ahlgren, J., Nordgren, H., Norberg, T., Klaar, S., Holmberg, L., and Bergh, J. (2004b). Overexpression of cyclin E protein is associated with specific mutation types in the p53 gene and poor survival in human breast cancer. *Carcinogenesis* 25, 375–380.
- Liu, J., Ma, L., Xu, J., Liu, C., Zhang, J., Liu, J., Chen, R., and Zhou, Y. (2013). Spheroid body-forming cells in the human gastric cancer cell line MKN-45 possess cancer stem cell properties. *Int. J. Oncol.* 42, 453–459.
- Liu, X., Zheng, H., and Qu, C.-K. (2012). Protein tyrosine phosphatase Shp2 (Ptpn11) plays an important role in maintenance of chromosome stability. *Cancer Res.* 72, 5296–5306.
- Liu, Y.-J., Yan, P.-S., Li, J., and Jia, J.-F. (2005). Expression and significance of CD44s, CD44v6, and nm23 mRNA in human cancer. *World J. Gastroenterol. WJG* 11, 6601–6606.
- Lobo, N.A., Shimono, Y., Qian, D., and Clarke, M.F. (2007). The biology of cancer stem cells. *Annu. Rev. Cell Dev. Biol.* 23, 675–699.
- De Luca, L.M. (1991). Retinoids and their receptors in differentiation, embryogenesis, and neoplasia. *FASEB J. Off. Publ. Fed. Am. Soc. Exp. Biol.* 5, 2924–2933.
- Luo, Y., Dallaglio, K., Chen, Y., Robinson, W.A., Robinson, S.E., McCarter, M.D., Wang, J., Gonzalez, R., Thompson, D.C., Norris, D.A., et al. (2012). ALDH1A isozymes are markers of human melanoma stem cells and potential therapeutic targets. *Stem Cells Dayt. Ohio* 30, 2100–2113.
- Luu, H.H., Zhang, R., Haydon, R.C., Rayburn, E., Kang, Q., Si, W., Park, J.K., Wang, H., Peng, Y., Jiang, W., et al. (2004). Wnt/beta-catenin signaling pathway as a novel cancer drug target. *Curr. Cancer Drug Targets* 4, 653–671.
- Ma, I., and Allan, A.L. (2011). The role of human aldehyde dehydrogenase in normal and cancer stem cells. *Stem Cell Rev.* 7, 292–306.
- Ma, J., Chen, J., Cai, S., Chen, C., Yang, D., Wu, H., He, Y., and Zhan, W. (2012). [Clinicopathologic features and prognostic analyses of Borrmann type IV gastric cancer]. *Zhonghua Yi Xue Za Zhi* 92, 2534–2537.
- Ma, S., Chan, K.-W., Hu, L., Lee, T.K.-W., Wo, J.Y.-H., Ng, I.O.-L., Zheng, B.-J., and Guan, X.-Y.

- (2007). Identification and characterization of tumorigenic liver cancer stem/progenitor cells. *Gastroenterology* *132*, 2542–2556.
- Ma, S., Chan, K.W., Lee, T.K.-W., Tang, K.H., Wo, J.Y.-H., Zheng, B.-J., and Guan, X.-Y. (2008). Aldehyde dehydrogenase discriminates the CD133 liver cancer stem cell populations. *Mol. Cancer Res. MCR* *6*, 1146–1153.
- Macdonald, J.S., Smalley, S.R., Benedetti, J., Hundahl, S.A., Estes, N.C., Stemmermann, G.N., Haller, D.G., Ajani, J.A., Gunderson, L.L., Jessup, J.M., et al. (2001). Chemoradiotherapy after surgery compared with surgery alone for adenocarcinoma of the stomach or gastroesophageal junction. *N. Engl. J. Med.* *345*, 725–730.
- MacLachlan, T.K., Sang, N., and Giordano, A. (1995). Cyclins, cyclin-dependent kinases and cdk inhibitors: implications in cell cycle control and cancer. *Crit. Rev. Eukaryot. Gene Expr.* *5*, 127–156.
- Maeda, S., Ogura, K., Yoshida, H., Kanai, F., Ikenoue, T., Kato, N., Shiratori, Y., and Omata, M. (1998). Major virulence factors, VacA and CagA, are commonly positive in *Helicobacter pylori* isolates in Japan. *Gut* *42*, 338–343.
- Maga, G., and Hubscher, U. (2003). Proliferating cell nuclear antigen (PCNA): a dancer with many partners. *J. Cell Sci.* *116*, 3051–3060.
- Magee, J.A., Piskounova, E., and Morrison, S.J. (2012). Cancer stem cells: impact, heterogeneity, and uncertainty. *Cancer Cell* *21*, 283–296.
- Mammano, E., Belluco, C., Sciro, M., Mencarelli, R., Agostini, M., Michelotto, M., Marchet, A., and Nitti, D. (2006). Epidermal growth factor receptor (EGFR): mutational and protein expression analysis in gastric cancer. *Anticancer Res.* *26*, 3547–3550.
- Mani, S.A., Guo, W., Liao, M.-J., Eaton, E.N., Ayyanan, A., Zhou, A.Y., Brooks, M., Reinhard, F., Zhang, C.C., Shipitsin, M., et al. (2008). The epithelial-mesenchymal transition generates cells with properties of stem cells. *Cell* *133*, 704–715.
- Mao, J., Fan, S., Ma, W., Fan, P., Wang, B., Zhang, J., Wang, H., Tang, B., Zhang, Q., Yu, X., et al. (2014). Roles of Wnt/ β -catenin signaling in the gastric cancer stem cells proliferation and salinomycin treatment. *Cell Death Dis.* *5*, e1039.
- Marangoni, E., Lecomte, N., Durand, L., de Pinieux, G., Decaudin, D., Chomienne, C., Smadja-Joffe, F., and Poupon, M.-F. (2009). CD44 targeting reduces tumour growth and prevents post-chemotherapy relapse of human breast cancers xenografts. *Br. J. Cancer* *100*, 918–922.
- Marcato, P., Dean, C.A., Pan, D., Araslanova, R., Gillis, M., Joshi, M., Helyer, L., Pan, L., Leidal, A., Gujar, S., et al. (2011). Aldehyde dehydrogenase activity of breast cancer stem cells is primarily due to isoform ALDH1A3 and its expression is predictive of metastasis. *Stem Cells Dayt. Ohio* *29*, 32–45.
- Marcato, P., Dean, C.A., Liu, R.-Z., Coyle, K.M., Bydoun, M., Wallace, M., Clements, D., Turner, C., Mathenge, E.G., Gujar, S.A., et al. (2014). Aldehyde dehydrogenase 1A3 influences breast cancer progression via differential retinoic acid signaling. *Mol. Oncol.*
- Martras, S., Alvarez, R., Martínez, S.E., Torres, D., Gallego, O., Duester, G., Farrés, J., de Lera, A.R., and Parés, X. (2004). The specificity of alcohol dehydrogenase with cis-retinoids. Activity with 11-cis-retinol and localization in retina. *Eur. J. Biochem. FEBS* *271*, 1660–1670.
- Masiá, S., Alvarez, S., de Lera, A.R., and Baretino, D. (2007). Rapid, nongenomic actions of retinoic acid on phosphatidylinositol-3-kinase signaling pathway mediated by the retinoic acid

receptor. *Mol. Endocrinol. Baltim. Md* 21, 2391–2402.

- Matsumoto, K., Arao, T., Hamaguchi, T., Shimada, Y., Kato, K., Oda, I., Taniguchi, H., Koizumi, F., Yanagihara, K., Sasaki, H., et al. (2012). FGFR2 gene amplification and clinicopathological features in gastric cancer. *Br. J. Cancer* 106, 727–732.
- Matsuoka, J., Yashiro, M., Doi, Y., Fuyuhiko, Y., Kato, Y., Shinto, O., Noda, S., Kashiwagi, S., Aomatsu, N., Hirakawa, T., et al. (2013). Hypoxia stimulates the EMT of gastric cancer cells through autocrine TGF β signaling. *PLoS One* 8, e62310.
- Matthay, K.K., Reynolds, C.P., Seeger, R.C., Shimada, H., Adkins, E.S., Haas-Kogan, D., Gerbing, R.B., London, W.B., and Villablanca, J.G. (2009). Long-term results for children with high-risk neuroblastoma treated on a randomized trial of myeloablative therapy followed by 13-cis-retinoic acid: a children's oncology group study. *J. Clin. Oncol. Off. J. Am. Soc. Clin. Oncol.* 27, 1007–1013.
- Matysiak-Budnik, T., and Mégraud, F. (2006). Helicobacter pylori infection and gastric cancer. *Eur. J. Cancer Oxf. Engl.* 1990 42, 708–716.
- Mégraud, F., and Broutet, N. (2000). [Epidemiology, acquisition and transmission of Helicobacter pylori]. *Rev. Prat.* 50, 1414–1417.
- Mégraud, F., Brassens-Rabbé, M.P., Denis, F., Belbouri, A., and Hoa, D.Q. (1989). Seroepidemiology of Campylobacter pylori infection in various populations. *J. Clin. Microbiol.* 27, 1870–1873.
- Merten, O.W. (2002). Development of serum-free media for cell growth and production of viruses/viral vaccines--safety issues of animal products used in serum-free media. *Dev. Biol.* 111, 233–257.
- Mic, F.A., Haselbeck, R.J., Cuenca, A.E., and Duester, G. (2002). Novel retinoic acid generating activities in the neural tube and heart identified by conditional rescue of Raldh2 null mutant mice. *Dev. Camb. Engl.* 129, 2271–2282.
- Miyake, H., Eto, H., Arakawa, S., Kamidono, S., and Hara, I. (2002). Over expression of CD44V8-10 in urinary exfoliated cells as an independent prognostic predictor in patients with urothelial cancer. *J. Urol.* 167, 1282–1287.
- Modiano, M.R., Dalton, W.S., Lippman, S.M., Joffe, L., Booth, A.R., and Meyskens, F.L. (1990). Phase II study of fenretinide (N-[4-hydroxyphenyl]retinamide) in advanced breast cancer and melanoma. *Invest. New Drugs* 8, 317–319.
- Mohamed, M.S., Chen, Y., and Yao, C.-L. (2014). A serum-free medium developed for in vitro expansion of murine intestinal stem cells. *Biotechnol. J.* 9, 962–970.
- Monzani, E., Facchetti, F., Galmozzi, E., Corsini, E., Benetti, A., Cavazzin, C., Gritti, A., Piccinini, A., Porro, D., Santinami, M., et al. (2007). Melanoma contains CD133 and ABCG2 positive cells with enhanced tumorigenic potential. *Eur. J. Cancer Oxf. Engl.* 1990 43, 935–946.
- Moreb, J., Schweder, M., Suresh, A., and Zucali, J.R. (1996). Overexpression of the human aldehyde dehydrogenase class I results in increased resistance to 4-hydroperoxycyclophosphamide. *Cancer Gene Ther.* 3, 24–30.
- Moreb, J.S., Ucar, D., Han, S., Amory, J.K., Goldstein, A.S., Ostmark, B., and Chang, L.-J. (2012). The enzymatic activity of human aldehyde dehydrogenases 1A2 and 2 (ALDH1A2 and ALDH2) is detected by Aldefluor, inhibited by diethylaminobenzaldehyde and has significant effects on cell proliferation and drug resistance. *Chem. Biol. Interact.* 195, 52–60.

- Moutinho, C., Mateus, A.R., Milanezi, F., Carneiro, F., Seruca, R., and Suriano, G. (2008). Epidermal growth factor receptor structural alterations in gastric cancer. *BMC Cancer* 8, 10.
- Moy, K.A., Fan, Y., Wang, R., Gao, Y.-T., Yu, M.C., and Yuan, J.-M. (2010). Alcohol and tobacco use in relation to gastric cancer: a prospective study of men in Shanghai, China. *Cancer Epidemiol. Biomark. Prev. Publ. Am. Assoc. Cancer Res. Cosponsored Am. Soc. Prev. Oncol.* 19, 2287–2297.
- Mulholland, D.J., Xin, L., Morim, A., Lawson, D., Witte, O., and Wu, H. (2009). Lin-Sca-1+CD49high stem/progenitors are tumor-initiating cells in the Pten-null prostate cancer model. *Cancer Res.* 69, 8555–8562.
- Muramaki, M., Miyake, H., Kamidono, S., and Hara, I. (2004). Over expression of CD44V8-10 in human bladder cancer cells decreases their interaction with hyaluronic acid and potentiates their malignant progression. *J. Urol.* 171, 426–430.
- Nakatake, Y., Fukui, N., Iwamatsu, Y., Masui, S., Takahashi, K., Yagi, R., Yagi, K., Miyazaki, J.-I., Matoba, R., Ko, M.S.H., et al. (2006). Klf4 cooperates with Oct3/4 and Sox2 to activate the Lefty1 core promoter in embryonic stem cells. *Mol. Cell. Biol.* 26, 7772–7782.
- Naor, D., Sionov, R.V., and Ish-Shalom, D. (1997). CD44: structure, function, and association with the malignant process. *Adv. Cancer Res.* 71, 241–319.
- Naor, D., Nedvetzki, S., Golan, I., Melnik, L., and Faitelson, Y. (2002). CD44 in cancer. *Crit. Rev. Clin. Lab. Sci.* 39, 527–579.
- Napoli, J.L. (1996). Retinoic acid biosynthesis and metabolism. *FASEB J. Off. Publ. Fed. Am. Soc. Exp. Biol.* 10, 993–1001.
- Nashimoto, A., Akazawa, K., Isobe, Y., Miyashiro, I., Katai, H., Kodera, Y., Tsujitani, S., Seto, Y., Furukawa, H., Oda, I., et al. (2013). Gastric cancer treated in 2002 in Japan: 2009 annual report of the JGCA nationwide registry. *Gastric Cancer Off. J. Int. Gastric Cancer Assoc. Jpn. Gastric Cancer Assoc.* 16, 1–27.
- Nguyen, L.V., Vanner, R., Dirks, P., and Eaves, C.J. (2012). Cancer stem cells: an evolving concept. *Nat. Rev. Cancer* 12, 133–143.
- Nilsson, I., and Hoffmann, I. (2000). Cell cycle regulation by the Cdc25 phosphatase family. *Prog. Cell Cycle Res.* 4, 107–114.
- Noda, S., Soejima, K., and Inokuchi, K. (1980). Clinicopathological analysis of the intestinal type and diffuse type of gastric carcinoma. *Jpn. J. Surg.* 10, 277–283.
- O'Brien, C.A., Pollett, A., Gallinger, S., and Dick, J.E. (2007). A human colon cancer cell capable of initiating tumour growth in immunodeficient mice. *Nature* 445, 106–110.
- Occhialini, A., Marais, A., Urdaci, M., Sierra, R., Muñoz, N., Covacci, A., and Mégraud, F. (2001). Composition and gene expression of the cag pathogenicity island in *Helicobacter pylori* strains isolated from gastric carcinoma and gastritis patients in Costa Rica. *Infect. Immun.* 69, 1902–1908.
- Oda, T., Kanai, Y., Oyama, T., Yoshiura, K., Shimoyama, Y., Birchmeier, W., Sugimura, T., and Hirohashi, S. (1994). E-cadherin gene mutations in human gastric carcinoma cell lines. *Proc. Natl. Acad. Sci. U. S. A.* 91, 1858–1862.
- Ogaki, S., Shiraki, N., Kume, K., and Kume, S. (2013). Wnt and Notch signals guide embryonic stem cell differentiation into the intestinal lineages. *Stem Cells Dayt. Ohio* 31, 1086–1096.

- Ogden, A.T., Waziri, A.E., Lochhead, R.A., Fusco, D., Lopez, K., Ellis, J.A., Kang, J., Assanah, M., McKhann, G.M., Sisti, M.B., et al. (2008). Identification of A2B5+CD133- tumor-initiating cells in adult human gliomas. *Neurosurgery* 62, 505–514; discussion 514–515.
- Ohata, H., Kitauchi, S., Yoshimura, N., Mugitani, K., Iwane, M., Nakamura, H., Yoshikawa, A., Yanaoka, K., Arii, K., Tamai, H., et al. (2004). Progression of chronic atrophic gastritis associated with *Helicobacter pylori* infection increases risk of gastric cancer. *Int. J. Cancer J. Int. Cancer* 109, 138–143.
- Ohtsuka, T., Ishibashi, M., Gradwohl, G., Nakanishi, S., Guillemot, F., and Kageyama, R. (1999). *Hes1* and *Hes5* as notch effectors in mammalian neuronal differentiation. *EMBO J.* 18, 2196–2207.
- Okayama, H., Kumamoto, K., Saitou, K., Hayase, S., Kofunato, Y., Sato, Y., Miyamoto, K., Nakamura, I., Ohki, S., Sekikawa, K., et al. (2009). CD44v6, MMP-7 and nuclear Cdx2 are significant biomarkers for prediction of lymph node metastasis in primary gastric cancer. *Oncol. Rep.* 22, 745–755.
- Oliveira, C., Seruca, R., and Carneiro, F. (2006). Genetics, pathology, and clinics of familial gastric cancer. *Int. J. Surg. Pathol.* 14, 21–33.
- Osei-Sarfo, K., and Gudas, L.J. (2014). Retinoic acid suppresses the canonical Wnt signaling pathway in embryonic stem cells and activates the noncanonical Wnt signaling pathway. *Stem Cells Dayt. Ohio* 32, 2061–2071.
- Oue, N., Motoshita, J., Yokozaki, H., Hayashi, K., Tahara, E., Taniyama, K., Matsusaki, K., and Yasui, W. (2002). Distinct promoter hypermethylation of p16INK4a, CDH1, and RAR-beta in intestinal, diffuse-adherent, and diffuse-scattered type gastric carcinomas. *J. Pathol.* 198, 55–59.
- Oue, N., Oshimo, Y., Nakayama, H., Ito, R., Yoshida, K., Matsusaki, K., and Yasui, W. (2003). DNA methylation of multiple genes in gastric carcinoma: association with histological type and CpG island methylator phenotype. *Cancer Sci.* 94, 901–905.
- Palli, D., Russo, A., and Decarli, A. (2001). Dietary patterns, nutrient intake and gastric cancer in a high-risk area of Italy. *Cancer Causes Control CCC* 12, 163–172.
- Pan, J., Kao, Y.-L., Joshi, S., Jeetendran, S., Dipette, D., and Singh, U.S. (2005). Activation of Rac1 by phosphatidylinositol 3-kinase in vivo: role in activation of mitogen-activated protein kinase (MAPK) pathways and retinoic acid-induced neuronal differentiation of SH-SY5Y cells. *J. Neurochem.* 93, 571–583.
- Park, I., Qian, D., Kiel, M., Becker, M.W., Pihalja, M., Weissman, I.L., Morrison, S.J., and Clarke, M.F. (2003). *Bmi-1* is required for maintenance of adult self-renewing haematopoietic stem cells. *Nature* 423, 302–305.
- Patrawala, L., Calhoun-Davis, T., Schneider-Broussard, R., and Tang, D.G. (2007). Hierarchical organization of prostate cancer cells in xenograft tumors: the CD44+alpha2beta1+ cell population is enriched in tumor-initiating cells. *Cancer Res.* 67, 6796–6805.
- Peinado, H., Olmeda, D., and Cano, A. (2007). Snail, Zeb and bHLH factors in tumour progression: an alliance against the epithelial phenotype? *Nat. Rev. Cancer* 7, 415–428.
- Peng, S., Kuang, Z., Sheng, C., Zhang, Y., Xu, H., and Cheng, Q. (2010). Association of microRNA-196a-2 gene polymorphism with gastric cancer risk in a Chinese population. *Dig. Dis. Sci.* 55, 2288–2293.

- Perez-Perez, G.I., Garza-Gonzalez, E., Portal, C., and Olivares, A.Z. (2005). Role of cytokine polymorphisms in the risk of distal gastric cancer development. *Cancer Epidemiol. Biomark. Prev. Publ. Am. Assoc. Cancer Res. Cosponsored Am. Soc. Prev. Oncol.* *14*, 1869–1873.
- Perissi, V., Jepsen, K., Glass, C.K., and Rosenfeld, M.G. (2010). Deconstructing repression: evolving models of co-repressor action. *Nat. Rev. Genet.* *11*, 109–123.
- Pharoah, P.D., Guilford, P., Caldas, C., and International Gastric Cancer Linkage Consortium (2001). Incidence of gastric cancer and breast cancer in CDH1 (E-cadherin) mutation carriers from hereditary diffuse gastric cancer families. *Gastroenterology* *121*, 1348–1353.
- Piazuelo, M.B., Epplein, M., and Correa, P. (2010). Gastric cancer: an infectious disease. *Infect. Dis. Clin. North Am.* *24*, 853–869, vii.
- Piazzi, G., Fini, L., Selgrad, M., Garcia, M., Daoud, Y., Wex, T., Malfertheiner, P., Gasbarrini, A., Romano, M., Meyer, R.L., et al. (2011). Epigenetic regulation of Delta-Like1 controls Notch1 activation in gastric cancer. *Oncotarget* *2*, 1291–1301.
- Polakis, P. (2000). Wnt signaling and cancer. *Genes Dev.* *14*, 1837–1851.
- Qiao, X.T., Ziel, J.W., McKimpton, W., Madison, B.B., Todisco, A., Merchant, J.L., Samuelson, L.C., and Gumucio, D.L. (2007). Prospective identification of a multilineage progenitor in murine stomach epithelium. *Gastroenterology* *133*, 1989–1998.
- Quintana, E., Shackleton, M., Sabel, M.S., Fullen, D.R., Johnson, T.M., and Morrison, S.J. (2008). Efficient tumour formation by single human melanoma cells. *Nature* *456*, 593–598.
- Rahadiani, N., Ikeda, J., Mamat, S., Matsuzaki, S., Ueda, Y., Umehara, R., Tian, T., Wang, Y., Enomoto, T., Kimura, T., et al. (2011). Expression of aldehyde dehydrogenase 1 (ALDH1) in endometrioid adenocarcinoma and its clinical implications. *Cancer Sci.* *102*, 903–908.
- Rattner, A., Hsieh, J.C., Smallwood, P.M., Gilbert, D.J., Copeland, N.G., Jenkins, N.A., and Nathans, J. (1997). A family of secreted proteins contains homology to the cysteine-rich ligand-binding domain of frizzled receptors. *Proc. Natl. Acad. Sci. U. S. A.* *94*, 2859–2863.
- Ren, C., Qiu, M., Wang, D., Luo, H., Zhang, D., Wang, Z., Wang, F., Li, Y., Zhou, Z., and Xu, R. (2012). Prognostic effects of 25-hydroxyvitamin D levels in gastric cancer. *J. Transl. Med.* *10*, 16.
- Reya, T., and Clevers, H. (2005). Wnt signalling in stem cells and cancer. *Nature* *434*, 843–850.
- Reya, T., Morrison, S.J., Clarke, M.F., and Weissman, I.L. (2001). Stem cells, cancer, and cancer stem cells. *Nature* *414*, 105–111.
- Ricardo, S., Vieira, A.F., Gerhard, R., Leitão, D., Pinto, R., Cameselle-Teijeiro, J.F., Milanezi, F., Schmitt, F., and Paredes, J. (2011a). Breast cancer stem cell markers CD44, CD24 and ALDH1: expression distribution within intrinsic molecular subtype. *J. Clin. Pathol.* *64*, 937–946.
- Ricardo, S., Vieira, A.F., Gerhard, R., Leitão, D., Pinto, R., Cameselle-Teijeiro, J.F., Milanezi, F., Schmitt, F., and Paredes, J. (2011b). Breast cancer stem cell markers CD44, CD24 and ALDH1: expression distribution within intrinsic molecular subtype. *J. Clin. Pathol.* *64*, 937–946.
- Rieder, G., Fischer, W., and Haas, R. (2005). Interaction of *Helicobacter pylori* with host cells: function of secreted and translocated molecules. *Curr. Opin. Microbiol.* *8*, 67–73.
- Rizzo, S., Hersey, J.M., Mellor, P., Dai, W., Santos-Silva, A., Liber, D., Luk, L., Titley, I., Carden,

- C.P., Box, G., et al. (2011). Ovarian cancer stem cell-like side populations are enriched following chemotherapy and overexpress EZH2. *Mol. Cancer Ther.* *10*, 325–335.
- Roberts, M.R., Hendrickson, A., McGuire, C.R., and Reh, T.A. (2005). Retinoid X receptor (gamma) is necessary to establish the S-opsin gradient in cone photoreceptors of the developing mouse retina. *Invest. Ophthalmol. Vis. Sci.* *46*, 2897–2904.
- Rochette-Egly, C., and Germain, P. (2009). Dynamic and combinatorial control of gene expression by nuclear retinoic acid receptors (RARs). *Nucl. Recept. Signal.* *7*, e005.
- Rowitch, D.H., S-Jacques, B., Lee, S.M., Flax, J.D., Snyder, E.Y., and McMahon, A.P. (1999). Sonic hedgehog regulates proliferation and inhibits differentiation of CNS precursor cells. *J. Neurosci. Off. J. Soc. Neurosci.* *19*, 8954–8965.
- Ryu, H.S., Park, D.J., Kim, H.H., Kim, W.H., and Lee, H.S. (2012). Combination of epithelial-mesenchymal transition and cancer stem cell-like phenotypes has independent prognostic value in gastric cancer. *Hum. Pathol.* *43*, 520–528.
- Sakai, Y., Meno, C., Fujii, H., Nishino, J., Shiratori, H., Saijoh, Y., Rossant, J., and Hamada, H. (2001). The retinoic acid-inactivating enzyme CYP26 is essential for establishing an uneven distribution of retinoic acid along the antero-posterior axis within the mouse embryo. *Genes Dev.* *15*, 213–225.
- Sakakura, C., Hagiwara, A., Tsujimoto, H., Ozaki, K., Sakakibara, T., Oyama, T., Ogaki, M., and Takahashi, T. (1994). Inhibition of gastric cancer cell proliferation by antisense oligonucleotides targeting the messenger RNA encoding proliferating cell nuclear antigen. *Br. J. Cancer* *70*, 1060–1066.
- Sangiorgi, E., and Capecchi, M.R. (2008). *Bmi1* is expressed in vivo in intestinal stem cells. *Nat. Genet.* *40*, 915–920.
- Savory, J.G.A., Edey, C., Hess, B., Mears, A.J., and Lohnes, D. (2014). Identification of novel retinoic acid target genes. *Dev. Biol.* *395*, 199–208.
- Schaller, J., Glander, H.J., and Dethloff, J. (1993). Evidence of beta 1 integrins and fibronectin on spermatogenic cells in human testis. *Hum. Reprod. Oxf. Engl.* *8*, 1873–1878.
- Schatton, T., and Frank, M.H. (2010). The in vitro spheroid melanoma cell culture assay: cues on tumor initiation? *J. Invest. Dermatol.* *130*, 1769–1771.
- Schenk, T., Stengel, S., and Zelent, A. (2014). Unlocking the potential of retinoic acid in anticancer therapy. *Br. J. Cancer* *111*, 2039–2045.
- Schmitz, B., Radbruch, A., Kümmel, T., Wickenhauser, C., Korb, H., Hansmann, M.L., Thiele, J., and Fischer, R. (1994). Magnetic activated cell sorting (MACS)--a new immunomagnetic method for megakaryocytic cell isolation: comparison of different separation techniques. *Eur. J. Haematol.* *52*, 267–275.
- Shenoy, A., Butterworth, E., and Huang, E.H. (2012). ALDH as a marker for enriching tumorigenic human colonic stem cells. *Methods Mol. Biol. Clifton NJ* *916*, 373–385.
- Sheridan, C., Kishimoto, H., Fuchs, R.K., Mehrotra, S., Bhat-Nakshatri, P., Turner, C.H., Goulet, R., Badve, S., and Nakshatri, H. (2006). CD44+/CD24- breast cancer cells exhibit enhanced invasive properties: an early step necessary for metastasis. *Breast Cancer Res. BCR* *8*, R59.
- Shi, C., Tian, R., Wang, M., Wang, X., Jiang, J., Zhang, Z., Li, X., He, Z., Gong, W., and Qin, R. (2010). CD44+ CD133+ population exhibits cancer stem cell-like characteristics in human

gallbladder carcinoma. *Cancer Biol. Ther.* *10*, 1182–1190.

- Shibuya, A., Takeuchi, A., Shibata, H., Saigenji, K., and Yoshida, A. (1994). Immunohistochemical study of hepatocellular carcinoma-specific aldehyde dehydrogenase. *Alcohol Alcohol. Oxf. Oxf. Suppl.* *29*, 119–123.
- Shmelkov, S.V., Butler, J.M., Hooper, A.T., Hormigo, A., Kushner, J., Milde, T., St Clair, R., Baljevic, M., White, I., Jin, D.K., et al. (2008). CD133 expression is not restricted to stem cells, and both CD133+ and CD133- metastatic colon cancer cells initiate tumors. *J. Clin. Invest.* *118*, 2111–2120.
- Ben-Shushan, E., Feldman, E., and Reubinoff, B.E. (2015). Notch signaling regulates motor neuron differentiation of human embryonic stem cells. *Stem Cells Dayt. Ohio* *33*, 403–415.
- Shutoh, M., Oue, N., Aung, P.P., Noguchi, T., Kuraoka, K., Nakayama, H., Kawahara, K., and Yasui, W. (2005). DNA methylation of genes linked with retinoid signaling in gastric carcinoma: expression of the retinoid acid receptor beta, cellular retinol-binding protein 1, and tazarotene-induced gene 1 genes is associated with DNA methylation. *Cancer* *104*, 1609–1619.
- Shyu, R.Y., Jiang, S.Y., Huang, S.L., Chang, T.C., Wu, K.L., Roffler, S.R., and Yeh, M.Y. (1995). Growth regulation by all-trans-retinoic acid and retinoic acid receptor messenger ribonucleic acids expression in gastric cancer cells. *Eur. J. Cancer Oxf. Engl.* *1990* *31A*, 237–243.
- Shyu, R.-Y., Huang, S.-L., and Jiang, S.-Y. (2003). Retinoic acid increases expression of the calcium-binding protein S100P in human gastric cancer cells. *J. Biomed. Sci.* *10*, 313–319.
- Silva, I.A., Bai, S., McLean, K., Yang, K., Griffith, K., Thomas, D., Ginestier, C., Johnston, C., Kueck, A., Reynolds, R.K., et al. (2011). Aldehyde dehydrogenase in combination with CD133 defines angiogenic ovarian cancer stem cells that portend poor patient survival. *Cancer Res.* *71*, 3991–4001.
- Singh, S.K., Clarke, I.D., Terasaki, M., Bonn, V.E., Hawkins, C., Squire, J., and Dirks, P.B. (2003). Identification of a cancer stem cell in human brain tumors. *Cancer Res.* *63*, 5821–5828.
- Singh, S.K., Hawkins, C., Clarke, I.D., Squire, J.A., Bayani, J., Hide, T., Henkelman, R.M., Cusimano, M.D., and Dirks, P.B. (2004). Identification of human brain tumour initiating cells. *Nature* *432*, 396–401.
- Sipponen, P., and Kimura, K. (1994). Intestinal metaplasia, atrophic gastritis and stomach cancer: trends over time. *Eur. J. Gastroenterol. Hepatol.* *6 Suppl 1*, S79–S83.
- Sirbu, I.O., Gresh, L., Barra, J., and Duester, G. (2005). Shifting boundaries of retinoic acid activity control hindbrain segmental gene expression. *Dev. Camb. Engl.* *132*, 2611–2622.
- Sládek, N.E., Kollander, R., Sreerama, L., and Kiang, D.T. (2002). Cellular levels of aldehyde dehydrogenases (ALDH1A1 and ALDH3A1) as predictors of therapeutic responses to cyclophosphamide-based chemotherapy of breast cancer: a retrospective study. Rational individualization of oxazaphosphorine-based cancer chemotherapeutic regimens. *Cancer Chemother. Pharmacol.* *49*, 309–321.
- Smith, L.M., Nesterova, A., Ryan, M.C., Duniho, S., Jonas, M., Anderson, M., Zabinski, R.F., Sutherland, M.K., Gerber, H.-P., Van Orden, K.L., et al. (2008). CD133/prominin-1 is a potential therapeutic target for antibody-drug conjugates in hepatocellular and gastric cancers. *Br. J. Cancer* *99*, 100–109.
- Sneath, R.J., and Mangham, D.C. (1998). The normal structure and function of CD44 and its role in neoplasia. *Mol. Pathol. MP* *51*, 191–200.

- Son, M.J., Woolard, K., Nam, D.-H., Lee, J., and Fine, H.A. (2009). SSEA-1 is an enrichment marker for tumor-initiating cells in human glioblastoma. *Cell Stem Cell* 4, 440–452.
- Soukka, T., Salmi, M., Joensuu, H., Häkkinen, L., Sointu, P., Koulu, L., Kalimo, K., Klemi, P., Grénman, R., and Jalkanen, S. (1997). Regulation of CD44v6-containing isoforms during proliferation of normal and malignant epithelial cells. *Cancer Res.* 57, 2281–2289.
- Spangrude, G.J., Heimfeld, S., and Weissman, I.L. (1988). Purification and characterization of mouse hematopoietic stem cells. *Science* 241, 58–62.
- Sriuranpong, V., Borges, M.W., Ravi, R.K., Arnold, D.R., Nelkin, B.D., Baylin, S.B., and Ball, D.W. (2001). Notch signaling induces cell cycle arrest in small cell lung cancer cells. *Cancer Res.* 61, 3200–3205.
- Srivastava, D., Singh, R.K., Moxley, M.A., Henzl, M.T., Becker, D.F., and Tanner, J.J. (2012). The three-dimensional structural basis of type II hyperproliferinemia. *J. Mol. Biol.* 420, 176–189.
- Su, Y., Qiu, Q., Zhang, X., Jiang, Z., Leng, Q., Liu, Z., Stass, S.A., and Jiang, F. (2010). Aldehyde dehydrogenase 1 A1-positive cell population is enriched in tumor-initiating cells and associated with progression of bladder cancer. *Cancer Epidemiol. Biomark. Prev. Publ. Am. Assoc. Cancer Res. Cosponsored Am. Soc. Prev. Oncol.* 19, 327–337.
- Subramaniam, V., Vincent, I.R., Gilakjan, M., and Jothy, S. (2007). Suppression of human colon cancer tumors in nude mice by siRNA CD44 gene therapy. *Exp. Mol. Pathol.* 83, 332–340.
- Sugihara, E., and Saya, H. (2013). Complexity of cancer stem cells. *Int. J. Cancer J. Int. Cancer* 132, 1249–1259.
- Sugihara, E., Shimizu, T., Kojima, K., Onishi, N., Kai, K., Ishizawa, J., Nagata, K., Hashimoto, N., Honda, H., Kanno, M., et al. (2012). Ink4a and Arf are crucial factors in the determination of the cell of origin and the therapeutic sensitivity of Myc-induced mouse lymphoid tumor. *Oncogene* 31, 2849–2861.
- Sugimura, R., and Li, L. (2010). Noncanonical Wnt signaling in vertebrate development, stem cells, and diseases. *Birth Defects Res. Part C Embryo Today Rev.* 90, 243–256.
- Sullivan, J.P., Spinola, M., Dodge, M., Raso, M.G., Behrens, C., Gao, B., Schuster, K., Shao, C., Larsen, J.E., Sullivan, L.A., et al. (2010). Aldehyde dehydrogenase activity selects for lung adenocarcinoma stem cells dependent on notch signaling. *Cancer Res.* 70, 9937–9948.
- Sun, Q., Gu, H., Zeng, Y., Xia, Y., Wang, Y., Jing, Y., Yang, L., and Wang, B. (2010). Hsa-mir-27a genetic variant contributes to gastric cancer susceptibility through affecting miR-27a and target gene expression. *Cancer Sci.* 101, 2241–2247.
- Sun, Y., Gao, X., Liu, J., Kong, Q.-Y., Wang, X.-W., Chen, X.-Y., Wang, Q., Cheng, Y.-F., Qu, X.-X., and Li, H. (2011). Differential Notch1 and Notch2 expression and frequent activation of Notch signaling in gastric cancers. *Arch. Pathol. Lab. Med.* 135, 451–458.
- Sung, N.Y., Choi, K.S., Park, E.C., Park, K., Lee, S.Y., Lee, A.K., Choi, I.J., Jung, K.W., Won, Y.J., and Shin, H.R. (2007). Smoking, alcohol and gastric cancer risk in Korean men: the National Health Insurance Corporation Study. *Br. J. Cancer* 97, 700–704.
- Sutton, L.M., Warmuth, M.A., Petros, W.P., and Winer, E.P. (1997). Pharmacokinetics and clinical impact of all-trans retinoic acid in metastatic breast cancer: a phase II trial. *Cancer Chemother. Pharmacol.* 40, 335–341.
- Tabata, T., and Kornberg, T.B. (1994). Hedgehog is a signaling protein with a key role in patterning

Drosophila imaginal discs. *Cell* 76, 89–102.

- Tahara, E. (2002). Histone Acetylation and Retinoic Acid Receptor beta DNA Methylation as Novel Targets for Gastric Cancer Therapy. *Drug News Perspect.* 15, 581–585.
- Takaishi, S., Okumura, T., Tu, S., Wang, S.S.W., Shibata, W., Vigneshwaran, R., Gordon, S.A.K., Shimada, Y., and Wang, T.C. (2009). Identification of gastric cancer stem cells using the cell surface marker CD44. *Stem Cells Dayt. Ohio* 27, 1006–1020.
- Takaishi, S., Okumura, T., Tu, S., Wang, S.S.W., Shibata, W., Vigneshwaran, R., Gordon, S.A.K., Shimada, Y., and Wang, T.C. (2009c). Identification of gastric cancer stem cells using the cell surface marker CD44. *Stem Cells Dayt. Ohio* 27, 1006–1020.
- Takeda, M., Arao, T., Yokote, H., Komatsu, T., Yanagihara, K., Sasaki, H., Yamada, Y., Tamura, T., Fukuoka, K., Kimura, H., et al. (2007). AZD2171 shows potent antitumor activity against gastric cancer over-expressing fibroblast growth factor receptor 2/keratinocyte growth factor receptor. *Clin. Cancer Res. Off. J. Am. Assoc. Cancer Res.* 13, 3051–3057.
- Takehana, T., Kunitomo, K., Suzuki, S., Kono, K., Fujii, H., Matsumoto, Y., and Ooi, A. (2003). Expression of epidermal growth factor receptor in gastric carcinomas. *Clin. Gastroenterol. Hepatol. Off. Clin. Pract. J. Am. Gastroenterol. Assoc.* 1, 438–445.
- Takeyama, K., Kojima, R., Ohashi, R., Sato, T., Mano, H., Masushige, S., and Kato, S. (1996). Retinoic acid differentially up-regulates the gene expression of retinoic acid receptor alpha and gamma isoforms in embryo and adult rats. *Biochem. Biophys. Res. Commun.* 222, 395–400.
- Tanaka, T., Suh, K.S., Lo, A.M., and De Luca, L.M. (2007). p21WAF1/CIP1 is a common transcriptional target of retinoid receptors: pleiotropic regulatory mechanism through retinoic acid receptor (RAR)/retinoid X receptor (RXR) heterodimer and RXR/RXR homodimer. *J. Biol. Chem.* 282, 29987–29997.
- Tang, D.G. (2012). Understanding cancer stem cell heterogeneity and plasticity. *Cell Res.* 22, 457–472.
- Tang, X.-H., and Gudas, L.J. (2011). Retinoids, retinoic acid receptors, and cancer. *Annu. Rev. Pathol.* 6, 345–364.
- Tang, K.H., Ma, S., Lee, T.K., Chan, Y.P., Kwan, P.S., Tong, C.M., Ng, I.O., Man, K., To, K.-F., Lai, P.B., et al. (2012). CD133(+) liver tumor-initiating cells promote tumor angiogenesis, growth, and self-renewal through neurotensin/interleukin-8/CXCL1 signaling. *Hepatology* 55, 807–820.
- Al Tanoury, Z., Piskunov, A., and Rochette-Egly, C. (2013). Vitamin A and retinoid signaling: genomic and nongenomic effects. *J. Lipid Res.* 54, 1761–1775.
- Al Tanoury, Z., Piskunov, A., Andriamorsiresy, D., Gaouar, S., Lutzing, R., Ye, T., Jost, B., Keime, C., and Rochette-Egly, C. (2014). Genes involved in cell adhesion and signaling: a new repertoire of retinoic acid receptor target genes in mouse embryonic fibroblasts. *J. Cell Sci.* 127, 521–533.
- Thiery, J.P. (2002). Epithelial-mesenchymal transitions in tumour progression. *Nat. Rev. Cancer* 2, 442–454.
- Todaro, M., Gaggianesi, M., Catalano, V., Benfante, A., Iovino, F., Biffoni, M., Apuzzo, T., Sperduti, I., Volpe, S., Cocorullo, G., et al. (2014). CD44v6 is a marker of constitutive and reprogrammed cancer stem cells driving colon cancer metastasis. *Cell Stem Cell* 14, 342–356.

- Torres, J., Pérez-Pérez, G., Goodman, K.J., Atherton, J.C., Gold, B.D., Harris, P.R., la Garza, A.M., Guarner, J., and Muñoz, O. (2000). A comprehensive review of the natural history of *Helicobacter pylori* infection in children. *Arch. Med. Res.* *31*, 431–469.
- Torres, V.J., VanCompernelle, S.E., Sundrud, M.S., Unutmaz, D., and Cover, T.L. (2007). *Helicobacter pylori* vacuolating cytotoxin inhibits activation-induced proliferation of human T and B lymphocyte subsets. *J. Immunol. Baltim. Md 1950* *179*, 5433–5440.
- Tseng, Y.-C., Tsai, Y.-H., Tseng, M.-J., Hsu, K.-W., Yang, M.-C., Huang, K.-H., Li, A.F.-Y., Chi, C.-W., Hsieh, R.-H., Ku, H.-H., et al. (2012). Notch2-induced COX-2 expression enhancing gastric cancer progression. *Mol. Carcinog.* *51*, 939–951.
- Turner, N., and Grose, R. (2010). Fibroblast growth factor signalling: from development to cancer. *Nat. Rev. Cancer* *10*, 116–129.
- Utsunomiya, T., Yonezawa, S., Sakamoto, H., Kitamura, H., Hokita, S., Aiko, T., Tanaka, S., Irimura, T., Kim, Y.S., and Sato, E. (1998). Expression of MUC1 and MUC2 mucins in gastric carcinomas: its relationship with the prognosis of the patients. *Clin. Cancer Res. Off. J. Am. Assoc. Cancer Res.* *4*, 2605–2614.
- Varjosalo, M., and Taipale, J. (2008). Hedgehog: functions and mechanisms. *Genes Dev.* *22*, 2454–2472.
- Varon, C., Dubus, P., Mazurier, F., Asencio, C., Chambonnier, L., Ferrand, J., Giese, A., Senant-Dugot, N., Carlotti, M., and Mégraud, F. (2012). *Helicobacter pylori* infection recruits bone marrow-derived cells that participate in gastric preneoplasia in mice. *Gastroenterology* *142*, 281–291.
- Vasiliou, V., Pappa, A., and Petersen, D.R. (2000). Role of aldehyde dehydrogenases in endogenous and xenobiotic metabolism. *Chem. Biol. Interact.* *129*, 1–19.
- Vasiliou, V., Pappa, A., and Estey, T. (2004). Role of human aldehyde dehydrogenases in endobiotic and xenobiotic metabolism. *Drug Metab. Rev.* *36*, 279–299.
- Vasiliou, V., Sandoval, M., Backos, D.S., Jackson, B.C., Chen, Y., Reigan, P., Lanaspá, M.A., Johnson, R.J., Koppaka, V., and Thompson, D.C. (2013). ALDH16A1 is a novel non-catalytic enzyme that may be involved in the etiology of gout via protein-protein interactions with HPRT1. *Chem. Biol. Interact.* *202*, 22–31.
- Vassilopoulos, A., Wang, R.-H., Petrovas, C., Ambrozak, D., Koup, R., and Deng, C.-X. (2008). Identification and characterization of cancer initiating cells from BRCA1 related mammary tumors using markers for normal mammary stem cells. *Int. J. Biol. Sci.* *4*, 133–142.
- Vermeulen, L., Todaro, M., de Sousa Mello, F., Sprick, M.R., Kemper, K., Perez Alea, M., Richel, D.J., Stassi, G., and Medema, J.P. (2008a). Single-cell cloning of colon cancer stem cells reveals a multi-lineage differentiation capacity. *Proc. Natl. Acad. Sci. U. S. A.* *105*, 13427–13432.
- Vermeulen, L., Todaro, M., de Sousa Mello, F., Sprick, M.R., Kemper, K., Perez Alea, M., Richel, D.J., Stassi, G., and Medema, J.P. (2008b). Single-cell cloning of colon cancer stem cells reveals a multi-lineage differentiation capacity. *Proc. Natl. Acad. Sci. U. S. A.* *105*, 13427–13432.
- Vescovi, A.L., Galli, R., and Reynolds, B.A. (2006). Brain tumour stem cells. *Nat. Rev. Cancer* *6*, 425–436.
- Vinion-Dubiel, A.D., McClain, M.S., Czajkowsky, D.M., Iwamoto, H., Ye, D., Cao, P., Schraw, W.,

- Szabo, G., Blanke, S.R., Shao, Z., et al. (1999). A dominant negative mutant of *Helicobacter pylori* vacuolating toxin (VacA) inhibits VacA-induced cell vacuolation. *J. Biol. Chem.* *274*, 37736–37742.
- Visvader, J.E. (2011). Cells of origin in cancer. *Nature* *469*, 314–322.
- Wagers, A.J., and Weissman, I.L. (2004). Plasticity of adult stem cells. *Cell* *116*, 639–648.
- Wallasch, C., Crabtree, J.E., Bevec, D., Robinson, P.A., Wagner, H., and Ullrich, A. (2002). *Helicobacter pylori*-stimulated EGF receptor transactivation requires metalloprotease cleavage of HB-EGF. *Biochem. Biophys. Res. Commun.* *295*, 695–701.
- Wang, X.-Q., Terry, P.-D., and Yan, H. (2009a). Review of salt consumption and stomach cancer risk: epidemiological and biological evidence. *World J. Gastroenterol.* *WJG* *15*, 2204–2213.
- Wang, Y.H., Li, F., Luo, B., Wang, X.H., Sun, H.C., Liu, S., Cui, Y.Q., and Xu, X.X. (2009b). A side population of cells from a human pancreatic carcinoma cell line harbors cancer stem cell characteristics. *Neoplasma* *56*, 371–378.
- Warrell, R.P., Frankel, S.R., Miller, W.H., Scheinberg, D.A., Itri, L.M., Hittelman, W.N., Vyas, R., Andreeff, M., Tafuri, A., and Jakubowski, A. (1991). Differentiation therapy of acute promyelocytic leukemia with tretinoin (all-trans-retinoic acid). *N. Engl. J. Med.* *324*, 1385–1393.
- Watanabe, T., Takahashi, A., Suzuki, K., Kurusu-Kanno, M., Yamaguchi, K., Fujiki, H., and Saganuma, M. (2014). Epithelial-mesenchymal transition in human gastric cancer cell lines induced by TNF- α -inducing protein of *Helicobacter pylori*. *Int. J. Cancer* *134*, 2373–2382.
- Weck, M.N., Gao, L., and Brenner, H. (2009). *Helicobacter pylori* infection and chronic atrophic gastritis: associations according to severity of disease. *Epidemiol. Camb. Mass* *20*, 569–574.
- Weigmann, A., Corbeil, D., Hellwig, A., and Huttner, W.B. (1997). Prominin, a novel microvilli-specific polytopic membrane protein of the apical surface of epithelial cells, is targeted to plasmalemmal protrusions of non-epithelial cells. *Proc. Natl. Acad. Sci. U. S. A.* *94*, 12425–12430.
- Weng, A.P., Millholland, J.M., Yashiro-Ohtani, Y., Arcangeli, M.L., Lau, A., Wai, C., Del Bianco, C., Rodriguez, C.G., Sai, H., Tobias, J., et al. (2006). c-Myc is an important direct target of Notch1 in T-cell acute lymphoblastic leukemia/lymphoma. *Genes Dev.* *20*, 2096–2109.
- Whiting, J.L., Sigurdsson, A., Rowlands, D.C., Hallissey, M.T., and Fielding, J.W.L. (2002). The long term results of endoscopic surveillance of premalignant gastric lesions. *Gut* *50*, 378–381.
- Williams, K., Motiani, K., Giridhar, P.V., and Kasper, S. (2013). CD44 integrates signaling in normal stem cell, cancer stem cell and (pre)metastatic niches. *Exp. Biol. Med.* *Maywood NJ* *238*, 324–338.
- Wu, Q., Chen, Z., and Su, W. (2002). Anticancer effect of retinoic acid via AP-1 activity repression is mediated by retinoic acid receptor alpha and beta in gastric cancer cells. *Int. J. Biochem. Cell Biol.* *34*, 1102–1114.
- Xia, P. (2014). Surface markers of cancer stem cells in solid tumors. *Curr. Stem Cell Res. Ther.* *9*, 102–111.
- Xie, C., Huang, H., Sun, X., Guo, Y., Hamblin, M., Ritchie, R.P., Garcia-Barrio, M.T., Zhang, J., and Chen, Y.E. (2011a). MicroRNA-1 regulates smooth muscle cell differentiation by repressing

Kruppel-like factor 4. *Stem Cells Dev.* 20, 205–210.

- Xie, C., Ritchie, R.P., Huang, H., Zhang, J., and Chen, Y.E. (2011b). Smooth muscle cell differentiation in vitro: models and underlying molecular mechanisms. *Arterioscler. Thromb. Vasc. Biol.* 31, 1485–1494.
- Xie, L., Su, X., Zhang, L., Yin, X., Tang, L., Zhang, X., Xu, Y., Gao, Z., Liu, K., Zhou, M., et al. (2013). FGFR2 gene amplification in gastric cancer predicts sensitivity to the selective FGFR inhibitor AZD4547. *Clin. Cancer Res. Off. J. Am. Assoc. Cancer Res.* 19, 2572–2583.
- Xu, W., Xu, J., Liu, S., Chen, B., Wang, X., Li, Y., Qian, Y., Zhao, W., and Wu, J. (2011). Effects of common polymorphisms rs11614913 in miR-196a2 and rs2910164 in miR-146a on cancer susceptibility: a meta-analysis. *PloS One* 6, e20471.
- Yaghoobi, M., Rakhshani, N., Sadr, F., Bijarchi, R., Joshaghani, Y., Mohammadkhani, A., Attari, A., Akbari, M.R., Hormazdi, M., and Malekzadeh, R. (2004). Hereditary risk factors for the development of gastric cancer in younger patients. *BMC Gastroenterol.* 4, 28.
- Yamada, H., Shinmura, K., Ikeda, S., Tao, H., Otani, T., Hanaoka, T., Tsuneyoshi, T., Tsugane, S., and Sugimura, H. (2007). Association between CDH1 haplotypes and gastric cancer risk in a Japanese population. *Scand. J. Gastroenterol.* 42, 1479–1485.
- Yamaguchi, A., Saito, M., Gio, T., Iida, A., Takeuchi, K., Hirose, K., Nakagawara, G., Urano, T., Furukawa, K., and Shiku, H. (1995). Expression of CD44 variant exons 8-10 in gastric cancer. *Jpn. J. Cancer Res. Gann* 86, 1166–1171.
- Yamaguchi, A., Goi, T., Yu, J., Hirono, Y., Ishida, M., Iida, A., Kimura, T., Takeuchi, K., Katayama, K., and Hirose, K. (2002). Expression of CD44v6 in advanced gastric cancer and its relationship to hematogenous metastasis and long-term prognosis. *J. Surg. Oncol.* 79, 230–235.
- Yamaoka, Y., Kato, M., and Asaka, M. (2008). Geographic differences in gastric cancer incidence can be explained by differences between *Helicobacter pylori* strains. *Intern. Med. Tokyo Jpn.* 47, 1077–1083.
- Yan, F., Cao, H., Chaturvedi, R., Krishna, U., Hobbs, S.S., Dempsey, P.J., Peek, R.M., Jr, Cover, T.L., Washington, M.K., Wilson, K.T., et al. (2009). Epidermal growth factor receptor activation protects gastric epithelial cells from *Helicobacter pylori*-induced apoptosis. *Gastroenterology* 136, 1297–1307, e1–e3.
- Yang, J., and Weinberg, R.A. (2008). Epithelial-mesenchymal transition: at the crossroads of development and tumor metastasis. *Dev. Cell* 14, 818–829.
- Yang, Y.M., and Chang, J.W. (2008). Bladder cancer initiating cells (BCICs) are among EMA-CD44v6+ subset: novel methods for isolating undetermined cancer stem (initiating) cells. *Cancer Invest.* 26, 725–733.
- Yang, J., Mani, S.A., Donaher, J.L., Ramaswamy, S., Itzykson, R.A., Come, C., Savagner, P., Gitelman, I., Richardson, A., and Weinberg, R.A. (2004). Twist, a master regulator of morphogenesis, plays an essential role in tumor metastasis. *Cell* 117, 927–939.
- Yang, J., Mani, S.A., and Weinberg, R.A. (2006). Exploring a new twist on tumor metastasis. *Cancer Res.* 66, 4549–4552.
- Yang, M.-H., Wu, M.-Z., Chiou, S.-H., Chen, P.-M., Chang, S.-Y., Liu, C.-J., Teng, S.-C., and Wu, K.-J. (2008a). Direct regulation of TWIST by HIF-1 α promotes metastasis. *Nat. Cell Biol.* 10, 295–305.

- Yang, Z.F., Ho, D.W., Ng, M.N., Lau, C.K., Yu, W.C., Ngai, P., Chu, P.W.K., Lam, C.T., Poon, R.T.P., and Fan, S.T. (2008b). Significance of CD90+ cancer stem cells in human liver cancer. *Cancer Cell* 13, 153–166.
- Yao, C.-T., Cheng, C.-A., Wang, H.-K., Chiu, S.-W., Chen, Y.-C., Wang, M.-F., Yin, S.-J., and Peng, G.-S. (2011a). The role of ALDH2 and ADH1B polymorphism in alcohol consumption and stroke in Han Chinese. *Hum. Genomics* 5, 569–576.
- Yao, T., Chen, Q., Zhang, B., Zhou, H., and Lin, Z. (2011b). The expression of ALDH1 in cervical carcinoma. *Med. Sci. Monit. Int. Med. J. Exp. Clin. Res.* 17, HY21–HY26.
- Yasuda, M., Tanaka, Y., Fujii, K., and Yasumoto, K. (2001). CD44 stimulation down-regulates Fas expression and Fas-mediated apoptosis of lung cancer cells. *Int. Immunol.* 13, 1309–1319.
- Yeh, T.-S., Wu, C.-W., Hsu, K.-W., Liao, W.-J., Yang, M.-C., Li, A.F.-Y., Wang, A.-M., Kuo, M.-L., and Chi, C.-W. (2009). The activated Notch1 signal pathway is associated with gastric cancer progression through cyclooxygenase-2. *Cancer Res.* 69, 5039–5048.
- Yin, A.H., Miraglia, S., Zanjani, E.D., Almeida-Porada, G., Ogawa, M., Leary, A.G., Olweus, J., Kearney, J., and Buck, D.W. (1997). AC133, a novel marker for human hematopoietic stem and progenitor cells. *Blood* 90, 5002–5012.
- Ying, M., Wang, S., Sang, Y., Sun, P., Lal, B., Goodwin, C.R., Guerrero-Cazares, H., Quinones-Hinojosa, A., Lathera, J., and Xia, S. (2011). Regulation of glioblastoma stem cells by retinoic acid: role for Notch pathway inhibition. *Oncogene* 30, 3454–3467.
- Yoshimura, K., Uchida, G., Okazaki, M., Kitano, Y., and Harii, K. (2003). Differential expression of heparin-binding EGF-like growth factor (HB-EGF) mRNA in normal human keratinocytes induced by a variety of natural and synthetic retinoids. *Exp. Dermatol.* 12 Suppl 2, 28–34.
- You, W.C., Zhang, L., Gail, M.H., Chang, Y.S., Liu, W.D., Ma, J.L., Li, J.Y., Jin, M.L., Hu, Y.R., Yang, C.S., et al. (2000). Gastric dysplasia and gastric cancer: Helicobacter pylori, serum vitamin C, and other risk factors. *J. Natl. Cancer Inst.* 92, 1607–1612.
- Yu, H., Zeng, J., Liang, X., Wang, W., Zhou, Y., Sun, Y., Liu, S., Li, W., Chen, C., and Jia, J. (2014). Helicobacter pylori promotes epithelial-mesenchymal transition in gastric cancer by downregulating programmed cell death protein 4 (PDCD4). *PLoS One* 9, e105306.
- Zhang, C., Li, C., He, F., Cai, Y., and Yang, H. (2011). Identification of CD44+CD24+ gastric cancer stem cells. *J. Cancer Res. Clin. Oncol.* 137, 1679–1686.
- Zhang, H.M., Wakisaka, N., Maeda, O., and Yamamoto, T. (1997). Vitamin C inhibits the growth of a bacterial risk factor for gastric carcinoma: Helicobacter pylori. *Cancer* 80, 1897–1903.
- Zhang, S., Balch, C., Chan, M.W., Lai, H.-C., Matei, D., Schilder, J.M., Yan, P.S., Huang, T.H.-M., and Nephew, K.P. (2008). Identification and characterization of ovarian cancer-initiating cells from primary human tumors. *Cancer Res.* 68, 4311–4320.
- Zhang, X.-F., Wang, Y.-M., Ge, H., Cao, Y.-Y., Chen, Z.-F., Wen, D.-G., Guo, W., Wang, N., Li, Y., and Zhang, J.-H. (2008c). Association of CDH1 single nucleotide polymorphisms with susceptibility to esophageal squamous cell carcinomas and gastric cardia carcinomas. *Dis. Esophagus Off. J. Int. Soc. Dis. Esophagus ISDE* 21, 21–29.
- Zhang, Y., Jia, S., Liu, Y., Li, B., Wang, Z., Lu, H., and Zhu, C. (2007). A clinical study of all-trans-retinoid-induced differentiation therapy of advanced thyroid cancer. *Nucl. Med. Commun.* 28, 251–255.

- Zhao, Q., Tao, J., Zhu, Q., Jia, P.-M., Dou, A.-X., Li, X., Cheng, F., Waxman, S., Chen, G.-Q., Chen, S.-J., et al. (2004). Rapid induction of cAMP/PKA pathway during retinoic acid-induced acute promyelocytic leukemia cell differentiation. *Leukemia* 18, 285–292.
- Zhou, G.-B., Zhang, J., Wang, Z.-Y., Chen, S.-J., and Chen, Z. (2007). Treatment of acute promyelocytic leukaemia with all-trans retinoic acid and arsenic trioxide: a paradigm of synergistic molecular targeting therapy. *Philos. Trans. R. Soc. Lond. B. Biol. Sci.* 362, 959–971.
- Zhu, H., Yang, X., Zhang, C., Zhu, C., Tao, G., Zhao, L., Tang, S., Shu, Z., Cai, J., Dai, S., et al. (2013). Red and processed meat intake is associated with higher gastric cancer risk: a meta-analysis of epidemiological observational studies. *PloS One* 8, e70955.
- Zhu, Z., Hao, X., Yan, M., Yao, M., Ge, C., Gu, J., and Li, J. (2010). Cancer stem/progenitor cells are highly enriched in CD133+CD44+ population in hepatocellular carcinoma. *Int. J. Cancer J. Int. Cancer* 126, 2067–2078.
- Zöller, M. (2011). CD44: can a cancer-initiating cell profit from an abundantly expressed molecule? *Nat. Rev. Cancer* 11, 254–267.

ANNEXES

**Article 3 – *Helicobacter pylori* infection
generates cells with cancer stem cells
properties via epithelial to mesenchymal-like
changes**

Oncogene. 2014 Aug 7;33(32):4123-31.

ORIGINAL ARTICLE

Helicobacter pylori generates cells with cancer stem cell properties via epithelial–mesenchymal transition-like changes

E Bessède^{1,2}, C Staedel^{3,4}, LA Acuña Amador^{1,2}, PH Nguyen^{1,2}, L Chambonnier^{1,2}, M Hatakeyama⁵, G Belleannée⁶, F Mégraud^{1,2} and C Varon^{1,2}

Helicobacter pylori infection is the major risk factor for gastric adenocarcinoma. The link with gastric adenocarcinoma is partly due to the *H. pylori* CagA oncoprotein. CagA is responsible for a particular cell phenotype *in vitro*, the ‘hummingbird’ phenotype, that corresponds to an elongation of the cells, mimicking an epithelial–mesenchymal transition (EMT). EMT participates in the carcinogenesis process, and is involved in the generation of cancer stem cells (CSCs). However, its involvement in gastric carcinogenesis has yet not been studied. Therefore, the aim of this study was to determine the role of *H. pylori* in EMT and in the emergence of gastric CSCs. For this purpose, gastric epithelial cells were cocultured with a *cagA*-positive *H. pylori* strain or its isogenic-deleted mutants or were transfected with CagA expression vectors. Study of the expression of epithelial and mesenchymal markers showed that *H. pylori*, via CagA, is responsible for an EMT phenotype associated with an increase in mesenchymal markers as well as CD44 expression, a known gastric CSC marker. Moreover, infection led to an increased ability to migrate, to invade and to form tumorspheres. Cell sorting experiments showed that only the CD44^{high} cells induced by *H. pylori* infection displayed the mesenchymal phenotype and CSC properties *in vitro*, and had higher tumorigenic properties than CD44^{low} cells in xenografted mice. Immunohistochemistry analyses on human and mouse gastric mucosa tissue samples confirmed a high expression of CD44 and mesenchymal markers in *H. pylori*-infected cases, and in gastric dysplasia and carcinoma. All of these data suggest that *H. pylori*, via CagA, unveils CSC-like properties by induction of EMT-like changes in gastric epithelial cells.

Oncogene advance online publication, 7 October 2013; doi:10.1038/onc.2013.380

Keywords: gastric cancer; infection; CD44

INTRODUCTION

Gastric adenocarcinoma remains the second cause of cancer-related mortality worldwide. *H. pylori* infection has a crucial role in this carcinogenesis process, and this bacterium has been classified as a class 1 carcinogen by the WHO.¹ Approximately 1% of infected persons develop a gastric adenocarcinoma (in Japan, ~10% of the infected individuals develop gastric cancers), and in certain parts of the world up to 80% of the population are infected with *H. pylori*. Thus, it is very important to investigate how the bacteria can lead to gastric adenocarcinoma. Several pathogenic factors of this bacterium are known to be involved in carcinogenesis. Among them, the *cag* pathogenicity island (*cagPAI*) is certainly the most important,^{2–4} as strains harboring the *cagPAI* are more carcinogenic than those that are *cagPAI* negative. The *cagPAI* encodes a type 4 secretion system (T4SS) and an oncoprotein named CagA. The T4SS forms a pilus allowing the injection of CagA inside the cell. It permits the interference with intercellular junctions via different pathways and leads to the appearance of a particular cell shape called the ‘hummingbird’ phenotype.^{5,6} This phenotype is characterized by an extremely elongated shape that is similar to that observed during an epithelial–mesenchymal transition (EMT), as the essential features of EMT are the disruption of intercellular contacts and the enhancement of cell motility.⁷ EMT is a developmental process in which epithelial cells acquire the motile, migratory properties of

mesenchymal cells. Recent evidence also suggests that cells that undergo EMT acquire stem cell-like properties.^{8,9} In particular, Mani *et al.*⁸ showed that the induction of EMT in immortalized mammary epithelial cells generated a subpopulation of CD44⁺/CD24[–] cells with the phenotype and properties of breast cancer stem cells (CSCs). CSCs correspond to a unique subpopulation of cells within the tumors; these cells possess the ability to initiate tumor growth and sustain tumor self-renewal. In breast, ovarian, pancreatic, prostate and colorectal cancers, CSCs have been described and characterized with different specific cell surface markers, and among these markers, CD44 was always present.^{10–17} Concerning gastric carcinoma, CD44 has also been identified as a marker of gastric CSCs,¹⁸ but the role of *H. pylori* in the emergence of gastric CSCs has never been explored. Thus, the aim of our study was to investigate the role of *H. pylori* and its virulence factors in the EMT, and in the emergence of gastric CSCs.

RESULTS

Infection of gastric epithelial cells with CagA-positive *H. pylori* strains generates cells with mesenchymal and stem cell features by an epithelial–mesenchymal-like transition

To determine whether *H. pylori* infection could generate cells with CSC properties by an epithelial–mesenchymal-like transition, coculture experiments with the AGS gastric epithelial cell line

¹Université de Bordeaux, Laboratoire de Bactériologie, Bordeaux, France; ²INSERM, U853, Bordeaux, France; ³RNA: Natural and Artificial Regulation (ARNA) Laboratory, Université de Bordeaux, Bordeaux, France; ⁴INSERM, U869, Bordeaux, France; ⁵Division of Microbiology, Graduate School of Medicine, University of Tokyo, Tokyo, Japan and ⁶Pathology Department, Haut Leveque Hospital, University Hospital Center, Bordeaux, France. Correspondence: Dr E Bessède, Université de Bordeaux, Laboratoire de Bactériologie, INSERM, U853, Bordeaux F-33000, France.

E-mail: emilie.bessede@chu-bordeaux.fr

Received 8 November 2012; revised 22 July 2013; accepted 30 July 2013

were performed and confirmed on MKN-45 and MKN-74 cell lines (Supplementary Figure S1). To assess the role of bacterial virulence factors, particularly those encoded by the *cagPAI* (the CagA protein and the T4SS component CagE, which is necessary for T4SS assembly), knock-out mutants of the *cagPAI*-positive 7.13, 7.13 Δ *cagA* and 7.13 Δ *cagE* strains were tested. As expected, the wild-type (WT) 7.13 *cagA*-positive strain induced morphological changes, characterized by a loss of polygonal shape, a disruption of cell clusters and the appearance of elongated cells with membrane ruffles at the cellular periphery, suggesting a mesenchymal phenotype (Figure 1a, Supplementary Figure S1A). Quantification of cells harboring a mesenchymal-like phenotype, ranging from approximately 30% in AGS cells to 7% in MKN-45 cells and 8% in MKN-74 cells (Supplementary Figure S1B),

confirmed that cellular elongation and particularly the 'humming-bird' phenotype were dependent on CagA injected by the T4SS (Figure 1a), as it is significantly higher in response to the WT strain than to 7.13 Δ *cagA* and 7.13 Δ *cagE* strains (Figure 1b).

RT-quantitative PCR (RT-qPCR) analyses of the expression of standard EMT markers upon infection revealed a significant increase in the mesenchymal markers Snail1, Vimentin and ZEB1, along with the stem cell marker CD44, all in a CagA-dependent manner (Figure 1c). A decreased expression of the epithelial markers Cytokeratin 7 (CK7) and Osteopontin (SSP-1) were also observed in a CagA-dependent manner (Figure 1c and Supplementary Figure S1H). CD44 expression was quantified by measuring the mean fluorescence intensity of immunostained cells, as the percentage of CD44-positive cells increased only

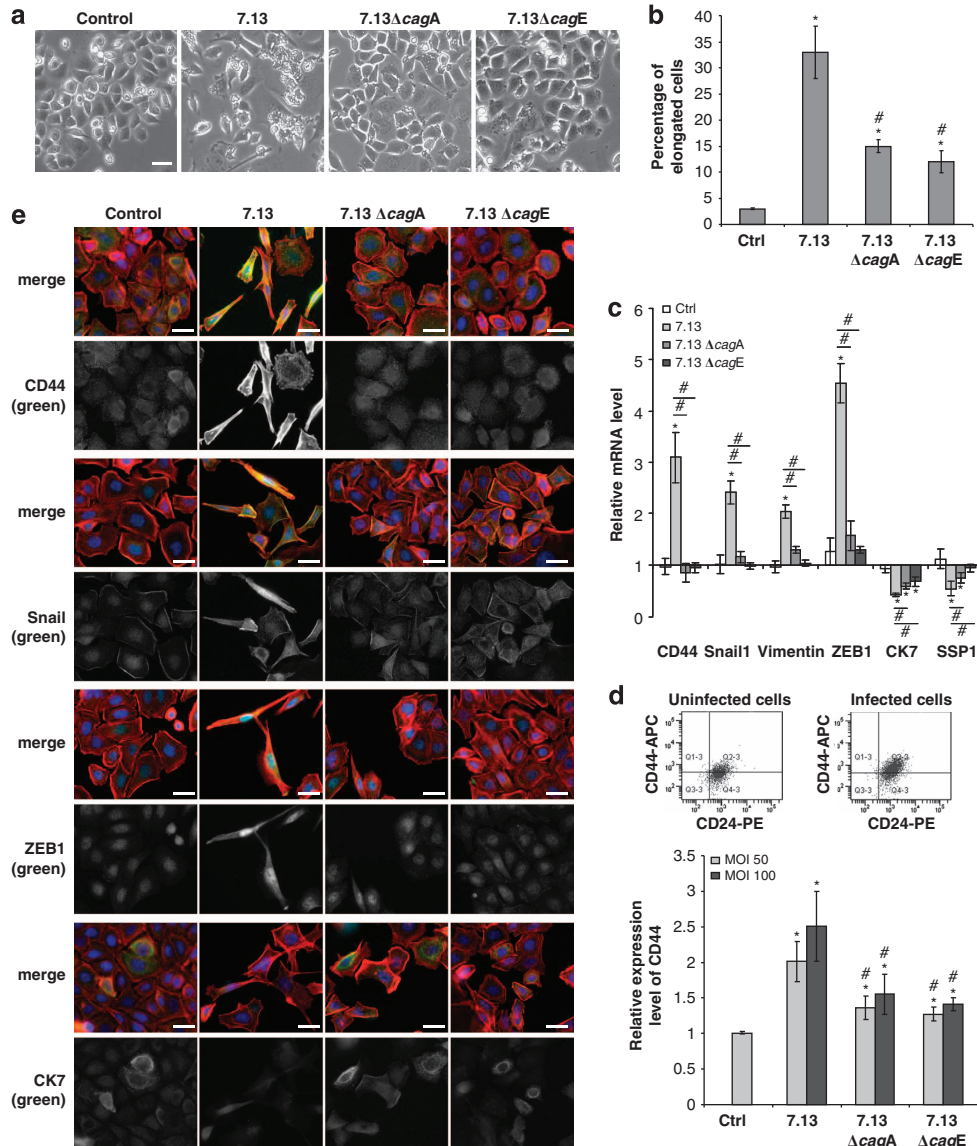


Figure 1. Infection with *cagPAI*-positive *H. pylori* induces an EMT-like phenotype and CD44 expression in gastric epithelial cells. AGS cells were cocultured with *H. pylori* 7.13 WT or Δ *cagA* or Δ *cagE* strains for 24 h. (a) Representative phase-contrast images of uninfected cells (control) or cells infected with different *H. pylori* strains. Scale bar, 20 μ m. (b) Quantification of the percentage of cells harboring an elongated phenotype ($n = 5$). (c) Relative expression levels of the mRNA encoding CD44, Snail1, Vimentin, ZEB1, Cytokeratin 7 and Osteopontin (SSP1) in uninfected cells (Ctrl) or infected with the different *H. pylori* strains determined by RT-qPCR (relative to the control HPRT1 housekeeping gene mRNA) ($n = 4$). (d) Relative CD44 expression quantified using flow cytometry in AGS cells infected with *H. pylori* strains at different MOI vs uninfected cells (Ctrl) ($n = 6$). (a–d) Data are reported as mean \pm s.d., * $P < 0.05$ vs control cells (Ctrl), # $P < 0.05$ vs 7.13-infected cells. (e) Representative images of immunofluorescent staining of cells after infection or not (Ctrl) with the different *H. pylori* strains. Black and white pictures correspond to the indicated single staining (in green), and colored images correspond to the merge with F-actin (in red) and nucleus (in blue) stainings. Scale bars, 10 μ m.

slightly after *H. pylori* infection (data not shown, $74\% \pm 5\%$ in 7.13-infected cells vs $63\% \pm 8\%$ in uninfected control cells, no significant). Flow cytometry data confirmed CD44 regulation, which depends on both the multiplicity of infection (MOI) of the *H. pylori* WT strain and the *cagPAI* integrity (Figure 1d, Supplementary Figure S1C). CD24 expression, considered as a CSC marker in some cancer models,^{19,20} was also evaluated but showed no significant variation in AGS cells in response to *H. pylori* infection ($CD24 > 97\%$ in AGS cells uninfected and infected with *H. pylori*, see Figure 1d). This result is in agreement with those of Takaishi et al.¹⁸ who reported that CD24 cannot be considered as a marker of gastric CSC in gastric cancer cell lines.

To identify which cells expressed the different pre-cited markers at a higher rate in response to *H. pylori* infection, immunofluorescent stainings were performed (Figure 1e). Cells with the 'hummingbird' phenotype showed a clearly higher expression of CD44, Snail and ZEB1 than the cells without the 'hummingbird' phenotype. Thus, the WT *H. pylori* strain induced a marked increase in CD44 and the mesenchymal markers Snail and ZEB1 compared with the knock-out strains. CK7 expression was moderately affected, with a mild decrease observed in cells with the 'hummingbird' phenotype induced by the WT *H. pylori* strain.

Cells infected by CagA-positive *H. pylori* exhibit CSC properties. CSCs express specific markers and are defined by their self-renewal capacity, their ability to generate a new tumor and an increased capacity for migration and invasion. In published studies, many different approaches have been described to identify CSC.^{8,16,18} Several techniques allow the study of their properties using *in vivo* models of cancer cell xenografts in mice to follow tumorigenesis or *in vitro* tumorsphere and migration assays. The tumorsphere assay is one of the most frequently used and consists of the *in vitro* formation of spheroids under non-adherent culture conditions in defined media after several days. This assay is ideal to identify CSC properties, as it highlights the capacity of cells for self-renewal and ability to form a three-dimensional sphere like a tumor.

The ability of AGS cells to form spheroids was studied *in vitro* under non-adherent culture conditions. Although AGS cells are cancer cells, under basal conditions, they do not share high tumorigenic properties, as their ability to spontaneously form tumorspheres after 5 days of culture under non-adherent conditions is limited. However, infection with the WT *H. pylori* strain led to a significant increase in spheroid formation compared with uninfected control cells in AGS cell line, with similar results obtained with both MKN-45 and MKN-74 cell lines (Figures 2a and b, Supplementary Figure S1F). Infection with the *cagA*- or *cagE*-deleted strains did not stimulate spheroid formation, indicating that formation is completely dependent on CagA. Moreover, cells infected with the WT *H. pylori* strain led to spheroids that were bigger than those generated by cells under other conditions, as shown on Figure 2a.

To evaluate the migration of cells and invasion properties, experiments using Transwells with 8- μ m pore size filters were performed. Infection with the WT *H. pylori* strain significantly stimulated the properties of migration and invasion through a type I collagen matrix of cells compared with the basal levels recorded in the uninfected control (Figures 2c and d and Supplementary Figures S1D and E). Cells infected with *cagA*- or *cagE*-deleted mutant strains migrated to a significantly lesser degree than cells infected with WT *H. pylori* (Figure 2c). Thus, migration and invasion properties of cells increased with CagA-positive *H. pylori* infection.

CD44^{high} cells isolated from *H. pylori* CagA-positive-infected AGS cells display mesenchymal features and stem cell properties. Cell sorting by flow cytometry was performed on *H. pylori* 7.13-infected AGS and MKN-45 cells in order to separate the CD44^{high}

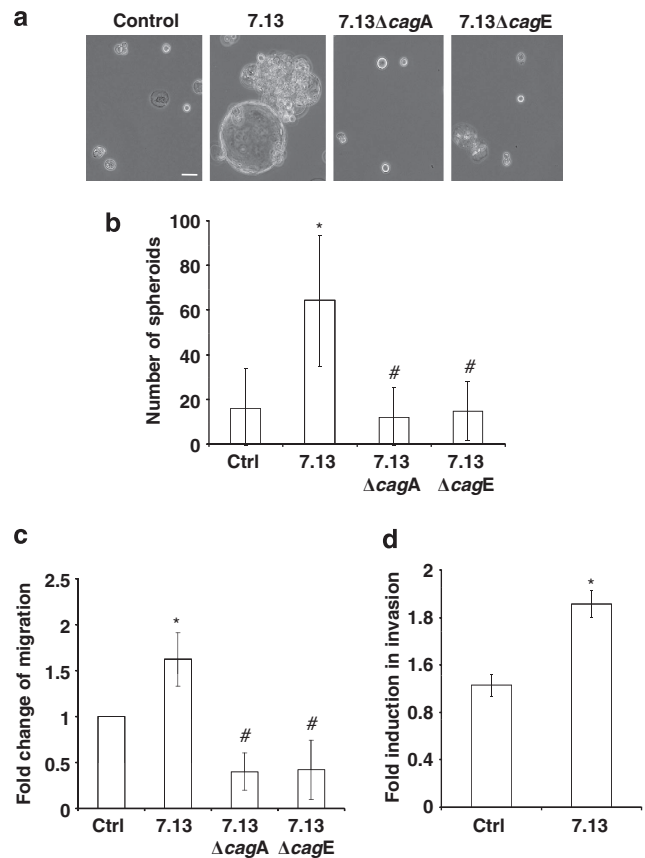


Figure 2. Infection with *cagPAI*-positive *H. pylori* stimulates migration, invasion and the formation of tumorspheres. AGS cells were cocultured with *H. pylori* 7.13 WT or Δ *cagA* or Δ *cagE* strains for 24 h, then recovered and seeded under non-adherent culture conditions for spheroid formation (a, b) or submitted to the migration and invasion assays in Transwells (c). (a) Representative phase-contrast images of spheroid colonies. Scale bar, 25 μ m. (b) Quantification in absolute number of spheroids after 5 days. (c) Quantification of migration after 18 h. (d) Quantification of invasion after 18 h. (b–d) Data are reported as fold induction vs uninfected cells (Ctrl) \pm s.d. ($n = 3$). * $P < 0.05$ vs Ctrl; # $P < 0.05$ vs 7.13-infected cells.

cells from the CD44^{low} cells. Cells were also stained for CD24 that was used as a positive control for the staining procedure, as it is expressed in all AGS cells, and with 4',6'-diamidino-2-phenylindol (DAPI) to exclude positive dead cells by cell sorting. The features and properties of the two cellular subpopulations obtained, CD44^{high} and CD44^{low}, were then studied in comparison with those of the unsorted and uninfected cells. Phase-contrast imaging revealed that CD44^{high} cells corresponded to cells with the 'hummingbird' phenotype, and the phenotype of CD44^{low} sorted cells was closer to that of control cells (Figure 3a and Supplementary Figure S1A). In addition, these CD44^{high} cells formed more tumorspheres (Figures 3b and c, Supplementary Figure S1F) and exhibited higher migration and invasion capacities than the CD44^{low} cells (Figure 3d, Supplementary Figures S1D and E). Interestingly, the same CD44^{high} sorted cells (*H. pylori* infected) expressed a higher level of mesenchymal markers (Snail1, Vimentin and ZEB1) and a lower level of epithelial markers (SSP-1 and CK7) than the CD44^{low} cells (Figure 3e). As AGS cells were described to be poorly tumorigenic *in vivo*,¹⁸ *in vivo* tumorigenicity experiments were performed with *H. pylori*-infected MKN-45 cells by subcutaneous injection in immunodeficient mice. Results from these xenograft experiments indicate that the CD44^{high} cells led to tumors with a significantly higher volume than the CD44^{low} cells after 6 weeks

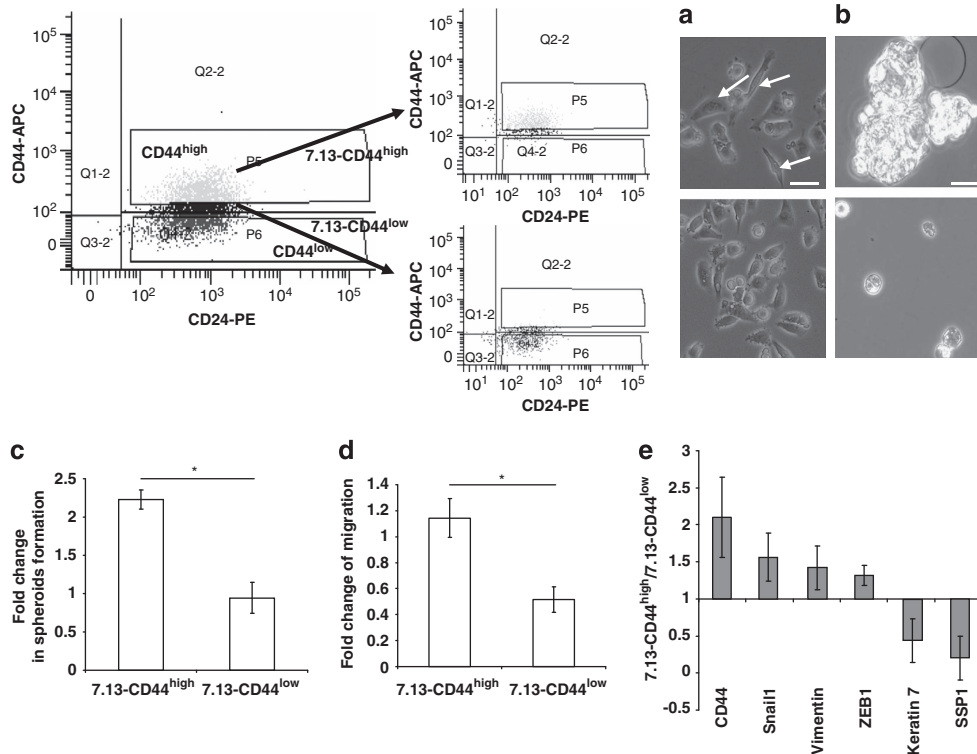


Figure 3. The CD44^{high} cells generated by infection with *cagPAI*-positive *H. pylori* share EMT features and CSC properties. AGS cells were cocultured with WT *H. pylori* 7.13 strain for 24 h, then stained with DAPI, anti-CD24-PE and anti-CD44-APC antibodies, and DAPI-negative/CD24-positive/CD44^{high} or CD44^{low} cells were sorted by FACS as illustrated. **(a)** Representative phase-contrast images of DAPI/CD24⁺CD44^{high} (upper panel) or DAPI/CD24⁺CD44^{low} (lower panel) sorted cells after 24 h plating under adherent culture conditions. Arrows point to cells having preserved the 'hummingbird' phenotype in DAPI/CD24⁺CD44^{high} sorted cells. **(b)** Same as **a**, but after 5 days of culture of sorted cells under non-adherent conditions to allow spheroid formation, which developed mainly with DAPI/CD24⁺CD44^{high} sorted cells (**a**, **b**). Scale bars, 10 μ m. **(c)** Quantification of spheroids after 5 days ($n = 3$). **(d)** Quantification of sorted cells submitted to the migration assay after 18 h ($n = 6$). **(b–d)** Data are reported as the mean of fold induction vs control uninfected and unsorted cells \pm s.d. * $P < 0.05$. **(e)** Relative expression levels of the mRNA encoding CD44, Snail1, Vimentin, ZEB1, Cytokeratin 7 and Osteopontin (SSP1) in CD44^{high} vs CD44^{low} sorted cells from 7.13-infected cells determined by RT-qPCR ($n = 4$). Data are reported as the mean ratio of CD44^{high} cells vs CD44^{low} cells \pm s.d.

(Supplementary Figure S1G). These results together demonstrate that CD44^{high} cells induced in response to infection with CagA-positive *H. pylori* display mesenchymal and stem cell properties.

CagA is responsible for *H. pylori*-induced EMT-like changes and CD44 upregulation

In coculture experiments with the *H. pylori* 7.13 *cagA*-positive strain, CagA was detected at higher levels in the cytoplasm of cells harboring the 'hummingbird' phenotype than in cells that maintained a polygonal shape, suggesting that the intracellular level of cytosolic CagA is associated with the formation of the 'hummingbird' phenotype (Figure 4a). To confirm the role of CagA in the induction of the EMT-like process and the upregulation of CD44 expression, transfection experiments were performed using a plasmid encoding for a hemagglutinin (HA)-tagged WT CagA (pCagA) alone or in combination with a plasmid-encoding green fluorescent protein (pGFP) in AGS cells. Experiments using immunofluorescent staining revealed that transfected cells expressing CagA (HA positive) displayed the 'hummingbird' phenotype, which was associated with a higher expression of CD44, Snail and ZEB1 expression than untransfected cells (HA negative) (Figure 4b). CagA-induced upregulation of the mesenchymal and stem cell markers was confirmed by RT-qPCR (Figure 4c). The upregulation of CD44 was also confirmed by flow cytometry on whole cells transfected with pCagA in comparison with control cells (transfected with an empty plasmid), and on GFP-positive

cells co-transfected with pCagA in comparison with control pGFP cells (the percentage of pCagA-transfected cells analyzed being higher within the GFP-positive cells than in the whole population) (Figure 4d).

The expression of epithelial markers remained quite unaffected by CagA expression, with a light downregulation of SSP-1 and CK7 transcripts or protein (Figures 4b and c). These results combined with those of coculture experiments with WT and mutant *H. pylori* strains indicate that CagA is mostly responsible for the upregulation of mesenchymal and stem cell markers induced by *H. pylori*, even though the downregulation of epithelial markers remained more discreet.

H. pylori-induced CD44^{high} cells with mesenchymal and stem cell features involve mitogen-activated protein kinase signaling. Several signaling pathways have been implicated in the signal transduction downstream of the T4SS and particularly CagA. The nuclear factor κ B (NF- κ B) signaling pathway was described as the major signaling pathway activated in response to the delivery by the T4SS of CagA and the bacterial peptidoglycan, both leading to the proinflammatory response.^{6,21} Concerning CagA, one of the major signaling pathways concerns the mitogen-activated protein kinase (MAPK) family members and particularly extracellular regulated kinases (ERK)1/2, which is involved in cytoskeleton remodeling and polarization disturbance.^{22,23} In order to evaluate the involvement of NF- κ B in the induction of CD44^{high} cells with the 'hummingbird' phenotype by

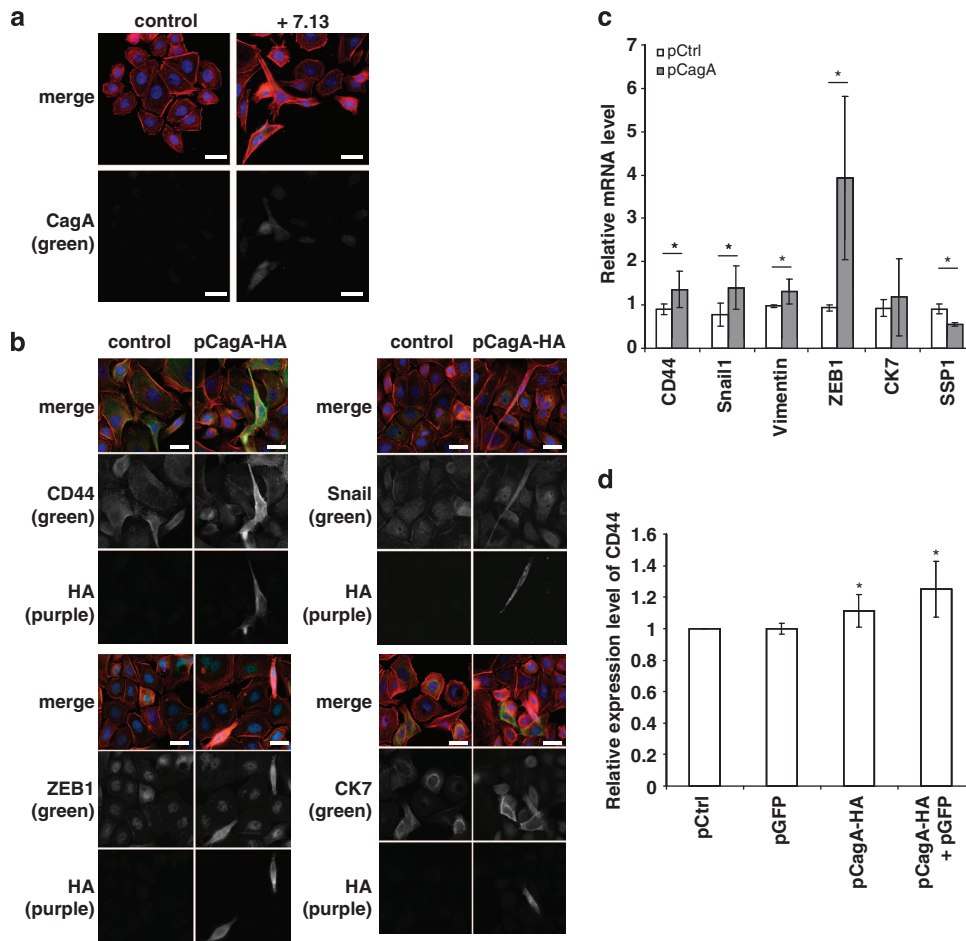


Figure 4. Expression of CagA-induced CD44^{high} cells with EMT features. AGS cells were analyzed 48 h after transfection with a negative control empty plasmid (pCtrl), a plasmid-encoding HA-tagged CagA (pCagA-HA) or a plasmid encoding the GFP (pGFP). **(a)** Representative images of immunofluorescence staining of cells after infection or not (control) with *H. pylori* 7.13. **(b)** Representative images of immunofluorescent staining of cells after transfection with the different plasmids. **(a, b)** Black and white pictures correspond to the indicated single staining alone (in green, HA in purple), and multi-colored images correspond to the merge with F-actin (in red) and nucleus (in blue) stainings. Scale bars, 10 μ m. **(c)** Relative expression levels of the mRNA encoding CD44, snail1, vimentin, ZEB1, cytokeratin 7 and osteopontin (SSP1) in cells transfected with pCagA-HA relative to pCtrl determined by RT-qPCR ($n=4$). Data are reported as mean \pm s.d. * $P<0.05$ vs pCtrl. **(d)** Relative CD44 expression quantified using flow cytometry in cells transfected with pCtrl and pCagA-HA alone, or in GFP-positive cells resulting from single transfection of pGFP or from the co-transfection of pCagA-HA + pGFP at a ratio of 3:1. Data are reported as the mean of relative expression vs pCtrl \pm s.e.m. ($n=6$). * $P<0.05$ vs pCtrl.

CagA-positive *H. pylori*, small interfering RNA (siRNA) targeting the p65 subunit of NF- κ B was transiently transfected in AGS cells before infection. P65 silencing in transfected AGS cells was confirmed by western blot analysis (Supplementary Figure S2A). Transfection with p65-siRNA did not induce a variation in basal CD44 expression compared with transfection with the non-silencing siRNA (NS-siRNA) control (Supplementary Figure S2B). However, the upregulation of CD44 induced by *H. pylori* infection was reduced in p65-siRNA-infected cells compared with NS-siRNA-infected cells, whereas it remained significant compared with the uninfected control. These results suggest that NF- κ B may have a minor role in *H. pylori*-induced upregulation of CD44 expression. In order to evaluate the signaling pathways such as the MAPK pathway, which is well known to regulate morphological changes and cytoskeleton remodeling, coculture experiments were performed in the presence of specific pharmacological inhibitors targeting the MAPK p38, ERK1/2 and c-Jun N-terminal kinase (JNK). Addition of the different pharmacological inhibitors showed no impact on the basal CD44 expression of AGS cells. Inhibition of ERK (inhibitors PD98059 and U0126) and JNK (SP600125) separately induced a significant reduction in *H. pylori* 7.13-induced CD44 expression, and when

used together, abolished the expression, whereas p38 MAPK inhibition (SB203580) did not, on both AGS and MKN-45 cells (Figure 5b and Supplementary Figure S3C). The inhibition of ERK and JNK was also associated with a significant inhibition of the 'hummingbird' phenotype induced by *H. pylori* 7.13 and, to a lesser extent, with the inhibition of the capacity to form tumorspheres (Figures 5a–c and Supplementary Figures S3B and C). These results suggest that ERK and JNK are involved in *H. pylori* cagA-positive strains and induced EMT-like changes, CD44 overexpression and the ability to form tumorspheres *in vitro*.

CD44^{high} cells and mesenchymal markers related to EMT are detected in *H. pylori*-infected gastric mucosa and dysplastic lesions in humans and mice

To evaluate the *in vivo* relevance of the *H. pylori*-induced EMT-like process, the expression of CD44 and mesenchymal markers was investigated by immunohistochemistry on serial tissue sections of tumors and healthy gastric mucosa tissue samples (distant from the tumor site) from patients who underwent a gastrectomy for gastric adenocarcinoma, and on gastric tissue sections of C57BL/6 mice infected with *H. pylori* and having developed dysplasia, as

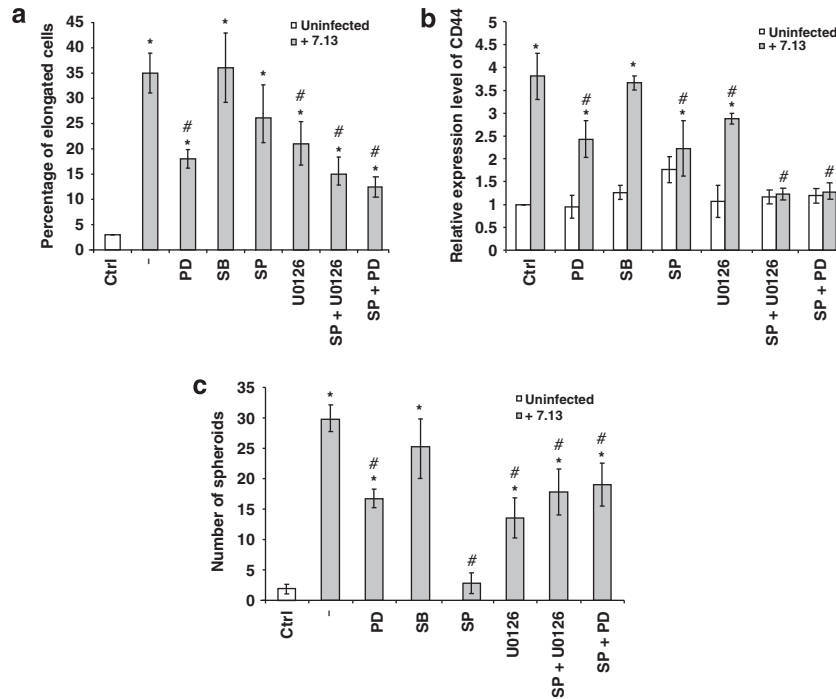


Figure 5. Effects of MAPK inhibition on 'hummingbird' phenotype, CD44 upregulation and tumorsphere formation induced by *H. pylori*. AGS cells were pre-treated (1 h) with inhibitors of ERK (PD98059 and U0126), p38 (SB203580) and JNK (SP600125) alone or combined as indicated and infected with *H. pylori* 7.13 strain for 24 h ($n = 4$). (a) Percentage of AGS cells harboring the 'hummingbird' phenotype at 24 h. (b) Relative CD44 expression quantified using flow cytometry at 24 h ($n = 6$). (c) Number of spheroids formed by cells infected during 24 h and submitted to the spheroid assays for 5 days ($n = 3$). (a–c) Data are reported as mean \pm s.d. * $P < 0.05$ vs Ctrl; # $P < 0.05$ vs 7.13-infected cells.

previously described.²⁴ Results revealed a significantly higher expression of CD44, ZEB1 and Snail in human cases presenting a gastritis associated with *H. pylori* infection compared with *H. pylori*-negative cases (Figure 6a, Supplementary Table S2). In addition, these markers were also overexpressed in dysplastic lesions of *H. pylori*-infected mice and in human gastric adenocarcinoma (Figures 6b and c, Supplementary Table S2).

These results suggest that *H. pylori* infection could promote the development of cells with mesenchymal and stem cell features and properties *in vivo*, which could further initiate gastric CSC and gastric carcinoma development.

DISCUSSION

In this study, we show that *H. pylori* generates CD44^{high} cells that display properties reminiscent of those of CSC, through an EMT-like process. Indeed, when cells are infected with *H. pylori*, mesenchymal markers increase significantly, whereas epithelial markers are downregulated. In this study, we used gastric epithelial cell lines with a basal tumorigenic potential, AGS, MKN-45 and MKN-74, to study their tumorigenic properties in response to *H. pylori* infection. In order to work with cells able to form tumorspheres, Mani *et al.*⁸ used a cell immortalization procedure using oncogenes Ras to make them tumorigenic. Another limit is that primary gastric epithelial cells cannot be easily isolated and cultured, nor can they be amplified *in vitro*. As it has been recently shown that *H. pylori* induces an EMT-like process,^{25,26} our main goal was to determine whether *H. pylori* was implicated in CSC emergence by an EMT. The *cdh1* gene encoding E-cadherin is mutated in AGS cells, and they do not express a functional E-cadherin protein. As a consequence, AGS can be naturally predisposed to encompass the EMT. Interestingly we showed that *H. pylori*-infected AGS cells, and to a lesser extent MKN-45 and MKN-74 cells, are heterogeneous and composed of (1) cells that preserve a polyagonal shaped phenotype similar to

uninfected cells and (2) cells affected by the EMT-like process and harboring the 'hummingbird' phenotype. We showed that *H. pylori* infection induced a strong upregulation of the mesenchymal markers Snail1, ZEB1 and Vimentin, associated with a repression of the expression of epithelial markers other than E-cadherin, including Cytokeratin 7 and Osteopontin, as previously reported.^{25,26} These results confirm that *H. pylori* infection can affect the level of epithelial differentiation. These phenotypic and molecular changes were not observed when cells were infected with *H. pylori cagA*- or *cagE*-deleted mutants, hence they are due to CagA. CagA is already recognized as being responsible for the acquisition of the 'hummingbird' phenotype.²⁷ In this study, we confirmed that *cagA*- and *cagE*-deleted strains did not induce an upregulation of mesenchymal markers. It is also interesting to note that the cells, having acquired the most elongated phenotype, corresponding to the 'hummingbird' phenotype mimicking the EMT presented more mesenchymal markers than the other cells, confirming that 'hummingbird' cells represent cells that have experienced an EMT. Moreover, the 'hummingbird' cells had a very high CD44 expression as shown by immunofluorescence staining (Figure 1). In addition, cells infected with WT *H. pylori* showed higher migration properties and were far more potent in generating tumorspheres than those infected with *H. pylori cagA*- or *cagE*-deleted strains. In addition, the CagA protein was detected at higher levels in 'hummingbird' cells induced by *cagA*-positive *H. pylori* infection of AGS cells *in vitro*. These results suggest that cells are heterogeneous, and that all cells do not respond in the same way to the infection and particularly to CagA. The role of CagA was confirmed by transient transfection with a CagA encoding vector in AGS cells, which was sufficient to generate cells undergoing the 'hummingbird' phenotype while overexpressing mesenchymal markers and CD44. ERK, JNK and to a lesser extent NF- κ B are involved in CagA-induced EMT-like changes and induction of CD44^{high} cells with tumorigenic properties, as their inhibition reduced the effects observed in response to *cagA*-positive

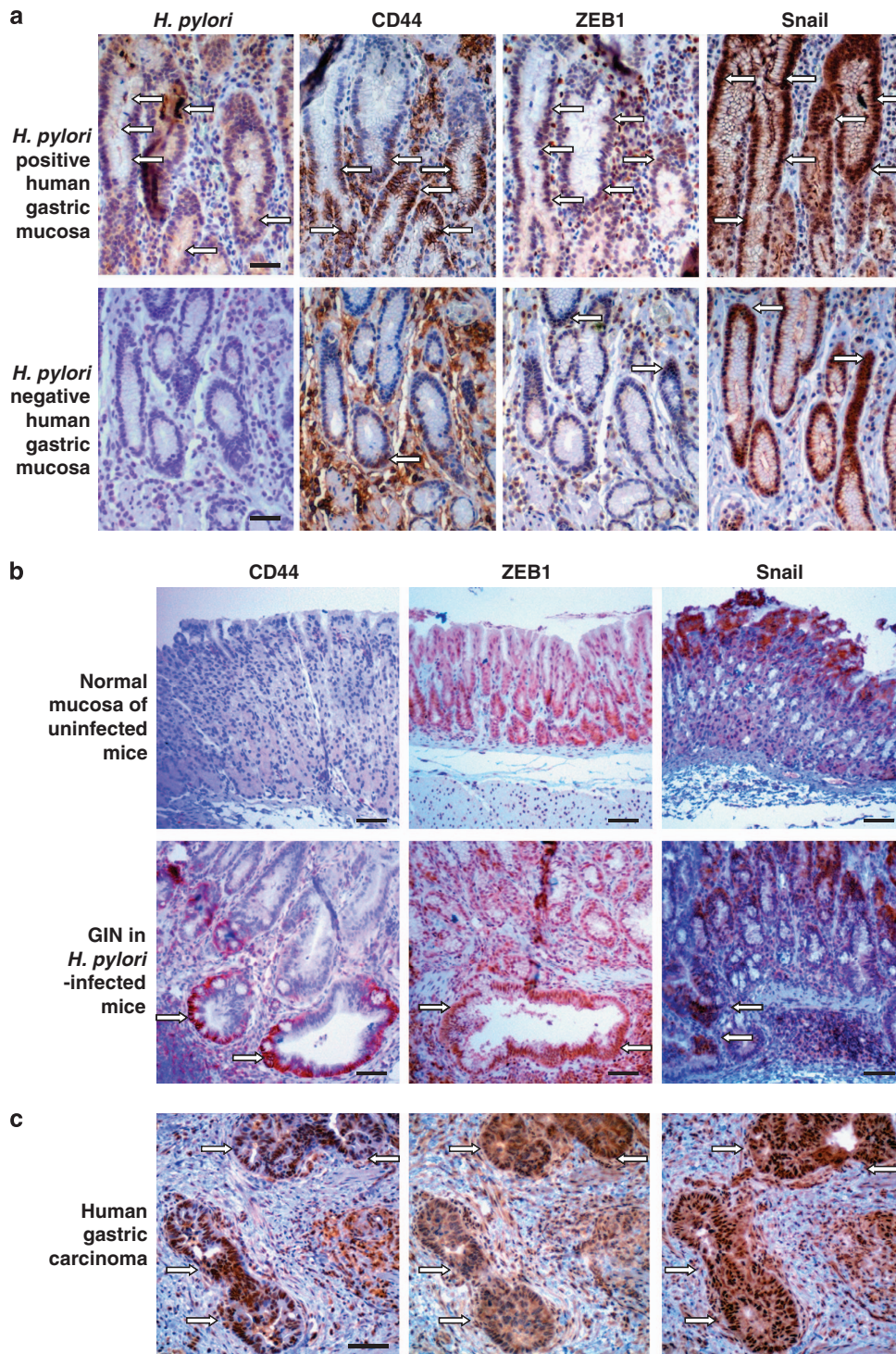


Figure 6. Mesenchymal markers related to EMT and CD44 are expressed in *H. pylori*-infected gastric mucosa and dysplastic lesions in humans and mice. Representative images of immunohistochemistry detection (in brown) of *H. pylori* and the indicated proteins on gastric tissue sections. **(a)** Representative staining on gastric tissue sections from *H. pylori*-negative cases ($n=4$, no gastritis) and *H. pylori*-positive cases ($n=6$, with chronic gastritis), as determined by RT-PCR (data not shown) and immunohistochemistry with anti-*H. pylori* antibodies (first vertical panel). **(b)** Representative staining on gastric tissue sections from C57BL/6 mice after 12 months of infection with *H. pylori* SS1 strain or not (Ctrl). Arrows point to gastrointestinal intraepithelial neoplasia (GIN) with an intense staining of the indicated proteins. **(c)** Representative images obtained with gastric tissue sections from patients with intestinal-type adenocarcinoma ($n=6$). **(a-c)** Arrows indicate an intense staining of the indicated proteins. Scale bars, 50 μm .

H. pylori. Our results combined with those of others with a particular emphasis on CagA-transgenic mice in which CagA overexpression leads to gastric carcinoma development,²⁸ reinforce the role of CagA

as an oncoprotein associated with gastric carcinoma. Previous work performed by Mani *et al.*⁸ and Yang *et al.*²⁹ described EMT induction by transforming growth factor beta 1 (TGF β 1) or by a

sustained expression of Snail or Bmi1, which led to the emergence of CD44^{high}/CD24^{low} cells with breast CSC properties. Contrary to breast epithelial cell lines, all AGS cells expressed CD24 and its expression level was not affected by *H. pylori* infection. Furthermore, only CD44 but not CD24 was identified to be a gastric CSC marker by Takaishi et al.¹⁸ Our results indicate that the CD44^{high} subpopulation of cells induced by infection with CagA-positive *H. pylori* strains share similar properties with CSC in terms of phenotype and ability to migrate, to invade and to form tumorspheres *in vitro* and larger tumors *in vivo* in comparison with their CD44^{low} counterpart. This is a very important finding as *H. pylori* is considered as the major risk factor to develop a gastric carcinoma. In this study, we report for the first time that *H. pylori*, and more precisely CagA, is responsible for the emergence of cells with CSC properties. EMT cannot be observed *in vivo* as in an *in vitro* model, but we confirmed that CD44 and the mesenchymal markers ZEB1 and Snail are overexpressed in epithelial cells of the gastric mucosa of *H. pylori*-infected patients. These overexpressions were detected in the upper part of the gastric mucosa that *H. pylori* colonizes, and particularly the isthmus region where local epithelial stem cells reside. The appearance of epithelial cells that overexpress CD44 and mesenchymal markers in chronic *H. pylori* infection as compared with normal healthy gastric mucosa suggests that these cells could correspond to an extension of the stem cell compartment leading to an incomplete and/or altered differentiation status. These markers were also detected in *H. pylori*-induced gastric dysplasia in experimentally infected mice, suggesting that the relationship observed *in vitro* also exists *in vivo* between chronic *H. pylori* infection and the emergence of cells expressing CD44 and mesenchymal markers. CD44^{high} cells and mesenchymal markers were also observed in carcinoma cells in human gastric adenocarcinoma, suggesting that gastric dysplasia and carcinoma could originate from these CD44^{high} cells. Indeed, the expansion of these cells, which may be naturally present in the gastric mucosa and associated with the acquisition of mesenchymal features in the context of a chronic infection and inflammation induced by CagA-positive *H. pylori* strains, could predispose them to transform and to generate CSCs. Further work is necessary to determine whether the detection of CD44^{high} positive cells can be correlated to gastric disease progression in *H. pylori*-infected patients. In conclusion, we report for the first time, that infection with an *H. pylori* CagA-positive strain induces EMT-like changes and the emergence of CD44^{high} cells with CSC properties. This effect was linked to CagA. Our results, combined with those of others, allow a better understanding of the cellular mechanisms involved in response to the oncogenic properties of CagA during *H. pylori* infection.

MATERIALS AND METHODS

Epithelial cell culture

Adenocarcinoma gastric epithelial cell lines AGS, MKN-45 and MKN-74 were cultured in DMEM/F12 Glutamax or RPMI1640 Glutamax media, respectively, with 10% fetal bovine serum and 50 µg/ml vancomycin (all from Invitrogen, Cergy-Pontoise, France), as previously described.³⁰

Bacterial culture

H. pylori 7.13 WT and knock-out strains (Δ cagA and Δ cagE) were obtained from R. Peek (Vanderbilt University, Nashville, TN, USA).³¹ Culture of *H. pylori* strains and coculture experiments were performed as previously described.^{24,30,32} Cocultures were performed at a MOI of 50 (unless otherwise specified) for 24 h at 37 °C in a humidified 5% CO₂ atmosphere before analysis.

Flow cytometry analysis

Cells were recovered and 100 000 cells per condition were stained with anti-CD44-APC and anti-CD24-PE antibodies (1:25 each, BD Pharmingen,

San Jose, CA, USA) in PBS, 0.5% bovine serum albumin, 2 mM EDTA solution. Flow cytometry was performed using a FACScan instrument and DIVA software (both from Becton Dickinson, Le Pont de Claix, France). Results were based on the analysis of 10 000 cells.

For cell sorting, cells were triple stained for CD44, CD24 (positive control) and DAPI (to exclude positive dead cells), and sorted according to their CD44 expression level on a FACSria (Becton Dickinson).

Migration and invasion assays

Cells were recovered and 50 000 cells per condition were placed in the upper side of a 8-µm pore size Transwell insert in 24-well culture plates with medium containing 5% fetal bovine serum. For invasion assays, inserts were prealably coated with 0.05 mg/ml rat type I collagen (BD Biosciences, Le Pont de Claix, France) for 40 min at 37 °C. After 18 h of incubation at 37 °C, the Transwell inserts were fixed in cold methanol and processed for hematoxylin staining, as described previously.³² Cells having migrated through the lower side of the inserts were counted on five different randomly chosen fields per insert under light microscopy using a × 20 objective.

Spheroid colony formation

Cells were recovered and 500 cells were plated on non-adherent 96-well culture plates (coated with a 10% polyHEMA (Sigma, Saint-Quentin Fallavier, France) solution in absolute ethanol and dried overnight at 56 °C). After plating, cells were incubated for 5 days at 37 °C in a serum-free medium consisting of DMEM-F12 Glutamax supplemented with 20 ng/ml of EGF, 10 ng/ml of basic-FGF, 1:100 N₂-supplement 100x, 0.3% glucose, 5 µg/ml of gentamicin, 50 IU/ml of penicillin and 2.5 µg/ml of amphotericin B (all from Invitrogen and Sigma). The number of spheroids per well was counted under light microscopy using a × 20 objective.

Transfection

Cells were transfected with plasmids using Lipofectamine 2000 (Invitrogen) following the manufacturer's instructions. The pSP65SRα plasmid containing the cagA gene of *H. pylori* strain NCTC11637 fused to a HA tag was used for transient expression of CagA.³³ The pSP65SRα empty plasmid and the pEGFP plasmid encoding the GFP (Clontech, provided by V. Moreau, INSERM U889, Bordeaux, France) were used as negative or positive controls of transfection, respectively.

Pharmacological inhibitors and siRNA transfection

For signaling pathway targeting, selective inhibitors of ERK MAPK (PD98059, 50 µM and U0126, 25 µM; Invivogen, Toulouse, France), p38 MAPK (SB203580 40 µM, provided by E. Génot, INSERM U889, Bordeaux, France,) and JNK (SP600125 25 µM, provided by E. Chevet, INSERM U889, Bordeaux, France,) were added to AGS cells 1 h before infection. Transfection of siRNA and western blotting experiments were performed as described previously³⁰ and included in the Supplementary Materials and methods.

Human and mouse gastric tissues

Gastric tissue samples from consenting patients (male and female, aged 68–85-year old) undergoing gastrectomy for distant non-cardia gastric adenocarcinoma were included in the study, in agreement with the tumor bank of the Bordeaux University Hospital Center (France). Tumors (intestinal-type adenocarcinoma according to Lauren's classification criteria, moderately differentiated and invading (T3, TNM7 staging criteria) or perforating subserosa and invading adjacent structures (T4b), with lymph node invasion (N1 to N3b)) and healthy gastric mucosa distant from the tumor site, and presenting a normal histology or a gastritis associated to a positive *H. pylori* detection were studied.

The stomachs of C57BL/6 mice experimentally infected with *H. pylori* SS1 strain for 12 months as previously described,²⁴ were studied.

See Supplementary Materials and methods for RNA extraction and quantitative RT-PCR, *H. pylori* detection on human gastric tissues, siRNA transfection, western blotting, use of pharmacological inhibitors, immunohistochemistry and immunofluorescence procedures and antibodies and statistical analyses.

CONFLICT OF INTEREST

The authors declare no conflict of interest.

ACKNOWLEDGEMENTS

This project was supported by the French 'Association pour la Recherche contre le Cancer' (grant number 8412), 'Institut du Cancer' (grant number 07/3D1616/IABC-23-12/NC-NG), 'Conseil Regional d'Aquitaine' (grant number 20071301017 and 20081302203). We thank D Collet (Digestive Surgery of Hospital Haut-Lévêque, University Hospital Center of Bordeaux, France) and Professor JP Merlio (Tumor Bank of University Hospital Center of Bordeaux, France) for providing human gastric tissue samples from consenting patients. We thank A Giese (EA2406, Bordeaux, France), B Rousseau (level 2 animal facilities, Université de Bordeaux), V Pitard and S Gonzalez (cytometry platform, Université de Bordeaux), A Ménard, M Alibert, E Siffre and L Biguet for technical support.

REFERENCES

- 1 IARC Working Group. *Schistosomes, liver flukes and Helicobacter pylori: Views and expert opinion of IARC Working Group on the evaluation of carcinogenic risks to humans*. IARC Monographs (International Agency for Research on Cancer): Lyon, France 1994; **61**: 177–240.
- 2 Blaser MJ, Perez-Perez GI, Kleanthous H, Cover TL, Peek RM, Chyou PH et al. Infection with *Helicobacter pylori* strains possessing CagA is associated with an increased risk of developing adenocarcinoma of the stomach. *Cancer Res* 1995; **55**: 2111–2115.
- 3 Gwack J, Shin A, Kim CS, Ko KP, Kim Y, Jun JK et al. CagA-producing *Helicobacter pylori* and increased risk of gastric cancer: a nested case-control study in Korea. *Br J Cancer* 2006; **95**: 639–641.
- 4 Murata-Kamiya N, Kurashima Y, Teishikata Y, Yamahashi Y, Saito Y, Higashi H et al. *Helicobacter pylori* CagA interacts with E-cadherin and deregulates the beta-catenin signal that promotes intestinal transdifferentiation in gastric epithelial cells. *Oncogene* 2007; **26**: 4617–4626.
- 5 Amieva MR, Vogelmann R, Covacci A, Tompkins LS, Nelson WJ, Falkow S. Disruption of the epithelial apical-junctional complex by *Helicobacter pylori* CagA. *Science* 2003; **300**: 1430–1434.
- 6 Backert S, Selbach M. Role of type IV secretion in *Helicobacter pylori* pathogenesis. *Cell Microbiol* 2008; **10**: 1573–1581.
- 7 Guarino M, Rubino B, Ballabio G. The role of epithelial-mesenchymal transition in cancer pathology. *Pathology* 2007; **39**: 305–318.
- 8 Mani SA, Guo W, Liao MJ, Eaton EN, Ayyanan A, Zhou AY et al. The epithelial-mesenchymal transition generates cells with properties of stem cells. *Cell* 2008; **133**: 704–715.
- 9 Morel AP, Lievre M, Thomas C, Hinkal G, Ansieau S, Puisieux A. Generation of breast cancer stem cells through epithelial-mesenchymal transition. *PLoS One* 2008; **3**: e2888.
- 10 Al-Hajj M, Wicha MS, Benito-Hernandez A, Morrison SJ, Clarke MF. Prospective identification of tumorigenic breast cancer cells. *Proc Natl Acad Sci USA* 2003; **100**: 3983–3988.
- 11 Bellizzi A, Sebastian S, Ceglia P, Centonze M, Divella R, Manzillo EF et al. Co-expression of CD133(+) /CD44(+) in human colon cancer and liver metastasis. *J Cell Physiol* 2012; **228**: 408–155.
- 12 Hao J, Madigan MC, Khatri A, Power CA, Hung TT, Beretov J et al. In vitro and in vivo prostate cancer metastasis and chemoresistance can be modulated by expression of either CD44 or CD147. *PLoS One* 2012; **7**: e40716.
- 13 Kure S, Matsuda Y, Hagio M, Ueda J, Naito Z, Ishiwata T. Expression of cancer stem cell markers in pancreatic intraepithelial neoplasias and pancreatic ductal adenocarcinomas. *Int J Oncol* 2012; **41**: 1314–1324.
- 14 Meng E, Long B, Sullivan P, McClellan S, Finan MA, Reed E et al. CD44+ /CD24- ovarian cancer cells demonstrate cancer stem cell properties and correlate to survival. *Clin Exp Metastasis* 2012; **29**: 939–948.

- 15 O'Brien CA, Pollett A, Gallinger S, Dick JE. A human colon cancer cell capable of initiating tumour growth in immunodeficient mice. *Nature* 2007; **445**: 106–110.
- 16 Ricci-Vitiani L, Lombardi DG, Pilozzi E, Biffoni M, Todaro M, Peschle C et al. Identification and expansion of human colon-cancer-initiating cells. *Nature* 2007; **445**: 111–115.
- 17 Su YJ, Lai HM, Chang YW, Chen GY, Lee JL. Direct reprogramming of stem cell properties in colon cancer cells by CD44. *EMBO J* 2011; **30**: 3186–3199.
- 18 Takaishi S, Okumura T, Tu S, Wang SS, Shibata W, Vigneshwaran R et al. Identification of gastric cancer stem cells using the cell surface marker CD44. *Stem Cells* 2009; **27**: 1006–1020.
- 19 Klarman GJ, Hurt EM, Mathews LA, Zhang X, Duhagon MA, Mistree T et al. Invasive prostate cancer cells are tumor initiating cells that have a stem cell-like genomic signature. *Clin Exp Metastasis* 2009; **26**: 433–446.
- 20 Li C, Lee CJ, Simeone DM. Identification of human pancreatic cancer stem cells. *Methods Mol Biol* 2009; **568**: 161–173.
- 21 Viala J, Chaput C, Boneca IG, Cardona A, Girardin SE, Moran AP et al. Nod1 responds to peptidoglycan delivered by the *Helicobacter pylori* cag pathogenicity island. *Nat Immunol* 2004; **5**: 1166–1174.
- 22 Mitsuno Y, Yoshida H, Maeda S, Ogura K, Hirata Y, Kawabe T et al. *Helicobacter pylori* induced transactivation of SRE and AP-1 through the ERK signalling pathway in gastric cancer cells. *Gut* 2001; **49**: 18–22.
- 23 Saito Y, Murata-Kamiya N, Hirayama T, Ohba Y, Hatakeyama M. Conversion of *Helicobacter pylori* CagA from senescence inducer to oncogenic driver through polarity-dependent regulation of p21. *J Exp Med* 2010; **207**: 2157–2174.
- 24 Varon C, Dubus P, Mazurier F, Asencio C, Chambonnier L, Ferrand J et al. *Helicobacter pylori* infection recruits bone marrow-derived cells that participate in gastric preneoplasia in mice. *Gastroenterology* 2012; **142**: 281–291.
- 25 Baud J, Varon C, Chabas S, Chambonnier L, Darfeuille F, Staedel C. *Helicobacter pylori* initiates a mesenchymal transition through ZEB1 in gastric epithelial cells. *PLoS One* 2013; **8**: e60315.
- 26 Yin Y, Grabowska AM, Clarke PA, Whelband E, Robinson K, Argent RH et al. *Helicobacter pylori* potentiates epithelial:mesenchymal transition in gastric cancer: links to soluble HB-EGF, gastrin and matrix metalloproteinase-7. *Gut* 2010; **59**: 1037–1045.
- 27 Backert S, Moese S, Selbach M, Brinkmann V, Meyer TF. Phosphorylation of tyrosine 972 of the *Helicobacter pylori* CagA protein is essential for induction of a scattering phenotype in gastric epithelial cells. *Mol Microbiol* 2001; **42**: 631–644.
- 28 Ohnishi N, Yuasa H, Tanaka S, Sawa H, Miura M, Matsui A et al. Transgenic expression of *Helicobacter pylori* CagA induces gastrointestinal and hematopoietic neoplasms in mouse. *Proc Natl Acad Sci USA* 2008; **105**: 1003–1008.
- 29 Yang MH, Hsu DS, Wang HW, Wang HJ, Lan HY, Yang WH et al. Bmi1 is essential in Twist1-induced epithelial-mesenchymal transition. *Nat Cell Biol* 2010; **12**: 982–992.
- 30 Varon C, Duriez A, Lehours P, Menard A, Laye S, Zerbib F et al. Study of *Helicobacter pullorum* proinflammatory properties on human epithelial cells *in vitro*. *Gut* 2009; **58**: 629–635.
- 31 Franco AT, Johnston E, Krishna U, Yamaoka Y, Israel DA, Nagy TA et al. Regulation of gastric carcinogenesis by *Helicobacter pylori* virulence factors. *Cancer Res* 2008; **68**: 379–387.
- 32 Ferrand J, Lehours P, Schmid-Alliana A, Mégraud F, Varon C. *Helicobacter pylori* infection of gastrointestinal epithelial cells *in vitro* induces mesenchymal stem cell migration through an NF-kappaB-dependent pathway. *PLoS One* 2011; **6**: e29007.
- 33 Higashi H, Tsutsumi R, Muto S, Sugiyama T, Azuma T, Asaka M et al. SHP-2 tyrosine phosphatase as an intracellular target of *Helicobacter pylori* CagA protein. *Science* 2002; **295**: 683–686.

Supplementary Information accompanies this paper on the Oncogene website (<http://www.nature.com/onc>)

Article 4 – Inhibition of gastric tumor cell growth using seed-targeting LNA as specific, long-lasting microRNA inhibitors.

In revision for Molecular Therapy – Nucleic Acids

De : mtna@molther.org
Objet : 2015MTNA000115 Decision Letter
Date : 19 janvier 2015 19:30:51 HNEC
À : cathy.staedel@inserm.fr
Cc : jrossi@coh.org, mtna@molther.org
Répondre à : mtna@molther.org

19th Jan 2015

Dear Dr STAEDEL:

Thank you for allowing us to review your manuscript 2015MTNA000115 entitled "Inhibition of gastric tumor cell growth using seed-targeting LNA as specific, long-lasting microRNA inhibitors." Your manuscript has been through peer review (see comments at the bottom of this message). While the reviewers found the work of potential interest, important concerns have been raised that preclude publication, at least at this time. We would like to request that you prepare a revision in response to the comments below, which will need to be seen again by one or more of the reviewers.

If you choose to submit the revision, please do so by clicking on the link provided below. Please DO NOT click on this link until you are actually ready to submit:

<http://mts-mtna.nature.com/cgi-bin/main.plex?el=A7CP5IK7A3Rvd4I5A9ftdTeFvsFrybRQ4gI84u0yd1wZ>

** Please remember to include your response to the reviewers' comments in an accompanying letter. If you disagree with any of the points raised by the referee/referees, then please provide adequate justification in your letter. You also have the option to withdraw your paper and submit it elsewhere, in which case we should be notified. However if you choose to revise it and resubmit it here, we will be pleased to consider the manuscript further.

Authors of accepted peer-reviewed articles must pay an article processing charge in order for their article to be published Open Access.

The article processing charge is a one-off payment of £1700/\$2500/€2137 for manuscripts with a first or corresponding/senior author who is an Active ASGCT member or £2500/\$3200/€2900 for manuscripts with a first or corresponding/senior author who is a non-ASGCT or associate member. This is plus VAT where applicable.

Your membership status is determined by a query to the ASGCT membership database at the time of acceptance. If not already a member, you are encouraged to become one; or, if a member, renew your membership when you submit your manuscript. You also have the option to do this immediately following acceptance (but PRIOR to online publication), although registration/ renewal following acceptance must also be flagged via an email to rzimmer@asgct.org.

Thank you for your interest in Molecular Therapy-Nucleic Acids.

With best regards,

Robert M. Frederickson, Ph.D.
Editor
Molecular Therapy-Nucleic Acids
214 Summit Avenue East, Suite 302
Seattle, WA 98102
206-724-7760
editor@molther.org

John J. Rossi, Ph.D.
Editor in chief
Molecular Therapy-Nucleic Acids
Dept. of Molecular and Cellular Biology
Beckman Research Institute of the City of Hope
Duarte, CA 91010

Reviewer #1 (Comments to the Author):

This paper by Staedel, et al., examines LNA phosphorothioate anti-miR oligos of only 8mer in length, and shows they are active in upregulating LATS2 in human tumor xenografts. I have a number of minor and major comments.

p. 1 "passive uptake" I've never heard this term used before and whatever is involved in uptake, it is definitely not passive. The same term is used on p. 5 in the first paragraph. Uptake can, however, be "gymnotic", or sometimes the word "free" has been used. It is never passive.

p.2 "TL155 raised against the miR-155 oncomir....." Do the authors mean targeted against?

The authors should specify their chemistry more carefully. Are these oligos all-LNA, meaning an LNA moiety at each sugar? Not that this is a criticism, but this is a rather odd chemistry for an anti-miR oligo, which are usually mix-mers (i.e., alternating DNA-LNA). It would be interesting to know what the T_m is of the heteroduplex formed between the 8mer anti-miR oligo and the microRNA. The amount that each LNA can raise the T_m is variable, and can range from 2-3°C to 6°C. But a priori, without a determination of T_m , there is no way to tell. To further complicate matters, the PS moieties will depress the T_m . The determination of T_m is not a difficult experiment to do (but the authors should be reminded to perform it in sodium arsenate buffer, which does not change ionic strength with increasing temperature, as sodium chloride buffer does. Further, I would like to add one additional comment-vive la France. All America is with you. Nous somme Charlie).

Fig. 1C; The 1 nM concentration can probably be eliminated.

p. 6 I do not see any evidence for the assertion that "TL372 also partly retains miR93..." Similarly, I do not see the evidence that "TL17 forms a stable heteroduplex with miR93....."

In my version, the "smeary duplex with miR 373" may or may not be present. There is a smear in Fig 1C with miR17 and TL372, however. Perhaps that is what the authors are referring to.

Fig 2C: This is a very poor quality Western. How many times was this experiment performed?

p. 7: The authors should note that just because the data in Fig. 2E shows diminished cell growth, that does not mean that the effect on cell growth is specific. LNA phosphorothioate oligos can bind to proteins, and given that the anti-miR oligos are all- LNA, they can bind to a number of other targets as well, both miR and mRNA. This may produce numerous off-target effects that can contribute to diminished rates of cell growth. The same is true in Fig. 3A. The TLCo may be having a effect at slowing growth, but by how much is not certain as the authors have not shown us tumor growth in the absence of any oligonucleotide treatment.

p. 8 "subcutaneously injected at the tumor periphery..." Why not IP or by tail vein intravenous injection?

Fig 3B: Why in the AGS-Mut372 line, when treated with TL, does luciferase expression decrease? I thought this line is insensitive to the miR372/3. Am I missing something? In any event, the data in this figure seems rather weak.

P. 9: "the northern blot clearly shows a slower migrating miR372/TL372 heteroduplex..." Yes, it does show that, but the question is how it got that way. The oligo may in the cells but sequestered in vesicles. As the cells are broken up and their contents mixed, the anti-miR oligo are now free to bind to their miR targets. This is a real problem in oligo biology, i.e., experiments not done in real time with cell fractionations. While I like the experiments in 4c and 4d, and they do suggest the authors are correct, a strict comparison nevertheless cannot be made.

Fig 5 A: It is difficult to know what to make of experiments in Fig. 5A that have an n =5 and overlapping SDs.

Reviewer #2 (Comments to the Author):

Dear Editor

This manuscript describes a series of logical and straight forward experiments regarding tiny LNAs targetting the seed region of the mir 372 and mir 373. The authors show that these seed targetting LNAs may be used as research tool to study oncomirs and maybe can be used in therapeutic strategies in the future,

This work is within the scope and acceptable for publication in MTNA with some minor revisions.

1: Please provide information about the purity of the LNAs used. Please provide data using HPLC or MALDI of the actual batches used to show purity of LNA. Only desalting as is done here can result in relatively low purities causing side effects and or lower amounts/dosages of

functional LNA oligo than anticipated. In general >90% purity (preferably >95%) is needed for in vivo work in my opinion

2: TL372+373 (page 7 and further); Is this an equimolar mix of the two LNAs? Please provide information in text.

3: Figures general remark: Make sure you provide the units of measurements for the axis. This is sometimes missing (fig 5A)

Figures 3 and 4 : Double labeling of figures with two letters can be confusing: For instance you have a Figure 3Ca and a 3Cd or a 4Ad etc. Maybe you should try a different labeling strategy.

4: What types of control experiments were done for the in situ hybridizations? There are no control experiments specified in manuscript. Please provide this information.

Inhibition of gastric tumor cell growth using seed-targeting tiny LNA as microRNA inhibitors

Cathy Staedel¹, Christine Varon², Phu Hung Nguyen², Brune Vialet¹, Lucie Chambonnier², Benoît Rousseau³, Isabelle Soubeyran⁴, Serge Evrard⁵, Franck Couillaud⁶ and Fabien Darfeuille¹

1 Univ. Bordeaux, ARNA Laboratory, F-33000 Bordeaux, France; INSERM, U869, ARNA Laboratory, F-33000 Bordeaux, France

2 Univ. Bordeaux, Laboratoire de Bactériologie, F-33000 Bordeaux, France; INSERM, U853, , F-33000 Bordeaux, France

3 Univ. Bordeaux, Service commun des animaleries, A2 animal facilities, F-33000 Bordeaux, France

4 Department of Biopathology, Institut Bergonié, Bordeaux, France ; INSERM U916, Institut Bergonié, Bordeaux, France.

5 Digestive Tumors Unit, Institut Bergonié, 33076 Bordeaux Cedex, France;

6 Univ. Bordeaux, Résonance Magnétique des Systèmes Biologiques, F-33000 Bordeaux, France; UMR CNRS 5536, Résonance Magnétique des Systèmes Biologiques, F-33000 Bordeaux, France

Correspondance to Drs Cathy Staedel and/or Fabien Darfeuille, Université de Bordeaux, INSERM U869, F-33076 Bordeaux Cedex, France. cathy.staedel@inserm.fr and fabien.darfeuille@inserm.fr

ABSTRACT

Small non-coding microRNAs (miRNAs) regulate eukaryotic gene expression upon pairing onto target mRNAs, subsequently inhibiting their translation. The targeting of mRNAs by miRNAs is influenced by the complementarity between the “seed” sequence at the 5′ end of the miRNA and the seed-matching sequences in the mRNA. Here, we assess the efficiency and specificity of 8-mer locked nucleic acid (LNA)-modified oligonucleotides raised against the seed of miR-372 and miR-373, two embryonic stem cell-specific miRNAs prominently expressed in the human gastric adenocarcinoma AGS cell line. These tiny antimiRs inhibit miR-372/373 functions and de-repress their common target, the cell cycle regulator LATS2. They are able to decrease cell proliferation *in vitro* upon either transfection at nanomolar concentrations or passive uptake at micromolar concentrations. Subcutaneously delivered 8-mer seed-targeting LNAs reduce tumor growth of AGS xenografts in mice, upon formation of a stable, specific heteroduplex with the targeted miRNA and LATS2 upregulation. The therapeutic potential of these tiny antimiRs is confirmed in fast-growing, miR-372-positive primary human gastric adenocarcinoma xenografts in mice. Thus, miRNA silencing by 8-mer seed-targeting LNAs appears a valuable approach for both loss-of-function studies aimed at elucidating miRNA functions and for miRNA-based therapeutic strategies.

INTRODUCTION

MicroRNAs (miRNAs) are small, evolutionarily conserved, non-coding RNAs of approximately 22 nucleotides in length, which are prominently involved in gene regulation in nearly every biological process. Thirty thousands of mature miRNA sequences have been identified in multiple organisms and deposited into the miRBase database (<http://www.mirbase.org/>). MiRNA bind to partly complementary sequences preferentially located in the 3'-untranslated region (3' UTR) of mRNAs of target genes. For most miRNAs, the targeting of cognate mRNAs is strongly influenced by the complementarity between the short 'seed' sequence at nucleotides 2–8 at the 5' end of the miRNA and the seed matching sequences contained in the mRNA. The pairing of a miRNA onto target mRNAs most often decreases the mRNA translation and stability, subsequently leading to decreased production of the target protein (1). MiRNAs sharing the same seed sequence are grouped into families and are theorized to target overlapping sets of genes.

Perturbations in miRNA biogenesis or expression contribute to diseases, including cancer, immune pathologies or infection. The widespread alterations in the miRNA profiles are ubiquitous features of cancer and affect all steps of the malignant phenotype from cellular transformation to tumor progression. In the same way as protein-coding genes, some miRNA behave as cancer “drivers” (the so-called oncomirs) or tumor suppressors depending on the cellular context in which they are expressed (2).

The involvement of deregulated miRNA expression in the malignant phenotype prompts the exploitation of miRNAs as anti-cancer therapeutic targets. Numerous studies have demonstrated the utility of inhibiting miRNAs using complementary anti-miRNA oligonucleotides, also called antimiRs. AntimiRs sequester the miRNA in competition with target mRNAs, leading to functional inhibition of the miRNA and de-repression of the direct targets. AntimiR-mediated miRNA inhibition requires optimization of the oligonucleotides for increased binding affinity, improved nuclease resistance and efficient *in vivo* delivery. This can be achieved using a variety of chemical modifications, which show particular promise *in vivo*. In most studies, fully complementary 22-mer antimiRs have been used to target the mature miRNA. Introduction of locked nucleic acids (LNA), in which the furanose ring in the sugar-phosphate backbone is chemically locked in a RNA mimicking N-type (C3'-endo) conformation by a 2'-O,4'-C methylene bridge, into an antisense sequence dramatically enhances its affinity for the target (3). Thus, an efficient antagonism of several miRNAs has been reported using either high affinity 15-16-mer LNA/DNA antimiRs targeting the 5' region of the mature miRNA, or even 12-14-mer seed-directed LNA

oligonucleotides with a phosphodiester backbone (4). Furthermore, the outstanding binding affinity of LNAs has been exploited in an approach using 8-mer LNA-phosphorothioate oligonucleotides complementary to the miRNA seed sequence (5). These 8-mer oligos, designated as tiny LNAs (TL), enable specific inhibition of miRNA function with concomitant de-repression of direct targets in cultured cells. In an orthotopic mouse model of breast tumor xenografts, unconjugated anti-miR-21 TL21 efficiently reached the miR-21 oncomir within the tumors upon systemic injection and de-repressed one of its target, the tumor suppressor PDCD4 (5). This strategy has been thereafter successfully applied to other miRNA-associated diseases. TL21 are able to reduce autoimmune splenomegaly in lupus mice (6). TL155 raised against the miR-155 oncomir inhibit the tumor growth in a mouse xenograft model of a B-cell lympho-proliferative disease (7). TL17 and TL19 targeting the miRNA seed family expressed by the oncogenic miR-17~92 and miR-106b~25 clusters inhibit medulloblastoma growth *in vivo* and prolong mice survival (8). TL33 targeting the miR-33 family, which regulates lipid/cholesterol homeostasis, increase circulating high-density lipoprotein cholesterol at long-term in obese and insulin-resistant nonhuman primates (9). Altogether, these data stress the potential of these tiny oligonucleotides in the therapeutic targeting of aberrantly expressed miRNAs.

We previously reported that the human gastric adenocarcinoma-derived AGS cell line express high levels of miR-372, which confer an active proliferation rate to these cells (10). MiR-372 belongs to the miRNA-371-372-373 (miR-371-373) cluster, originally found to be specifically expressed in human embryonic stem cells (11) and involved in both stem cell pluripotency and cell cycle regulation (12; 13). In this cluster, miR-372 and miR-373 are homologous and likely target the same protein-coding genes. The miR-371-373 cluster is frequently deregulated in some human tumors, leading to high expression of miR-372 and -373 in testicular germ cell tumors (14; 15), esophageal carcinoma (16), thyroid adenoma (17), hepatoblastoma (18), colorectal carcinoma (19) and gastric carcinoma (20). The oncogenic role of this miRNA cluster has been defined through the identification of some of the miR-372 and -373 targets, which are silenced in tumor cells expressing high levels of these miRNAs: the tumor suppressor protein kinase *ecrite en entier* (LATS2) regulating cell cycle progression (14; 16; 10), the hyaluronic acid receptor CD44 regulating tumor invasion and metastasis (21), the *écriture en entier* Transforming Growth Factor β Receptor 2 (TGF β R2), which upon TGF β binding controls cell growth and promotes epithelial to mesenchymal transition (22), or else the tumor necrosis factor α -induced protein 1 (TNFAIP1) involved in the regulation of the *écriture en entier* (NF- κ B) signaling pathway (20). Besides, miR-372 and

miR-373 belong to the miR-17 family along with miR-17-5p, miR-20a, miR-106b and miR-93 (Table 1). All these miRNAs harbor similar seed sequence (23)(Table 1) and share similar cell growth stimulating functions.

Based on both the efficient silencing of miRNA families by seed-targeting tiny LNAs (5) and our previous results on the high miR-372 and -373 expression in the human gastric adenocarcinoma AGS cells (10), the present work aims at applying this anti-miR approach to inhibit gastric adenocarcinoma cell growth both *in vitro* and *in vivo*. We report here that tiny LNAs targeting miR-372 and -373 seeds are as efficient as full-length anti-miR-372/373 oligonucleotides upon transfection to antagonize the function of these oncomirs in cultured AGS cells, de-repress LATS2 and subsequently inhibit their growth rate. They enter passively into cultured cells at micromolar concentrations to achieve cell growth inhibition. Moreover, they are able to specifically sequester their target miRNAs within tumor cells in AGS xenografts in mice and impair tumor growth. Their anti-tumor effect is particularly noticeable in fast-growing primary human gastric adenocarcinoma xenografts in mice.

MATERIAL AND METHODS

Synthesis of LNA oligonucleotides. LNA oligonucleotides were synthesized on an automated Expedite 8909 DNA synthesizer. The LNA phosphoramidite solutions were prepared with commercially available LNA-amidites (ABz, Gdmf, mCBz, T) from Exiqon and diluted in anhydrous acetonitrile (Glen Research) and 25% of tetrahydrofuran (Sigma) for LNA-mCBz. DNA SynBase CPG (1000Å, loading 60-100µmol/g, Link Technologies) were used as solid supports. The oligonucleotides were synthesized with a phosphorothioate backbone, using Sulfurizing Reagent II (Glen Research). After the synthesis the oligonucleotides were cleaved from the supports and the nucleobases were deprotected with ammonium hydroxide at 55°C for 4h. The tiny LNA were then desalted and concentrated by 85% ethanol precipitation. Concentrations were determined by absorbance at 260 nm and the respective molar extinction coefficient.

Cell culture. All the tissue culture reagents were from Invitrogen. AGS gastric epithelial cell line (ATCC CRL 1739) was routinely grown in DMEM/F-12 medium, supplemented with 10% heat-inactivated fetal bovine serum (FBS) and 2 mM L-glutamine at 37°C in a humidified 5% CO₂ atmosphere.

RNA extraction. Total RNA was extracted using Trizol reagent (Invitrogen), according to the manufacturer's protocol. Trizol was directly added onto the drained cell layers in cell culture wells, or onto the resected tumor pieces in a 2-mL Eppendorf tube containing a 5 mm steel bead. The tumor was completely disrupted after 90 sec at 30 Hz in a Tissue-Lyser (Qiagen). RNA concentrations were determined using a NanoDrop spectrophotometer (NanoDrop Technologies, Inc.). RNA quality was analyzed on a 2100 Bioanalyzer (Agilent Technologies).

Quantitative RT-PCR. Total RNA (500 ng) was retro-transcribed in 10 µL using the miScript Reverse Transcription kit (Qiagen), according to the manufacturer's instructions. Mature miRNA expressions were quantified on 1/200 RT reaction volume by real-time PCR using the 2x Quantitect SYBR Green PCR Master mix (Qiagen) with universal and miRNA-specific primers (both from Qiagen). Real-time PCRs were run on ROTORGENE (Qiagen). MiRNAs levels were normalized to the small non-coding RNA snor25 and U6, using the comparative Ct method.

Northern blots. Total RNA (10 µg) was resolved on a 20% denaturing polyacrylamide gel in 1X TBE and blotted onto nylon membranes (Hybond-N, GE Healthcare) according to standard procedures. Membranes were incubated with 5'-³²P-radiolabelled LNA/DNA anti-miRNA probes (Table S1) in 50% formamide, 5X SSPE, 5X Denhardt solution, 0.5% SDS, 20 µg/mL salmon sperm DNA, at 42°C overnight in a hybridization oven. After two washes for 5 min each in 2X SSC, 0.1% SDS at 42°C, blots were analyzed by phospho-imaging (Molecular imager PharosFXplus, Biorad).

Luciferase reporter systems. The pGL3 and pRL-SV40 vectors harboring the firefly luciferase and the *Renilla* luciferase coding sequences, respectively, under the control of the SV40 promoter were from Promega. The pGL3-3'UTR-LATS2wt and pGL3-3'UTR-LATS2mut constructs were kindly provided by R. Agami (Amsterdam, The Netherlands) (14). The pGL4-PM372 and pGL4-mut372 vectors were obtained upon the following cloning steps on the basis of the pGL4.15 vector (Promega) backbone harboring the firefly luciferase and hygromycin B phosphotransferase coding sequences: 1) insertion of the SV40 promoter retrieved by PCR from the pRL-SV40 vector between *Bgl II* and *Hind III* sites into the multi-cloning site upstream of the luciferase coding sequence; 2) site-directed mutagenesis of the *Xba I* site at 3' of the luciferase coding sequence into a *Pca I* site; 3) insertion of a synthetic DNA fragment corresponding to *Pac I* site/single perfect-match target site for miR-372 (or single mutated target site)/SV40 late poly(A)region/*BamH I* site (synthesized by Millegen Biotechnologies) between the *Pac I* and *BamH I* sites downstream of the luciferase coding sequence. Molecular cloning was performed according to standard protocols and the final constructs were verified by sequencing.

Transient transfections. Cells were plated at 5.10⁴ cells/well in a 24-well plate. Transfections were performed using Lipofectamine 2000 (Invitrogen) according to the manufacturer's protocol. Cells were co-transfected with 10 nM of either 22-mer full-length miRNA antisense (AS372, AS373), 22-mer scrambled oligonucleotides (sc372-373), 8-mer tiny LNA (TL372, TL373) or the 8-mer negative control (TLsc), mixed with 10 ng pRL-SV40 control vector (Promega) and 100 ng of either pGL3, pGL3-wt3'UTR-LATS2, pGL3-mut3'UTR-LATS2. Firefly and *Renilla* luciferase activities were measured 48 h post-transfection using the Dual Luciferase Assay (Promega). Firefly luciferase activities were normalized for transfection efficiency by *Renilla* luciferase activity.

Western Blot. Cells were washed twice with ice cold PBS and harvested in ice cold ProteoJET™ Mammalian Cell lysis reagent (Fermentas) supplemented with 5 mM EDTA and 1X ProteoBlock™ Protease inhibitor cocktail (Fermentas). Proteins (40 µg) were separated by SDS-PAGE and western blot performed using Immobilon-P transfer membrane (Millipore), according to standard procedures. Anti-LATS2 (clone ST-3D10, Abnova) and anti- α -tubulin (clone B-5-1-2, Sigma-Aldrich) antibodies were used at a 1:500 and 1:30,000 dilutions, respectively. Protein detection was carried out using HRP-conjugate anti-mouse IgG and enhanced chemoluminescence according to the manufacturer (Immobilon Western Chemiluminescent HRP substrate, Millipore). The luminescence on the blots was detected using a DS ImageQuant LAS (GE) analyzer.

Cell growth. Cells were grown in a 96 well microplate, starting at 1,500 cells per well. Cell viability was assessed using the CellTiter96 AQueous One Solution Reagent (Promega), as recommended by the manufacturer. Absorbance at 492nm was read on a Bio-Tek spectrophotometric microplate reader.

Immunofluorescence: Cells were grown on glass coverslips, fixed with 3% buffered paraformaldehyde and permeabilized in Triton 0,2%. After blocking with 3% bovine serum albumin in PBS (PBS-BSA), they were stepwise incubated overnight at 8°C with a rabbit anti-LATS2 antibody (Bethyl, 1/200 dilution), washed four times in PBS-BSA and then 30 min at room temperature with a secondary anti-rabbit IgG antibody coupled to Alexafluor488 (Invitrogen; 1/200 dilution). After extensive washes in PBS, the coverslips were mounted on glass slides using Slowfade reagent (Invitrogen) prior to imaging in epifluorescence on a Zeiss microscope.

Establishment of stable reporter AGS cell lines

Cells (10^5 per well) were plated in a 24-well plate and transfected the following day with 500 ng of either pGL4-PM372 or pGL4-mut372 vectors using Fugene HP transfection reagent ($3\mu\text{l}/\mu\text{g}$ DNA; Promega) as recommended. 24 hour post-transfection, the cells were detached and plated in a 10 cm diameter tissue culture plate in non-selective growth medium. After 24 hr growth, hygromycin B was added at a final concentration of 0.7 mg/mL to select the AGS cells having integrated the luciferase reporter DNA. Stable pGL4-mut372 reporter clones were chosen on the basis of the intensity of their firefly luciferase

specific activity, and stable pGL4-PM372 reporter clones were chosen on the basis of the intensity of the luciferase activity upon specific de-repression by anti-miR-372 antisense oligonucleotides.

***In vivo* experiments**

Ethics Statement: approval was obtained from the French Committee of Genetic Engineering (approval number 4608) and the local Central Animal Facility Committee of the University of Bordeaux before initiation of the study. All animal experiments were performed in level 2 animal facilities of the University of Bordeaux, in accordance with national institutional guidelines and with the agreement of the local Ethic Committee on Animal Experiments CEEA50 of Bordeaux (agreement number 50120151-A).

Studies on fresh tumors from primary gastric adenocarcinoma cases were performed in agreement with the Direction for Clinical Research and the Tumor and Cell Bank of the Institut Bergonié of Bordeaux. Fresh tumors samples were collected from gastric surgical wastes from consenting patients (written consent), who underwent gastrectomy for gastric cancer. Activities of conservation and preparation of elements of human origin are declared at the French Ministry of Research (reference number DC-2008-412).

Mouse xenografts of AGS cells and in vivo imaging: Immunodeficient non obese diabetous/shi-severe combined immunodeficiency/interleukin-2Rgammanull (NSG) mice under 2.5 % isoflurane anesthesia (Belamont) were injected subcutaneously into the right flank with 10^5 AGS reporter cells, GC10 or GC06 gastric tumor cells resuspended in 100 μ L of 7 mg/mL Matrigel (BD Biosciences) in ice cold PBS. Tumor growth was periodically monitored by measuring the length (L) and width (W) of the tumor with a caliper, and tumor volume was calculated according to the formula $\frac{1}{2}(L \times W^2)$, as previously described (24). After 10 days to 5 weeks upon engraftment of either AGS, GC10 or GCO6 cells, when the tumor was visible through the skin of the animal and reached ~ 100 mm³, 100 μ L of tiny LNA solutions at the indicated concentrations were injected subcutaneously at the tumor periphery on 3 consecutive days. For AGS reporter cells, *in vivo* luciferase imaging was performed at the indicated periods of time upon tiny LNA injection on isoflurane-anesthetized and shaved animals, previously injected intra-peritoneally with 3 mg D-luciferin (Promega) per mouse in 100 μ L PBS. *In vivo* luciferase activity was recorded within the region of interest in the flank of the animal, for 30 min following luciferin injection using a real time PhotonIMAGER (Biospace). At the end of the experiments (4-5 weeks post engraftment), mice were sacrificed by cervical dislocation and tumors immediately harvested and processed for further analyses.

Primary human gastric adenocarcinoma-derived cells. GC10 and GC06 gastric adenocarcinoma xenografts were established in NSG mice from tumor samples collected from primary human gastric adenocarcinoma. Primary tumor samples were xenografted subcutaneously in isofluran-anesthetized NSG mice. Secondary tumors were amplified in mice by serial transplantation. Briefly, tumors were collected for cell isolation when reaching ~500 mm³: after mechanical mincing, samples were dissociated by collagenase IV and hyaluronidase (all from Sigma) as previously described (25). Viability was evaluated by trypan blue exclusion, before counting for analysis or resuspension in matrigel for xenograft experiments. Histopathological characteristics were confirmed to be similar to those of the primary tumor after histological analysis of the tumor xenografts processed following standard procedures (hematoxylin and eosin, alcian blue and periodic acid Schiff stainings) (26). Expression of human epithelial markers was verified by immunostaining of ESA (StemCell Technologies) and CD24 (BD Biosciences) and flow cytometry analysis as previously described (25). According to Lauren's classification, GC10 and GC06 are intestinal (moderately differentiated) and diffuse types, respectively, both infiltrating the sub-serosa.

Tumor immunohistochemistry (IHC) and *in situ* hybridization of miRNA.

For histology processing, the tumor samples were fixed for 24 h in 3.7 % neutral-buffered formalin (Sigma), followed by standard histological processing and paraffin embedding. Sections of 3 µm thickness from paraffin-embedded tissues were used for standard IHC protocols with anti-LATS2 antibodies (Bethyl; 1/400 dilution) for 1 hr at room temperature, and then with labeled Polymer-Horse Radish Peroxidase anti-rabbit EnVision System (DAKO) for 30 min at room temperature. Immunolabeling was revealed by 10 min incubation in liquid substrate-diaminobenzidine-chromogen (DAKO) at room temperature. Slides were counterstained with hematoxylin, dehydrated and mounted with Eukit-mounting medium (Labonord).

For *in situ* hybridization of miR-372, de-paraffinized and rehydrated tissue sections of 5 µm thickness were digested by Proteinase K (Invitrogen, 10 µg/mL in Tris 50 mM pH 7.6) for 15 min at room temperature, and post-fixed in 4% paraformaldehyde in PBS for 10 min. After 3 washes in PBS and one in SSC buffer 4x, the tissues were prehybridized for 2 hrs at 52 °C in formamide 50%, SSC 4x, dextran sulfate 200 mg/mL, tRNA 500 µg/mL, and hybridized overnight at 52°C in the same buffer containing 25 nM anti-miR-372 DNA/LNA antisense (Table S1) labeled at both 3' and 5' ends with digoxigenin. After

2 stringent washes in SSC 0.2x at 52°C, the hybridized antisense was revealed with an anti-digoxigenin antibody coupled to alkaline phosphatase (Roche, 1/400 dilution, overnight incubation at 8°C), followed after 4 washes by a 2 hr incubation at room temperature in a 1-Step™NBT/BCIP plus Suppressor solution (Pierce). Slides were dehydrated and mounted with Eukit-mounting medium.

Statistical analysis.

Statistical significance ($***P < 0.001$, $**P < 0.01$, $*P < 0.05$) was calculated using the unpaired, one-tailed Student *t*-test.

RESULTS

Specificity of 8-mer LNAs targeting miR-372 and miR-373 seeds.

We previously reported the efficiency of full-length antisense oligonucleotides to miR-372 and miR-373 (AS372, AS373) to inhibit the functions of these miRNAs in AGS cells (10). To assess whether miR-372 seed-targeting LNAs (TL372) are as efficient as AS372 in antagonizing miR-372, 8-mer TL372, 22-mer AS372 or their respective controls TLCo and SC372 were transfected into growing AGS cells at final concentration of 10 nM and miR-372 expression was evaluated by RT-qPCR and non-denaturing northern blot analyses. Upon AS372 transfection, the miR-372 level is drastically reduced as determined by RT-qPCR, and becomes undetectable by northern blot analyses, compared to untransfected cells or SC372-transfected ones (Fig. 1A and B, respectively), in agreement with our previous data (10). Similar results were obtained by determining miR-373 content upon AS373 transfection (data not shown). However, RT-qPCR data suggest that TL372 does not reduce the miR-372 content as efficiently as AS372 (Fig. 1A). Northern blot analysis of miR-372 revealed a slower-migrating band in TL372-transfected cells, as compared to TLCo-, SC-transfected or untransfected cells (Fig. 1B), likely being the miR-372/TL372 heteroduplex: indeed, anti-miR LNAs may sequester their targeted miRNA without degrading it (5). There is still room left in the miR-372/TL372 heteroduplex for the anti-miR-372 probe or the qPCR primers to pair onto the miR-372 sequence and to make it detectable both by northern blot or RT-qPCR analyses (lower part of Fig. 1B). On the contrary, in AS372-transfected cells, miR-372 remains sequestered on its full length by the specific 22-mer antisense oligonucleotide, and hence unable to bind either the probe or the primers: this makes it undetectable either on the northern blot or by RT-qPCR. Thus, using anti-miR 8-mer LNAs, quantification of residual miRNA levels by RT-qPCR may be misleading.

MiR-372 and miR-373 share similar seed sequences, which resemble those of miR-17-5p, miR-20a, miR-106b and miR-93 (Table 1). We synthesized 8-mer TL372, TL373 and TL17 LNAs perfectly matching the 2-9 nucleotides of miR-372, miR-373 or miR-17-5, respectively (Table S1). In order to assess their respective ability to target the different miRNAs of this miRNA family, we transfected them in AGS cells at 1 or 10 nM and, 4 days later, we analyzed their ability to form a stable TL/miRNA heteroduplex in the cells. TLCo and the miR-21-targeting TL21 were used as negative controls. Fig. 1C shows the northern blot analyses of miR-372, miR-373, miR-17-5p and miR-93 in non-denaturing conditions, and Table 2 summarizes the results, along with the likely pairing of the 8-mer LNAs to the

miRNA sequences. As expected, TL372 is able to sequester miR-372, which appears as a shifted band as compared to mock, TLCo and TL21-treated cells, in a dose-dependent manner. TL372 also partly retains miR-93, with which it pairs beyond the seed from nucleotides 3 to 10. TL373 does not form a heteroduplex with any miRNA but miR-373, and the 10 nM concentration seems insufficient to sequester the whole amount of miR-373 of the AGS cells. TL17 at 10nM forms stable heteroduplexes with miR-17-5p and miR-93, as expected, as well as with miR-372, to which it pairs from nucleotides 1 to 8. It forms a smeary duplex with miR-373, to which it pairs from nucleotides 2 to 8. All combined, these data suggest that the ability of a 8-mer LNAs to efficiently target miRNAs of a same family resides in the perfect pairing over all the 8 nucleotides and starting at nucleotide 2 or 1 at the 5' end of the miRNA. Moving forward at nucleotide 3 of the miRNA and/or mispairing at nucleotide 9 lead to substantial or complete loss of their efficacy to sequester this miRNA. Therefore, although they harbor similar seeds, but differ on nucleotide 9, miR-372 and miR-373 cannot be targeted efficiently by a unique 8-mer seed-targeting sequence.

The 8-mer LNAs against miR-372 and miR-373 de-repress LATS2 and inhibit AGS cell growth *in vitro*.

LATS2 is one of the major targets of both miR-372 and miR-373, and contains two miR-372 and -373 pairing sites in its 3'UTR (10). It has been validated in other cancer cells (14; 16; 10). To compare the efficiency of the 8-mer LNA and full-length AS against miR-372 and miR-373 to de-repress LATS2, the luciferase reporter plasmid containing the 3'UTR of LATS2, named pGL3-3'UTR-LATS2wt, was transiently transfected into AGS cells along with 8-mer LNAs or 22-mer AS. The resulting luciferase activity was compared to that of either the control pGL3 vector or the pGL3-3'UTR-LATS2mut vector harboring mutated miR-372 and -373 pairing sites. In the absence of oligonucleotides, the luciferase activity generated by pGL3-3'UTR-LATS2wt, which senses the endogenous miR-372 and miR-373 levels, represented 30% of that of the control pGL3 reporter (Fig. 2 A, B) and 40% of that of the pGL3-3'UTR-LATS2mut vector (Fig. 2B). In the presence of TL372+373, but not TLCo or SC372, the luciferase activity of the pGL3-3'UTR-LATS2wt increased in the same extent that in the presence of AS372+373 (Fig. 2A). The TL372+373-derepressed luciferase activity reached the level of that generated by the pGL3-3'UTR-LATS2mut (Fig. 2B). This indicates that the 8-mer LNAs are as efficient as the AS372+373 to inhibit miR-372 and -373 functions and de-repress LATS2. In consequence, LATS2 protein

accumulated in cells treated by either 8-mer or full-length antisenses against miR-372 and miR-373, but not in cells treated by the respective control oligonucleotides, in which LATS2 expression pattern remained as faint as in untreated cells (Fig. 2C and D). The de-repressed LATS2 mainly accumulated in the cell nucleus upon treatment with either 22-mer AS or 8-mer LNAs (Fig. 2D). TL372+373-transfected AGS cells exhibit a noticeably reduced proliferation rate, which is slowed down by 40% compared to that of TLCo-transfected cells (Fig. 2E). Of note, TL21 targeting the seed of miR-21, another oncogenic miRNA that is also highly expressed in AGS cells (10), has no effect on AGS proliferation rate, suggesting that this cell line may not be particularly dependent on miR-21 for its growth. All together, these results show that 8-mer LNAs, inhibiting miR-372 and -373 functions and de-repressing LATS2, inhibit AGS cell growth at the same extent as did AS in our previous data (10).

The experiments shown in Fig. 1 and 2 have been performed by transfecting the 8-mer LNAs with lipofectamin, which allows using concentrations in nanomolar range. As tiny LNA have been proven to enter cells unassisted (5), we verified this property by treating AGS cell cultures with them without any transfection agent. We established a stable AGS cell line containing the pGL4-PM372 luciferase reporter system, which contains a single site perfectly matching miR-372 downstream of the *luc* coding sequence. This AGS-luc-PM372 line was compared to the AGS-luc-mut372, a stable cell line constitutively expressing the pGL4-mut372 reporter system, in which the sequence pairing the miR-372 seed contains 3 mismatches and is thereby unable to sense miR-372. AGS-luc-PM372 cells express a low luciferase activity as compared to AGS-luc-mut372 cells ($5,611 \pm 1,018$ RLU/ μ g protein versus $1332,000 \pm 178,000$ RLU/ μ g protein), due to the miR-372-mediated post-transcriptional *luc* repression. AGS-luc-PM372 cells specifically respond to TL372+373 at 2.5 μ M by a significant increase of the luciferase activity, whereas AGS-luc-mut372 cells do not, as shown in Fig.S1A. These data suggest that 8-mer LNAs at micromolar range concentrations have entered freely into the cells to specifically inhibit the target miRNAs. Subsequently, they induce a significant dose-dependent decrease in AGS growth rate (Fig. S1B).

Seed-targeting 8-mer LNAs silence miR-372 and mir-373 in AGS cells grown in mice and inhibit tumor growth.

We then determined whether the 8-mer LNAs could be used to target miR-372 and -373 in solid tumors *in vivo* and subsequently reduce their growth rate. Therefore, we subcutaneously engrafted the stable

reporter cell lines AGS-luc-PM372 or AGS-luc-mut372 into female NSG mice (n = 5, one tumor per mouse). The xenografts grew at a similar rate independently on the reporter they harbor (AGS-luc-PM372 and AGS-luc-mut372 tumor size: $119.6 \text{ mm}^3 \pm 46.2$ and $108.6 \text{ mm}^3 \pm 61.2$, respectively, after 2 weeks, p-value = 0.22; $157.6 \text{ mm}^3 \pm 42.3$ and 150.5 ± 54.7 respectively after 4 weeks, p-value = 0.43). Ten days after tumor initiation, increasing concentrations of TL372+373 or TLCo were subcutaneously injected at the tumor periphery for three consecutive days. Both the size of the tumor and *in vivo* bioluminescence images were periodically recorded, starting at the day of the first injection (Fig. 3).

A noticeable delay was observed in the growth kinetics of the tumors treated with 5 or 50 nmoles/mouse TL372+373 as compared to TLCo-treated ones, leading to a significant reduction of tumor size after 2 weeks following the first injection (Fig.3A). Bioluminescence images recorded at day 9 following the first injection show the luciferase activity appearing in the AGS-PM372 tumors upon treatment with TL372+373 but not with TLCo (Fig.3B, and 3Ce versus 3Cd), whereas in mock conditions luciferase activity of AGS-PM372 tumors remains undetectable as compared to that of AGS-mut372 tumors (Fig.3B, and 3Cc versus 3Ca). These data indicate that the injected TL372+373 may have reached the tumor cell cytoplasm to inhibit the function of the endogenous miR-372 and miR-373 levels. The TL372+373-mediated up-regulation of the luciferase activity in the AGS-PM372 tumors likely results from the combined effects on de-repression of the luciferase reporter sensing miR-372, on the one side, and reduction of the tumor size, on the other side. These combined effects could explain why the luciferase activity recorded in TL372+373-treated mice bearing the AGS-Mut372 xenografts is lower than that of the untreated ones (Fig. 3B and 3Cb versus a).

Three weeks post-treatment, the mice were euthanized. The residual tumors were removed and processed for further RNA analyses and histology. The northern blot analysis of miR-372 clearly shows a slower-migrating miR-372/TL372 heteroduplex in TL372+373-treated AGS xenografts, compared to TLCo or untreated tumors (Fig. 4A, a). A similar band shift is observed on the northern blot analyzed for miR-373 expression in TL372+373-treated tumors and corresponds to the miR-373/TL373 heteroduplex (Fig. S2). The heteroduplex is formed in a TL372+373 dose-dependent manner at doses over 5 nanomoles/mouse (Fig. 4A, b) and further confirm that they have reached their targeted miRNA and form a long lasting duplex with it. On the contrary, the northern blot analysis of miR-21 does not show any band shift in the TL372+373-treated cells (Fig. 4A, c and d), further stressing the specificity of miRNA targeting by 8-mer LNAs. Along with TL372+373-mediated miR-372 and miR-373

sequestrations and tumor growth inhibition, LATS2 is up-regulated upon TL372+373 treatment, as compared to TLCo treatment, and accumulates in the carcinoma cell nucleus and cytoplasm (Fig. 4B).

8-mer LNAs targeting miR-372 and miR-373 inhibit the growth of human gastric carcinoma xenografts

To assess whether the human gastric AGS cell line is relevant of other human gastric carcinoma, we selected two tumors in our collection of resected tumors from gastric cancer patients, to be xenografted in mice and treated with the TL372+373. GC10 is a highly aggressive, fast growing gastric carcinoma of intestinal type; it expressed both miR-200b, which attests for its epithelial origin, and miR-372 in every epithelial cell, as shown by *in situ* hybridization (Fig. S3 left panels). GC06 is a gastric carcinoma of diffuse type that grows slower than GC10; it homogenously expressed miR-200b in every cell, but miR-372 only in some cell clusters (Fig. S3, right panels). Fig. 5A shows that untreated GC10 tumors gain 200% volume in 2 weeks, while GC06 tumors gain only 60% volume during the same time, suggesting a causal relationship between the high miR-372 expression and rapid tumor growth. Indeed, TL372+373 treatment markedly inhibits GC10 growth at doses as low as 5 nanomoles per mouse. It is much less efficient on GC06, for which a trend of growth reduction is noticeable only with TL372+373 at 50 nanomoles/mouse (Fig. 5A). TL372+373-treated GC10 xenografts exhibit an up-regulated LATS2 expression as compared to TLCo-treated ones (Fig. 5B).

DISCUSSION

MiRNA silencing by chemically modified antimir oligonucleotides has become an important and widely used approach in studies aimed at unveiling miRNA functions, as well as in miRNA-based therapeutic strategies, when those miRNAs are aberrantly over-expressed in pathologies. Whereas satisfying oligonucleotide uptake can be accomplished in *in vitro* cultured cells using commercial transfection agents, efficient delivery of antimirs remains a critical factor for their successful use *in vivo*. We here applied an antimir strategy based on the use of seed-targeting 8-mer LNA oligonucleotides and originally developed by Obad et al. (5), to antagonize the function of miR-372 and miR-373 in gastric carcinoma cells. Whereas these two miRNAs are specific of embryonic stem cells and not expressed in adult tissues, they may be expressed at high levels in some tumors of various tissue origins (16-20), in which they behave as oncomirs, silencing tumor suppressor genes such as the cell cycle regulator LATS2, and triggering cell growth. Using the AGS cell line as a model of gastric adenocarcinoma, in which miR-

372 is the most expressed of its miRnome (10), we found that 8-mer LNAs complementary to the miR-372 and miR-373 seeds specifically antagonize the growth-promoting functions of these miRNAs and reduce the growth rate of both *in vitro* cultured cells and *in vivo* mouse xenografts. Moreover, they are also highly efficient on mouse xenografts of human gastric adenocarcinoma that express miR-372.

The seed region comprises the nucleotides 2 to 8 of the miRNA, with nucleotides 2 to 7 being most critical for binding specificity (27). The efficiency of targeting the miRNA seed has been interpreted by the high accessibility of this particular region, exposed and pre-organized in the Argonaute (Ago) complex to favor efficient pairing to the seed-match site in a target mRNA (28; 29). Ago proteins form the functional core of the RNA-induced silencing complexes (RISC) that mediate RNA silencing in eukaryotes. LNA oligonucleotides, in which the bicyclic furanose unit is locked in an RNA-mimicking sugar conformation, resemble natural nucleic acids with respect to Watson–Crick base-pairing and display outstanding hybridization affinity toward complementary single-stranded RNA or DNA (3). 8-mer LNAs have been shown to pair to mature miRNAs bound to Ago2 (5). Thus TL372 and TL373 sequestering miR-372 and miR-373 within the Ago complex competes out the miR372 and -373 binding sites on the targeted mRNAs, among which the tumor suppressor LATS2, and alleviates their miRNA-dependent repression.

The length of 8-mer LNAs complementary to the miRNA nu 2-9 including the seed sequence has been found to be optimal to sequester the miRNA in competition with the targeted mRNA, 6-7-mer or 9-10-mer LNAs both being less or no efficient (5). Despite miR-372 and miR-373 harbor the same nu 2-8 seed sequence and both target LATS2 through interactions at two sites in the LATS2 3' UTR (10; 14), their 5' end differs at the 9th nucleotide, which pairs with the first nucleotide at the 5' end of the tiny LNA. According to our analysis of the miRNA/8-mer LNA duplex formation, the 8-mer LNA targeting miR-372 is not able to sequester miR-373, and *vice versa*. In comparison, Obad *et al.* reported that a mismatch between the first nucleotide of TL21 and the 9th nu of miR-21 decreased by 60% its efficiency to de-repress the miR-21 reporter (5). Thus, our data confirm that the optimal antimir tiny LNA activity indeed requires the perfect pairing of all the 8 nucleotides with the target miRNA. A 8-mer LNA targeting the seed of miR-17 would have been a more “universal” antimir sequestering also miR-372, -373, -93, and likely also miR-106b and miR-20a (Table 1), in addition to miR-17-5p. We choose to target miR-372 and -373 because, contrarily to miR-17-5p, they are not expressed in healthy adult tissue (except placenta), and therefore their targeting should not lead to undesirable side effects on normal tissue, a potential risk

targeting miR-17. Nevertheless, deleterious effects on healthy tissues of 8-mer LNAs targeting broadly expressed miRNA have not been found (5; 9).

An additional quality of 8-mer LNAs is the possibility to be delivered as simple unconjugated oligonucleotides without the use of any transfection agents. This property could be demonstrated in tissue culture, but requires micromolar ranges of TL concentrations instead of nanomolar concentrations in complex with a transfection agent such as lipofectamin. Nevertheless, micromolar concentrations are still acceptable and comparable to those used for pharmacological inhibitors of signaling pathways. The simple oligonucleotide delivery is highly valuable *in vivo*, and the antitumor properties of TL372+373 are emphasized in a human gastric carcinoma xenograft model in mice. They are associated with long-lasting growth inhibition and apparent lack of toxicity. Indeed, we noticed no sign of inflammation/ulceration at the site of injection and a good general state of the animals without any significant loss of the animal weight. The lack of toxicity of TL372+373 is consistent with other data that have pointed out the safety of these oligonucleotides in mice (6-8) as well as in nonhuman primates (9). Gastric cancers, which constitute the third cause of cancer-related mortality worldwide, are more often adenocarcinomas that derive from the malignant transformation of the gastric mucosa in the context of a chronic infection with *Helicobacter pylori* (30). Gastric adenocarcinomas exist in either diffuse or intestinal histological subtypes. Specific alterations in the miRNA expression pattern have been identified in human gastric adenocarcinoma since the earliest steps of tumorigenesis, and involve the oncomir miR-21 (31) and miRNAs of the oncogenic *miR-17-92* and *miR-106-25* clusters (32). Despite the fact that, in our experience, the strong miR-372 or miR-373 expression is not a feature as common as that of those mentioned oncomirs (C. Staedel and C. Varon, unpublished results), it nevertheless confers a remarkably active growth potential to the tumor cells, as observed here for GC10 versus GC06 and by others in gastric cancer (20) or in other localizations (14-19). As embryonic stem cell markers (11), miR-372 and miR-373 in tumors could be a signature of cancer stem cells (CSC), a tumor cell reservoir to be preferentially targeted in anticancer therapies, because they supply tumor growth and metastasis by their self-renewal capacities combined to their general resistance to chemo- and radiotherapy. Interestingly, CD44 is both a gastric CSC marker (23) and a miR-373 target (21). LATS2 constitute the core of the Hippo pathway, which regulates organ size during development (33). The particular CD44/miR-372&373/LATS2 relationship would therefore deserve further exploration in the context of gastric adenocarcinoma.

In conclusion, our study confirms the importance of 8-mer seed-targeting LNAs as important tools to antagonize highly expressed oncomirs and de-repress tumor suppressor genes to recover growth control. Targeting of miR-372 and -373 may be applicable to other cancer subsets depending on these oncomir for their growth.

SUPPLEMENTARY DATA

Table S1

Figure S1

Figure S2

ACKNOWLEDGEMENT

We thank the former PhD students of the authors' lab, C. Belair, J. Baud and J. Ferrand, who developed the cell systems involved in this study, and the technical team of the Animal Facilities of the University of Bordeaux.

FUNDING

This work was supported by the SFR "Technology for Health" of Bordeaux, by the Conseil Regional d'Aquitaine (Grants # 20091301007, 20091301027, and 20081302203), by the INSERM U869 (France), by the Association pour la Recherche contre le Cancer (grant # 8412), 'Institut National du Cancer' (grant # 07/3D1616/IABC-23-12/NC-NG), the French Société Nationale Française de Gastroenterologie and the SIRIC BRIO (Site de Recherche Intégrée sur le Cancer –Bordeaux Recherche Intégrée Oncologie) [Grant: INCa-DGOS-Inserm 6046].

REFERENCES

1. Huntzinger, E. and Izaurralde, E. (2011) Gene silencing by microRNAs: contributions of translational repression and mRNA decay. *Nat. Rev. Genet.*, **12**, 99–110.
2. Di Leva, G. and Croce, C.M. (2013) miRNA profiling of cancer. *Curr. Opin. Genet. Dev.*, **23**, 3–11.
3. Vester, B. and Wengel, J. (2004) LNA (locked nucleic acid): high-affinity targeting of complementary RNA and DNA. *Biochemistry*, **43**, 13233–13241.

4. Thomas, M., Lange-Grünweller, K., Dayyoub, E., Bakowsky, U., Weirauch, U., Aigner, A., Hartmann, R.K. and Grünweller, A. (2012) PEI-complexed LNA antiseeds as miRNA inhibitors. *RNA Biol*, **9**, 1088–1098.
5. Obad, S., dos Santos, C.O., Petri, A., Heidenblad, M., Broom, O., Ruse, C., Fu, C., Lindow, M., Stenvang, J., Straarup, E.M., et al. (2011) Silencing of microRNA families by seed-targeting tiny LNAs. *Nat. Genet.*, **43**, 371–378.
6. Garchow, B.G., Bartulos Encinas, O., Leung, Y.T., Tsao, P.Y., Eisenberg, R.A., Caricchio, R., Obad, S., Petri, A., Kauppinen, S. and Kiriakidou, M. (2011) Silencing of microRNA-21 in vivo ameliorates autoimmune splenomegaly in lupus mice. *EMBO Mol Med*, **3**, 605–615.
7. Zhang, Y., Roccaro, A.M., Rombaoa, C., Flores, L., Obad, S., Fernandes, S.M., Sacco, A., Liu, Y., Ngo, H., Quang, P., et al. (2012) LNA-mediated anti-miR-155 silencing in low-grade B-cell lymphomas. *Blood*, **120**, 1678–1686.
8. Murphy, B.L., Obad, S., Bihannic, L., Ayrault, O., Zindy, F., Kauppinen, S. and Roussel, M.F. (2013) Silencing of the miR-17~92 Cluster Family Inhibits Medulloblastoma Progression. *Cancer Res.*, **73**, 7068–7078.
9. Rottiers, V., Obad, S., Petri, A., McGarrah, R., Lindholm, M.W., Black, J.C., Sinha, S., Goody, R.J., Lawrence, M.S., deLemos, A.S., et al. (2013) Pharmacological inhibition of a microRNA family in nonhuman primates by a seed-targeting 8-mer antimiR. *Sci Transl Med*, **5**, 212ra162.
10. Belair, C., Baud, J., Chabas, S., Sharma, C.M., Vogel, J., Staedel, C. and Darfeuille, F. (2011) *Helicobacter pylori* interferes with an embryonic stem cell micro RNA cluster to block cell cycle progression. *Silence*, **2**, 7.
11. Suh, M.-R., Lee, Y., Kim, J.Y., Kim, S.-K., Moon, S.-H., Lee, J.Y., Cha, K.-Y., Chung, H.M., Yoon, H.S., Moon, S.Y., et al. (2004) Human embryonic stem cells express a unique set of microRNAs. *Dev. Biol.*, **270**, 488–498.
12. Judson, R.L., Babiarz, J.E., Venere, M. and Blelloch, R. (2009) Embryonic stem cell-specific microRNAs promote induced pluripotency. *Nat. Biotechnol.*, **27**, 459–461.
13. Wang, Y. and Blelloch, R. (2009) Cell cycle regulation by MicroRNAs in embryonic stem cells. *Cancer Res.*, **69**, 4093–4096.

14. Voorhoeve, P.M., le Sage, C., Schrier, M., Gillis, A.J.M., Stoop, H., Nagel, R., Liu, Y.-P., van Duijse, J., Drost, J., Griekspoor, A., et al. (2006) A genetic screen implicates miRNA-372 and miRNA-373 as oncogenes in testicular germ cell tumors. *Cell*, **124**, 1169–1181.
15. Palmer, R.D., Murray, M.J., Saini, H.K., van Dongen, S., Abreu-Goodger, C., Muralidhar, B., Pett, M.R., Thornton, C.M., Nicholson, J.C., Enright, A.J., et al. (2010) Malignant germ cell tumors display common microRNA profiles resulting in global changes in expression of messenger RNA targets. *Cancer Res.*, **70**, 2911–2923.
16. Lee, K.-H., Goan, Y.-G., Hsiao, M., Lee, C.-H., Jian, S.-H., Lin, J.-T., Chen, Y.-L. and Lu, P.-J. (2009) MicroRNA-373 (miR-373) post-transcriptionally regulates large tumor suppressor, homolog 2 (LATS2) and stimulates proliferation in human esophageal cancer. *Exp. Cell Res.*, **315**, 2529–2538.
17. Rippe, V., Flor, I., Debler, J.W., Drieschner, N., Rommel, B., Krause, D., Junker, K. and Bullerdiek, J. (2012) Activation of the two microRNA clusters C19MC and miR-371-3 does not play prominent role in thyroid cancer. *Mol Cytogenet*, **5**, 40.
18. Cairo, S., Wang, Y., de Reyniès, A., Duroure, K., Dahan, J., Redon, M.-J., Fabre, M., McClelland, M., Wang, X.W., Croce, C.M., et al. (2010) Stem cell-like micro-RNA signature driven by Myc in aggressive liver cancer. *Proc. Natl. Acad. Sci. U.S.A.*, **107**, 20471–20476.
19. Yamashita, S., Yamamoto, H., Mimori, K., Nishida, N., Takahashi, H., Haraguchi, N., Tanaka, F., Shibata, K., Sekimoto, M., Ishii, H., et al. (2012) MicroRNA-372 is associated with poor prognosis in colorectal cancer. *Oncology*, **82**, 205–212.
20. Zhang, X., Li, X., Tan, Z., Liu, X., Yang, C., Ding, X., Hu, X., Zhou, J., Xiang, S., Zhou, C., et al. (2013) MicroRNA-373 is upregulated and targets TNFAIP1 in human gastric cancer, contributing to tumorigenesis. *Oncol Lett*, **6**, 1427–1434.
21. Huang, Q., Gumireddy, K., Schrier, M., le Sage, C., Nagel, R., Nair, S., Egan, D.A., Li, A., Huang, G., Klein-Szanto, A.J., et al. (2008) The microRNAs miR-373 and miR-520c promote tumour invasion and metastasis. *Nat. Cell Biol.*, **10**, 202–210.
22. Subramanyam, D., Lamouille, S., Judson, R.L., Liu, J.Y., Bucay, N., Derynck, R. and Blelloch, R. (2011) Multiple targets of miR-302 and miR-372 promote reprogramming of human fibroblasts to induced pluripotent stem cells. *Nat. Biotechnol.*, **29**, 443–448.

23. Borgdorff, V., Lleonart, M.E., Bishop, C.L., Fessart, D., Bergin, A.H., Overhoff, M.G. and Beach, D.H. (2010) Multiple microRNAs rescue from Ras-induced senescence by inhibiting p21(Waf1/Cip1). *Oncogene*, **29**, 2262–2271.
24. Bessède, E., Staedel, C., Acuña Amador, L.A., Nguyen, P.H., Chambonnier, L., Hatakeyama, M., Belleannée, G., Mégraud, F. and Varon, C. (2013) Helicobacter pylori generates cells with cancer stem cell properties via epithelial-mesenchymal transition-like changes. *Oncogene*, 10.1038/onc.2013.380.
25. Ferrand, J., Noël, D., Lehours, P., Prochazkova-Carlotti, M., Chambonnier, L., Ménard, A., Mégraud, F. and Varon, C. (2011) Human bone marrow-derived stem cells acquire epithelial characteristics through fusion with gastrointestinal epithelial cells. *PLoS ONE*, **6**, e19569.
26. Varon, C., Dubus, P., Mazurier, F., Asencio, C., Chambonnier, L., Ferrand, J., Giese, A., Senant-Dugot, N., Carlotti, M. and Mégraud, F. (2012) Helicobacter pylori infection recruits bone marrow-derived cells that participate in gastric preneoplasia in mice. *Gastroenterology*, **142**, 281–291.
27. Lewis, B.P., Burge, C.B. and Bartel, D.P. (2005) Conserved seed pairing, often flanked by adenosines, indicates that thousands of human genes are microRNA targets. *Cell*, **120**, 15–20.
28. Wang, Y., Juraneck, S., Li, H., Sheng, G., Tuschl, T. and Patel, D.J. (2008) Structure of an argonaute silencing complex with a seed-containing guide DNA and target RNA duplex. *Nature*, **456**, 921–926.
29. Elkayam, E., Kuhn, C.-D., Tocilj, A., Haase, A.D., Greene, E.M., Hannon, G.J. and Joshua-Tor, L. (2012) The Structure of Human Argonaute-2 in Complex with miR-20a. *Cell*, **150**, 100–110.
30. Cover, T.L. and Blaser, M.J. (2009) Helicobacter pylori in health and disease. *Gastroenterology*, **136**, 1863–1873.
31. Zhang, Z., Li, Z., Gao, C., Chen, P., Chen, J., Liu, W., Xiao, S. and Lu, H. (2008) miR-21 plays a pivotal role in gastric cancer pathogenesis and progression. *Lab. Invest.*, **88**, 1358–1366.
32. Petrocca, F., Visone, R., Onelli, M.R., Shah, M.H., Nicoloso, M.S., de Martino, I., Iliopoulos, D., Pilozi, E., Liu, C.-G., Negrini, M., et al. (2008) E2F1-regulated microRNAs impair TGFbeta-dependent cell-cycle arrest and apoptosis in gastric cancer. *Cancer Cell*, **13**, 272–286.
33. Harvey, K.F., Zhang, X. and Thomas, D.M. (2013) The Hippo pathway and human cancer. *Nat. Rev. Cancer*, **13**, 246–257.

FIGURES LEGENDS

Figure 1. Specificity of miRNA targeting by 22-mer full-length antisense or 8-mer seed-directed oligonucleotides in cultured AGS cells. AGS cells were transfected with either the 22-mer full-length anti-miR-372 LNA/DNA antisense (AS372) or its scrambled sequence (SC372), or with the 8-mer LNA oligonucleotide targeting the nu 2-9 of miR-372 including the seed (TL372), or its negative control sequence (TLCo), at a final concentration of 10 nM in the presence of Lipofectamine 2000. Cells were grown for 5 days. (A) RT-qPCR analysis of miR-372 levels; the bars represent the miR-372 level normalized with snor25 and U6 and compared to mock treated cells (mean \pm SD, n = 4). (B) Northern blot analysis of miR-372 (medium panel) and U6 (upper panel) in non-denaturing conditions; the lower panel schematizes miR-372 (full line) paired or not with the specific anti-miR (dotted line) for each lane. (C) Non-denaturing northern blot analyses of miR-372, miR-373, miR-17-5p and miR-93 in AGS cells transfected with either TL372, TL373, TL17, TL21 or TLCo at 10 nM or 1 nM.

Figure 2. Tiny LNA against miR-372 and miR-373 de-repress LATS2 and inhibit the growth of cultured AGS cells. (A) and (B) Relative luciferase activity (mean \pm SD, n = 3) of the LATS2 reporter system pGL3-LATS2wt containing the wt LATS2 3'UTR, or of the mutated LATS2 reporter system pGL3-LATS2mut, compared to that of the control vector pGL3. The vectors have been co-transfected with pRL-SV40 and 10 nM of the indicated oligonucleotides using lipofectamin, and their expression was analyzed 48 hrs later. (C) Western blot analysis of LATS2 (upper panel) and α -tubulin (lower panel) protein expression in untreated MKN74 cells (positive control) or in AGS cells treated with either 22-mer anti-miR-372+miR-373 antisenses (AS) or their scrambled sequence (SC), or with 8-mer tiny LNA against miR-372 and miR-373 (TL) or their negative control (TLCo). (D) LATS2 immunofluorescent staining in AGS cells in the same conditions than in (C). E. Relative growth rate (mean \pm SD, n = 6) of tiny LNA-transfected cultured AGS cells between day 2 and day 5 post-treatment, compared to TLCo-treated cells.

Figure 3. Tiny LNA inhibit miR-372 in AGS cells grown in mice and delay tumor growth. (A) Kinetics of the AGS tumor size expressed in mm³ (mean \pm SD, n = 5) following the first injection (T0) of TLCo, or TL372+373 (TL) at 0.5, 5 or 50 nmol /mouse. Tumors were measured the 3rd (T3), the 9th (T9) and the 14th (T14) day following the first injection. (B) Quantification of *in vivo* luciferase activity at

T9 on AGS-PM372 or AGS-mut372 xenografts, either untreated (mock) or treated with TL or TLCo at 5 nanomoles/mouse: bars represent the mean \pm SD ($n = 5$) of radiance (photons/s/cm²/steradian) of the region of interest relative to the background radiance (out of the region of interest). (C) Representative *in vivo* bioluminescence images of AGS-mut372 xenografts in mice either untreated (a) or TL-treated (b), and AGS-PM372 xenografts either untreated (c), TLCo- (d) or TL-treated (e) as in (B).

Figure 4. Tiny LNA stably sequester miR-372 in AGS xenografts and de-repress LATS2. (A) Non denaturing northern blot analysis of miR-372 (a, b) and miR-21 (c, d) in AGS-PM372 tumors treated with TLCo or TL372+373 at 5 nanomoles/mouse (a, c) or with increasing doses (b, d). (B) Representative images of LATS2 immunostaining in AGS -PM372 tumors treated with either TLCo or TL372+373 at 5 nanomoles/mouse. Scale bars, 25 μ m.

Figure 5. Tiny LNA inhibit the growth of a miR-372-positive human gastric tumor. (A) TL372+373 (TL) dose-dependent effects on tumor growth: bars represent the mean \pm SD ($n = 5$) of the relative tumor size increase during the 14 days following the first day of injection. (B) Representative images of LATS2 immunostaining in GC10 xenografts treated with either TLCo or TL372+373 at 5 nanomoles/mouse. Scale bars, 25 μ m.

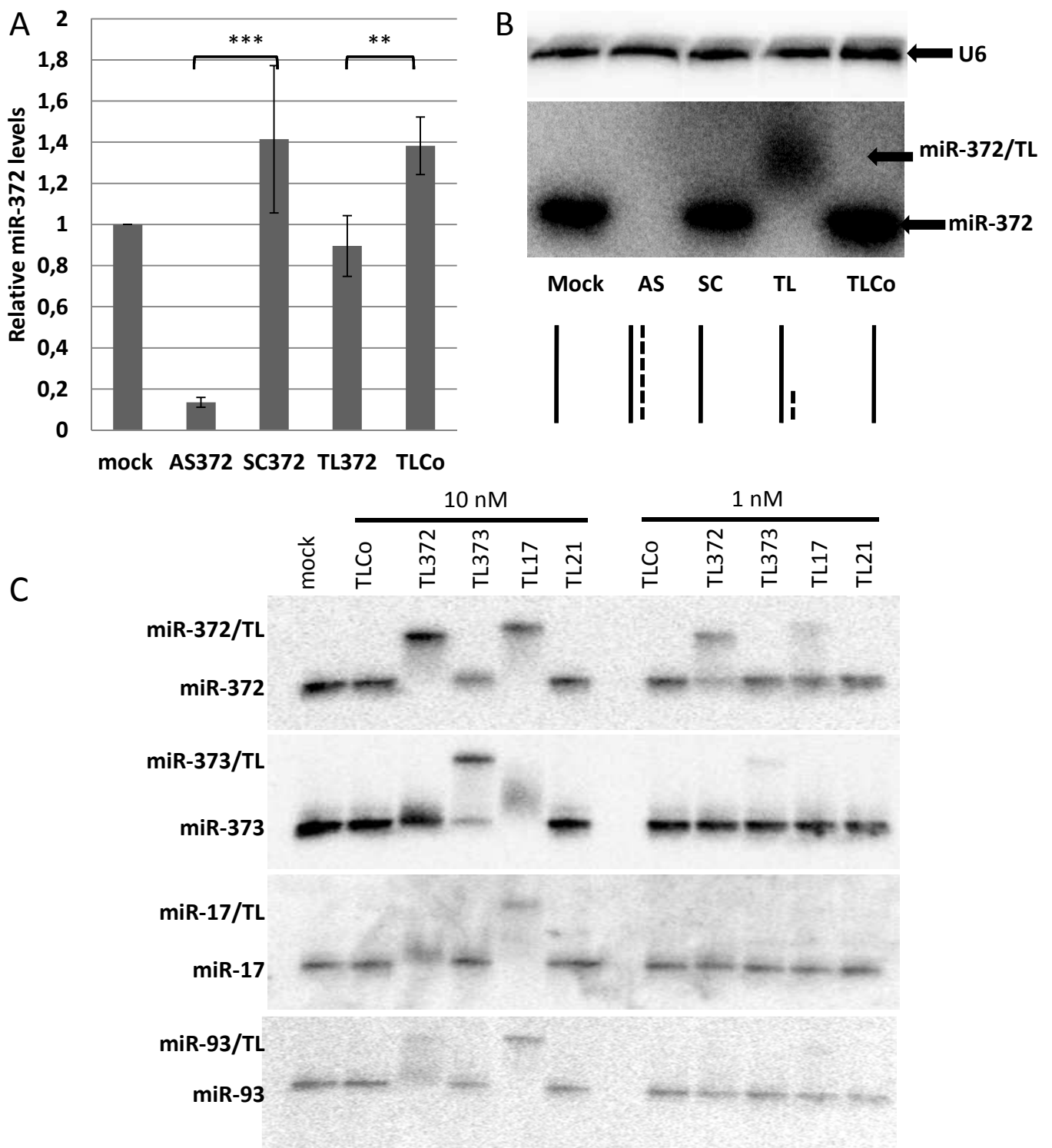


Figure 1

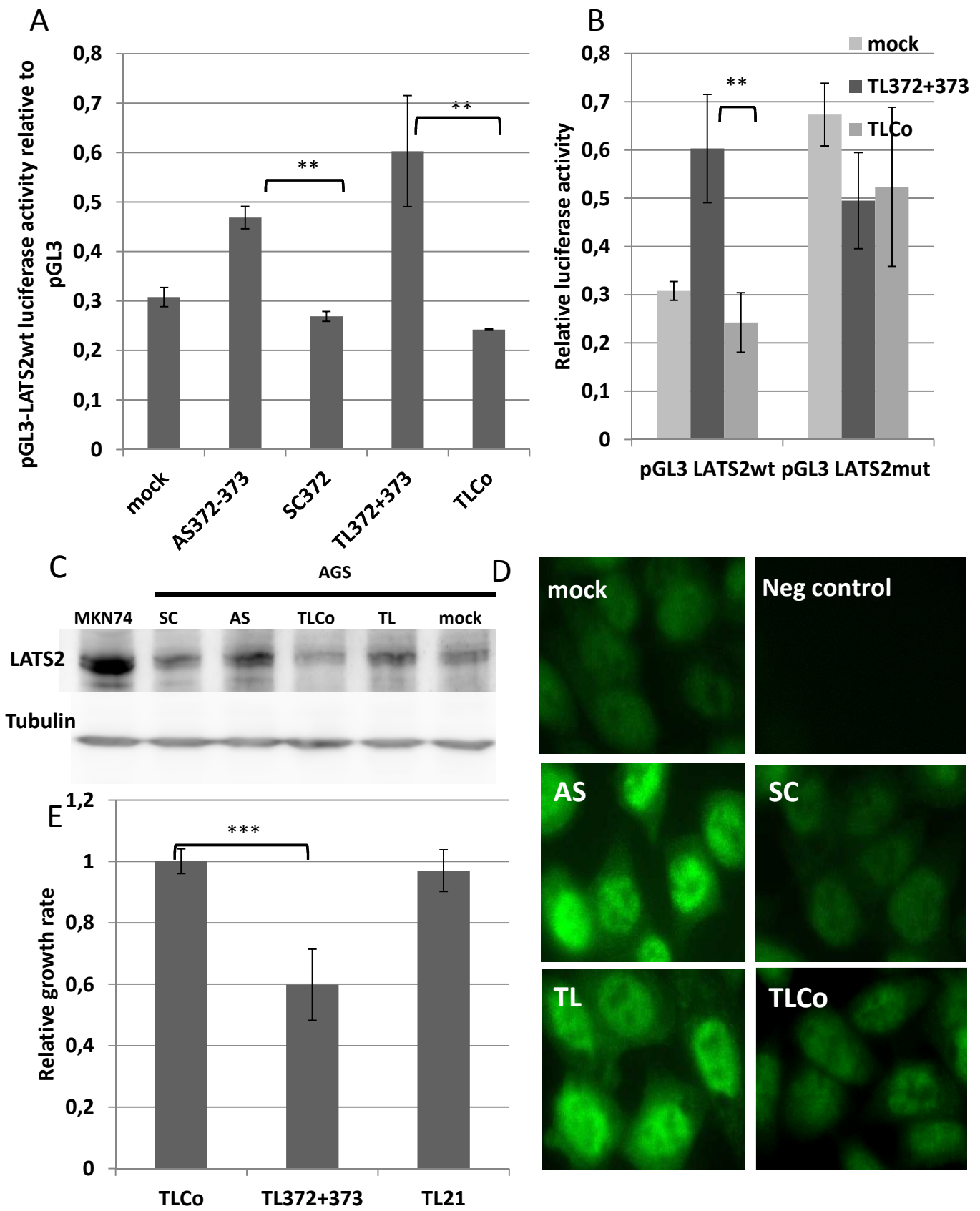


Figure 2

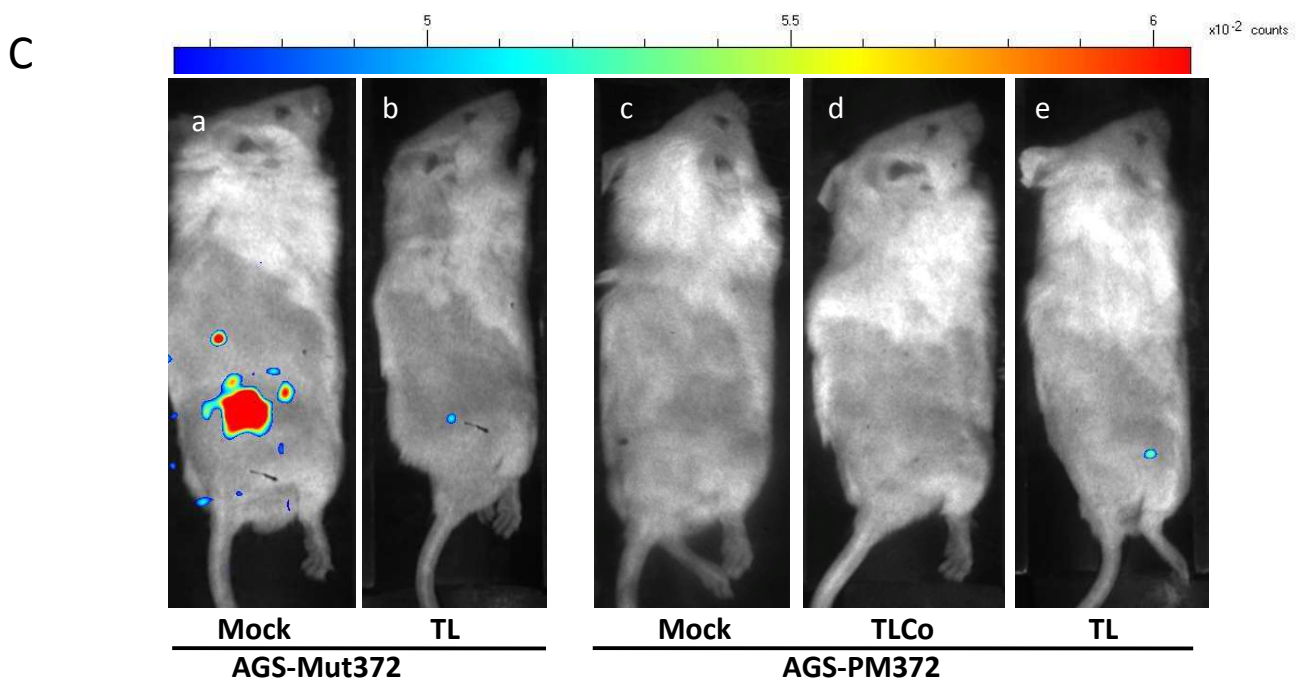
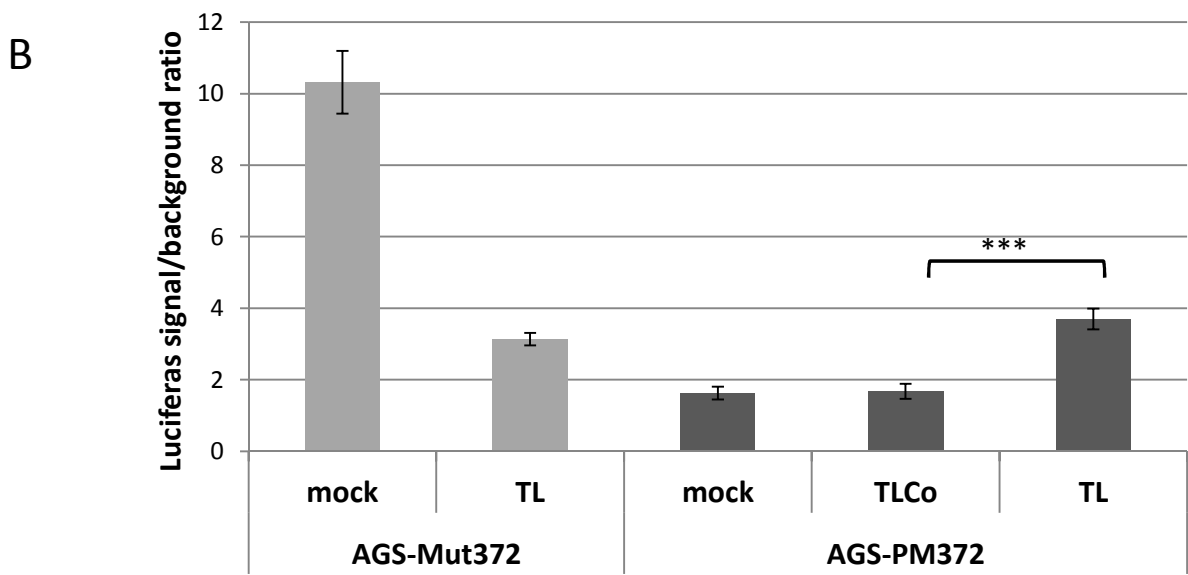
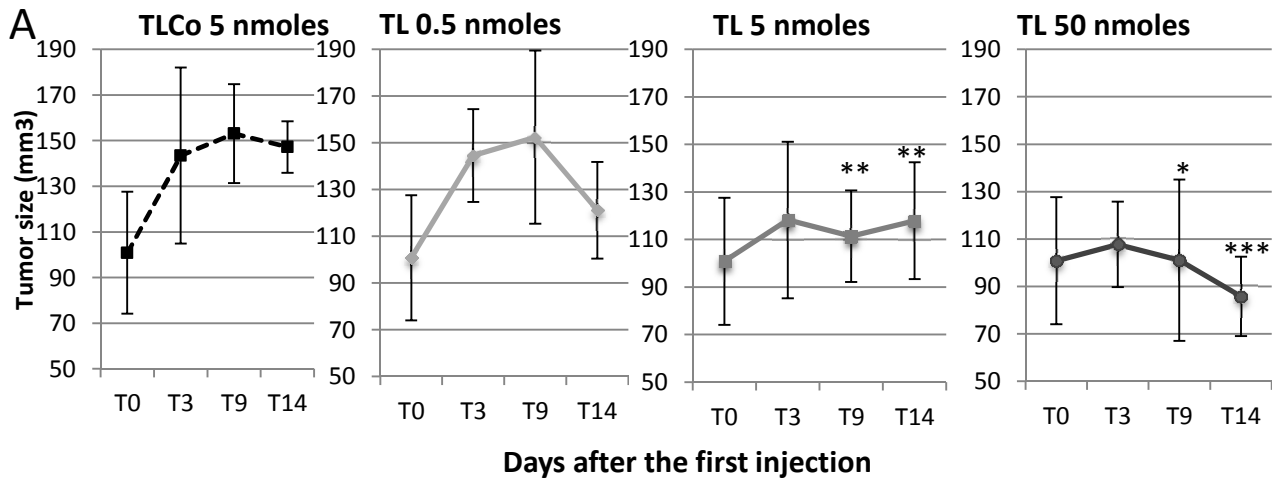


Figure 3

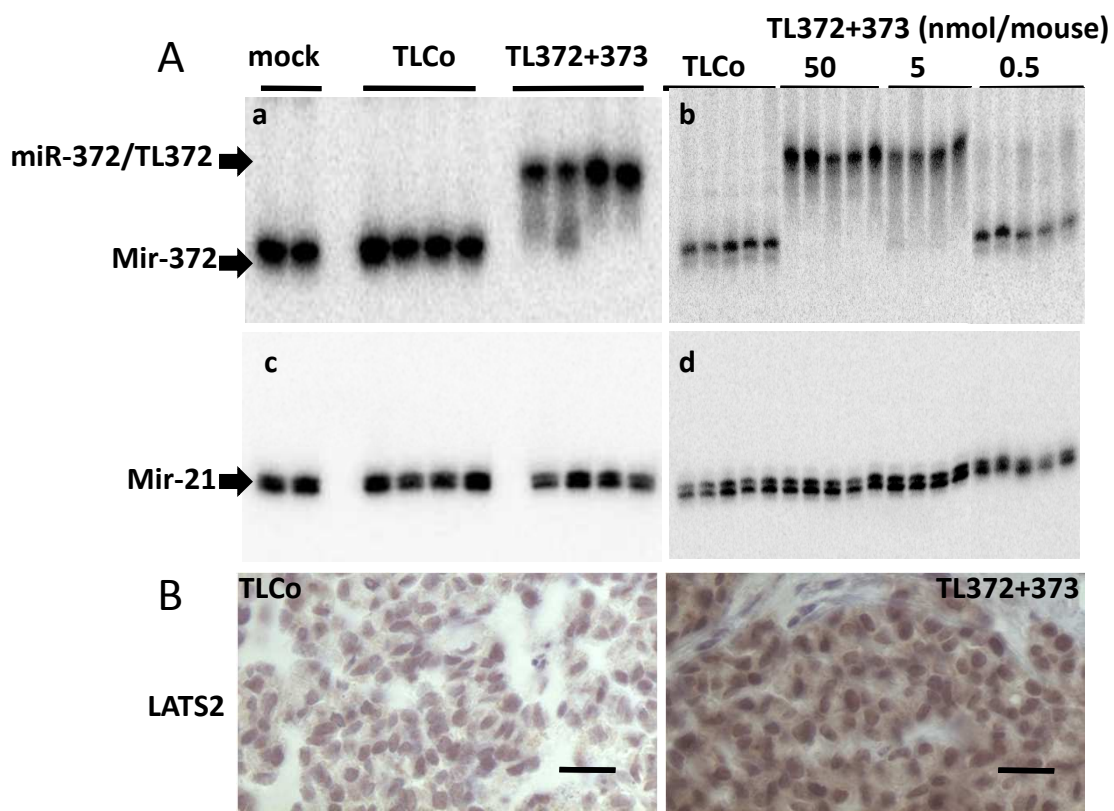


Figure 4

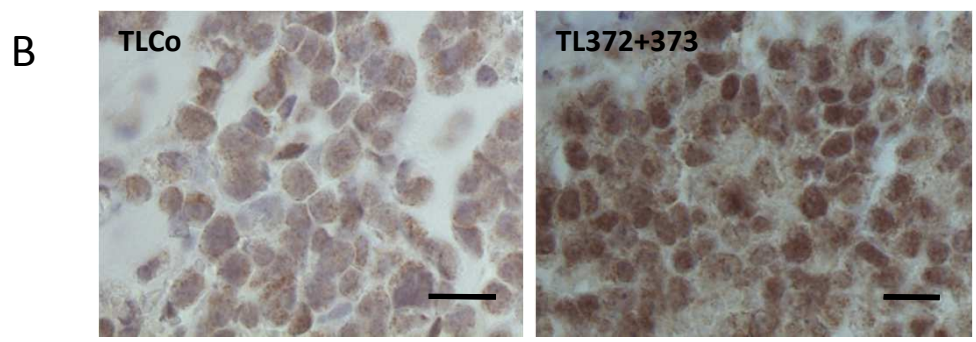
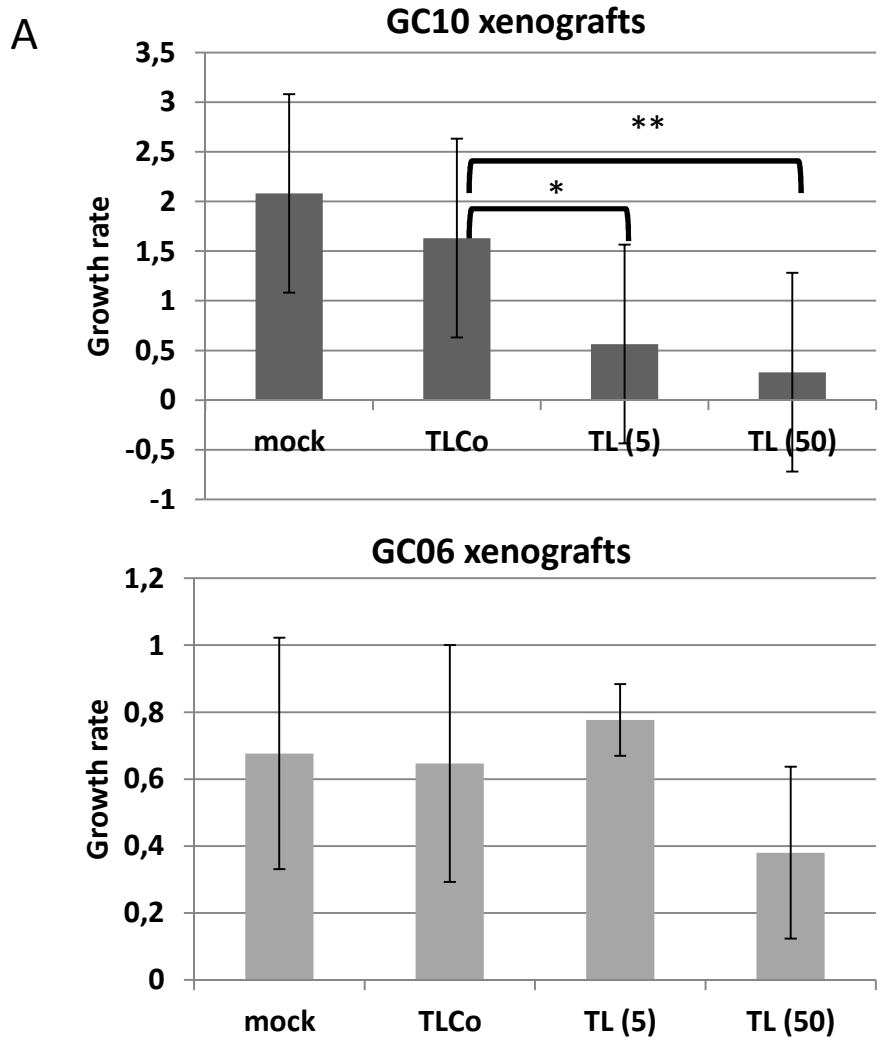


Figure 5

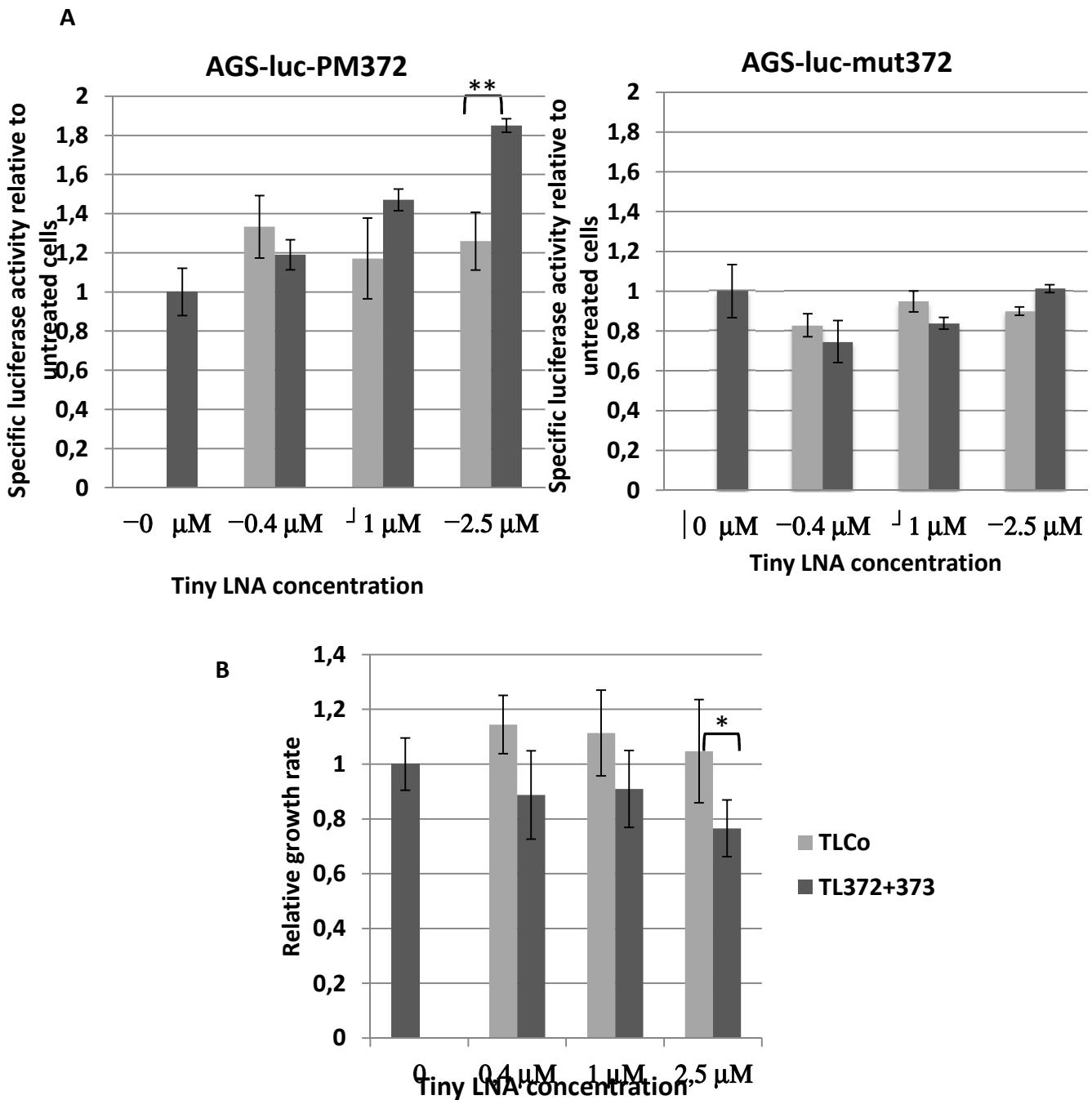


Figure S1. Unassisted tiny LNA inhibit miR-372 and miR-373 functions.

(A) The stable reporter cell lines AGS-luc-PM372 (left) and AGS-luc-mut372 (right) were treated with increasing concentrations of TLCo (light grey), TL372+373 (dark grey) for 5 days. The bars represent the relative luciferase activities (mean \pm SD, $n = 6$) of each reporter cell line normalized to total protein content and compared to untreated cells.

(B) Relative growth rate (mean \pm SD, $n = 6$) of tiny LNA-treated cultured AGS cells between day 2 and day 5 post-treatment, compared to untreated cells.

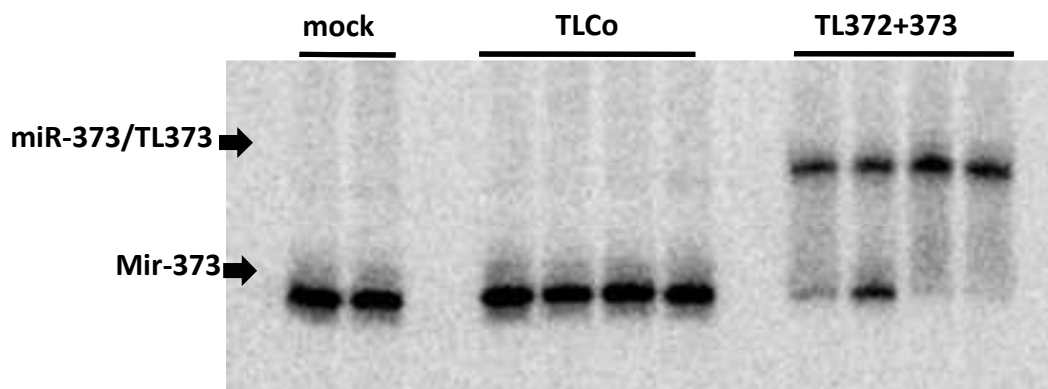


Figure S2: Non denaturing northern blot analysis of miR-373 in AGS-PM372 tumors treated with TL372+373 or TLCo at 5 nanomoles/mouse

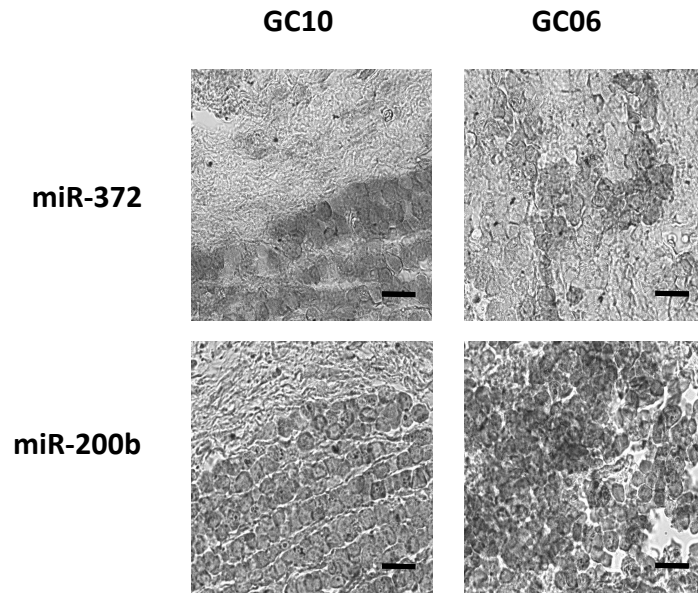


Figure S3: MiR-372 and miR-200b *in situ* hybridization.

The human gastric adenocarcinoma xenografts in mice GC10 (left panels) and GC06 (right panels) have been probed for miR-372 (upper panels) or miR-200b (lower panels). Scale bars, 25 μm .

Table 1. Sequences of the miRNAs of the miR-17 family

| miRNA cluster | miRNA name | MiRNA sequence, showing the seed (nu 2-8) underlined |
|-------------------------|--|---|
| Cluster miR-371-372-373 | hsa-miR-372-3p MIMAT0000724 | 5' <u>AAAGUGCUGCGACA</u> UUUGAGCGU 3' |
| | hsa-miR-373-3p MIMAT0000726 | 5' <u>GAAGUGC</u> UUCGAUUUUUGGGGUGU 3' |
| Cluster miR-17~92 | hsa-miR-17-5p MIMAT0000070 | 5' <u>CAAAGUGC</u> UUACAGUGCAGGUAG 3' |
| | hsa-miR-20a-5p MIMAT0000075 | 5' <u>UAAAGUGC</u> UUAUAGUGCAGGUAG 3' |
| Cluster miR-106b-93-25 | hsa-miR-93-5p MIMAT0000093 | 5' <u>CAAAGUGC</u> UGUUCGUGCAGGUAG 3' |
| | hsa-miR-106b-5p MIMAT0000680 | 5' <u>UAAAGUGC</u> UGACAGUGCAGAU 3' |

Table 2. Theoretical 8-mer LNA pairing with the miRNAs of the miR-17 family

| Tiny LNA | Targeted miRNA | Pairing with the miRNA and duplex formation |
|--------------|--|---|
| TL372 | miR-372 3' TTCACGAC 5' 5' a <u>AAGUGC</u> Ugcgacauuugagcgu 3' | nu 2 to 9 : duplex |
| | miR-93 3' TTCACGAC 5' 5' ca <u>AAGUGC</u> UGuucgugcagguaG 3' | nu 3 to 10 : loose duplex |
| | miR-17 3' TTCACGAC 5' 5' ca <u>AAGUGC</u> Uuacagugcagguag 3' | nu 3 to 9 : no duplex |
| | miR-373 3' TTCACGAC 5' 5' g <u>AAGUGC</u> Uucgauuuuggggugu 3' | nu 2 to 8 : no duplex |
| TL373 | miR-373 3' TTCACGAA 5' 5' g <u>AAGUGC</u> Uucgauuuuggggugu 3' | nu 2 to 9 : duplex |
| | miR-372 3' TTCACGAA 5' 5' a <u>AAGUGC</u> Ugcgacauuugagcgu 3' | nu 2 to 8 : no duplex |
| | miR-17 3' TTCACGAA 5' 5' c <u>AAAGUGC</u> Uuacagugcagguag 3' | nu 3 to 10 : no duplex |
| | miR-93 3' TTCACGAA 5' 5' c <u>AAAGUGC</u> Uguucgugcagguag 3' | nu 3 to 9 : no duplex |
| TL17 | miR-17 3' TTTCACGA 5' 5' c <u>AAAGUGC</u> Uuacagugcagguag 3' | nu 2 to 9 : duplex |
| | miR-93 3' TTTCACGA 5' 5' c <u>AAAGUGC</u> UguucgugcagguaG 3' | nu 2 to 9 : duplex |
| | miR-372 3' TTTCACGA 5' 5' <u>AAAGUGC</u> Ugcgacauuugagcgu 3' | nu 1 to 8 : duplex |
| | miR-373 3' TTTCACGA 5' 5' g <u>AAGUGC</u> Uucgauuuuggggugu 3' | nu 2 to 8 : loose duplex |

In each miRNA, the seed is underlined and the nucleotides paired with the 8-mer LNA are in capitals

Table S1 Oligonucleotides used in this study

| Oligonucleotide | Sequence (5' – 3') |
|--|---------------------------|
| Anti-miR-372 AS372 | acGctCaaAtgTcgCagCacTtt |
| Anti-miR-373 AS373 | acAccCcaAaaTcgAagCacTtc |
| Scrambled oligonucleotide SC372/373 | caCgtAcaTagTgcAccGatAtt |
| Tiny anti-miR-372 TL372 | CAGCACTT |
| Tiny anti-miR-373 TL373 | AAGCACTT |
| Tiny anti-miR-17-5p TL17 | AGCACTTT |
| Tiny anti-miR-21 TL21 | GATAAGCT (*) |
| Tiny negative control (TLCo) | TCATACTA (*) |
| Anti-miR-21 | tcAacAtcAgtCtgAtaAgcTa |
| Anti-miR-17-5p | aCtaCCtGCaCtGtaaGCaCtttg |
| Anti-miR-93 | ctAccTgcAcgAacAgcActTtg |
| U6 | caCgaAttTgcGtgTcaTccTt |

LNA nucleotides are shown in upper case and DNA nucleotides in lowercase.

(*) according to Obad, S., dos Santos, C.O., Petri, A., Heidenblad, M., Broom, O., Ruse, C., Fu, C., Lindow, M., Stenvang, J., Straarup, E.M., et al. (2011) Silencing of microRNA families by seed-targeting tiny LNAs. *Nat. Genet.*, **43**, 371–378.

